

The synthesis of water-soluble polymers with drag reducing properties

Edyta Lam

November 2012

A dissertation submitted in partial fulfilment of the requirements for the degree of
Doctor of Philosophy
and the Diploma of Imperial College London

Department of Chemical Engineering
Imperial College London
London, SW7 2AZ, UK

Declaration

This dissertation is a description of the work carried out in the Department of Chemical Engineering at Imperial College London between May 2008 and May 2012. Except where acknowledged, the material is the original work of the author and includes nothing, which is the outcome of work in collaboration and no part of it has been submitted for a degree at this or any other university.

Edyta Lam

November 2012

Abstract

The objective of work described in this thesis was to synthesize water soluble polymers with drag reducing properties that would expand the understanding of the relationship between the molecular structure of polymers and drag reduction performance. The additional aim of this study was to identify suitable additives that would enable removal of associating polymers from the low permeability reservoirs. The copolymers of acrylamide and two hydrophobic monomers, n-decyl- and n-octadecyl acrylamide were prepared using micellar polymerisation. Polymers of N-hydroxyethyl acrylamide were also prepared via the same method. Water soluble polymers of styrene and butadiene were acquired by sulfonation of poly(styrene-*block*-butadiene) with acetyl sulfate. The evidence of the incorporation of hydrophobic monomers, sulfonic acid groups into copolymers and the concentration of hydrophobic moieties was studied using NMR, FT-IR and Elemental Analysis. The influence of the degree of sulfonation on the flexibility of polymers and polymer degradation temperatures were investigated by DSC, DMA and TGA. The associating properties of polymers were studied using Dynamic Light Scattering and rheology. The drag reducing properties were quantified using a standard rheometer equipped with a Couette double-gap measuring geometry, by calculating the percentage of drag reduction (% DR) based on apparent viscosity. The extent of adsorption and desorption of polymers from silica was studied by Total Organic Carbon.

From the obtained results it was clear that the associating properties of polymers synthesised in this thesis were dependent on the concentration of hydrophobic moieties. In addition, the formation of hydrophobic associations and the polymer coil dimensions were found to greatly influence the drag reducing properties and shear resistance of copolymers. It was found that hydrophobically modified polyacrylamide promoted higher drag reduction in comparison to unmodified polyacrylamide. In addition, introduction of a small amount of hydrophobic moieties was found to impart drag reducing properties in poly(N-hydroxyethyl acrylamide). Moreover, water soluble sulfonated poly(styrene-*block*-butadiene) showed high drag reduction efficiency at extremely low molecular weights below the required lower molecular weight limit necessary to produce excellent drag reduction effect. Furthermore, the sulfonation of poly(styrene-*block*-

butadiene) resulted in the reduced thermal stability of polymers and an increase in the degree of sulfonation resulted in the decrease in the flexibility of polymer chains.

The extent of adsorption of polymers of acrylamide on silica was found to increase with molecular weight of polymers and was higher for hydrophobically modified polyacrylamide due to the formation of intermolecular associations between copolymer chains. The desorption capability of copolymers with the aid of Cyclodextrin was demonstrated and was found to depend on the type of Cyclodextrin used and on the concentration of hydrophobic moieties. Nearly 100 % of the adsorbed polymer was recovered when even small concentrations of β -Cyclodextrin were applied. Additionally, partial desorption of polyacrylamide with the aid of α and β -Cyclodextrin was also achieved.

Table of Contents

Declaration.....	2
Abstract.....	3
Acknowledgments.....	8
Publications.....	10
Poster Presentations	10
List of Figures.....	11
List of Tables	19
Abbreviations.....	21
Symbols.....	24
CHAPTER 1 INTRODUCTION.....	26
1.1. Project Aims.....	29
1.2. Thesis structure	30
CHAPTER 2 BACKGROUND.....	31
2.1. Drag reduction	31
2.2. Polymeric drag reducing agents.....	33
2.3. Water soluble polymeric drag reducing agents.....	37
2.4. Degradation of polymeric drag reducing agents.....	39
2.5. Association of polymers and drag reduction	40
2.6. Intra- and intermolecular association breakers	42
2.7. Synthesis of hydrophobically modified water soluble polymers.....	44
2.7.1. Polyacrylamide (PAAm).....	45
2.7.2. Polyacrylic acid (PAA).....	47
2.7.3. Poly(ethylene oxide) (PEO).....	49
2.7.4. Poly(vinyl alcohol) (PVA).....	51
2.7.5. Poly(N-hydroxyethylacrylamide) (PHEAAm)	54
2.7.6. Biopolymers.....	56
2.7.7. Polystyrene polymers, copolymers and terpolymers	58
2.7.8. Polyisoprene copolymers and terpolymers	63
CHAPTER 3 EXPERIMENTAL METHODS.....	65
3.1. Materials	65
3.2. Synthesis of hydrophobically modified polyacrylamide copolymers.....	66
3.2.1. Micellar copolymerisation of acrylamide and n-decyl acrylamide.....	66
3.2.2. Micellar copolymerisation of acrylamide and n-octadecyl acrylamide	70

3.2.3. Synthesis of polyacrylamide (PAAm0)	71
3.3. Synthesis of hydrophobically modified poly(N-hydroxyethyl acrylamide) copolymers	72
3.3.1. Micellar copolymerisation of N-hydroxyethyl acrylamide and n-decyl acrylamide	72
3.3.3. Synthesis of poly(N-hydroxyethyl acrylamide) (PHEAAm0).....	74
3.4. Synthesis of sulfonated poly(styrene- <i>block</i> -butadiene)	75
3.4.1. The synthesis of acetyl sulfate	75
3.4.3. Sulfonation of poly(styrene- <i>block</i> -butadiene) with acetyl sulfate	77
3.5. Characterisation methods.....	78
3.5.1. Nuclear Magnetic Resonance Spectroscopy (NMR)	78
3.5.2. Fourier Transform Infrared Spectroscopy (FT-IR).....	79
3.5.3. Gel Permeation Chromatography (GPC)	79
3.5.4. Differential Scanning Calorimetry (DSC)	80
3.5.5. Dynamic Mechanical Analysis (DMA)	80
3.5.6. Thermal Gravimetric Analysis (TGA).....	80
3.5.7. Elemental Analysis (EA)	80
3.5.8. Determination of hydrophobic monomer content in copolymers	81
3.5.9. Determination of the degree of sulfonation	84
3.5.10. Dynamic Light Scattering (DLS).....	85
3.5.11. Rheology	86
3.5.12. Instantaneous and time dependent drag reduction measurements	87
3.5.13. Adsorption and desorption study of polymers on silica.....	90
3.5.14. Determination of solubility of sulfonated polymers	91
3.5.15. Determination of solubility of hydrophobically modified polyacrylamide and poly(N-hydroxyethylacrylamide) copolymers	92

CHAPTER 4 HYDROPHOBICALLY MODIFIED POLYMERS OF ACRYLAMIDE 93

4.1. Introduction.....	93
4.2. Results and discussion	94
4.2.1. Synthesis and characterisation of polymers of acrylamide.....	94
4.2.2. Rheology of polymers of acrylamide.....	102
4.2.3. Instantaneous drag reduction study of polymers of acrylamide	105
4.2.4. Time dependent drag reduction of polymers of acrylamide	109
4.2.5. Influence of solvent quality on drag reduction of polymers of acrylamide	115
4.3. Summary	117

CHAPTER 5 INFLUENCE OF CYCLODEXTRINS ON THE BEHAVIOUR OF THE POLYMERS OF ACRYLAMIDE 120

5.1. Introduction.....	120
------------------------	-----

5.2. Results and discussion	121
5.2.1. Influence of Cyclodextrins on the deactivation of hydrophobic interactions in polymers of acrylamide.....	121
5.2.3. Adsorption of polymers of PAAm and desorption from silica using Cyclodextrins	136
5.3. Summary	139

CHAPTER 6 HYDROPHOBICALLY MODIFIED POLYMERS OF N-

HYDROXYETHYL ACRYLAMIDE.....	141
6.1. Introduction.....	141
6.2. Results and Discussion	142
6.2.1. Synthesis and characterisation of polymers of N-hydroxyethyl acrylamide	142
6.2.2. Rheology of polymers of N-hydroxyethyl acrylamide	147
6.2.3. Instantaneous drag reduction study of polymers of N-hydroxyethyl acrylamide.....	151
6.3. Summary	155

CHAPTER 7 SULFONATED COPOLYMERS OF STYRENE AND BUTADIENE 157

7.1. Introduction.....	157
7.2. Results and discussion	158
7.2.1. Sulfonation of poly(styrene- <i>block</i> -butadiene)	158
7.2.3. Characterisation of sulfonated poly(styrene- <i>block</i> -butadiene)	163
7.2.4. Thermal analysis of sulfonated poly(styrene- <i>block</i> -butadiene).....	166
7.2.5. Rheology of water soluble sulfonated poly(styrene- <i>block</i> -butadiene)	172
7.2.6. Instantaneous drag reduction of sulfonated poly(styrene- <i>block</i> -butadiene)	175
7.2.7. Time dependent drag reduction of sulfonated poly(styrene- <i>block</i> -butadiene)	177
7.3. Summary	180

CHAPTER 8 SUMMARY AND FUTURE WORK 183

8.1. Summary of the results	183
8.2. Future work	188
References.....	190

Acknowledgments

First I would like to express my biggest gratitude to Prof Alexander Bismarck and Dr Joachim Steinke for guidance, advice and encouragement while supervising this project. Further I would like to acknowledge Halliburton Energy Services and EPSRC for funding this project, Dr Lewis Norman and Dr Ian Robb from Halliburton for the technical advice. I would also like to express my gratitude to Prof Paul Luckham, my collaborating academic, for the useful advice and discussions about rheological studies. Special thanks to Ms Patricia Carry from Analytical Lab for the help with analytical equipment and testing, Mr Alan Dickerson from University of Cambridge and Exeter Analytical Services for carrying out elemental analysis, Dick Sheppard and Peter Haycock for their help with NMR studies, Dr Mohammad (Reza) Moghareh Abed for help with TOC and Rajeev Dattani for his help with DLS.

I would also like to thank Prof Alexander Bismarck, Prof Geoffrey Maitland, Dr Dominic McCann and Dr Kevin Forbes for the opportunity to work on challenging project during interruption of studies.

I am pleased to thank Dr Natasha Shirshova, Dr Ivan Zadrazil and Dr Emilia Kot for their advice, especially Ivan for sharing his extensive knowledge on drag reduction and for his help in drag reduction studies.

I would like to thank past and present members of PaCE and Steinke group: Ling Ching Wong, Bernice Oh, Dr Siti Rosminah Shamsuddin, Dr Sascha Wettmarshausen, Puja Bharadia, Dr Dan Cegla, Hele Diao, Su Bai, Dr Hui (Sherry) Qian, Dr Atif Javaid, Tomi Herceg, Jing Li, Henry Maples, Dr Koon-Yang Lee, Dr Angelika Menner, Qixiang Jiang, Marta Fortea Verdejo, Dr Kingsley Ho, Dr Sheema Riaz, Nadine Graeber, Dr Anthony Abbot, Dr Johny Blaker, Dr Vivian Ikem, Dr David Anthony, Ain Kamal, Michael Tebboth, Steven Wakefield, Dr Apostolos Georgiadis, Nikoforos Maragos, Dr Michael (Big Mike) Bajomo, Dr John Hodgkinson, Dr Ann Delille, Dr Ki Heung Kim, Dr Juntaro Julasak, Dr Charnwit Tridech, Dr Ryo Murakami, Dr Steven Lamoriniere, Dr Andreas Mautner, Dr Shengzhong Zhou, Sally Ewen, Dr Chirag Patel, Bryn Monnery, Dr Beeta Mood-Balali, Dr Stephen Jones, Wei Yuan, Dr Julian Farmer, Muge

Gulesci, Dr Caroline Knapp, David Rees, Dr Martin Hornung, Dr Mustafa Bayazit, Dr Beinn Muir, Dr James Seginson, Nikolay Vaklev and Hin Chun Yau.

I would like to thank especially Ling Ching Wong, Bernice Oh and Dr Siti Rosminah Shamsuddin for being supportive and being there in good and bad times.

Great thanks must go to Susi Underwood, Sarah Payne, Alexandra Szymanska, Anusha Sri-Pathmanthan, Keith Walker, Ben Kristnah and people I have met during my time at Imperial: Dr Joao Cabral, Dr Edo Boek, Emily Chapman, Dr Jerzy Pental, Dr Francisco Garcia Garcia, Dr Him Cheng, Joanna Davies, Dr Alisyn Nedoma, Stephanie Glassford, Carlos Gonzalez Lopez, Dr Bojan Tamburic, Angus Bailey, Ashok Barua and others I forgot to mention (this was unintentional).

Finally, sincere thanks to my parents Alicja and Romuald Sidorowicz, my mother in-law Anna Lam and my family for unconditional support. My special thanks must go to my husband Dr Darren Lam for unconditional support, love, patience and for always being there for me.

Publications

1. “*Fluid Identification System and Production and Use Thereof*” Dominic P.J. McCann, Kevin J. Forbes, Edyta Lam, Geoffrey Maitland, Alexander Bismarck, Patent GB 2490207.

Poster Presentations

1. “*Novel Water Soluble Drag Reducing Agents*” Edyta Sidorowicz, Alexander Bismarck, Joachim H.G. Steinke and Lewis Norman, Macro Group Young Researchers Meeting, University of Nottingham, April 2010.

List of Figures

Figure 1.1. Four stages of hydraulic fracturing; 1. Drilling, 2. Casing, 3. Creating a fracture, 4. Propagation of a fracture.	27
Figure 1.2. Schematic of the conformation of adsorbed layers formed by associating polyacrylamide at solid/liquid interface [25].....	28
Figure 2.1. Schematic illustration of laminar (a) and turbulent (b) flow (image reproduced from www.ceb.cam.ac.uk).	32
Figure 2.2. Structure of water soluble drag reducing biopolymers [10].....	37
Figure 2.3. Structure of water soluble drag reducing synthetic polymers.	38
Figure 2.4. Chemical structures of α - (1), β - (2) and γ - (3) Cyclodextrin.	43
Figure 2.5. Schematic representation of the influence of the number of hydrophobic monomers per micelle on the copolymer microstructure [152].	45
Figure 2.6. Schematic of modification of materials by transamidation.....	47
Figure 2.7. Modification of polyacrylic acid with alkylamine.	49
Figure 2.8. Structures of poly(ethylene oxide-co-glycidol) and poly(ethylene oxide-block-glycidol) [171].	50
Figure 2.9. Anionic polymerisation of ethylene oxide initiated by potassium alkoxide and subsequent synthesis of asymmetric end-capped polymers by esterification [151, 152].	51
Figure 2.10. Hydrolysis of poly(vinyl acetate) in methanol.	52
Figure 2.11. Reaction scheme for the hydrophobic modification of PVA [158].....	52
Figure 2.12. The reaction scheme for the Williamson ether synthesis, $R = C_{15}H_{31}$ [159].....	53
Figure 2.13. Reaction scheme for the Michael addition of acrylamide and subsequent Hoffman degradation [159].....	53
Figure 2.14. Polymerisation of HEAA using ECP, CuCl, and Me6TREN and subsequent additions of DMAA, NAM, and DMAPAA, producing PHEAA-b-PDMAA, PHEAA-b-PNAM, and PHEAA-b-PDMPAA, respectively.....	55
Figure 2.15. Synthesis of PHEAA-b-PS copolymers. PS- Polystyrene, PMDTA- N,N,N,N,N-pentamethyldiethylenetriamine [164].....	56

Figure 2.16. Synthesis of guar gum polyoxyalkyleneamines derivatives [183]. DMS-dimethylsulfate.	57
Figure 2.17. Functionalisation of polystyrene by chloromethylation and quaternisation.....	59
Figure 2.18. Chloromethylation, quaternization and alkalization of SEBS.....	59
Figure 2.19. Commonly used sulfonating agent species.....	60
Figure 2.20. Reaction scheme of homogeneous sulfonation : (A) acetyl sulfate generation and (B) sulfonation of polystyrene (PS) [179].	61
Figure 2.21. Structure of sulfonated styrene-isoprene copolymers.	64
Figure 3.1. The reaction scheme for the synthesis of poly(acrylamide-co-n-decyl acrylamide)..	66
Figure 3.2. Reaction scheme for the synthesis of poly(acrylamide-co-n-octadecyl acrylamide).	70
Figure 3.3. Reaction scheme for the synthesis of PAAm0	71
Figure 3.4. Reaction scheme for the synthesis of poly(N-hydroxyethyl acrylamide-co-n-decyl acrylamide).	72
Figure 3.5. Reaction scheme for the synthesis of HEOD1	73
Figure 3.6. Reaction scheme for the synthesis of PHEAAm0	74
Figure 3.7. The reaction scheme for the synthesis of acetyl sulfate.	75
Figure 3.8. The reaction scheme for the sulfonation of poly(styrene- <i>block</i> -butadiene).	77
Figure 3.9. ¹ H NMR spectrum of poly(acrylamide-co-n-decyl acrylamide) (AD7).....	82
Figure 3.10. ¹ H NMR spectrum of poly(N-hydroxyethyl acrylamide-co-n-decyl acrylamide) (HED1).....	82
Figure 3.11. ¹ H NMR spectrum of poly(acrylamide-co-n-octadecyl acrylamide) (AOD3).....	83
Figure 3.12. ¹ H NMR spectrum of poly(N-hydroxyethyl acrylamide-co-n-octadecyl acrylamide) (HEOD1).....	83
Figure 3.13. Schematic representation of the double gap cell with axial symmetry used for drag reduction study. The measuring cell active rotor height is H = 111.00 mm and the radii are R1 = 22.25mm, R2 = 22.75mm, R3 = 23.50mm and R4 = 24.00mm. The sample volume was 17 ml.....	87
Figure 3.14. Taylor onset of polyacrylamide at M _w = 1085 kDa at 0.1 mg•g ⁻¹	88

Figure 3.15. The apparent viscosity as a function of time at constant rotor speed of 2250 rpm (11200 s ⁻¹) for polyacrylamide M _w = 1085 kDa at 0.1 mg•g ⁻¹	89
Figure 4.1. ¹ H NMR spectrum of n-decyl acrylamide recorded in CDCl ₃	97
Figure 4.2. ¹ H NMR spectrum of polyacrylamide acquired in D ₂ O (PAAm0).....	97
Figure 4.3. The example of ¹ H NMR spectrum of poly(acrylamide-co-n-decyl acrylamide) in D ₂ O (AD7 , 0.65 mol% DAAM).....	98
Figure 4.4. ¹ H NMR spectrum of n-octadecyl acrylamide recorded in CDCl ₃	98
Figure 4.5. ¹ H NMR spectrum of poly(acrylamide-co-n-octadecyl acrylamide) in D ₂ O (AOD3 , 0.09 mol% ODAAM).....	99
Figure 4.6. The apparent viscosity at $\dot{\gamma} = 10 \text{ s}^{-1}$ and at T= 25°C of the aqueous solutions of PAAm and its copolymers with n-decyl acrylamide as a function of polymer concentration (inset shows close-up of low concentrations).....	102
Figure 4.7. The apparent viscosity at 10 s^{-1} and at T= 25°C of the aqueous solutions of PAAm and its copolymer with n-octadecyl acrylamide (AOD3 , 0.09 mol% ODAAM) as a function of concentration (inset shows close-up of low concentrations).....	103
Figure 4.8. Percentage drag reduction as a function of polymer concentration for commercial PAAm (PAAmC , M _w = 1085 kDa), control PAAm0 (M _w = 1896 kDa) and copolymers of PAAm with n-decyl acrylamide. Measured at shear rate $\dot{\gamma} = 11200 \text{ s}^{-1}$ and 25°C.....	106
Figure 4.9. Percentage drag reduction as a function of polymer concentration for PAAm0 (M _w = 1896 kDa) and its copolymer with n-octadecyl acrylamide (AOD3 , M _w = 1345 kDa). Measured at shear rate $\dot{\gamma} = 11200 \text{ s}^{-1}$ and 25°C.....	106
Figure 4.10. Evolution of drag reduction with shearing time for the polymers of acrylamide. Studied at a shear rate of 11200 s^{-1} , 25°C and at polymer C= 0.5 mg•g ⁻¹ . Error 0.5 to 1.5 %. 1 to 6 is the number of a shearing cycle.	110
Figure 4.11. The variation of drag reduction as a function of shearing cycle number in Taylor flow for copolymers of PAAm. Measured with a double-gap cell at shear rate of 11200 s^{-1} , 25°C and at polymer C=0.5 mg•g ⁻¹	112
Figure 4.12. The schematic illustration of the proposed mechanism for the interaction of associating polymers of PAAm containing hydrophobic moieties with turbulent vortices. 1.	

Quiescent conditions, polymer in the intra- or/and intermolecularly associated form; 2. Collision of turbulent vortices and the resulting polymer elongation and vortices destruction; 3. Formation of a gel-like transient network with elongated chains containing associating groups; 4. Collision of turbulent vortices and gel-like network; 5. Dissociation of gel-like network under the shear; 6. Recovered associating polymer in quiescent conditions.	113
Figure 4.13. Apparent viscosity of poly(acrylamide-co-n-decyl acrylamide) (AD8 , 0.54 mol% DAAM) as a function of time. Measured at 1000 s^{-1} after 1 st shearing cycle and after 60 min. relaxation at 0 shear rate.....	114
Figure 4.14 Percent drag reduction as a function of concentration for copolymers of acrylamide and polyacrylamide (PAAm0). Studied in deionised water, API brine ($1.711\text{ mol}\cdot\text{L}^{-1}\text{ NaCl}$ and $0.084\text{ mol}\cdot\text{L}^{-1}\text{ CaCl}_2\cdot 2\text{H}_2\text{O}$ and 2% w/w ($0.268\text{ mol}\cdot\text{L}^{-1}$) KCl (for selected polymers).	116
Figure 5.1. An example of ^1H NMR spectrum in D_2O of poly(acrylamide-co-n-decyl acrylamide) (AD8), α -CD and inclusion complex of poly(acrylamide-co-n-decyl acrylamide) (AD8) with 100 meq α -CD.	123
Figure 5.2. An example of ^1H NMR spectrum of poly(acrylamide-co-n-decyl acrylamide) (AD8), β -CD and inclusion complex of poly(acrylamide-co-n-decyl acrylamide) (AD8) and 100 meq β -CD studied in D_2O	123
Figure 5.3. Part of the ^1H NMR spectrum in D_2O showing protons in poly(acrylamide-co-n-decyl acrylamide) (AD8) and inclusion complexes at 1 and 100 meq of β -CD and 100 meq α -CD.	124
Figure 5.4. Part of the ^1H NMR spectrum in D_2O showing protons in α -Cyclodextrin (CD) and inclusion complex of poly(acrylamide-co-n-decyl acrylamide) (AD8 , 0.54 mol% of DAAM) with 100 meq α -CD.	124
Figure 5.5. Part of the ^1H NMR spectrum in D_2O showing protons of β -Cyclodextrin (CD) and inclusion complex of poly(acrylamide-co-n-decyl acrylamide) (AD8 , 0.54 mol% of DAAM) with 100 meq of β -CD.....	125

Figure 5.6. Photographs of the transition of the polymer gel formed by poly(acrylamide-co-n-decyl acrylamide) AD8 (0.54 mol% of DAAM) at $C=5 \text{ mg}\cdot\text{g}^{-1}$ (left) into solution (right) upon addition of 100 meq of β -CD.....	126
Figure 5.7. Influence of α - and β -Cyclodextrin addition on the apparent viscosity of solutions of poly(acrylamide-co-n-decyl acrylamide) (AD7 , 0.65 mol% DAAM). Studied at polymer $C=0.5 \text{ mg}\cdot\text{g}^{-1}$ and 25°C	126
Figure 5.8. Influence of α - and β -Cyclodextrin addition on the apparent viscosity of solutions of poly(acrylamide-co-n-decyl acrylamide) (AD8 , 0.54 mol% DAAM). Studied at polymer $C=0.5 \text{ mg}\cdot\text{g}^{-1}$ and 25°C	128
Figure 5.9. Influence of α - and β -Cyclodextrin addition on apparent viscosity of solutions of poly(acrylamide-co-n-decyl acrylamide) (AD9 , 0.33 mol% DAAM). Studied at $C=0.5 \text{ mg}\cdot\text{g}^{-1}$ and 25°C	128
Figure 5.10. Influence of α - and β -Cyclodextrin addition on the apparent viscosity of solutions of poly(acrylamide-co-n-decyl acrylamide) (AD10 , 0.21 mol% DAAM). Studied at $C=0.5 \text{ mg}\cdot\text{g}^{-1}$ and 25°C	129
Figure 5.11. Influence of α - and β -Cyclodextrin addition on apparent viscosity of solutions of poly(acrylamide-co-n-octadecyl acrylamide) (AOD3 , 0.09 mol% ODAAM). Studied at polymer $C=0.5 \text{ mg}\cdot\text{g}^{-1}$	130
Figure 5.12 Influence of α - and β -Cyclodextrin addition on apparent viscosity of solutions of PAAM0. Studied at polymer $C=0.5 \text{ mg}\cdot\text{g}^{-1}$	130
Figure 5.13. Influence of α -CD addition on the drag reduction of PAAM copolymers. Studied at 11200 s^{-1} , at 25°C and at polymer $C=0.5 \text{ mg}\cdot\text{g}^{-1}$	131
Figure 5.14. Influence of the addition of β -CD to aqueous solutions of PAAM copolymers on the drag reduction. Studied at 11200 s^{-1} , at 25°C and at polymer $C=0.5 \text{ mg}\cdot\text{g}^{-1}$	133
Figure 5.15. Percent DR of PAAM0 ($M_w=1896 \text{ kDa}$) as a function of α - and β -CD concentration studied in deionised water. Measured at 11200 s^{-1} , 25°C and polymer $C=0.5 \text{ mg}\cdot\text{g}^{-1}$	135
Figure 5.16. The adsorption of PAAM0 and its copolymers with n-decyl acrylamide AD10 and n-octadecyl acrylamide AOD3 on silica (specific surface area of silica $45 \text{ m}^2\cdot\text{g}$) as a function of polymer concentration. Measured in deionised water, at pH 7 and 25°C	137

Figure 6.1. ¹ H NMR spectrum of poly(N-hydroxyethyl acrylamide) acquired in D ₂ O (PHEAAm0).....	144
Figure 6.2. ¹ H NMR spectrum of poly(N-hydroxyethyl acrylamide-co-n-decyl acrylamide) acquired in D ₂ O (HED1 , 0.73 mol% DAAM).....	144
Figure 6.3. ¹ H NMR spectrum of poly(N-hydroxyethyl acrylamide-co-n-octadecyl acrylamide) acquired in D ₂ O (HEOD1 , 0.11 mol% ODAAM).....	145
Figure 6.4. Apparent viscosity of the aqueous solutions of polymers of N-hydroxyethyl acrylamide as a function of polymer concentration. Measured at 10 s ⁻¹ and 25°C (inset shows close-up of low concentrations).....	148
Figure 6.5. Apparent viscosity as a function of shear rate for aqueous solutions of poly(N-hydroxyethyl acrylamide) polymers at polymer concentration of 0.5 mg·g ⁻¹ and at 25°C (logarithmic scale).....	150
Figure 6.6. Apparent viscosity as a function of shear rate for aqueous solutions of poly(N-hydroxyethyl) polymers at polymer concentration of 1 mg·g ⁻¹ and at 25°C (logarithmic scale).....	151
Figure 6.7. Percentage drag reduction as a function of polymer concentration for polyacrylamide (PAAm, M _w = 1085 kDa), PHEAAm0 and poly(N-hydroxyethyl acrylamide-co-N-decylacrylamide) copolymers.....	152
Figure 6.8. Percentage drag reduction as a function of polymer concentration for HEAAM homopolymer (PHEAAm0) and its copolymer with n-octadecyl acrylamide (HEOD1)..	153
Figure 7.1. Yield of sulfonation of poly(styrene- <i>block</i> -butadiene) at 25°C and at a sulfonation time of 24 hours.....	160
Figure 7.2. The mechanism of sulfonation of poly(styrene- <i>block</i> -butadiene) by acetyl sulfate. For clarity 1,2 butadiene sulfonation is omitted.....	161
Figure 7.3. Time dependence of the degree of sulfonation of poly(styrene- <i>block</i> -butadiene). Studied at 25°C and with 5.74 mol eq. of acetyl sulfate to 1 mol eq. of polymer.	162
Figure 7.4. Infrared spectrum of poly(styrene- <i>block</i> -butadiene) before (a) and (b) after sulfonation (SSB1 , SD= 6.68 mol%).	163

Figure 7.5. Infrared spectrum of poly(styrene- <i>block</i> -butadiene) before (a) and (b) after sulfonation (SSB6 , SD= 66.28 mol%).	164
Figure 7.6. ¹ H NMR spectrum of poly(styrene- <i>block</i> -butadiene) before sulfonation in d8-THF.	165
Figure 7.7. ¹ H NMR spectrum of poly(styrene- <i>block</i> -butadiene) after sulfonation in a mixture of 25% d ₈ -THF and 75% D ₂ O (SSB6 , SD= 66.28 mol%).	165
Figure 7.8. Chemical structure of poly(styrene- <i>block</i> -butadiene) before and after sulfonation with acetyl sulfate.	166
Figure 7.9. Thermogravimetric curves of poly(styrene- <i>block</i> -butadiene) (PS- <i>b</i> -PB) and sulfonated water soluble poly(styrene- <i>block</i> -butadiene) SSB6 (SD= 66.28 mol%) and SSB10 (SD= 57.06 mol%).	167
Figure 7.10. Thermogravimetric derivative weight curves for poly(styrene- <i>block</i> -butadiene) (PS- <i>b</i> -PB) and sulfonated water soluble poly(styrene- <i>block</i> -butadiene) SSB6 (SD= 66.28 mol%) and SSB10 (SD= 57.06 mol%).	168
Figure 7.11. DSC curves of poly(styrene- <i>block</i> -butadiene) (PS- <i>b</i> -PB) and water soluble sulfonated poly(styrene- <i>block</i> -butadiene) SSB6 (SD= 66.28 mol%) and SSB10 (SD= 57.06 mol%) for the 1 st heating cycle.	169
Figure 7.12. DSC curves of poly(styrene- <i>block</i> -butadiene) (PS- <i>b</i> -PB) and water soluble sulfonated poly(styrene- <i>block</i> -butadiene) SSB6 (SD= 66.28 mol%) and SSB10 (SD= 57.06 mol%) for the 2 nd heating cycle.	170
Figure 7.13. DMA tan δ curves of poly(styrene- <i>block</i> -butadiene) (PS- <i>b</i> -PB) and water soluble sulfonated poly(styrene- <i>block</i> -butadiene) SSB6 and SSB10 obtained at 1 Hz.	171
Figure 7.14. Apparent viscosity as a function of concentration of the aqueous solutions of sulfonated polymers poly(styrene- <i>block</i> -butadiene) SSB6 (SD= 66.28 mol%) and SSB10 (SD= 57.06 mol%) at 10 s ⁻¹ and 25°C.	172
Figure 7.15. Shear rate dependence on the apparent viscosity of the aqueous solutions of sulfonated poly(styrene- <i>block</i> -butadiene) SSB6 (SD= 66.28 mol%) studied at various polymer concentrations at 25°C (logarithmic scale).	173

Figure 7.16. Shear rate dependence on the apparent viscosity of the aqueous solutions of sulfonated poly(styrene-block-butadiene) SSB10 (SD= 57.06 mol%) studied at various polymer concentrations at 25°C (logarithmic scale).	174
Figure 7.17. Illustration of shear-thickening behaviour in associating polymers [266].	175
Figure 7.18. Percentage drag reduction as a function of polymer concentration for sulfonated poly(styrene- <i>block</i> -butadiene) SSB6 (SD= 66.28 mol%) and SSB10 (SD= 57.06 mol%) and commercial PAAm (PAAmC M_w = 1085 kDa) obtained at 25°C in turbulent Taylor Flow.	176
Figure 7.19. Drag reduction as a function of time for sulfonated poly(styrene- <i>block</i> -butadiene) SSB6 (SD= 66.28 mol%) measured at $\gamma = 11200 \text{ s}^{-1}$ and polymer concentration $C = 0.5 \text{ mg}\cdot\text{g}^{-1}$. Error 0.5-1.5 %. 1 to 6 is the number of shearing cycle.	178
Figure 7.20. Drag reduction as a function of time for sulfonated poly(styrene- <i>block</i> -butadiene) SSB10 (SD= 57.06 mol%) measured at $\gamma = 11200 \text{ s}^{-1}$ and polymer concentration $C = 0.5 \text{ mg}\cdot\text{g}^{-1}$. Error 0.5-1.5 %. 1 to 6 is the number of shearing cycle.	179
Figure 7.21. Drag reduction as a function of number of shearing cycles for sulfonated poly(styrene- <i>block</i> -butadiene) SSB6 and SSB10 as measured at polymer $C = 0.5 \text{ mg}\cdot\text{g}^{-1}$ and $\gamma = 11200 \text{ s}^{-1}$. Error 0.5-1.5 %. %	180

List of Tables

Table 2.1. List of water and organic solvents soluble polymers known to reduce drag.	35
Table 3.1. Composition of the monomer mixture for polymerisations AD1-AD10	68
Table 3.2. Composition of the monomer mixture for polymerisations AOD1-AOD3	71
Table 3.3. Composition of the monomer mixture for polymerisations HED1-HED3	73
Table 3.4. The reaction conditions for sulfonation of poly(styrene- <i>block</i> -butadiene)	76
Table 4.1. Yield, molecular weight M_w , hydrophobic monomer content H and solubility of polymers in water and formamide obtained by micellar polymerisation. – or + denotes insoluble or soluble in deionised water or formamide, respectively. ns denotes insoluble in either GPC eluent, deionised water or D_2O , hence analysis not possible, AD = poly(acrylamide-co-n-decyl acrylamide). AOD = poly(acrylamide-co-n-octadecyl acrylamide).	95
Table 4.2. Weight average molecular weight M_w , polydispersity index PDI, hydrophobic monomer content H, drag reduction (DR) determined at $C=0.5\text{mg}\cdot\text{g}^{-1}$ and hydrodynamic radius R_H for copolymers and polymers of acrylamide; AD = poly(acrylamide-co-n-decyl acrylamide), AOD = poly(acrylamide-co-n-octadecyl acrylamide), PAAm0 and PAAmC are homopolymers of acrylamide synthesised under micellar polymerisation conditions and obtained from a commercial source, respectively.	108
Table 5.1. Weight average molecular weight M_w , polydispersity index PDI, hydrophobic moiety content H, and hydrodynamic radius R_H for PAAm and its copolymers with and without α - or β -Cyclodextrin addition; AD = poly(acrylamide-co-n-decyl acrylamide), AOD = poly(acrylamide-co-n-octadecyl acrylamide).	135
Table 5.2. The amount of PAAm and its hydrophobically modified copolymers adsorbed and desorbed on and from silica as measured by TOC; ¹ Amount desorbed with 100 α -CD, no desorption seen at 0.5 and 1 meq of α -CD, ² Amount desorbed with 100 β -CD, no desorption seen at 0.5 and 1 meq of β -CD, ³ Amount desorbed with 0.5 and 100 meq β -CD.....	139
Table 6.1. Yield, molecular weight M_w and the content of hydrophobic moieties H in the copolymers obtained by micellar polymerisation; PDI is the polydispersity index, HED =	

poly(N-hydroxyethyl acrylamide-co-n-decyl acrylamide), **HEOD**= poly(N-hydroxyethyl acrylamide-co-n-octadecyl acrylamide), **PHEAAm0**= poly(N-hydroxyethyl acrylamide).147

Table 6.2. Molecular parameters of the modified poly(N-hydroxyethyl acrylamide) copolymers obtained from the GPC analysis and Dynamic Light Scattering (DLS). Where N_H is the number of hydrophobes per surfactant micelle, M_w is the weight average molecular weight, PDI is the polydispersity index, H (mol%) is the molar percentage of hydrophobic moieties in polymer and R_H is the hydrodynamic radius. **HED**= poly(N-hydroxyethyl acrylamide-co-n-decyl acrylamide) **HEOD**= poly(N-hydroxyethyl acrylamide-co-n-octadecyl acrylamide), **PHEAAm0**= poly(N-hydroxyethyl acrylamide). 155

Table 7.1. Properties of sulfonated poly(styrene-*block*-butadiene). SD is the degree of sulfonation (extent of sulfonation) determined by elemental analysis and calculated from equations (14)-(18) in Chapter 3 section 3.5.9. 159

Table 7.2. T_g of polybutadiene and polystyrene segments and T_d with corresponding weight loss for poly(styrene-*block*-butadiene) and water-soluble sulfonated polymers **SSB6** and **SSB10** as measured by DSC, DMA and TGA. 171

Abbreviations

AAm	Acrylamide
AD	Poly(acrylamide-co-n-decyl acrylamide)
AIBN	2,2'-azobis(isobutyronitrile)
AMPDAC	[2-(acrylamido)-2-methylpropyl]dimethylammonium chloride
AOD	Poly(acrylamide-co-n-octadecyl acrylamide)
ATRP	Atom Transfer Radical Polymerisation
BET	Brunauer Emmett Teller (Particle Surface Area Analyser)
CD	Cyclodextrin
¹³ C NMR	Carbon Nuclear Magnetic Resonance
¹ H NMR	Hydrogen Nuclear Magnetic Resonance
CDCl ₃	Deuterated chloroform
CMC	Critical micellar concentration
DAAm	n-decyl acrylamide
DAAM	Diacetone acrylamide
DBTDL	Dibutyltin dilaurate
DCC	Dicyclohexylcarbodiimide
1,2-DCE	1,2-dichloroethane
DLS	Dynamic Light Scattering
DMA	Dynamic Mechanical Analysis
DMAA	Dimethylacrylamide
DMAP	(dimethylamino)pyridine
DMAPAA	N-[3-(dimethylamino)propyl]acrylamide
DMF	N,N'-dimethyl formamide
D ₂ O	Deuterium oxide
DSC	Differential Scanning Calorimetry
EA	Elemental Analysis
ECP	Ethyl 2-chloropropionate
FT-IR	Fourier Transform Infrared Spectroscopy

GPC	Gel Permeation Chromatography
HASE	Hydrophobically modified alkali-soluble emulsion polymers
HEAAm	N-hydroxyethyl acrylamide
HED	Copolymers of N-hydroxyethyl acrylamide and n-decyl acrylamide
HEOD	Copolymers of N-hydroxyethyl acrylamide and n-octadecyl acrylamide
HLB	Hydrophilic-Lipophilic Balance
MAPTAC	Methacrylamidopropyltrimethylammonium chloride
Me ₆ TREN	Tris[2-(dimethylamino)ethyl]amine
MPD	2-methyl-2,4-pentanediol
MWCO	Molecular weight cut-off
NaAMB	Sodium 3-(acrylamido)-3-methylbutanoate
NaAMPS	Sodium 2-(acrylamido)-2-methylpropanesulfonate
NAM	N-acyloymorpholine
NMP	n-methylpyrrolidinone
ODAAm	n-octadecyl acrylamide
PAAm	Polyacrylamide
PAA	Polyacrylic acid
PDI	Polydispersity index
PEG	Poly(ethylene glycol)
PEO	Poly(ethylene oxide)
PHEAAm	Poly(N-hydroxyethyl acrylamide) (also PHEAA)
PS	Polystyrene
PVA	Poly(vinyl alcohol)
SBS	Poly(styrene-butadiene-styrene)
SDS	Sodium dodecyl sulfate
SEBS	Polystyrene- <i>block</i> -poly(ethylene-ran-butylene)- <i>block</i> -polystyrene
SIBS	Poly(styrene-isobutylene-styrene)
SSS	Sodium styrene sulfonate
St	Styrene

TGA	Thermal Gravimetric Analysis
THEA	Tris(2-hydroxyethyl)amine
THF	Tetrahydrofuran
TOC	Total Organic Carbon Analyser
V50	2,2'-azobis (2-amidinopropane) dihydrochloride

Symbols

C_{agg}	Critical aggregation concentration
C_o/C_e	Initial and equilibrium liquid-phase polymer concentrations
C^*	Overlap concentration
d	Pipe diameter
$DR(\%)$	Percentage of drag reduction (%)
$H(\text{mol}\%)$	Molar percentage of hydrophobic monomer in copolymer
H	Height
$[I]_o$	Initial concentration of initiator
K_d	The initiator dissociation rate constant
k_p	The propagation rate constant
$k_{t(pp)}$	The termination rate constant
m_{CinPB}	The mass of the carbon in polybutadiene
$m_{C \text{ in EA}}$	The mass of carbon in the copolymer obtained from elemental analysis
$meq.$	Molar equivalent
m_{SEA}	The mass of sulphur obtained from elemental analysis
$m_{Total C}$	The total mass of carbon in polymer
$[M]$	Monomer concentration
M_C	The atomic mass of carbon atom
M_N	The atomic mass of nitrogen atom
M_n	Number average molecular weight (kDa or $\text{g}\cdot\text{mol}^{-1}$)
M_{PB}	The molecular weight of the butadiene repeat unit
M_{PS}	The molecular weight of styrene repeat unit
M_S	The atomic mass of sulfur
M_w	Weight average molecular weight (kDa or $\text{g}\cdot\text{mol}^{-1}$)
N_{agg}	The SDS aggregation number
n_{PB}	The number of moles butadiene in polymer
n_{PS}	The number of moles of styrene in polymer

N_H	The number of hydrophobic monomers per surfactant micelle
Δp_p	Pressure drop in pipe flow in presence of polymer
Δp_s	Pressure drop in pipe flow in solvent
Q_e	Amount of adsorbed polymer on the silica surface
R	Radius
Re	Reynolds Number
R_p	The rate of polymerisation
R_H	Hydrodynamic radius (nm)
W_m	The weight of the monomers
W_p	The weight of the freeze dried polymer
W_{sp}	The weight of purified sulfonated polymer
W_s	The mass of microsilica
W_t	The theoretical weight of polymer at the determined level of sulfonation
y_{PB}	The weight fraction of polybutadiene in poly(styrene- <i>block</i> -butadiene)
X_n	Average degree of polymerisation
Γ	Aspect ratio of the double-gap cell
η_N	Normalized viscosity
δ^*	Gap between the rotor and the stator in double-gap cell
μ	Dynamic viscosity of the fluid
λ	Wave number
ρ	Density of the fluid
v	Mean fluid velocity

Chapter 1

Introduction

Natural gas is a mixture of hydrocarbons, which is composed primarily of methane and other short chain hydrocarbons and common gases. This material is formed over millions of years due to high heat and compacting of organic materials such as plants and dead animals. Additionally it is formed by the transformation of organic matter by microorganisms or by interactions occurring under the Earth's crust between hydrogen rich gases, carbon molecules and minerals. The easily recoverable natural gas can be found under the surface of the earth. The low density of gas allows it to rise over time and either dissipate into the atmosphere or become trapped in porous rock forming a reservoir between impermeable layers of rock. This gas formation is recovered easily using conventional drilling techniques and utilising natural pressure of reservoir.

Over the last decade, economic growth and increase in world's population resulted in increase in demand of natural gas. The conventional resources of this material is finite and according to Skov [1], Holtberg and Conti [2], in the next decade the world would face a serious shortage and production will not be able to keep up with the world's demand. The utilisation of natural gas will also be found to increase since it is a cleaner energy source of low CO₂ emission compared to other materials [3]. The development of alternative gas sources such as shale gas was therefore inevitable. The shale reservoirs are known to contain great amount of natural gas. Shale gas is a natural gas that is stored in rocks rich in organic matter. It is typically interbedded within layers of shaley siltstone and sandstone [4]. The reservoirs of shale gas can be classified as a "continuous gas accumulation expanding through large areas which are of low permeability" [5, 6]. The creation of fractures to provide high gas production is therefore needed. The technology typically utilised to increase the permeability of these reservoirs is hydraulic fracturing, which creates broad artificial fractures around the well bore. This process involves drilling a borehole down the gas bearing formation, placing the piping and cementing it into place (casing). The

next stage of hydraulic fracturing is pumping fracturing fluid, usually water with an additive; at very high pressures down the well to create the vertical fracture. This propagates further in the opposite directions from a borehole. During hydraulic fracturing the pressure has to be high enough to exceed the rock strength such that the pumped fluid creates fractures in the rock [6-8] (Figure 1.1).

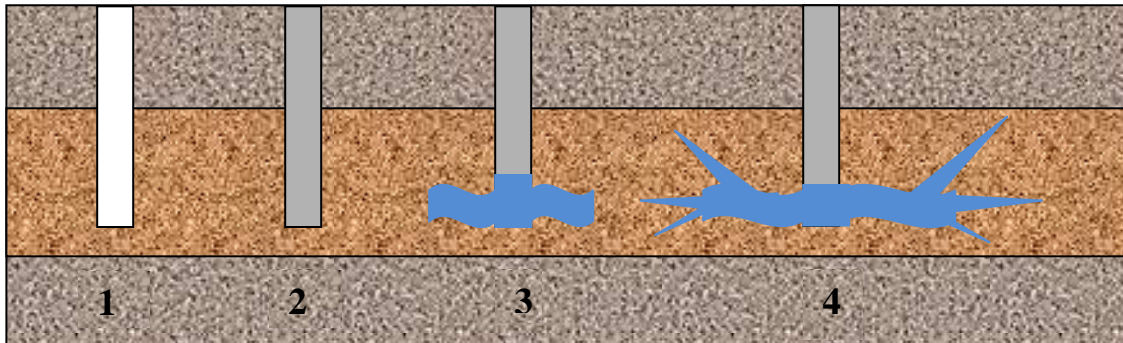


Figure 1.1. Four stages of hydraulic fracturing; 1. Drilling, 2. Casing, 3. Creating a fracture, 4. Propagation of a fracture.

Transportation of liquids using pipeline technology has its limitations, since turbulent flow inside the pipe involves a loss of energy. The net effect of this is that increasing the energy applied to the flow does not increase the flow rate. To overcome this flaw in turbulent flow, the drag reduction phenomenon was utilised in 1948 by Toms [9]. He discovered that upon addition of a small amount of polymer, a significant reduction in drag caused by turbulent flow occurred. Toms observed that poly(methyl methacrylate) dissolved in monochlororobenzene reduced the pressure drop required to pump fluid through the pipe at a constant flow rate below that of a pure solvent.

In the past 50 years, there has been extensive research activity in this field of fluid mechanics. Typically high molecular weight water soluble polymers such as polyacrylamide, polyethylene oxide or guar gum [10-16] are often investigated as potential water soluble drag reducers. It is known that the performance of the aforementioned polymers is highly dependent on molecular weight since increasing the molecular weight improves drag reduction. Unfortunately the drag reduction effectiveness can be reduced by mechanical degradation of the polymer solution.

Moreover the degradation of the drag reducing polymer is proportional to its molecular weight. A compromise between high molecular weight and shear stability is therefore required. Associating polymers have been shown to be of a great importance in drag reduction experiments since association creates high molecular weight macromolecules. Furthermore the shear degradation effect could be reduced for associating systems, since the breakage of secondary bonds would occur preferentially to the cleavage of the polymer backbone [10, 17-21]. However, the utilisation of polymers as drag reducing agents presents the serious problem of adsorption in reservoirs causing a decrease in the flow of natural gas into the well [22-25]. The adsorption of polymer is especially undesirable in shale gas reservoirs where permeability is extremely low. Moreover it has been shown that there is potentially higher risk of polymer adsorption when associating polymers are used comparing to non-associating homologues. The stronger adsorption of an associating polymer comparing to a non-associating polymer has been demonstrated by Argiller *et al.* [22], Lu and Huang [25] and is caused by the restoration of associations after the pressure is released (*Figure 1.2*).

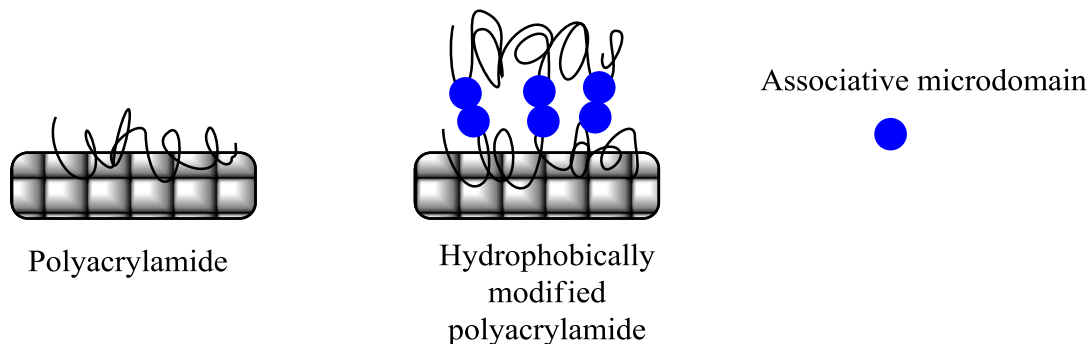


Figure 1.2. Schematic of the conformation of adsorbed layers formed by associating polyacrylamide at solid/liquid interface [25].

The application of associating polymers therefore requires more expensive clean up procedures and for the utilization in shale reservoirs, the availability of polymers able to dissociate under a specific trigger would be beneficial. A potential solution in achieving this would be to use stimuli sensitive associating polymers which can be switched between states: associated and dissociated. Whilst in associated state polymer would raise the viscosity of fluid and promote drag reduction. After hydraulic fracturing, the associations would be switched off allowing the

natural gas to flow freely towards the well. The associations would then be restored when the polymer flows back to the surface and the polymer could be then reused. This might be achieved by potentially injecting chemicals causing the dissociation of polymer, leading to a reduced viscosity and a lower adsorption of polymer in the shale reservoirs.

1.1. Project Aims

The main objective of this research was to synthesise water soluble polymers that would display improved drag reducing properties and resistance to shear degradation. Since it was demonstrated that associating polymers exhibit these properties, this class of polymers was primarily chosen for investigation [17, 20, 26]. In particular, hydrophobically modified water soluble polymers were selected due to the ability of these polymers to form micellar-like structures in water. Hydrophobically modified polyacrylamides have been reported to demonstrate effective drag reduction; however there are a number of unanswered questions with regards to this class of polymers that still remain [19, 26, 27]. Questions such as; the effect of alkyl chain length in the hydrophobic monomer, the concentration of the hydrophobic moieties in the copolymer, or the shear stability of hydrophobically modified polyacrylamide. These issues were tackled in this research work.

The investigation of the other associating water soluble polymers that could display drag reducing properties was also approached in this thesis. In particular, copolymers and homopolymers based on the water soluble poly(N-hydroxyethyl acrylamide) (a derivative of polyacrylamide) and partially sulfonated copolymers of styrene and butadiene (hydrophobic drag reducing polymers), were chosen to study the relationship between molecular characteristics and the drag reduction performance.

The final objective of this research was to identify suitable additives capable of dissociating (or breaking) the hydrophobic associations between polymers or within a polymer chain. Deactivation of hydrophobic interactions would result in reduced viscosity, quick partitioning of polymer into the water phase and reduced adsorption of polymer onto formation surfaces. The approach taken to solve this problem was to modify polyacrylamide, which is a well-known and inexpensive synthetic polymer used in subterranean applications. By modifying polyacrylamide

and exposing it to hydrophobic bond breakers, the likelihood of obtaining useful information on adsorption and desorption of these polymers was higher than in case of completely new polymer systems. Low molecular weight Cyclodextrins were chosen as potential materials capable of dissociating hydrophobic interactions. Hydrophobic core of water soluble Cyclodextrins can bind the hydrophobic moieties resulting in deactivation of the hydrophobic interactions.

1.2. Thesis structure

This thesis presents work on the synthesis of polymers with drag reducing properties for subterranean applications. **Chapter 2** reviews the relevant background literature. In **Chapter 3** the materials and experimental methods are described. **Chapter 4, Chapter 5, Chapter 6** and **Chapter 7** contain obtained results and the discussion of these results. Each of these chapters deals with different types of polymers: hydrophobically modified polyacrylamides (**Chapter 4**), homopolymer and copolymers of N-hydroxyethyl acrylamide (**Chapter 6**) and sulfonated block copolymers of styrene and butadiene (**Chapter 7**). Additionally the interaction of polymers with Cyclodextrins and their influence on adsorption of polymer on the silica surface is presented in **Chapter 5**. Finally, **Chapter 8** draws conclusions from the work and formulates suggestions for future work.

Chapter 2

Background

This chapter is divided into two main parts in which the relevant literature concerning the objectives of this research is introduced. The first section covers the concept of drag reduction and drag reducing agents used in subterranean applications. The desired properties of drag reducing agents and the importance of associations in drag reducing performance are also presented. Second section reviews the materials that can be used to deactivate hydrophobic associations and methods of synthesising water soluble associating polymers.

2.1. Drag reduction

Drag is caused by the resistance encountered by a flowing fluid in turbulent flow coming into contact with a solid substrate e.g. pipe wall. Addition of a drag reducing agent interferes with the formation of turbulent vortices thereby reducing drag. There are two types of flow regimes; laminar and turbulent and each of the flow type can be characterised by the linear dependence of the flow rate on the driving pressure (*Figure 2.1*). In laminar flow (*Figure 2.1a*) the motion of the particles of fluid occurs in ordered fashion and all of the particles are moving in straight lines parallel to the pipe walls. Increasing the pressure difference creates a proportional increase in flow rate; however at a certain point the pressure difference increases more rapidly than the flow rate and is known as turbulence onset.

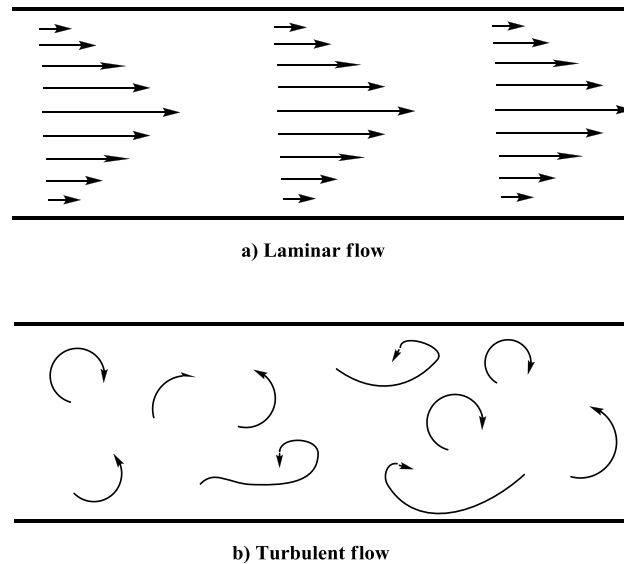


Figure 2.1. Schematic illustration of laminar (a) and turbulent (b) flow (image reproduced from www.ceb.cam.ac.uk).

The turbulent flow can be defined by intense mixing which leads to transfer of momentum between liquid layers in a spanwise direction (formation of vortices, *Figure 2.1b*) [28]. The flow pattern is dependent on a Reynolds number defined by Equation 1 and the turbulent flow starts to predominate at a Reynolds number above 2300 [29].

$$Re = \frac{\rho v d}{\mu} \quad (1)$$

Where v is the mean fluid velocity, d the pipe diameter, ρ the density of the fluid and μ the dynamic viscosity of the fluid.

Drag reduction works by reducing the intensity of the vortex in turbulent flow. The required pressure difference needed to obtain the desired flow rate in a pipe is lower for a liquid containing a small amount of drag reducing agent compared to pure liquid. This is illustrated by Equation 2:

$$DR(\%) = \frac{\Delta p_S - \Delta p_P}{\Delta p_S} \cdot 100 \quad (2)$$

Where DR (%) is the drag reduction percentage, Δp_s is the pressure drop for the solvent in a given length of pipe and Δp_p is the pressure drop after addition of a drag reducing agent with the same flow rate as of the pure fluid [16].

There are three main classes of drag reducing additives: polymers [16, 30-34], surfactants [35-38], suspensions of particles and fibres [39, 40] or microbubbles [41]. However, surface modification of solid substrate which the fluid interacts with is also known [42, 43]. The polymers in organic and aqueous media are the most researched materials in the field of drag reduction. Surfactants are less well researched but offer an attractive alternative due to the higher levels of drag reduction in comparison to polymers. In addition, surfactants demonstrate high shear stability due to the existence of micellar structures.

Drag reducing additives provide a major reduction in energy requirements; therefore their use is economically attractive for a variety of commercial applications. The best known application of drag reducing polymers is in oilfield industry and the first successful application of drag reduction phenomenon took place in 1979 and marked the beginning of transportation of crude oil through the Trans Alaskan Pipelines [44]. The other uses of the drag reducers include hydraulic fracturing and drilling fluids [45], sewers [46], fire-fighting [47], drainage and irrigation systems [48] as well as marine industry for the use as ship coating [49]. Drag reducing agents have been also trialled in biomedicine to potentially treat or prevent circulatory diseases [50]. It should be noted that drag reduction is a well known phenomenon in nature. Aquatic animals such as dolphins and eels produce slime containing drag reducing polysaccharides. This gives them the ability to quickly accelerate when hunting or fleeing [51].

2.2. Polymeric drag reducing agents

Since the discovery of the drag reduction phenomenon by Toms in 1948, a great amount of research have has been undertaken on the subject of drag reduction. There are a number of

important publications and include Lumley who presented a review on the drag reduction literature [34]. In his review, Lumley looked at publications regarding the aspects of drag reducing additives such as the effect of molecular structure, flexibility, length of polymeric molecules and the effect of the expansion of the random coil in various solvents on drag reducing properties. Lumley also investigated elasticity, viscosity and concentration, the physical appearance of solutions, the experimental methods of measurements of turbulence and the theoretical aspects of drag reduction. Also a few years later Virk presented his experimental data for turbulent pipe flow and explained the proposed mechanisms [52]. In this article, Virk introduced the term of “maximum drag reduction asymptote” for a given system. It also stated that the maximum drag reduction was dependent on the physical properties of the flow rather than on the polymer structure. In 1978, Berman investigated the influence of polymer physics and molecular parameters on the drag reduction effectiveness by polymers [30]. Nadolink and Haigh provided a list of references on the research regarding drag reduction spanning over 70 years and contained over 4900 references [53]. In 2006 Bismarck *et al.* published book chapters in Heat Exchanger Design Updates reviewing various aspects of drag reduction and discussed more closely drag reduction of polymers, surfactants and drag reduction in multiphase flow [16, 29, 37, 54]. More recent review by Benzi summarised models and suggested mechanisms of drag reduction, providing mathematical explanation for the observed features [55]. In the same year Brostow summarised the most important features found to date in regards to drag reduction such as influence of solvent type or polymer structure on the drag reducing performance and the mechanical degradation in relation to mechanism of drag reduction [56].

Drag reduction by polymers can be accomplished in water as well as in organic solvents and the list of polymers known to reduce drag is presented in *Table 2.1*.

Water soluble polymers	Hydrocarbon soluble polymers
Poly(ethylene oxide) [15, 52, 57-61]	
Polyacrylamide [15, 52, 57, 58]	Polyisobutylene [52, 69-71]
Hydrolysed polyacrylamide [12, 57, 62]	Poly α -olefin [72]
Poly(N-vinyl formamide) [63]	Polystyrene [73-75]
Guar gum [52, 64]	Poly(methyl methacrylate) [9, 52]
Xanthan gum [11, 64-66]	Polydimethylsiloxane [52, 76]
Carboxymethyl cellulose [64]	Poly(cis-isoprene) [52, 76]
Hydroxyethyl cellulose [52]	Polybutadiene [76]
DNA [31, 57, 67]	
Scleroglucan [68]	

Table 2.1. List of water and organic solvents soluble polymers known to reduce drag.

The parameters that decide the effectiveness of a specific polymer towards drag reduction are chemical structure, chain flexibility, solvent quality and a molecular weight above $5 \cdot 10^5 \text{ g} \cdot \text{mol}^{-1}$; however polymers of lower molecular weight capable of forming higher molecular weight aggregates have also been found to be effective drag reducers [10, 34, 77]. The relationship between polymer structure and drag reduction efficiency was extensively studied by McCormick's group [10, 19, 78-80]. They determined that generally linear polymers provide good drag reduction although graft and slightly branched polymers are also good drag reducing agents. The creation of branches and grafts onto some linear polymers can also offer enhanced shear stability. Kim *et al.* [81] studied linear and branched polyacrylamide and showed that both polymers have comparable drag reduction ability. Addition of a few branches onto the polyacrylamide backbone resulted in increased shear stability, since the shear forces that the polymer experienced were distributed among the individual chains. Lim *et al* [82] demonstrated that grafting polyacrylamide onto amylopectin can significantly increase the drag reduction of amylopectin even at very low concentrations. Moreover the polymer was found to be extremely resistant to shear degradation in comparison to unmodified homologues.

The molecular weight is an important factor deciding polymer's effectiveness to reduce drag, however it is believed that it is the coil volume rather than the molecular weight itself that

determines the effectiveness of drag reduction [19]. Zakin *et al.* [76] demonstrated that the high molecular weight fraction in a polydisperse polymer sample is responsible for high levels of drag reduction and suggested that there is a minimum molecular weight that is required to reduce drag. By studying polymer samples in various solvents they showed that for a constant polymer molecular weight and concentration, greater drag reduction was seen in solvents where intrinsic viscosity was greater. Virk also showed that the benefit from using high molecular weight polymer is that the onset of drag reduction is shifted towards lower Reynolds numbers indicating higher drag reduction efficiencies [52].

The efficiency of polymer in drag reduction depends largely on a solvent quality. Good solvents promoting coil expansion provide higher drag reduction. Poor solvents favour polymer-polymer interactions over polymer-solvent interactions and result in contracted coil. This in turn causes a decrease in drag reduction. Zadrazil [83] showed that upon addition of iso-propanol (a non-solvent for polyacrylamide) to an aqueous solution of polyacrylamide, the contraction of the random coil was observed and the efficiency of the drag reduction decreased. Conversely, the addition of formamide (a very good solvent for polyacrylamide) caused expansion of the random coil and improved the drag reduction. Zadrazil also found that the shear stability of polyacrylamide in poor solvent was higher than in good solvent, which was particularly evident at low concentration.

Drag reduction of polyelectrolytes such as polyacrylic acid can be modified by variations in pH and the addition of salt. It is well known that at certain conditions, drag reduction is high if the polyelectrolyte's coil is highly expanded due to charge-charge repulsion [84].

The most efficient drag reducing agents are polymers with flexible chains. Rigid polymers however offer more resistance to mechanical degradation. It has been stated that the comparative effectiveness is nevertheless dependent on other factors such as polymer concentration, flow rate and testing geometry, therefore in some cases rigid polymers can exceed the performance of flexible polymers [30].

2.3. Water soluble polymeric drag reducing agents

Water soluble drag reducing polymers can be divided into two classes: 1) biopolymers and 2) synthetic polymers. Biopolymers are reasonable drag reducing agents and the most commercialised biopolymers include guar gum [11, 62, 64], carboxymethyl [14] and hydroxyethyl cellulose [85] and xanthan gum [14, 64] (Figure 2.2). The natural polymers are usually obtained from plants (guar gum and cellulose derivatives) or produced by bacterium (xanthan gum) and all have semi-rigid backbones. They have higher shear stability than synthetic polymers; however they are less efficient drag reducing agents. The concentrations needed to obtain drag reduction compared to synthetic polymers are few hundred ppm in contrast to a few ppm for synthetic polymers.

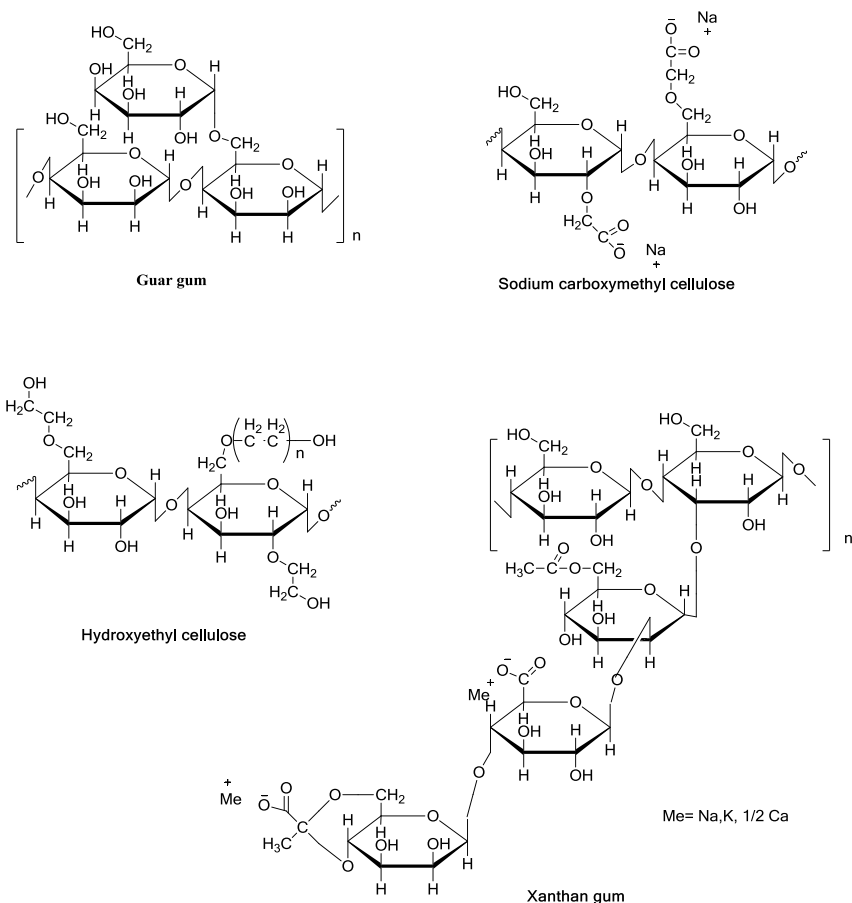


Figure 2.2. Structure of water soluble drag reducing biopolymers [10].

The structures of the most commonly used synthetic drag reducing polymers are shown in *Figure 2.3*. Among synthetic polymers, poly(ethylene oxide) is the most efficient known drag reducing agent. For instance, one of the earlier publications by Little [86] reported a drag reduction of 40 % at a concentration of just 25 ppm for poly(ethylene oxide) with a molecular weight of $5 \cdot 10^5 \text{ g}\cdot\text{mol}^{-1}$. Poly(ethylene oxide) is a linear, flexible molecule and its drag reduction efficiency has been tested in a range of parameters, such as temperature, concentration, molecular weight by various researchers such as Peyser and Little [87], Parker and Hedley [88], Choi and Jhon [33], Shetty and Solomon [21], Pereira and Soares [61] and Zadrazil *et al.* [60]. It was however revealed that its utility in multiple pass applications is limited due to extreme sensitivity to shear degradation [89].

Polyacrylamide is another linear, flexible and efficient polymeric drag reducing agent. It has been shown that it has higher shear stability than poly(ethylene oxide) [13] nevertheless it also degrades under high shear flow [83, 89]. Olivier and Bakhtiyarov [90] have demonstrated that at high molecular weight ($20\text{-}25 \cdot 10^6 \text{ g}\cdot\text{mol}^{-1}$), drag reduction of polyacrylamide can occur at concentration as low as 0.02 ppm.

Related to polyacrylamide, polyacrylic acid can be formed by the hydrolysis of polyacrylamide or by the polymerisation of acrylic acid. Depending on the pH, polyacrylic acid can either exist in an uncharged form or as a polyelectrolyte. Banijamali *et al.* [84], Zhang *et al.* [91] and Kim *et al.* [92] reported the drag reduction efficiencies of polyacrylic acid. In addition Banijamali *et al.* and Kim *et al.* studied the drag reduction of polyacrylic acid at different pH. An increase in drag reduction was demonstrated between a pH of 4.1 and 10 and the onset of drag reduction in the laminar region was observed.

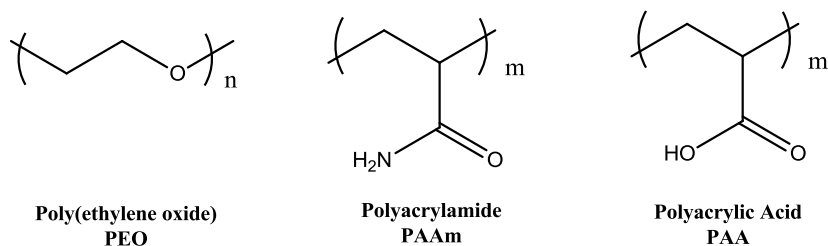


Figure 2.3. Structure of water soluble drag reducing synthetic polymers.

2.4. Degradation of polymeric drag reducing agents

Although high molecular weight drag reducing polymers provide many advantages, they can undergo mechanical degradation in turbulent flow and lose their effectiveness after a short interval of time. The theory of polymer degradation in a pipe flow was linked to the mechanism of drag reduction in which the coiled polymer is stretched and rotated, due to interactions with the vortices in a turbulent flow [93]. At a certain point, the strain that the polymer molecule is experiencing becomes too much and the polymer chain breaks.

The mechanical degradation of the polymer generally depends on the chemical structure, polymer concentration, molecular weight and distribution of molecular weight, interactions of polymer with solvent and the temperature as well as the diameter and geometry of the pipe. The mechanical degradation of polymers in turbulent flow has been extensively investigated and reviewed by many researchers for example Moussa *et al.* [94, 95], Den Toonder *et al.* [96], Brostow *et al.* [97, 98], Choi *et al.* [99, 100], Rho *et al.* [101] and Kim *et al.* [11]. It is well-known that the extent of the drag reduction increases with molecular weight and length of polymers, however their susceptibility to mechanical degradation also increases.

The findings on the flow induced degradation has been reviewed by Bueche [93]. He determined that correlations between certain parameters and degradation existed. Higher molecular weights and longer polymer chain lengths expedite flow induced degradation and rate of mechanical degradation. Bueche also found that the degradation depends on the compatibility of polymer to solvent with degradation being more pronounced in poor solvent with a low Reynolds number. The opposite occurs in solvents with a high Reynolds number. Furthermore, at a constant wall shear stress and pipe diameter, the degradation becomes proportional to the molecular weight but inversely proportional to polymer concentration, and at a constant wall shear stress and polymer concentration, the degradation becomes inversely proportional to the pipe diameter. Bueche also established that at a constant polymer concentration and pipe diameter, the degradation increased with wall shear stress and shear stability increasingly became a function of polymer solubility in a given solvent.

Different solutions to enhance drag reduction and shear stability have been tried, including grafting of polymers onto polysaccharides, which combine the efficiency of synthetic polymers

with the shear stability of natural polymers [64, 102, 103]. The reversible intermolecular associations in solutions have also been known to increase the molecular weight of polymer associates and provide mechanical stability [18, 20]. Additionally, cross-linking between polymer molecules such as guar gum provided an increase in the dimensions of the macromolecules resulting in enhanced drag reduction but degradation of polymer still occurred [104].

2.5. Association of polymers and drag reduction

The importance of molecular associations in drag reduction has been recognised for a long time. Since the early 70's, researchers have hypothesised that since high molecular weight polymers are the most successful drag reducing agents, higher molecular weight aggregates should provide even greater effect. Moreover, the effect of shear degradation might be lower for associating systems since the breakage of intermolecular associations could be favoured instead of mechanical degradation of the polymer backbone. The intermolecular interactions in the associating polymers can therefore reform upon lowering of the shear rate. The role of molecular aggregates in the drag reduction of water soluble polymers such as polyethylene oxide and polyacrylamide has been studied by Dunlop and Cox [105] and Shetty and Solomon [21]. They revealed that the formation of aggregates could be induced by shearing action at high concentrations and suggested that aggregates are almost always present in a solution of drag reducing agent. They also suggested that macromolecular aggregation could be used to explain the mechanism of drag reduction. Zadrazil studied the solvent mediated formation of aggregates in aqueous solution of polyacrylamide [83]. He suggested on a basis of the light scattering data that aggregates are formed upon variations in solvent quality. The pronounced shear stability of polyacrylamide dissolved in poor solvent and increase in observed drag reduction after a few minutes of shearing was suggested to be due to the presence of aggregates. These aggregates are elongated and unravel, whilst continuously releasing more individual polymer molecules into the flow.

Intermolecular complexes between water soluble copolymers have been found to improve drag reducing effect. Lundberg *et al.* [106] studied the drag reduction efficiency of a mixture of a

cationically charged poly(acrylamide-co-methacrylamidopropyltrimethylammonium chloride) (PAAm-co-MAPTAC) containing 3.7 mol% of MAPTAC and an anionically charged poly(acrylamide-co-sodium styrene sulfonate) (PAAm-co-SSS) containing 32.9 mol% of SSS. They have shown that the drag reduction of the mixture of aqueous solution of these copolymers (concentration of copolymer PAAm-co-MAPTAC equal to 375 ppm and concentration of copolymer PAAm-co-SSS equal to 125 ppm) increased 2-6 times as compared to the individual drag reduction of the aqueous solution of each copolymer.

The interpolymer complexes were also studied by Kowalik *et al.* [20] and Malik *et al.* [17, 18]. Kowalik *et al.* studied a series of hydrocarbon soluble polymers, which contained polar associating groups that could form concentration dependent intra- and intermolecular associations. They revealed that the intrapolymer associations decreased drag reduction performance whereas intermolecular resulted in its increase. Malik *et al.* studied the interactions of ionic groups and hydrogen bonded mediated interpolymer complexes. From the obtained results, the researchers revealed that the drag reduction effectiveness for associated complexes was increased 2-6 times comparing to non-associated species. The shear stability was also found to be improved. Sabadini *et al.* studied the influence of the supramolecular assembly of bis-urea-based monomers on drag reduction [107]. They revealed that two competitive polymeric structures were formed, tubes and filaments. Sabadini *et al.* demonstrated that only tubular like formation is capable of drag reduction due to its greater length. The solvent used was found to be the deciding factor as to which structure will prevail.

Bock *et al.* studied the drag reduction effectiveness of hydrophobically modified polyacrylamide with low concentrations of n-octyl- and n-dodecyl acrylamide [27]. They demonstrated that polymers exhibited drag reduction performance in deionised water, however no details on the role of association in drag reduction was revealed. Year later, McCormick *et al.* [19] studied the relationship between the drag reduction performance of water soluble polymers and various parameters including chemical structure, molecular weight, hydrodynamic volume, solvent nature and associations. In their research they examined commercial poly(ethylene oxide) and copolymers of acrylamide with sodium 3-(acrylamido)-3-methylbutanoate (NaAMB), sodium 2-(acrylamido)-2-methylpropanesulfonate (NaAMPS), [2-(acrylamido)-2-methylpropyl]

dimethylammonium chloride (AMPDAC), and diacetone acrylamide (DAAM). McCormick *et al.* indicated that the intermolecular hydrophobic association in copolymers of acrylamide and diacetone acrylamide was responsible for enhanced drag reduction. Intramolecular ionic associations in polyampholites were also demonstrated and a decrease of drag reduction was shown to occur due to collapsed polymer chains. In 2009 Camail *et al.* studied the rheological properties of copolymers of N-alkyl and N-arylalkyl acrylamides with acrylamide [26]. They demonstrated that the degree of association and radius of gyration was dependent on the type and the concentration of the incorporated hydrophobic group. The drag reduction efficiency of a copolymer of acrylamide and decylphenyl acrylamide at a level of 0.5 mol% was studied and demonstrated to be higher when compared to poly(ethylene oxide). Moreover, Camail *et al.* provided experimental evidence of the exceptional persistent drag reduction for the copolymer of acrylamide and n-decylphenyl acrylamide. The researchers suggested that the observed performance was attributed to strong intramolecular associations. As yet the amount of research into drag reduction in associating water soluble systems remains low and thus requires further investigation.

2.6. Intra- and intermolecular association breakers

Non-covalent interactions that direct intra- and intermolecular associations are weak and can be broken by physical (temperature) and chemical parameters (additives, pH and ionic strength). McCormick *et al.* suggested that the performance of polymers in the drag reduction is influenced by the structure of water therefore additives promoting changes in the structure of water (affecting hydrogen bond in water) decrease polymers drag reduction efficiency [19]. The hydrophobic bond is only seen in water and is independent of the pH or presence of salts, unless the structure of water is modified by surface charges or small ions in solution. That means in the presence of salts, hydrophobic interaction can be enhanced [108].

Mumick, Hester and McCormick demonstrated that urea diminished hydrogen bonding between polymer and the aqueous media, which resulted in lower binding of solvent to polymer [79]. This in turn resulted in decreased drag reduction in poly(acrylamide-co-N-isopropylacrylamide) containing varying concentrations of N-isopropylacrylamide. The authors also found that the

drag reduction of polyacrylamide was unaffected by urea. Camail *et al.* demonstrated that urea can dissociate the hydrophobic interaction in the hydrophobically modified polyacrylamide [109]. The authors showed that the viscosity of the polymer solution decreased with increasing urea concentration. However, urea was only capable of partially disrupting intermolecular associations.

Cyclodextrins (CDs) are cyclic oligosaccharides with cylindrical shape that have hydrophobic internal cavity and hydrophilic exterior (*Figure 2.4*).

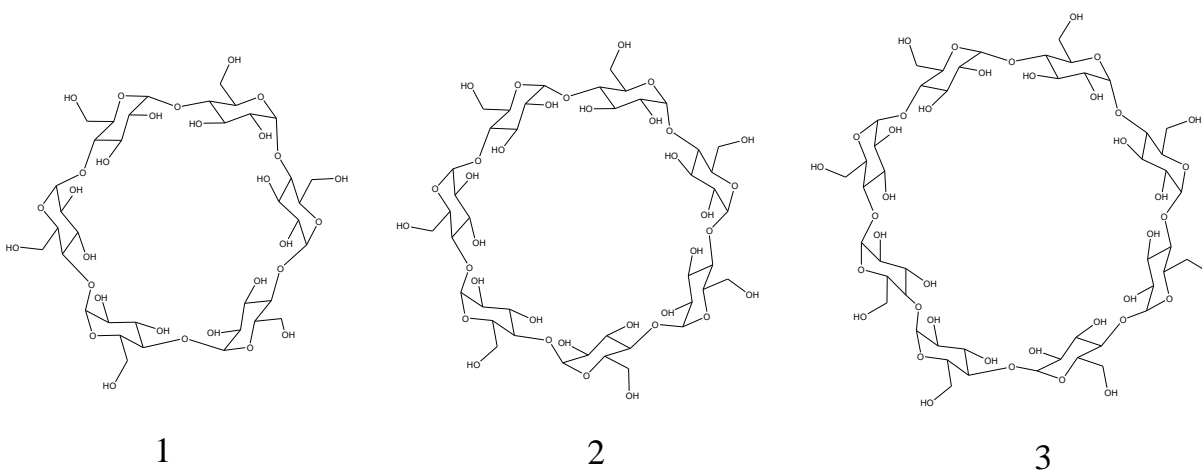


Figure 2.4. Chemical structures of α - (1), β - (2) and γ - (3) Cyclodextrin.

Cyclodextrins are molecules that form complexes with guest molecules by utilisation of hydrophobic interaction [110]. In 2002, Karlson investigated the inhibition of hydrophobic interactions in hydrophobically modified ethyl hydroxyethyl cellulose with nonyl phenyl or tetradecyl groups and hydrophobically modified poly(ethylene glycol) (PEG) by Cyclodextrins [111]. He showed that methyl- α -Cyclodextrin, methyl- β -Cyclodextrin and β -Cyclodextrin are all capable of decoupling the polymeric network as evidenced by a decrease in solution viscosity. Furthermore, Karlson demonstrated that methylated Cyclodextrins had more pronounced effect on polymers containing hydrophobic monomers with long hydrophobic chains.

Ogoshi *et al.* demonstrated the effect of α -Cyclodextrin on the complexes of hydrophobically modified polyacrylic acid and pyrene modified β -Cyclodextrin/Single-Walled Carbon Nanotubes (SWNTs) hybrids [112]. Mixing of polyacrylic acid containing 2 mol% of dodecyl groups and SWNTs hybrids resulted in hydrogel formation, which converted into solution upon addition of

100 mol equivalents of α -Cyclodextrin in respect to dodecyl groups in hydrophobically modified polyacrylic acid. This was attributed to stronger competitive interaction of dodecyl groups with α -Cyclodextrin than with β -Cyclodextrin. Mahammad, Roberts and Khan investigated the complexation of α - and β -Cyclodextrin with water soluble hydrophobically modified alkali-soluble emulsion polymers (HASE) [113]. They concluded that the addition of 30 moles of Cyclodextrins per mole of hydrophobic macromonomer resulted in the dissociation of hydrophobes from the polymer network, as evidenced by a decrease in dynamic moduli. The decrease in a value of dynamic moduli was found to be more pronounced for α -Cyclodextrin than β -Cyclodextrin. Similar findings were reported by Talwar *et al.* who reported the decrease in viscosity and dynamic moduli of HASE polymers upon addition of Cyclodextrins [114]. Moreover they also showed that the original viscosity could be recovered upon addition of a non-ionic surfactant.

More recently, Hashidzume and Harada presented an extensive review on the studies of polymer interactions with Cyclodextrins with particular attention to the application in biological systems [115]. In their review they summarized the steric effects in polymers such as polyacrylamide bearing hydrophobic side chains, on their ability to associate with α -, β - and γ -Cyclodextrin. Authors described NMR studies in which they studied complexation of polymers with Cyclodextrins. They concluded from their research that α -Cyclodextrin interacted strongest with linear alkyl chains and β -Cyclodextrin with branched chains, whereas γ -Cyclodextrin interacted weakly with both linear and branched alkyl chains.

2.7. Synthesis of hydrophobically modified water soluble polymers

Associative polymers contain segments that can interact via physical interactions. These segments can be distributed randomly along the chain or be present as blocks in the copolymer. Synthesis of water soluble drag reducing agents containing hydrophobic moieties can be acquired via different synthetic routes. One approach is the direct copolymerisation of hydrophilic and hydrophobic monomers; a second approach is to graft hydrophobic groups onto water soluble polymers via post functionalisation of homopolymers and a third route is via functionalisation of hydrophobic polymers to aid water solubility.

2.7.1. Polyacrylamide (PAAm)

Hydrophobically modified polyacrylamide can be obtained by micellar, micro- or macroemulsion and solution polymerisation. Copolymers with hydrophobic units randomly distributed as small blocks in the polyacrylamide backbone can be synthesised via micellar polymerisation. Copolymers synthesised via this type of polymerisation has been shown to display strong associative properties due to the incorporation of the hydrophobic monomers into the copolymer structure as random blocks. The pioneering work in the field of micellar polymerisation was led by Turner *et al.* in 1985 [116, 117]. They discovered that the copolymerisation of water soluble monomers with hydrophobic monomers could be achieved by the addition of a water soluble surfactant. Homogeneity of the system was accomplished since the hydrophobic monomers were solubilised in the interior of the surfactant micelles. The ratio of surfactant over the hydrophobic monomer was high and by varying the number of hydrophobic molecules per surfactant micelle, the copolymer microstructure was varied (*Figure 2.5*).

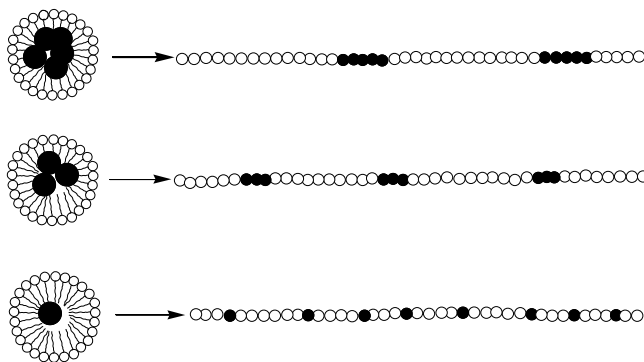


Figure 2.5. Schematic representation of the influence of the number of hydrophobic monomers per micelle on the copolymer microstructure [152].

Turner *et al.* have demonstrated that the block copolymers with randomly distributed blocks of hydrophobic monomer can be obtained when the ratio of hydrophobic monomer to surfactant is high and the higher is this ratio the greater is the length of the hydrophobic block. Since this revolutionary discovery, great amount of work has been performed in this field and many hydrophobic monomers have been tried including pyrenesulfonamide functionalities [118], N-vinylnaphtalene [119], poly(propylene oxide) [120], N-arylalkylacrylamides [26, 109, 121-124],

N-alkylacrylamides [26, 109, 123-127], N,N'-dialkylacrylamides [123, 127-130] and polymerisable surfactants e.g. 2-acrylamido-tetradecane sulfonate [131].

Candau and Selb [132] demonstrated in their review that the association of copolymers prepared in micellar polymerisation depends on various parameters, which include the nature and structure of the hydrophobic monomer. They showed that copolymers containing N,N'-dialkylacrylamide show much stronger interactions than copolymers containing N-alkylacrylamide. They also demonstrated that the longer the alkyl chains in the N-alkyl or N,N'-dialkylacrylamide, the stronger the association. Additionally, higher concentrations of hydrophobic monomers in the copolymer and higher hydrophobic block length favoured stronger association. More recently Camail, Margaillan and Martin showed that the incorporation of N-alkylarylacrylamide offered stronger association than the incorporation of N-alkylacrylamide and offered greater improvement in shear resistance [26, 109].

Although micellar polymerisation was mainly studied, for the polymerisation of acrylamide it is believed that any water soluble monomer that can undergo free radical initiation could be synthesised via this process.

Hydrophobically modified polyacrylamide can be also obtained by polymerisation in organic solvent. However, Hill *et al.* [122] demonstrated that the copolymers formed in such process produce weaker associations since the polymerisation results in singly and randomly distributed hydrophobic monomer(s) along the polymer backbone. Moreover, they revealed that numerous chain transfer reactions result in polymers with a low molecular weight, if the solvent is not selected carefully.

Emulsion polymerisation is another method to synthesise amphiphilic copolymers. Ivanova *et al.* [133] reported the synthesis of a high molecular weight copolymer of acrylamide and lauryl methacrylate using microemulsion polymerisation in which the oil phase was composed of 2,2'-azobis(isobutyronitrile) (AIBN) and SPAN 60 dissolved in cyclohexane. They demonstrated that the obtained copolymer showed strong associative behaviour and this behaviour was dependent on the concentration of lauryl methacrylate.

Kobitskaya reported the synthesis of polyacrylamide with lauryl methacrylate and styrene via inverse miniemulsion in which the oil phase comprised of hydrophobic monomer, AIBN and

SPAN 60 [134]. A miniemulsion process was studied in which a Ce^{4+} /SPAN 60 redox initiator pair was used instead of AIBN. Kobitskaya showed that polymers prepared by microemulsion and micellar polymerisation had similar thickening properties suggesting that hydrophobic monomers were distributed as blocks.

Hydrophobically modified polyacrylamide can be also prepared by chemical post-modification of polyacrylamide. Wu and Shanks [135] demonstrated the grafting of alkyl chains by direct N-alkylation via the transamidation with alkylamines (*Figure 2.6*). Substitution reactions with highly hydrophobic groups such as dodecyl chain were proved to be impossible due to the insolubility of these amines in water. Moreover, no substitution was seen in other polar solvents and this was attributed to the contraction of the polyacrylamide chain in poor solvent.

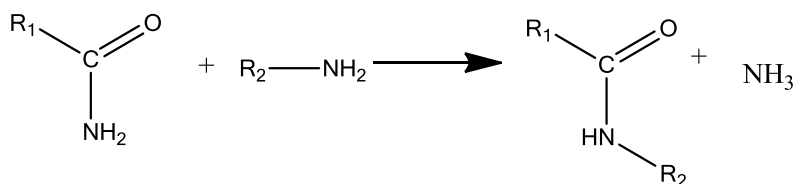


Figure 2.6. Schematic of modification of materials by transamidation.

2.7.2. Polyacrylic acid (PAA)

Hydrophobically modified polyelectrolytes such as polyacrylic acid can be prepared by free-radical copolymerisation of acrylic acid and a hydrophobic comonomer in organic solvents [136-138]. Zhou *et al.* described the synthesis in *tert*-butanol and solution properties of a copolymer of acrylic acid and 2-(N-ethylperfluorooctanesulfoamido)ethylacrylate or 2-(N-ethylperfluorooctanesulfoamido) ethylmethacrylate [138]. They demonstrated that the aqueous solutions of the synthesised copolymers exhibited associating behaviour that was dependent on salt addition, pH and temperature. The addition of salt favoured the hydrophobic interaction and at pH above 5.5 the polymer chain stiffened. This caused the intermolecular interactions to largely diminish.

Philippova *et al.* prepared hydrophobically modified pH responsive polymers of polyacrylic acid and hydrogels crosslinked with N,N-methylenebisacrylamide containing up to 20 % of n-alkyl acrylates in N,N-dimethylformamide using 2,2'-azobis(isobutyronitrile) (AIBN) as a radical initiator [137]. The random distribution of hydrophobic groups was observed by ^{13}C NMR and the negative effect on ionisation was observed at high amounts of hydrophobic monomer as evidenced by potentiometric titration. The swelling of hydrogels was found to be affected by the concentration of hydrophobic moieties and length of n-alkyl side chain in the hydrophobic monomer. The increase in the concentration of hydrophobic moieties and alkyl chain length in hydrophobic monomer resulted in polymer swelling in alkaline medium, due to stabilisation of the collapsed state of the gel by hydrophobic interactions.

Zhuang *et al.* prepared a series of copolymers of acrylic acid by free radical solution copolymerisation with n-alkyl acrylates in benzene and cyclohexane with AIBN as free radical initiator [139]. The influence of hydrophobic chain on intramolecular association of hydrophobically modified polyacrylic acid was demonstrated to be retarded at low ionic strength due to electrostatic repulsion. At high ionic strength however, a dramatic increase in viscosity was reported, which was dependent on the length of the alkyl chain in hydrophobic monomer.

Hydrophobically modified polyacrylic acid can be also devised by post-modification of polyacrylic acid [140-146]. For example Wang *et al.* [147] demonstrated the modification of polyacrylic acid via the reaction of an alkyl amine with the carboxyl groups in the presence of dicyclohexylcarbodiimide (DCC) and a protic solvent (MPD, 2-methyl-2,4-pentanediol) (*Figure 2.7*). They achieved 100 % yields for the modification of polyacrylic acid with 1, 3 and 10 % of n-octadecyl amine. Wang *et al.* found that the viscosity of the hydrophobically modified polyacrylic acid was higher than the viscosity of polyacrylic acid and the viscosity of hydrophobically modified polyacrylic acid increased with the content of hydrophobic moieties. They also found that with addition of salt the viscosity decreased for all polymers due to screening of charges on polyacrylic acid, however the association of the hydrophobic groups was more pronounced. The association of the hydrophobic groups led to polymer chain cross-linking and viscosity enhancement.

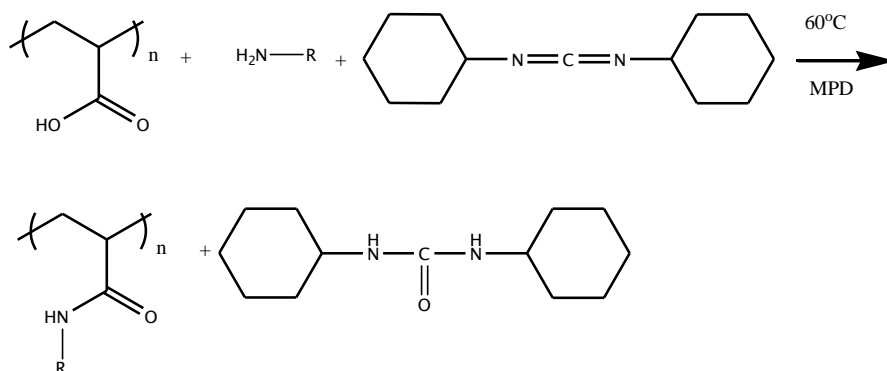
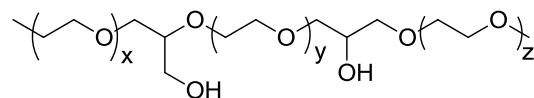


Figure 2.7. Modification of polyacrylic acid with alkylamine.

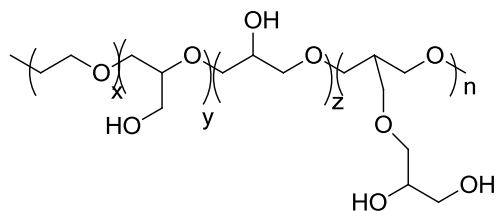
Shedge *et al.* synthesised hydrophobically modified polyacrylic acid by reaction with 3-pentadecylcyclohexylamine in the presence of dicyclohexylcarbodiimide (DCC), using *n*-methylpyrrolidinone (NMP) as solvent [145]. Rheological measurements of the polymer solutions in water demonstrated an increase in viscosity with increasing content of the hydrophobic modification, which was attributed to intermolecular hydrophobic interactions between polymer chains resulting in the formation of a transient network. The viscoelastic measurements indicated the development of a soft physical gel at semi-dilute polymer concentrations.

2.7.3. Poly(ethylene oxide) (PEO)

Hydrophobically modified poly(ethylene oxide) can be synthesised by anionic polymerisation and end-capping with hydrophobic groups. The synthesis of high molecular weight, hydrophobically modified poly(ethylene oxide) has been reported by Dimitrov *et al.* [148]. They used anionic suspension coordination polymerisation with a calcium amide-alkoxide initiating system to afford copolymers of poly(ethylene oxide-co-glycidol) and poly(ethylene oxide-*block*-glycidol) (Figure 2.8), producing molecular weights of $4\text{-}12\cdot 10^5 \text{ g}\cdot\text{mol}^{-1}$ and $3.4\text{-}14\cdot 10^5 \text{ g}\cdot\text{mol}^{-1}$ respectively. Hydrophobically modified water-soluble polymers bearing hydrophobic stearyl moieties were then obtained by modification of the poly(ethylene oxide-co-glycidol) or poly(ethylene oxide-*block*-glycidol) with stearic acid.



poly(ethylene oxide-co-glycidol)



poly(ethylene oxide-block-glycidol)

Figure 2.8. Structures of poly(ethylene oxide-co-glycidol) and poly(ethylene oxide-block-glycidol) [171].

Petrov *et al.* has also reported the synthesis of high molecular weight poly(ethylene oxide)-*b*-poly(alkylglycidyl ether) ($1.8 \cdot 10^6 \text{ g} \cdot \text{mol}^{-1}$ for poly(ethylene oxide-co-dodecyl/tetradecyl glycidyl ether)) via anionic coordination polymerisation [149]. They demonstrated that the polymerisation of alkylglycidyl ethers with ethylene oxide resulted in the formation of block copolymers containing water soluble ethylene oxide segments and hydrophobic blocks. Moreover, the hydrophobicity of the polymers was varied by altering the length of the alkyl chain in glycidyl ethers and the length of the oxyethylene spacer between the terminal hydrophobic groups and polymerisable epoxy group. Additionally they demonstrated, using experimental data obtained by fluorescence, light scattering and transmission electron microscopy, that the copolymers can associate in water, forming corona-core type micelles. Random and block-like gradient copolymers of ethylene oxide and propylene oxide have been synthesised by Petrov *et al.* [150] by utilisation of the anionic ring opening copolymerisation catalysed by a calcium amide/alkoxide initiator. Additionally they demonstrated a new method of synthesis of high molecular weight poly(ethylene oxide-co-propylene oxide) with block-like gradient structures, which was based on the repeated short-time feeds of ethylene oxide in regular time intervals.

Rufier *et al.* reported the synthesis of water soluble asymmetric end capped poly(ethylene oxide) by anionic polymerisation of ethylene oxide with alkoxide, followed by esterification with

carboxylic acid in the presence of *N,N*-dicyclohexylcarbodiimide (DCC) and (dimethylamino)pyridine (DMAP) (Figure 2.9) [151, 152]. The symmetric polymers were synthesised by the same method using carboxylic acids with various lengths of an alkyl chain.

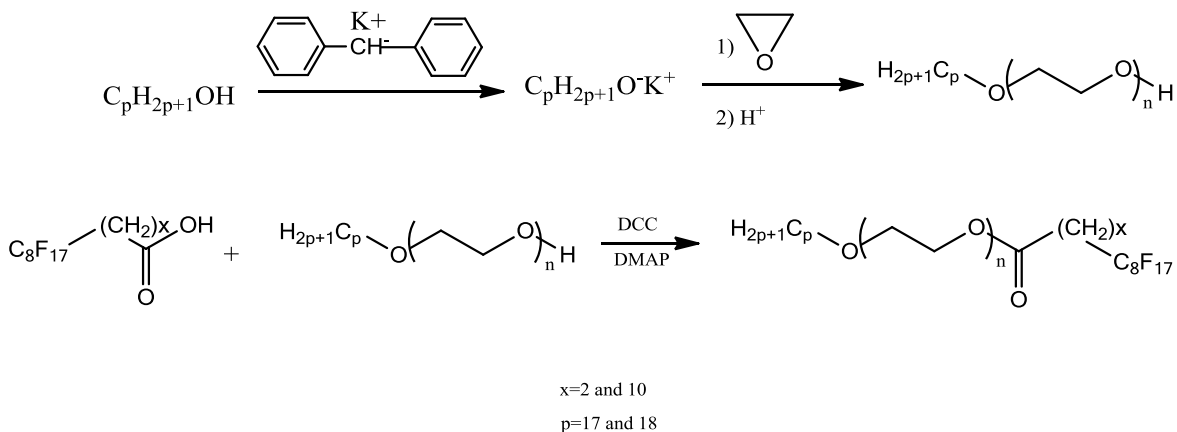


Figure 2.9. Anionic polymerisation of ethylene oxide initiated by potassium alkoxide and subsequent synthesis of asymmetric end-capped polymers by esterification [151, 152].

Rufier *et al.* demonstrated that bridge-like mixed aggregates were formed between hydrogenated and fluorinated groups that led to phase separation. Symmetric aggregates containing only alkyl end capped groups were found to be stable at low concentrations when polymers contained long alkyl chains and a whole range of concentrations studied when polymers contained short alkyl chains. The phase separation was avoided by the addition of surfactant. The viscosity of the asymmetric aggregates containing hydrogenated and fluorinated groups increased at the polymer concentrations above 1 wt% when the solution contained surfactant.

2.7.4. Poly(vinyl alcohol) (PVA)

Poly(vinyl alcohol) (PVA) was researched in the past by Kolnibolotchuk *et al.* [153] and Shakhovskaya *et al.* [154] as a potential drag reducing agent. Kolnibolotchuk *et al.* and Shakhovskaya *et al.* demonstrated that poly(vinyl alcohol) does not reduce drag. They have attributed this to the formation of supramolecular structures in turbulent flow. Kolnibolotchuk *et al.* observed a decrease in the degree of crystallinity upon an increase in hydrophobicity of the polymer and this influenced the polymers behaviour in turbulent flow. Moreover, Shakhovskaya

et al. showed that polymer's conformation can be changed and drag reducing properties can be induced into polymer by the high heat treatment of the polymer solutions.

Synthesis of polyvinyl alcohol is generally carried out by the hydrolysis of polyvinyl acetate, and the polymer with surfactant like behaviour can be obtained by partially hydrolysis of polyvinyl acetate (Figure 2.10). The reaction is usually carried out in presence of catalytic amounts of acid such as hydrochloric acid or base such as sodium hydroxide with the higher reaction rates and no side reactions achieved for the latter [155-157].

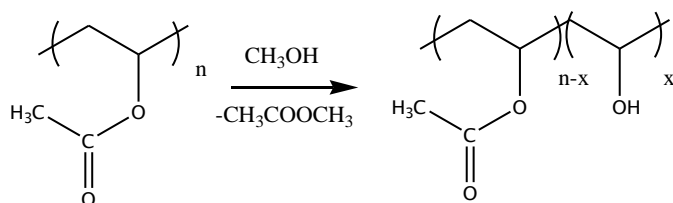


Figure 2.10. Hydrolysis of poly(vinyl acetate) in methanol.

Hydrophobically modified poly(vinyl alcohol) can be also prepared by partial urethanisation of polyvinyl alcohol followed by reaction with acid chloride [158] (Figure 2.11).

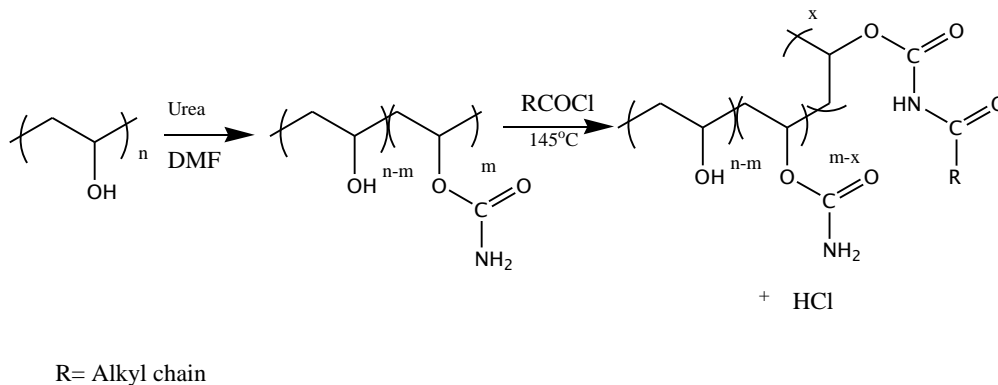


Figure 2.11. Reaction scheme for the hydrophobic modification of PVA [158].

The example given by Yahya *et al.* demonstrated that PVA modified with docosanoic, stearic and decanoic acid chlorides associated in deionised water and aqueous solution of sodium chloride [158]. The two polymers composed of PVA grafted with 0.5 mol% of docosanoic, 0.5 mol% of stearic and 1 mol% of decanoic alkyl chain; and PVA grafted with 2 mol % stearic and

1 mol% decanoic alkyl chain were studied and showed improved viscosity as compared to unmodified and urethanised PVA. This was due to formation of intermolecular association between polymer chains and the creation of large aggregates. The behaviour of the functionalised polymers was found to be unaffected by the variable of concentrations of NaCl and not even by harsh brine.

Marstokk and Roots reported two different routes for the preparation of hydrophobically modified poly(vinyl alcohol) [159]. The first was by Williamson ether synthesis and the second by Michael addition of acrylamide followed by Hoffman degradation (*Figure 2.12* and *Figure 2.13*).

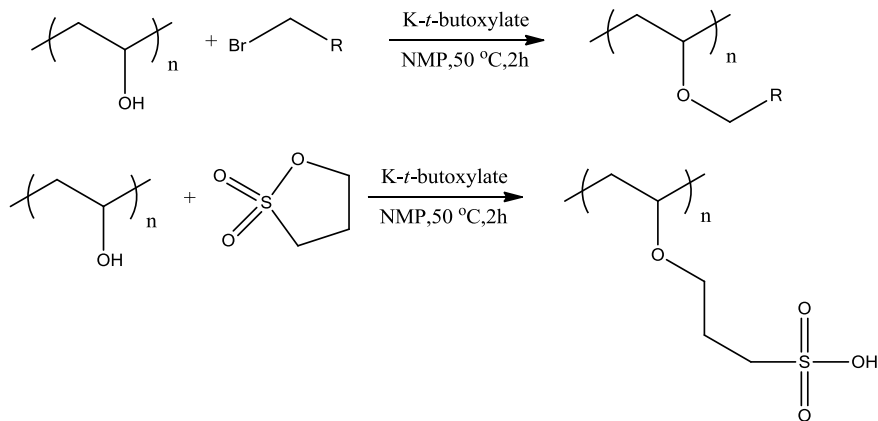


Figure 2.12. The reaction scheme for the Williamson ether synthesis, $R = C_{15}H_{31}$ [159].

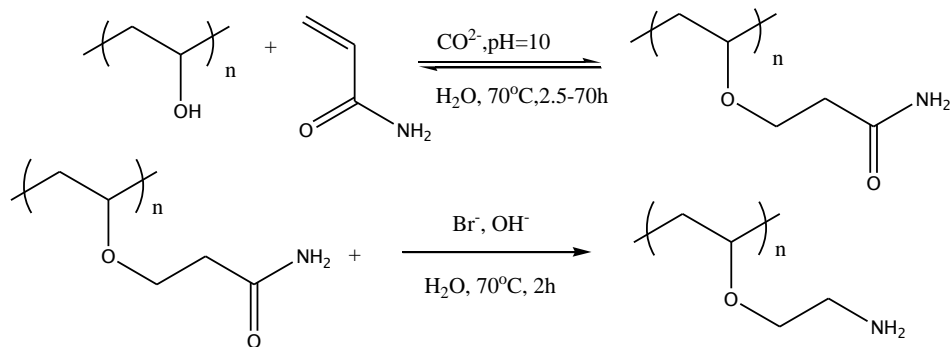


Figure 2.13. Reaction scheme for the Michael addition of acrylamide and subsequent Hoffman degradation [159].

The resulting ether linkages in the graft were more resistant to hydrolysis than the ester linkages reported by Yahya *et al.* [158]. The degree of substitution achieved in Williamson ether synthesis was reported to be 50 % for the alkylation and 30 % for the sulfopropylation, with no improvement in the yield at long reaction times and with possible elimination reaction occurring as a side reaction. The Michael addition and Hoffman degradation resulted in 6-9 % and 100 % yields, respectively and the maximum substitution of 60 %. Marstokk and Roots demonstrated that the yield of the reactions were independent on the time of reaction.

2.7.5. Poly(N-hydroxyethylacrylamide) (PHEAAm)

Poly(N-hydroxyethyl acrylamide) is a very hydrophilic homopolymer with a solubility number of 4, which is the highest ever known solubility number [160]. This polymer has been demonstrated to have potential use as a matrix in capillary electrophoresis of DNA since it has good electrosmotic mobility and high degree of adhesion [161]. The very high molecular weight homopolymer can be prepared by free radical polymerisation in N,N-dimethylformamide with 2,2'-azobis(isobutyronitrile) (AIBN) as the initiator at 60°C [160] and at 47°C in deionised water with 2,2'-azobis (2-amidinopropane) dihydrochloride (V50) as the initiator [161, 162].

Copolymers of poly(N-hydroxyethyl acrylamide) have not been researched widely and are synthesised mainly by Atom Transfer Radical Polymerisation (ATRP). ATRP is one of the methods to produce copolymers with well defined structures and narrowly distributed molecular weights.

Narumi *et al.* synthesised poly(N-hydroxyethylacrylamide) (PHEAAm) by ATRP using ethanol/water as a solvent, copper (I) chloride and ethyl 2-chloropropionate (ECP) as an initiator system and tris[2-(dimethylamino)ethyl]amine (Me₆TREN) as a ligand [163]. The copolymers were created by mixing prepolymer of PHEAAm with N,N-Dimethylacrylamide (DMAA), N-acryloylmorpholine (NAM), and N-[3-(dimethylamino)propyl]acrylamide (DMAPAA) and various copolymers of well defined molecular weights and low molecular weight distributions were obtained (*Figure 2.14*).

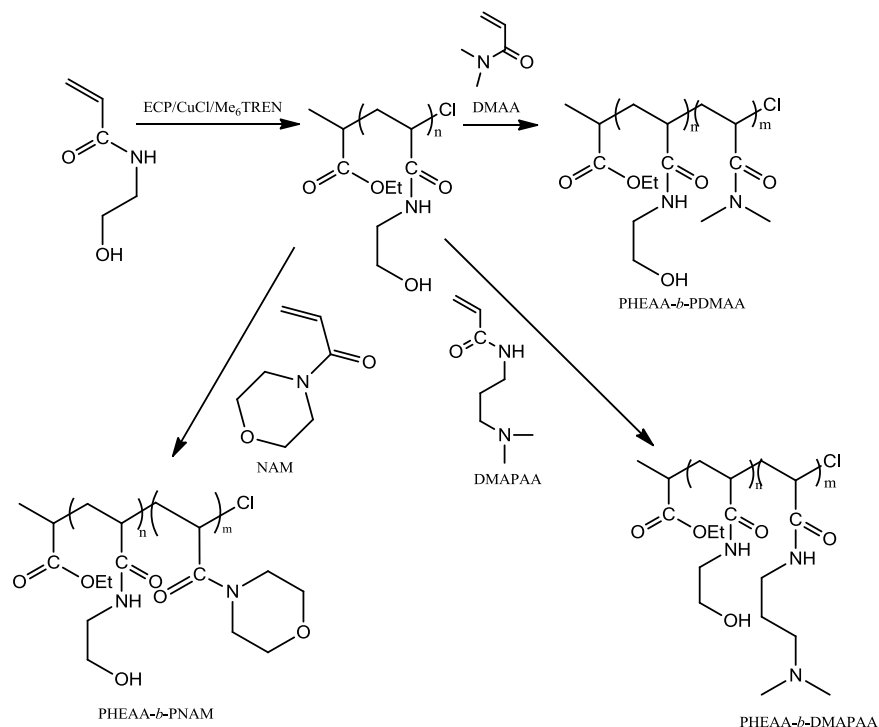


Figure 2.14. Polymerisation of HEAA using ECP, CuCl, and Me₆TREN and subsequent additions of DMAA, NAM, and DMAPAA, producing PHEAA-*b*-PDMAA, PHEAA-*b*-PNAM, and PHEAA-*b*-PDMAPAA, respectively.

Gunes *et al.* [164] recently used sequential ATRP to polymerise ethyl acrylate and styrene monomers and prepared hydrophobically modified poly(N-hydroxyethyl acrylamide) by the subsequent aminolysis of the acrylic block of copolymer with ethanolamine (*Figure 2.15*).

The synthesis resulted in well defined blocks and relatively low molecular weights were achieved with the highest reported number average molecular weight (M_n) of 2.06 kDa. Gunes *et al.* [164] demonstrated that copolymers associated in water and showed that the content of styrene in copolymer decided the polymer's solubility in water. The copolymer containing the shortest block of polystyrene, copolymer with 80 repeat units of N-hydroxyethyl acrylamide (HEAA) and 21 repeat units of styrene (St), formed micelles in water as evidenced by Dynamic Light Scattering (DLS) and fluorescence study at various polymer concentrations, with the hydrodynamic radius (R_H) of 78 nm and critical micellar concentration (CMC) of 38 mg·L⁻¹.

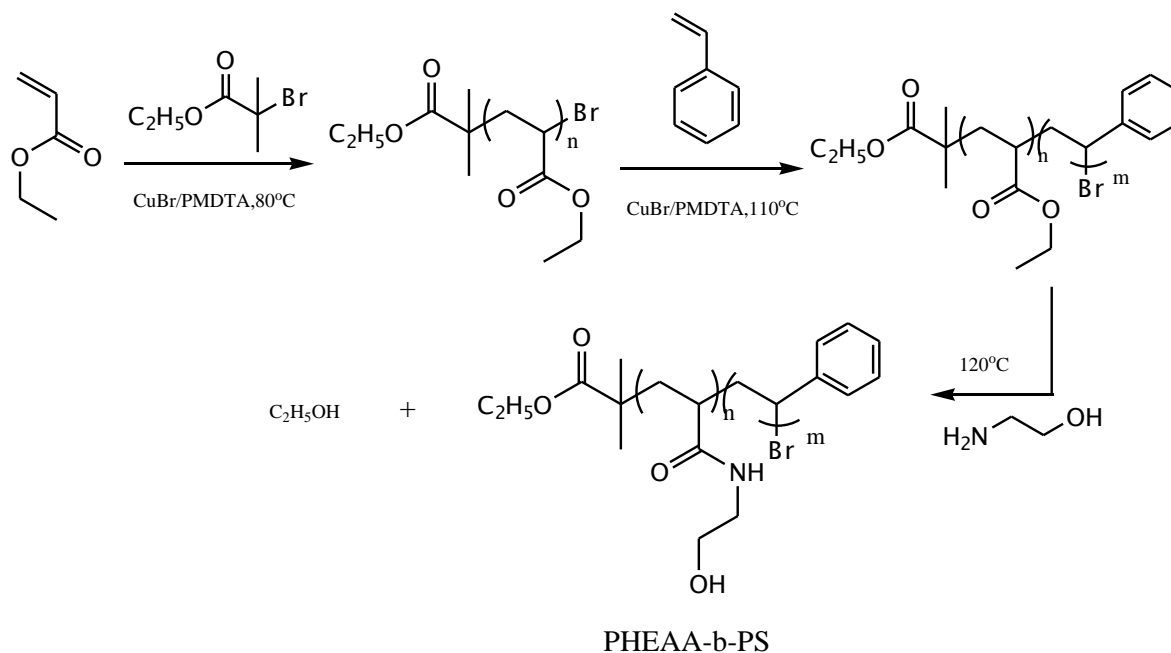


Figure 2.15. Synthesis of PHEAA-b-PS copolymers. PS- Polystyrene, PMDTA- N,N,N,N,N-pentamethyldiethylenetriamine [164].

2.7.6. Biopolymers

Hydrophobically modified biopolymers can be obtained by graft copolymerisation, reaction with alkyl halides, acid halides, acid anhydrides, isocyanates, epoxides and by amination. Bahamdan and Daly [165] carried out successful functionalisation of guar gum with polyalkoxyalkyleneamide in a three step process (*Figure 2.16*). The degree of functionalisation was dependent on the type of polyalkoxyalkyleneamine used and varied from 0.03 to 28.29 % for carboxymethylhydroxypropyl guar gum and 2.16 to 24.43 % for carboxymethyl guar gum. Additionally, the researchers showed that the viscosity of grafted guar gum was lower than the viscosity of an unmodified carboxymethylhydroxypropyl and carboxymethyl guar gum. Bahamdan and Daly explained this drop in viscosity in terms of the surfactant effect.

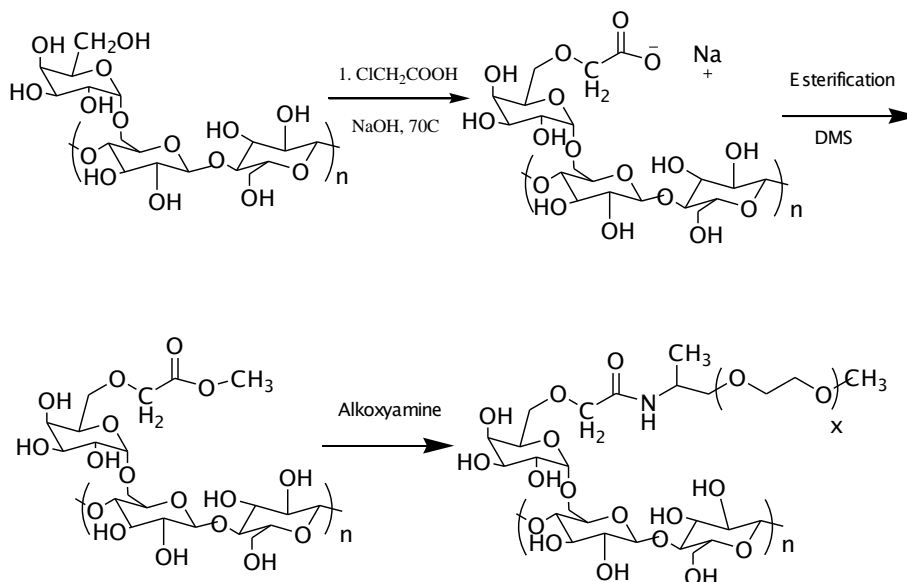


Figure 2.16. Synthesis of guar gum polyoxyalkyleneamines derivatives [183]. DMS-dimethylsulfate.

Nucleophilic substitution of guar gum was demonstrated by Lapasin *et al.* [166]. They reported a two step reaction in which guar gum underwent alkaline etherification with propylene oxide followed by alkaline etherification with docosylglycidylether. The degree of substitution determined by gas chromatography was in the range of 0.00015 and 0.00060. Lapasin *et al.* demonstrated from shear behaviour experiments that the degree of substitution controlled the rheological performance. Additionally all degrees of substitution showed improved rheological properties over the unmodified hydroxypropyl guar gum.

Cellulosic associative polymers can be obtained by reaction of the lateral groups with water soluble derivatives and by graft copolymerisation. Hydrophobically modified carboxymethyl and hydroxyethyl cellulose can be created by reactions with long alkyl chain epoxide, alkyl halides, acyl halides, isocyanates and anhydrides and those methods as well as graft copolymerisation methods have been reviewed by Zhang [167]. The reactions are generally carried out in alkaline slurry since the hydrophobic reagents are incompatible with hydrophilic cellulose. Landoll [168] used long n-alkyl chain terminated epoxides (1,2-epoxydecane, 1,2-epoxydodecane, a mixture of 1,2-epoxyeicosane, 1,2-epoxydocosane and 1,2-epoxytetracosane) to modify hydroxyethyl, methyl and hydroxypropyl cellulose with the degree of functionalisation ranging from 0.7 to 2.9

wt% with respect to epoxide. He reported that the viscosities of the hydrophobically modified celluloses were exceptionally enhanced as compared to unmodified celluloses, which he explained to be due to the formation of aggregates.

The synthesis of hydrophobically modified anionic cellulosic derivatives by amidation of carboxymethyl cellulose with dodecylamine has been reported by Cohen-Stuart *et al.* [169], who obtained a degree of substitution of 0.012 per glucose unit. Homogeneous etherification of cellulose with butyl glycidyl ether was described by Nishimura *et al.* [170], who reported a degree of substitution of between 0.4 and 2.0.

Some cellulosic associative thickeners have been synthesized by graft copolymerisation. In this case, the surfactant macromonomers with hydrophilic head group and a hydrophobic tail, as well as water-soluble (or dispersible) surface-active monomers have been widely used. Shih [171] for example, successfully grafted N-[1-(2-pyridinol)ethyl] acrylamide and methacrylamido propyltrimethyl ammonium chloride using a redox initiating system (hydrogen peroxide/ferrous ammonium sulfate/ethylene diamine tartaric acid disodium salt).

Hydrophobic functionality of carboxyethyl cellulose can be also achieved by modification with methyl ester of rapeseed oil. Tomanova *et al.* [172] carried out the chemical modification by a transesterification reaction in water and N,N'-dimethyl formamide mixture using microwave irradiation at various reaction conditions. They observed that the modified carboxyethyl cellulose associated via hydrophobic interactions.

2.7.7. Polystyrene polymers, copolymers and terpolymers

Hydrophobically modified water-soluble polymers can be also obtained by the functionalisation of hydrophobic polymers with groups imparting water solubility. Polystyrene copolymers and terpolymers can be modified by aromatic electrophilic substitution and this process is used on the industrial scale to obtain polymers with ion-exchange properties [173]. Luka *et al.* introduced water solubility into polystyrene by chloromethylation followed by quaternisation reaction with tris(2-hydroxyethyl)amine (THEA) in N,N'-dimethyl formamide (DMF) and benzene (*Figure 2.17*). However, the reaction that was carried out resulted in the formation of quaternary salts and

crosslinked byproduct. The crosslinking was explained by intermolecular rearrangement of ammonium quaternary groups during reaction [174].

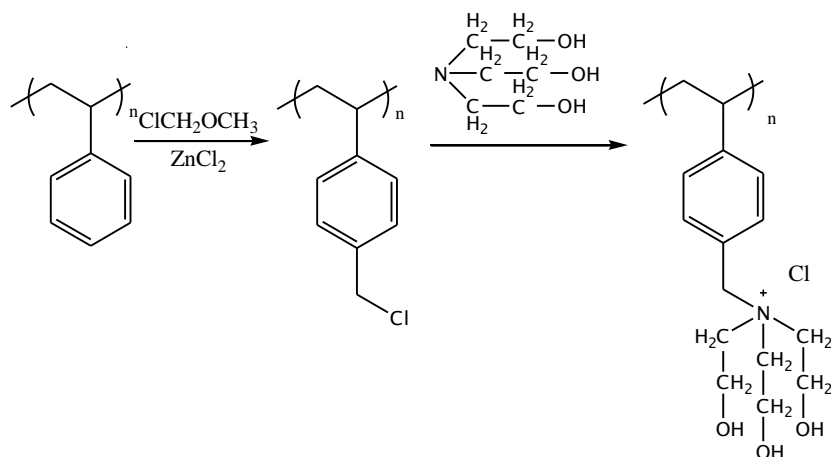


Figure 2.17. Functionalisation of polystyrene by chloromethylation and quaternisation.

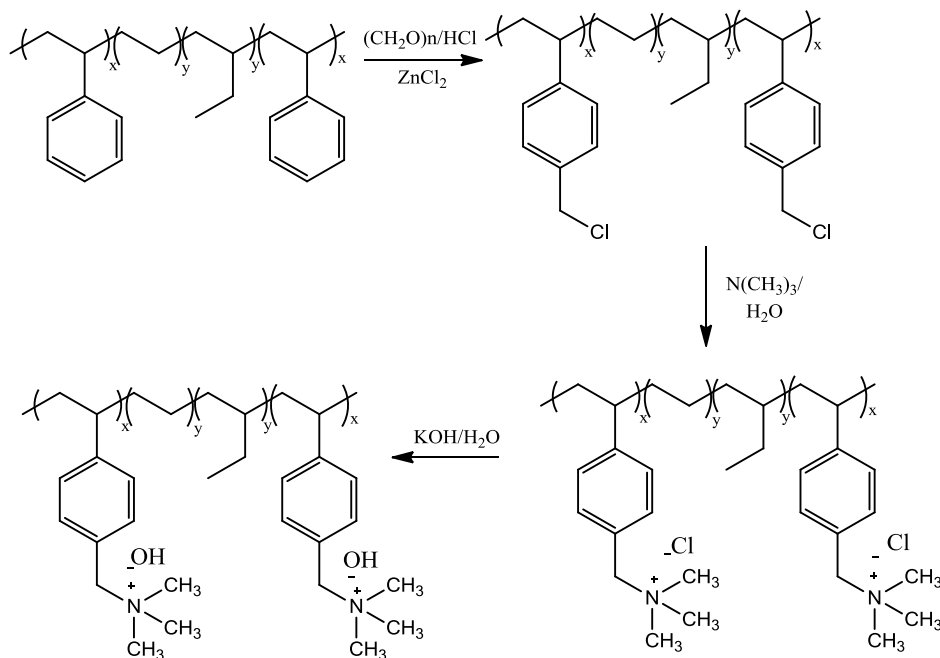


Figure 2.18. Chloromethylation, quaternization and alkalization of SEBS.

Polystyrene-*block*-poly(ethylene-*ran*-butylene)-*block*-polystyrene (SEBS) can be modified by chloromethylation followed by quaternisation and alkalisation as described by Zeng *et al.* [175]

(Figure 2.18). The functionalised SEBS showed reduced thermal stability, however chemical stability remained unchanged. A low degree of functionalisation resulted in improved water uptake of the terpolymers and the polymers showed high ionic conductivity.

Sulfonation is another method to functionalise polystyrene, polystyrene copolymers and terpolymers. The most commonly used sulfonating agents are shown in Figure 2.19 and have been summarized by Roth [176], Thaler [177], Kučera and Jančář [178].

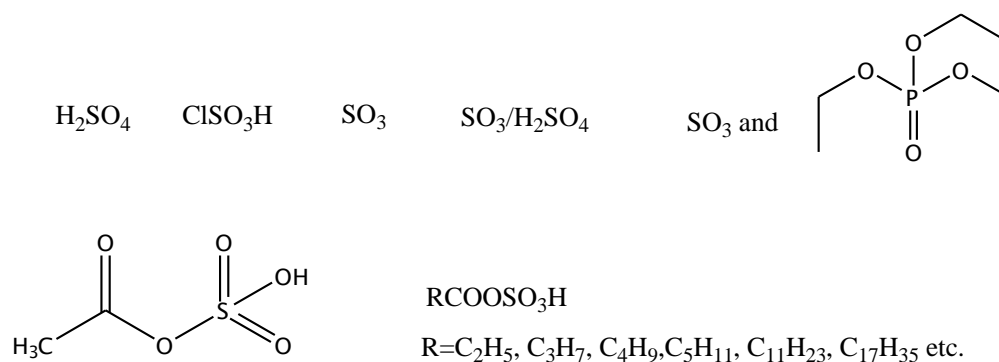


Figure 2.19. Commonly used sulfonating agent species.

Roth summarized the factors affecting the sulfonation of poly(vinyl aromatics). The type and molecular weight of polymer, type of solvent, concentration and purity of reactants, stoichiometry of reaction, rate of agitation, temperature and order of added reactants were described as reaction conditions that can affect the rate of sulfonation [176]. Thaler synthesised a novel hydrocarbon soluble sulfonating agent species based on higher molecular weight carboxylic acids prepared by reaction of carboxylic acids with sulfur trioxide or sulfonic acid. Improved sulfonation rates of polystyrene were demonstrated that were accredited to the higher solubility of sulfonating agents in the reaction medium. Kučera and Jančář reviewed the homogeneous and heterogeneous sulfonation of polymers especially polystyrene and the influence of the reaction conditions on the sulfonation [178]. Few commonly used sulfonating agents such as sulphuric acid, oleum, chlorosulfonic acid, fluorosulfonic acid, amidosulfonic acid, free sulfur trioxide and its complexes, halogen derivatives of sulfuric acid that were used for sulfonation of polymers, were named. Kučera and Jančář also described the most common problems with the sulfonation

reaction, such as desulfonation that is promoted by diluted solutions of acid and the presence of water as well as the formation of sulfone that occurs at high temperatures.

Preparation of sulfonated polystyrene was reported by Martins *et al.* [179], Carvalho and Curvelo [180]. The sulfonation was carried out in 1,2-dichloromethane under mild sulfonation conditions with the use of acetyl sulfate formed in-situ (*Figure 2.20*).

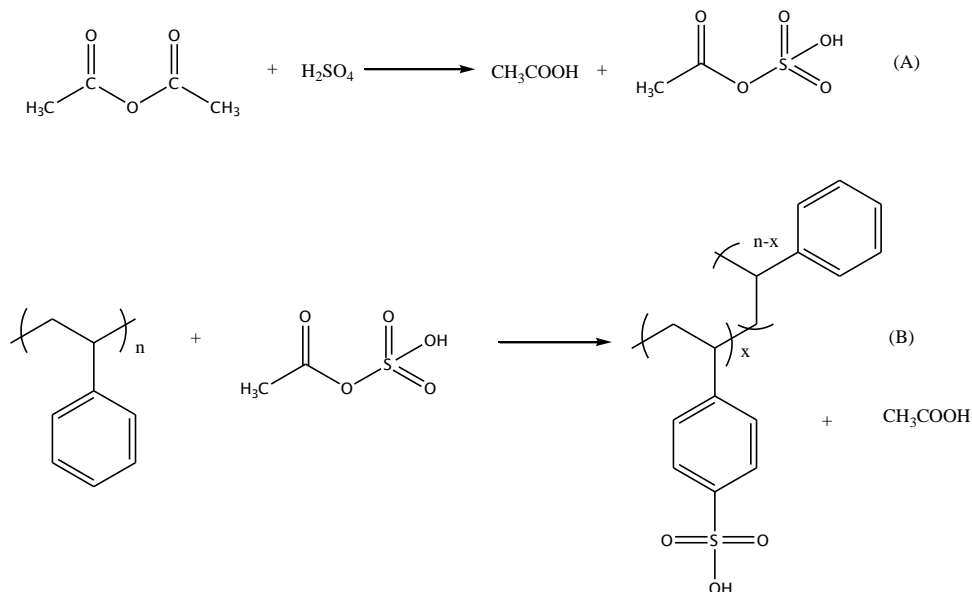


Figure 2.20. Reaction scheme of homogeneous sulfonation : (A) acetyl sulfate generation and (B) sulfonation of polystyrene (PS) [179].

Sulfonated polystyrene achieved by Martins *et al.* was prepared at 40°C with a maximum degree of sulfonation of ~20 mol%. The polymers showed decreased thermal stability as compared to polystyrene. Carvalho and Curvelo obtained water soluble sulfonated polystyrenes while carrying out sulfonation at room temperature. Polymers were found to be soluble in mixtures of tetrahydrofuran (THF) and water (50/50% v/v) and at 52 mol% degree of sulfonation the polymers were soluble in water. Polymer solutions dissolved in 1:1 (v/v) water: THF mixture demonstrated typical polyelectrolyte behaviour and an increase in viscosity of polymers was observed with increasing degree of sulfonation. A decrease in the viscosity was also observed with increases in the concentration of sodium chloride.

Sułkowski *et al.* demonstrated the modification of polystyrene with silica-sulfuric acid carried out in 1,2-dichloroethane at 30 to 60°C and at sulfonation time between 60 to 720 minutes [181]. The sulfonated polystyrene was not soluble in water but was characterised by high water absorption when reaction was carried out at 60°C and when 4 mol eq of sulfonating agent was used. Sułkowski *et al.* also showed that the degree of sulfonation increased with increases in reaction time and temperature. The products obtained had high ion exchange capacities.

Sulfonation of SEBS can be achieved by reaction with acetyl sulfate at 50-60 °C in 1,2-dichloroethane as reported by Picchioni *et al.* [182], Kim *et al.* [183], Hwang *et al.* [184, 185], Barra *et al.* [186] and Johnson *et al.* [187]. The sulfonated polymers were prepared for use in membrane applications and all the copolymers studied contained up to 30 wt % of styrene. The sulfonation was carried out for 2-3 hours and none of the polymers obtained was water soluble. All the authors demonstrated an increase in sulfonation level, proton conductivities and water/methanol uptake with increase in sulfonating agent concentration. Moreover, Picchioni *et al.* showed that the yield decreased upon an increase in the concentration of acetyl sulfate [182]. Furthermore, the thermal stability of the polymer increased with an increase in the degree of sulfonation.

The sulfonation of poly(styrene-isobutylene-styrene) (SIBS) containing 19 moles% of polystyrene was described by Elabd and Napadensky and was carried out with acetyl sulfate in methylene chloride at 40°C [188]. The authors demonstrated an increase in the degree of sulfonation, ionic conductivity, water solubility and a decrease in reaction efficiency with increasing concentration of the sulfonating agent. The latter was attributed to the decrease in solubility of polymer in the course of reaction.

Sulfonation of poly(styrene-butadiene-styrene) (SBS) with acetyl sulfate in a mixture of organic solvents or chlorosulfonic acid in 1,2-dichloroethane has been also reported by Xie *et al.* [189] and Idibie *et al.* [190]. Xie *et al.* reported sulfonation at room temperature in a mixture of cyclohexane and acetone as a method to reduce polymer insolubility and gelation problems during the reaction. The authors demonstrated an increase in the degree of sulfonation and an increase in the solution viscosity in toluene/methanol mixture with increases in the concentration of acetyl sulfate. The increase in viscosity was a result of the association of polymer.

Sulfonated SBS ionomers can be also prepared by emulsion polymerisation of sodium styrene sulfonate and butadiene; however research in this area is not as extensive as for post-sulfonation mainly due to the high crosslinking tendency during the course of polymerisation. Weiss, Lundberg and Werner prepared copolymers containing 0.5 to 4 mol% of sulfonated monomers in the presence of a triethylenetetramine and diisopropylbenzene hydroperoxide redox initiator pair [191]. It has been demonstrated that the polymerisation process was dependent on several factors such as Hydrophilic-Lipophilic Balance (HLB) of the surfactant used with the optimal reaction rate being achieved with a surfactant of a HLB of 29. The increase in the concentration of sulfonated monomer resulted in an increase in conversion, due to the surfactant like properties of sodium styrene sulfonate. The composition, molecular weight and solubility behaviour of the copolymers prepared were found to be strongly dependent on the conversion. Weiss, Lundberg and Werner also observed increase in tendency in polymer crosslinking with an increase in conversion.

2.7.8. Polyisoprene copolymers and terpolymers

The work on the selective sulfonation of polyisoprene block in polystyrene-isoprene copolymers and terpolymers was first pioneered by Japan Synthetic Rubber Co. and published by Szczubiałka, Ishikawa and Morishima [192, 193] and later by Gatsouli *et al.* [194] and Wang *et al.* [195]. The sulfonation of isoprene segment in block copolymers and terpolymers (*Figure 2.21*) was carried out with a sulphur trioxide/1,4-dioxane complex that was prepared in-situ by the reaction between concentrated sulphuric acid and 1,4-dioxane. Szczubiałka, Ishikawa and Morishima synthesised water soluble copolymers and terpolymers and demonstrated that the polymer molecules associate intermolecularly to form core-corona and flower type micelles. The diameter of core-corona micelles was found to be large and independent on the polymer concentration up to $1 \text{ g}\cdot\text{L}^{-1}$; however a decrease in the size of micelles was seen when salt was added. The hydrodynamic radius was also demonstrated to be dependent on the content of polystyrene and these polymers were found to have highest aggregation number. Based on a fluorescence and quasielastic light scattering study, Szczubiałka *et al.* demonstrated that the terpolymers formed oligomeric aggregates below the critical aggregation concentration. Above

critical aggregation concentration however, unimers, oligomeric aggregates and micelles were present. The type of structures formed by polymers was dependent on the content of styrene in terpolymer and bridged-micelles were present when content of styrene was the highest.

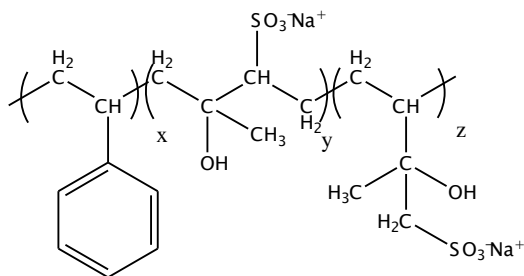


Figure 2.21. Structure of sulfonated styrene-isoprene copolymers.

Uchman *et al.* [196] and Pispas [197] have also investigated the behaviour of sulfonated terpolymer of styrene, isoprene and ethylene oxide and copolymer of isoprene and ethylene oxide. The authors sulfonated polymers with chlorosulfonyl isocyanate in dry diethyl ether. The copolymers were found to follow typical polyelectrolyte behaviour. Uchman *et al.* demonstrated the terpolymers containing styrene blocks to form multicomponent micelles with a polyethyleneoxide shell and a raspberry-like sulfonated polyisoprene core containing polystyrene domains. The behaviour of the aggregates was found to be dependent on the pH with smaller aggregates forming in alkaline medium. Complex aggregation mechanism dependent on pH was also demonstrated, which was attributed to the amphiphilic character of the polyisoprene block and the hydrogen bonding between the sulfonic acid groups and the PEO block.

Chapter 3

Experimental Methods

3.1. Materials

The following monomers were used in polymerisations: acrylamide (AAm) (99%, Sigma-Aldrich) was recrystallised twice from acetone (99.5%, VWR) and n-decyl acrylamide (DAAm) (>98%, Monomer-Polymer Dajac) was recrystallised twice from a mixture of acetone and hexane (99%, VWR) (1:2 v/v respectively). N-hydroxyethyl acrylamide (HEAAm) (97%, Sigma-Aldrich) and n-octadecyl acrylamide (ODAAm) (99%, Polysciences) were used without further purification. Potassium persulfate ($\geq 99\%$, Sigma-Aldrich) and sodium metabisulfate ($\geq 99\%$, Sigma-Aldrich) were used as initiators in polymerisation and used without further purification. Sodium dodecyl sulfate (SDS) ($\geq 99.0\%$, Sigma) was used as a surfactant in micellar polymerisation and used as received. Poly(styrene-*block*-butadiene) (SBR), block copolymer of styrene and butadiene was kindly provided by BASF. The copolymer contained 71.1 mol% of polystyrene (PS) and had a weight average molecular weight of 143 kDa and the PDI of 1.4 (data provided by the manufacturer). Poly(styrene-*block*-butadiene) was supplied as a mixture of block copolymer and ~ 5 (w/w) % of polystyrene homopolymer. The polymer pellets were dried under vacuum at 60°C for 24 hours and stored in a desiccator before use. Sulfuric acid (99.999%, Sigma-Aldrich) and acetic anhydride ($\geq 99\%$, Sigma-Aldrich) were used to prepare acetyl sulfate and used as acquired. Propan-2-ol (99.5%, VWR) used to quench sulfonation reaction was used as received. Dry 1,2-dichloroethane (0.003% of H₂O, $\geq 99\%$, Sigma-Aldrich) was stored under dried argon. Diethyl ether ($\geq 99.7\%$, VWR), 1,2-dichloromethane ($\geq 99.8\%$, VWR), acetone ($\geq 99.8\%$, VWR), tetrahydrofuran ($\geq 99\%$, VWR), dimethyl sulfoxide ($\geq 99.9\%$, VWR) and methanol ($\geq 99.8\%$, HPLC grade, VWR) were used as received. α -Cyclodextrin ($\geq 98\%$, Sigma-Aldrich), β -Cyclodextrin ($\geq 99\%$, Sigma-Aldrich), potassium chloride ($\geq 99.5\%$, BDH), sodium chloride ($\geq 99.5\%$, Fluka) and calcium chloride dihydrate ($\geq 99.5\%$, Sigma) were used as received. Polyacrylamide used in drag reduction study as a control sample (Polysciences Inc.,

$M_w=1085$ kDa, PDI= 2.05, values determined by GPC) was supplied as a solution in deionised water and was freeze dried before use. Sodium azide ($\geq 99\%$, Sigma-Aldrich) was used as antibacterial agent and sodium nitrate ($\geq 98\%$, BDH) was used to prepare the GPC eluent. These chemicals were used without further purification. Microsilica used in adsorption and desorption study (Dura-Sil E, Durapact), had a surface area of $48 \text{ m}^2\cdot\text{g}$ (value determined by BET, ASAP 2010 Micromeritics, UK). NMR solvents, deuterium oxide (D_2O , 99.8 atom% D, Merck), deuterated tetrahydrofuran ($\text{d}_8\text{-THF}$, 99.5 atom% D, Sigma) and deuterated chloroform ($\text{d}_1\text{-CDCl}_3$, 99.96 atom % D, Merck) were used as received. Pureshield argon (99.998%, BOC) and piped nitrogen (BOC) was passed through a calcium carbonate, sodium hydroxide and self-indicating silica drying column with the length of ~ 20 cm. The dialysis tubing (Biodesign, Fisher Scientific) used in purification of polymers had a molecular weight cut off (MWCO) of 3500 Da and was washed in deionised water for 5 minutes before use. Deionised water (“Option 4”, Water Purifier, Elga, UK) was used for all experiments.

The materials were weighed with an accuracy of ± 0.1 mg and solvents were weighed with an accuracy of ± 0.1 or 10 mg.

3.2. Synthesis of hydrophobically modified polyacrylamide copolymers

3.2.1. Micellar copolymerisation of acrylamide and n-decyl acrylamide

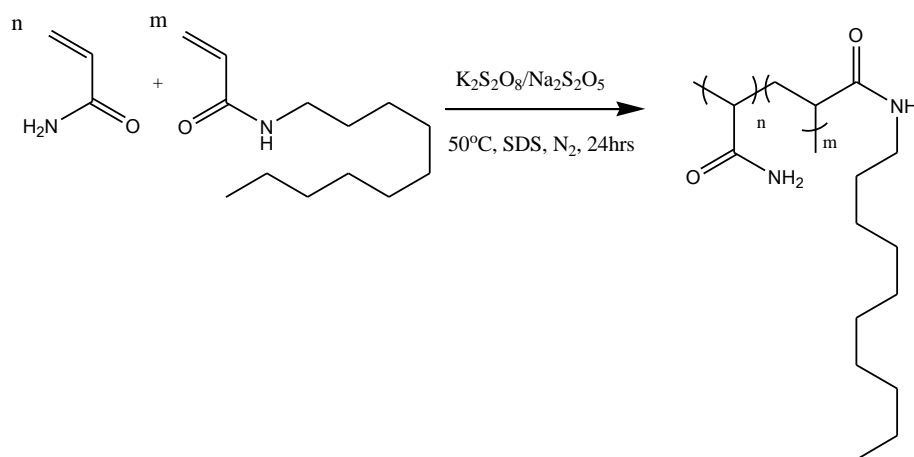


Figure 3.1. The reaction scheme for the synthesis of poly(acrylamide-co-n-decyl acrylamide).

Acrylamide (AAm), n-decyl acrylamide (DAAm) and sodium dodecyl sulfate (SDS) (for quantities see *Table 3.1*) were mixed with deionised water in a 50 ml round bottom flask equipped with magnetic stirrer, oil bath, external temperature probe, Young's adapter and nitrogen inlet and outlet. The mixture was stirred at room temperature for two hours until homogeneous and a transparent solution was obtained. The mixture was degassed by three successive freeze-pump-thaw cycles. The initiator solution was prepared by dissolving, potassium persulfate (2.5 mg, 9.24 μmol) and sodium metabisulfate (1.6 mg, 8.4 μmol) in 2 g of deionised water. This solution was also degassed by three successive freeze-pump-thaw cycles and purged with nitrogen for 60 seconds. The monomer mixture was heated to 50°C and the initiator solution was injected at temperature. The resulting solution was purged with nitrogen for an hour. Polymerisation was carried out for 24 hours before 100 ml of deionised water was added to a viscous polymer solution or hard gel (especially for polymers at higher content of hydrophobic monomer). The polymer was then gently stirred for 12 to 24 hours until dissolution was complete. The dissolution was determined visually. This solution was precipitated into 500 ml of acetone whilst being vigorously stirred. The clumpy white precipitate was cut into pellets smaller than 1 cm and gently agitated in acetone overnight. The solid was removed by filtration and redissolved in 150 ml of deionised water for 12 to 24 hours with gentle agitation. The polymer solution was then dialysed against 2 litres of deionised water for a week. Deionised water was replaced once every hour in the first 12 hours and then twice a day for the remainder of dialysis. The progress of the dialysis process was followed by measuring the conductivity of the extracting water phase. The polymer was transferred from dialysis tube into a clean beaker and recovered by lyophilisation to yield white fluffy solid (Edwards Modulyo freeze dryer, West Sussex, UK).

Sample	AAM (g) (mmol)	DAAM (g) (mmol) (mol% of total monomer)	SDS (g) (mmol)	DiH ₂ O (g)	N _H [126, 130]
AD1	2.354 33.13	0.369 1.745 5.01	2.529 8.772	75.19	13.0
AD2	2.354 33.12	0.216 1.020 2.99	2.528 8.7671	75.36	7.58
AD3	2.353 33.11	0.1062 0.5025 1.49	2.520 8.739	74.81	3.74
AD4	2.353 33.11	0.071 0.334 0.92	2.528 8.765	75.05	2.57
AD5	2.353 33.11	0.060 0.284 0.85	2.527 8.763	75.14	2.11
AD6	2.353 33.11	0.046 0.217 0.61	2.528 8.768	75.27	1.61
AD7	2.354 33.12	0.060 0.285 0.79	2.427 8.416	11.77	2.06
AD8	2.354 33.12	0.046 0.219 0.62	2.427 8.416	11.77	1.58
AD9	2.355 33.13	0.032 0.1495 0.45	2.4263 8.4141	11.77	1.08
AD10	2.353 33.11	0.017 0.083 0.29	2.427 8.417	11.77	0.60

Table 3.1. Composition of the monomer mixture for polymerisations **AD1-AD10**.

The polymers that were synthesised at high N_H (>2.1, *Table 3.1*) and formed a suspension in deionised water, were cut into pellets smaller than 1 cm after precipitation into 500 ml of acetone. The solid polymer was stirred gently in acetone overnight. The white polymer pellets were recovered by filtration, placed into 500 ml of fresh acetone and stirred in acetone overnight. This process was repeated 5 times. The white polymer pellets were then dried under vacuum at

room temperature to constant weight. Yield, molecular weights and hydrophobic monomer content are presented in Chapter 4 Section 4.2.1 *Table 4.1*. Typical ^1H NMR (400 MHz, D_2O): δ (ppm) 0.8 (m, 3H, CH_3 , DAAM), 1.2 (s, 16H, CH_2 , DAAM), 1.25-1.7 (br, 4H, CH_2 , DAAM and AAm, backbone), 2.0-2.35 (br, 2H, CH , DAAM and AAm, backbone), 3.1 (s, 2H, CH_2 , DAAM). The yield of polymerisation (Y) was determined gravimetrically:

$$Y(\%) = \frac{W_P}{W_M} \cdot 100 \quad (3)$$

Where W_P is the weight of the freeze dried polymer and W_M is the weight of the monomers.

$$N_H = \frac{[H]}{([SDS] - \text{CMC}_{SDS}) / N_{agg}} \quad (4)$$

Where N_H is the number of hydrophobic monomers per surfactant micelle, $[H]$ is the initial molar concentration of n-decyl acrylamide, $[SDS]$ is the molar concentration of surfactant, CMC_{SDS} is critical micellar concentration of SDS at 50°C ($9.2 \cdot 10^{-3} \text{ mol} \cdot \text{L}^{-1}$ [126]), N_{agg} is the aggregation number of SDS (60 at 50°C [128, 130])

3.2.2. Micellar copolymerisation of acrylamide and n-octadecyl acrylamide

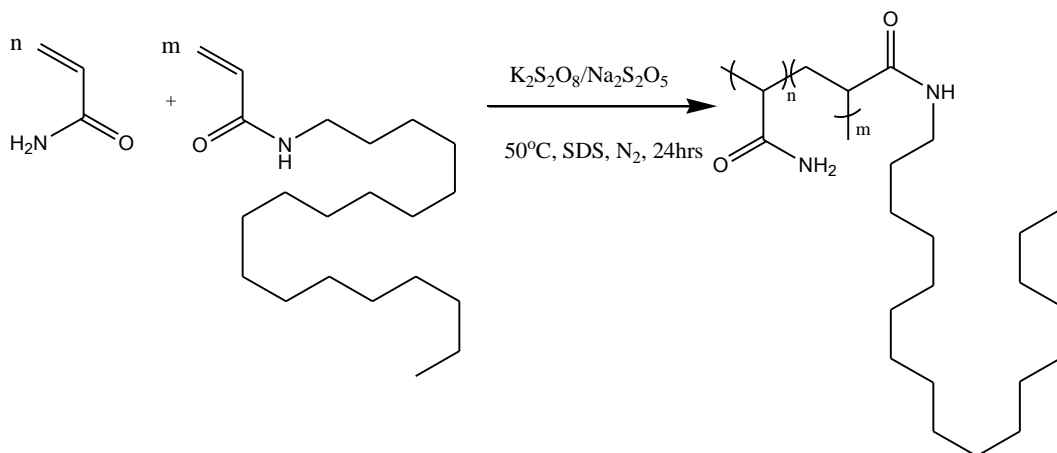


Figure 3.2. Reaction scheme for the synthesis of poly(acrylamide-co-n-octadecyl acrylamide).

The synthesis and purification of product was carried out according to the procedure used in Section 3.2.1 (for the reagent quantities see *Table 3.2*). The mixture of SDS, n-octadecyl acrylamide and deionised water was however stirred for 60 minutes at 80°C to allow dissolution of the hydrophobic monomer. Once the solution was homogeneous and transparent the temperature was decreased to 25°C and acrylamide (AAM) was mixed in. The polymerisation yielded a white fluffy product or polymer pellets for copolymers **AOD1** and **AOD2**. Yield, molecular weights and hydrophobic monomer content are presented in Chapter 4 Section 4.2.1 *Table 4.1*. Typical ¹H NMR (400 MHz, D₂O): δ (ppm) 0.8 (m, 3H, CH₃, ODAAm), 1.2 (s, 32H, CH₂, ODAAm), 1.25-1.7 (br, 4H, CH₂, ODAAm and AAm, backbone), 2.0-2.35 (br, 2H, CH, ODAAm and AAm, backbone), 3.1 (s, 2H, CH₂, ODAAm).

Sample	AAm (g) (mmol)	ODAAm (g) (mmol) (mol% of total monomer)	SDS (g) (mmol)	DiH ₂ O (g)	N _H
AOD1	2.354 33.11	0.048 0.150 0.430	2.427 8.418	11.77	1.08
AOD2	2.353 33.11	0.027 0.083 0.245	2.427 8.417	11.77	0.60
AOD3	2.352 33.10	0.011 0.033 0.099	2.427 8.418	11.77	0.24

Table 3.2. Composition of the monomer mixture for polymerisations **AOD1-AOD3**.

3.2.3. Synthesis of polyacrylamide (PAAm0)

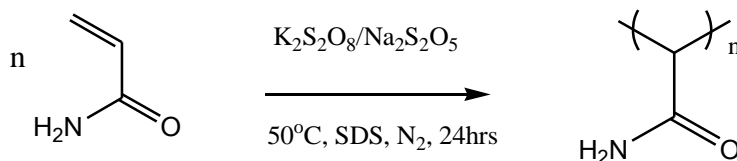


Figure 3.3. Reaction scheme for the synthesis of **PAAm0**.

The synthesis and purification of polyacrylamide was carried out according to the procedure used in Section 3.2.1. The following quantities of reagents were used: acrylamide (AAm, 2.355 g, 33.12 mmol), sodium dodecyl sulfate (SDS, 2.426 g, 8.414 mmol), potassium persulfate (2.5 mg, 9.24 μmol), sodium metabisulfate (1.6 mg, 8.4 μmol) and deionised water (11.78 g). The polymerisation yielded a white fluffy product (1.954 g). GPC: $M_w = 1896 \text{ kDa}$, $M_n = 1458.5 \text{ kDa}$, PDI = 1.3. $^1\text{H NMR}$ (400 MHz, D_2O): δ (ppm) 1.3-1.6 (br, 2H, CH_2), 2.0-2.35 (br, 1H, CH).

3.3. Synthesis of hydrophobically modified poly(N-hydroxyethyl acrylamide) copolymers

3.3.1. Micellar copolymerisation of N-hydroxyethyl acrylamide and n-decyl acrylamide

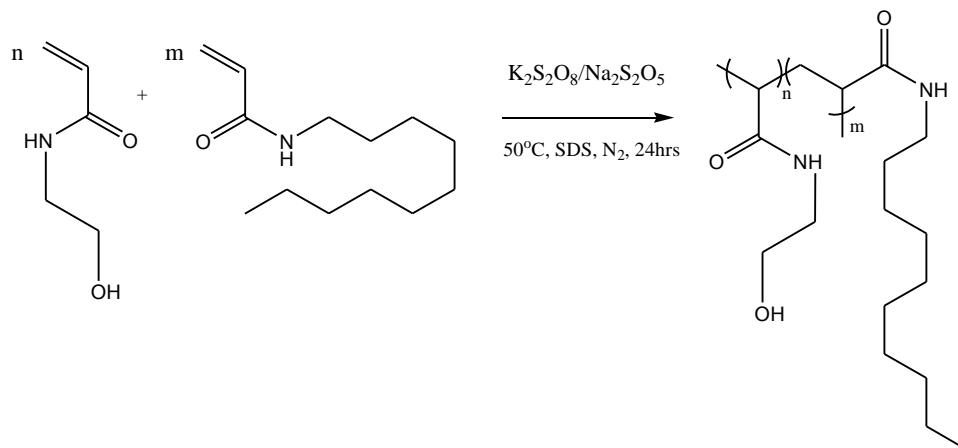


Figure 3.4. Reaction scheme for the synthesis of poly(N-hydroxyethyl acrylamide-co-n-decyl acrylamide).

The synthesis and purification of copolymers of poly(N-hydroxyethyl acrylamide) was carried out according to the procedure used in Section 3.2.1 (for quantities of reactants see *Table 3.3*). The quantities of other reagents were as follows: potassium persulfate (2.4 mg, 8.88 μ mol) and sodium metabisulfate (1.7 mg, 8.95 μ mol). The yield of polymerisation was calculated according to Equation 3 (see section 3.2.1). Yield, molecular weights and the hydrophobic monomer content are presented in Chapter 6 Section 6.2.1 *Table 6.1*. Typical ¹H NMR (400 MHz, D₂O): δ (ppm) 0.8 (m, 3H, CH₃, DAAm), 1.1 (s, 16H, CH₂, DAAm), 1.2-1.6 (br, 4H, CH₂, DAAm and HEAAm, backbone), 1.8-2.25 (br, 2H, CH, DAAm and HEAAm, backbone), 3.1-3.4 (s, 2H, CH₂, CH₂OH HEAAm and 2H, CH₂, DAAm), 3.5-3.6 (2H, CH₂, CH₂NH HEAAm).

Sample	HEAAm (g) (mmol)	DAAm (g) (mmol) (mol% of total monomer)	SDS (g) (mmol)	Di-H ₂ O (g)	N _H
HED1	2.114 18.36	0.028 0.133 0.72	1.515 5.25	11.77	1.55
HED2	2.117 18.39	0.020 0.093 0.50	1.515 5.25	11.77	1.08
HED3	2.117 18.39	0.011 0.052 0.28	1.514 5.25	11.77	0.61

Table 3.3. Composition of the monomer mixture for polymerisations **HED1-HED3**.

3.3.2. Micellar copolymerisation of N-hydroxyethylacrylamide and n-octadecyl acrylamide (**HEOD1**)

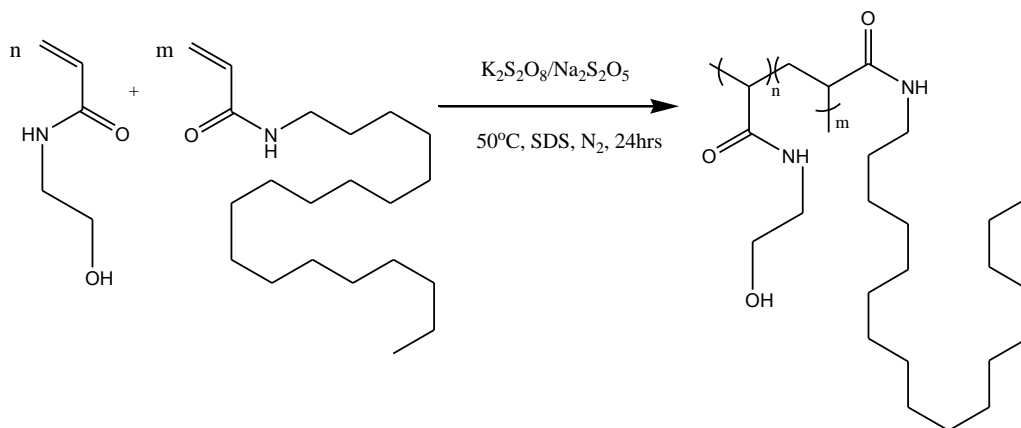


Figure 3.5. Reaction scheme for the synthesis of **HEOD1**.

The synthesis and purification of **HEOD1** was carried out according to the procedure used in Section 3.2.1. The following quantities of reagents were used: N-hydroxyethyl acrylamide (HEAAm, 2.253 g, 19.57 mmol), n-octadecyl acrylamide (0.007 g, 2·10⁻⁵ mol, 0.1 mol%), sodium dodecyl sulfate (SDS, 1.514 g, 5.25 mmol), potassium persulfate (2.4 mg, 8.88 μmol),

sodium metabisulfate (1.7 mg, 8.95 μmol) and deionised water (11.78 g). The mixture of SDS, n-octadecyl acrylamide and deionised water was stirred for 60 minutes at 80°C to allow dissolution of the hydrophobic monomer first. Once the solution was homogeneous and transparent the temperature was decreased to 25°C and N-hydroxyethyl acrylamide (HEAAm) was mixed in. The polymerisation yielded a white fluffy product (1.600 g). GPC: $M_w = 204$ kDa, $M_n = 136$ kDa, PDI = 1.5. H (mol%) by NMR: 0.11, ^1H NMR (400 MHz, D_2O): δ (ppm) 0.8 (m, 3H, CH_3 , ODAAm), 1.1 (s, 32H, CH_2 , ODAAm), 1.2-1.6 (br, 4H, CH_2 , ODAAm and HEAAm, backbone), 1.8-2.25 (br, 4H, CH , ODAAm and HEAAm, backbone), 3.1-3.4 (s, 2H, CH_2OH , HEAAm and 2H, CH_2 , ODAAm), 3.5-3.6 (2H, CH_2NH , HEAAm)

3.3.3. Synthesis of poly(N-hydroxyethyl acrylamide) (PHEAAm0)

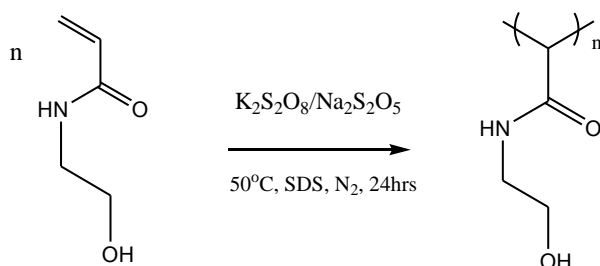


Figure 3.6. Reaction scheme for the synthesis of **PHEAAm0**.

The synthesis and purification of poly(N-hydroxyethyl acrylamide) was carried out according to the procedure used in Section 3.2.1. The following quantities of reagents were used: N-hydroxyethyl acrylamide (HEAAm 2.354 g, 20.44 mmol), sodium dodecyl sulfate (SDS 1.514 g, 5.252 mmol), potassium persulfate (2.4 mg, 8.88 μmol), sodium metabisulfate (1.7 mg, 8.95 μmol) and deionised water (11.777 g). The polymerisation yielded a white fluffy product (1.742 g). GPC: $M_w = 633$ kDa, $M_n = 352$ kDa, PDI = 1.8. ^1H NMR (400 MHz, D_2O): δ (ppm) 1.2-1.6 (br, 2H, CH_2 , Backbone), 1.8-2.25 (br, 1H, CH , Backbone), 3.1-3.4 (m, 2H, CH_2OH , HEAAm), 3.5-3.6 (m, 2H, CH_2NH , HEAAm)

3.4. Synthesis of sulfonated poly(styrene-*block*-butadiene)

3.4.1. The synthesis of acetyl sulfate

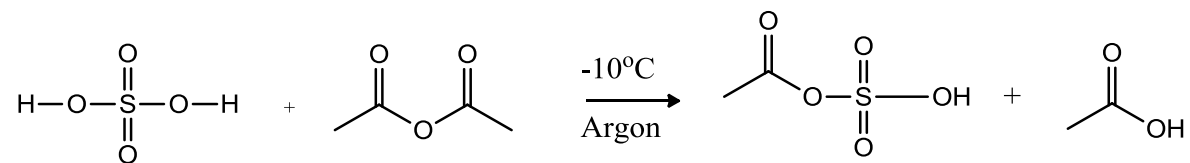


Figure 3.7. The reaction scheme for the synthesis of acetyl sulfate.

Acetyl sulfate was synthesized according to the procedure by Hwang *et al.* [184]. The glassware was dried in 100°C oven overnight, allowed to cool down in desiccator and flushed with dry argon before use. The reaction was carried out in 50 ml round bottom flask equipped with Young's tap, mercury thermometer and argon inlet and outlet. The predetermined amount of acetic anhydride (2 mol eq. with respect to concentrated sulfuric acid, *Table 3.4*) was added to a flask and cooled to -10°C using a CaCl₂/ice bath. Concentrated sulfuric acid in a predetermined amount (1 mol eq. with respect to acetic anhydride, *Table 3.4*) was then added dropwise over 30 minutes in such a way so that the temperature did not exceed 0°C. A viscous and transparent liquid mixture containing acetyl sulfate and acetic acid was formed which was allowed to warm to room temperature. The prepared mixture was used immediately. The yield of formation of acetyl sulfate could not be determined due to the instability of the product. A complete conversion of sulfuric acid was assumed based on the literature reports [180, 185, 188, 189].

Sample	Acetic anhydride (ml) (mmol)	c. H ₂ SO ₄ (ml) (mmol)	Poly(styrene- <i>block</i> -butadiene) (g)	Acetyl sulfate:polymer (meq:meq)	T (°C)	Time (hrs)	Work-up
SSB1	0.753 7.980	0.213 3.996	0.500	0.72:1	25	1	A
SSB2	0.753 7.980	0.213 3.996	0.500	0.72:1	25	24	A
SSB3	1.506 15.96	0.427 8.010	0.500	1.4:1	25	24	A
SSB4	3.013 31.93	0.850 15.94	0.502	2.9:1	25	24	A
SSB5	6.025 63.86	1.698 31.85	0.501	5.74:1	25	24	B
SSB6	6.025 63.86	1.700 31.85	0.500	5.74:1	40	24	B
SSB7	12.05 127.7	3.400 63.78	0.505	11.49:1	25	3	A
SSB8	12.05 127.7	3.400 63.78	0.502	11.49:1	25	24	B
SSB9	12.05 127.7	3.400 63.78	0.501	11.49:1	25	48	B
SSB10	12.05 127.7	3.400 63.78	0.502	11.49:1	40	24	B
SSB11	18.07 191.5	5.093 95.5	0.500	17.2:1	25	24	B
SSB12	24.1 255.4	6.791 127.4	0.501	22.95:1	25	24	B

Table 3.4. The reaction conditions for sulfonation of poly(styrene-*block*-butadiene)

3.4.3. Sulfonation of poly(styrene-*block*-butadiene) with acetyl sulfate

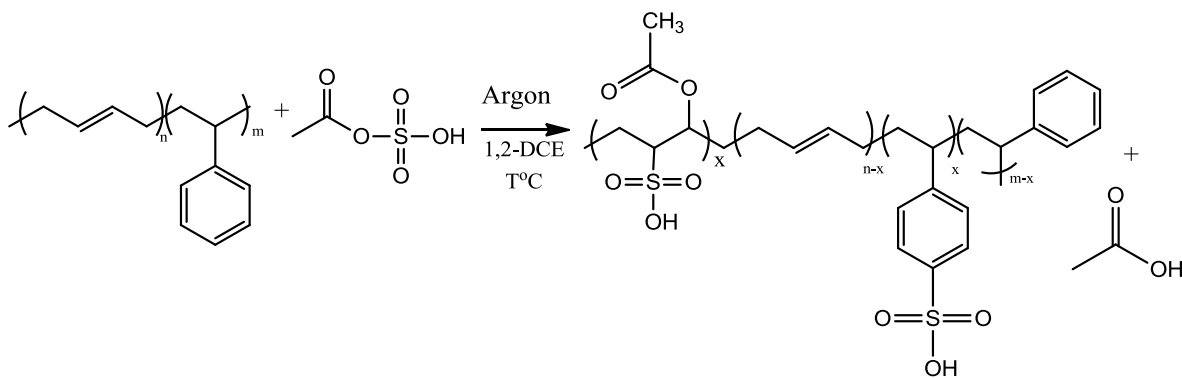


Figure 3.8. The reaction scheme for the sulfonation of poly(styrene-*block*-butadiene).

The glassware was dried in 100°C oven overnight, cooled down in a desiccator and flushed with dried argon before use. The reaction was carried out in a 2-neck 50 ml round bottom flask equipped with magnetic stirrer, reflux condenser, external thermocouple and argon inlet and outlet. Dried poly(styrene-*block*-butadiene) (0.501 g) was dissolved in dried 1,2-dichloroethane (1,2-DCE, 10 ml) at room temperature overnight under argon. A predetermined amount of mixture of acetyl sulfate and acetic acid that was synthesised in section 3.4.1 was added dropwise over 15 minutes to the polymer solution at a predetermined temperature (see *Table 3.4*). The mixture was stirred from 1 to 48 hours before the reaction was quenched with 10 ml of propan-2-ol. The quenching reagent was added slowly and dropwise over 10 minutes. Work-up A: The light brown slightly viscous mixture was precipitated in 500 ml of diethyl ether, filtered and washed with ~ 2 litres of diethyl ether until a neutral pH was attained. The pH was checked by the pH-indicator strips (pH 0-14, Merck Milipore Co.). The resulting samples were dried at room temperature in a desiccator under vacuum to a constant weight. The light brown to medium brown grainy solid was stored in a desiccator until required. Work-up B: The very dark brown and viscous mixtures were precipitated in 500 ml of 1,2-dichloromethane, filtered and diluted with 200 ml of water. The samples were placed inside dialysis tubing (MWCO=3500 Da) and dialysed against 2 litres of deionised water until neutral pH was achieved. Deionised water was replaced every hour for the first 12 hours then twice a day until neutral pH was reached (~ 1

week). The pH of extracting water phase was measured with pH-indicator strips (pH 0-14, Merck Milipore Co.). Polymer solutions were then transferred from the dialysis tube to a clean beaker and recovered by lyophilisation (Edwards Modulyo freeze dryer, West Sussex, UK). The dark brown fluffy product was stored in the desiccator until required.

The yield of sulfonation (Y) was determined gravimetrically:

$$Y(\%) = \frac{W_{sp}}{W_t} \cdot 100 \quad (5)$$

Where W_{sp} is the weight of purified sulfonated polymer and W_t is theoretical weight of polymer at the determined level of sulfonation.

The yield of sulfonation and degree of sulfonation is shown in *Chapter 7* section 7.2.1 *Table 7.1*. Typical ^1H NMR (**SSB6**) (400 MHz, 75% D_2O /25% d_8 -THF): δ (ppm) 1.0-2.0 (br, 19H, CH_2 and CH PS backbone, CH_2 and CH 1,2-PB backbone, CH_2 and CH 1,4-PB backbone, CH_3 acetyl, d_8 -THF), 3.1-3.4 (5H, $\underline{\text{CH}_2}\text{-SO}_3\text{H}$ and $\underline{\text{CH}}\text{-OCOCH}_3$, 1,2-PB and 1,4-PB, d_8 -THF), 4.5-4.8 (4H, $\underline{\text{CH}_2}=\text{CH}$ and $\text{CH}=\text{CH}$ PB if any present), 6.3 (2H, ArC-H , PS), 6.8-7.25 (3H, ArC-H PS), 7.25-7.75 (4H, ArC-H , PS sulf). FT-IR (neat) ν_{max} (cm^{-1}): 966 C=C, 1034 and 1162 O=S=O, 1650 $\text{ArC}=\text{C}$, 3100 C-H, 3490 OH.

The weight average molecular weight of the sulfonated copolymers could not be determined by Gel Permeation Chromatography, due to precipitation of the samples in GPC eluent arising from strong interactions between the sulfonate groups and interactions within the hydrophobic chains.

3.5. Characterisation methods

3.5.1. Nuclear Magnetic Resonance Spectroscopy (NMR)

^1H NMR was used to structurally characterize polymers and to determine the level of hydrophobic monomer incorporated into the copolymer. The NMR spectra of the monomers, synthesised polymers and poly(styrene-*block*-butadiene) were recorded on a 2 channel DRX-400 spectrometer (400 MHz, Bruker, Germany) using D_2O , $\text{d}_1\text{-CDCl}_3$ and d_8 -tetrahydrofurane as solvents at 25°C. Chemical shifts are expressed in parts per million (ppm, δ). The errors of the

measurements were limited by the accuracy of approximately 1-2% [198]. Spectra were processed using Mestrenova software version 7.0.2.

3.5.2. Fourier Transform Infrared Spectroscopy (FT-IR)

FT-IR spectra were recorded to determine the structure of polymers and acquired with a Fourier Transform-IR spectrometer with an ATR cell (Perkin Elmer, Spectrum 100, UK). The range of acquisition was from 4000 to 500 cm^{-1} at a resolution of 1 cm^{-1} . Twenty scans were acquired for each measurement.

3.5.3. Gel Permeation Chromatography (GPC)

GPC-50+ system (Polymer Laboratories Ltd) was used to analyse the molecular weight of the polymers. The system was equipped with a triple detector assembly: refractive index (PL-RI), viscosity (PL-BV 400RT) and light scattering (15° and 90° PL-LS) detectors. A guard column (PL Aquagel-OH Guard 8 μm 50x7.5 mm) and two columns (PL Aquagel-OH Mixed-H 8 μm 300x7.5 mm) were used in a series to separate the polymer molecules based on their hydrodynamic volume. The detectable molecular weight range is 100 to $10 \cdot 10^6$ $\text{g} \cdot \text{mol}^{-1}$. Polyethylene oxide (PEO) standards in a range of molecular weights 106 to 1258000 $\text{g} \cdot \text{mol}^{-1}$ (Polymer Laboratories Ltd) in form of Easy Vials and polyethylene oxide (PEO) of $M_w = 124700$ $\text{g} \cdot \text{mol}^{-1}$ (Polymer Labs) were used to calibrate all three detectors. The mobile phase used was composed of 20 % of methanol (HPLC Grade, VWR), 80 % of 0.1M NaNO_3 and 0.01% w/w NaN_3 in deionised water at the flow rate of 0.7 $\text{ml} \cdot \text{min}^{-1}$ at 25°C. Methanol was used to eliminate hydrophobic interaction in the polymers. The eluent was filtered through a series of in-line filters 0.25, 0.1 and 0.02 μm (Anodisc Millipore, Millipore Co. and Anotop 10 Plus with glass microfiber prefilter, Whatman) prior to use in order to remove any contamination that would interfere with the light scattering detector.

Samples were prepared by the dissolution of the polymers in filtered eluent for 24 hours at a concentration of 0.25 to 0.5 $\text{mg} \cdot \text{ml}^{-1}$ and additionally filtered through 0.22 μm polyethersulfone membrane Millex syringe filter (Millipore Co.) prior to injection. The chromatograms were analysed using PL Cirrus software v.3.0 (Polymer Laboratories Ltd).

3.5.4. Differential Scanning Calorimetry (DSC)

The thermal behaviour of the synthesised polymers and control samples was examined using a Differential Scanning Calorimeter (DSC, Q2000, TA Instruments, USA). The equipment was calibrated using indium and zinc standards to cover the studied temperature range between -150 °C to 250 °C. Samples were weighted into an aluminium Tzero pan with a hermetic Tzero lid and measured in a helium atmosphere at the rate of 10°C·min⁻¹. A sample size of 5 to 10 mg was used in each measurement.

3.5.5. Dynamic Mechanical Analysis (DMA)

The thermal behaviour and dynamic properties of the polymer samples were characterised using Dynamic Mechanical Analysis (DMA, Tritec 2000, Triton Technology Ltd, Keyworth, UK). DMA was performed in a dual beam cantilever bending mode with a gauge length of 10 mm. The sample was grinded mechanically using mortar and pestle. The ground sample of a weight approximately 15-20 mg was placed in the foldable stainless steel powder pocket (Triton Technology, Mettler Toledo). The storage modulus, loss modulus and tan delta ($\tan \delta$) were measured from 25°C to 250°C using a heating rate of 5°C·min⁻¹ at the frequency of 1 Hz.

3.5.6. Thermal Gravimetric Analysis (TGA)

The thermal degradation behaviour of the polymer samples was characterised using Thermal Gravimetric Analysis (TGA, Q500, TA Instruments, West Sussex, UK). A sample size of approximately 5 mg was used. The thermal behaviour was measured from 25 °C to 550°C at the heating rate of 10°C·min⁻¹. The measurements were carried out under a nitrogen atmosphere.

3.5.7. Elemental Analysis (EA)

Elemental analysis was used to determine carbon, hydrogen, nitrogen and sulfur content in polymer samples and to calculate the degree of sulfonation in sulfonated poly(styrene-*block*-butadiene). The analysis was carried out at University of Cambridge at the Department of Chemistry by Mr. Alan Dickerson and at University of Warwick by the Exeter Analytical-Elemental Analysis Services.

3.5.8. Determination of hydrophobic monomer content in copolymers

The content of n-decyl acrylamide in copolymers was determined by ^1H NMR and calculated using Equation 6 for polyacrylamide copolymers and Equation 7 for poly(N-hydroxyethyl acrylamide) copolymers:

$$DAAm (\text{mol}\%) = \frac{I_{0.8}}{3 \cdot I_{2.2} + I_{0.8}} \cdot 100 \quad (6)$$

$$DAAm (\text{mol}\%) = \frac{2 \cdot I_{0.8}}{3 \cdot I_{1.6} + 2 \cdot I_{0.8}} \cdot 100 \quad (7)$$

Since an intensity of a methyl peak in copolymers containing n-octadecyl acrylamide was too low, the integrals of methylene peak found at 1.2 ppm were used instead. Content of n-octadecyl acrylamide in copolymers was calculated using Equation 8 for polyacrylamide copolymers and Equation 9 for poly(N-hydroxyethyl acrylamide) copolymers:

$$ODAAM (\text{mol}\%) = \frac{I_{1.2}}{32 \cdot I_{2.2} + I_{1.2}} \cdot 100 \quad (8)$$

$$ODAAM (\text{mol}\%) = \frac{2 \cdot I_{1.2}}{32 \cdot I_{1.6} + 2 \cdot I_{1.2}} \cdot 100 \quad (9)$$

Where ODAAM is the content of n-octadecyl acrylamide in the copolymer in mol%, DAAm is the content of n-decyl acrylamide in the copolymer in mol%, $I_{0.8}$ is the integral area of methyl protons in n-decyl acrylamide, $I_{1.2}$ is the integral area of methylene protons in n-octadecyl acrylamide $I_{2.2}$ is the integral area of methine protons in the polyacrylamide backbone and $I_{1.6}$ is the integral area of methylene protons in poly(N-hydroxyethyl acrylamide) backbone (the exemplar ^1H NMR spectra of poly(acrylamide-co-n-decyl acrylamide) (**AD7**), poly(N-hydroxyethyl acrylamide-co-n-decyl acrylamide) (**HED1**), poly(acrylamide-co-n-octadecyl acrylamide) (**AOD3**) and poly(N-hydroxyethyl acrylamide-co-n-octadecyl acrylamide) (**HEOD1**) demonstrating integrals are shown in *Figure 3.9*, *Figure 3.10*, *Figure 3.11* and *Figure 3.12*).

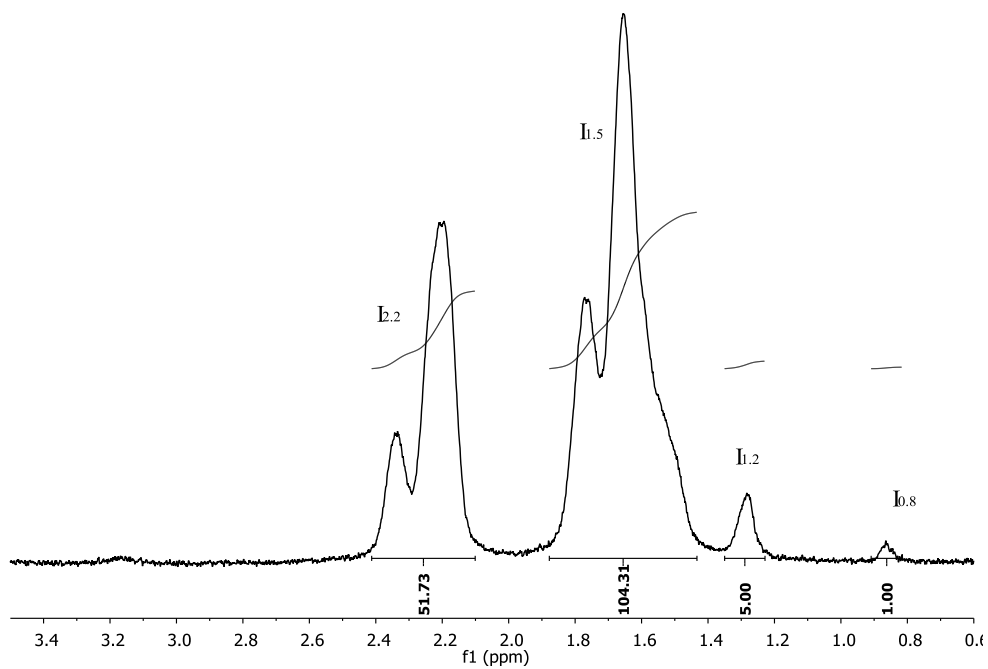


Figure 3.9. ^1H NMR spectrum of poly(acrylamide-co-n-decyl acrylamide) (**AD7**).

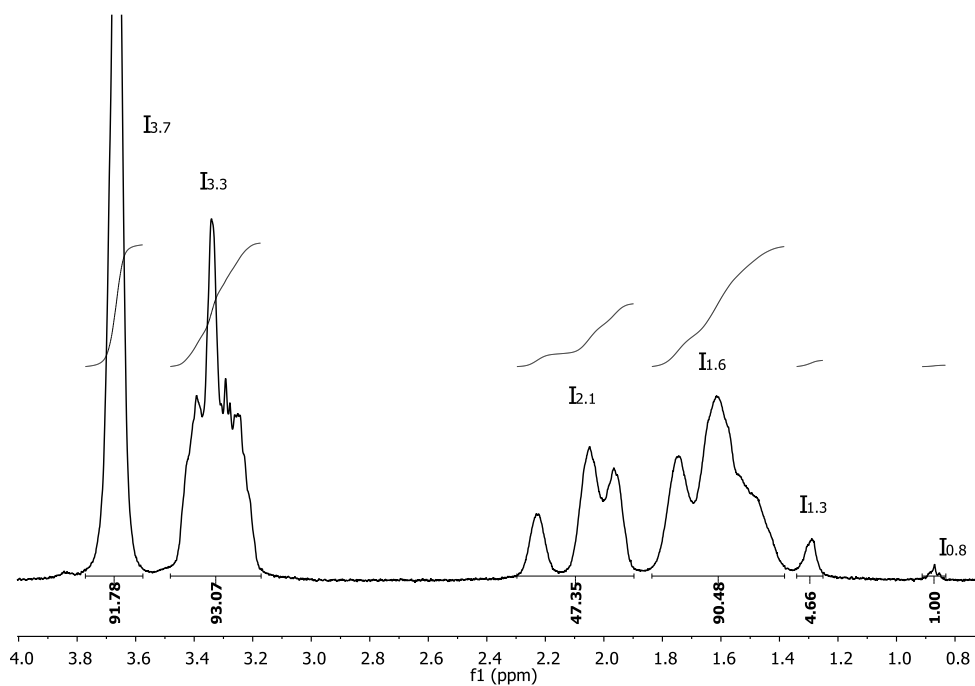


Figure 3.10. ^1H NMR spectrum of poly(N-hydroxyethyl acrylamide-co-n-decyl acrylamide) (**HED1**).

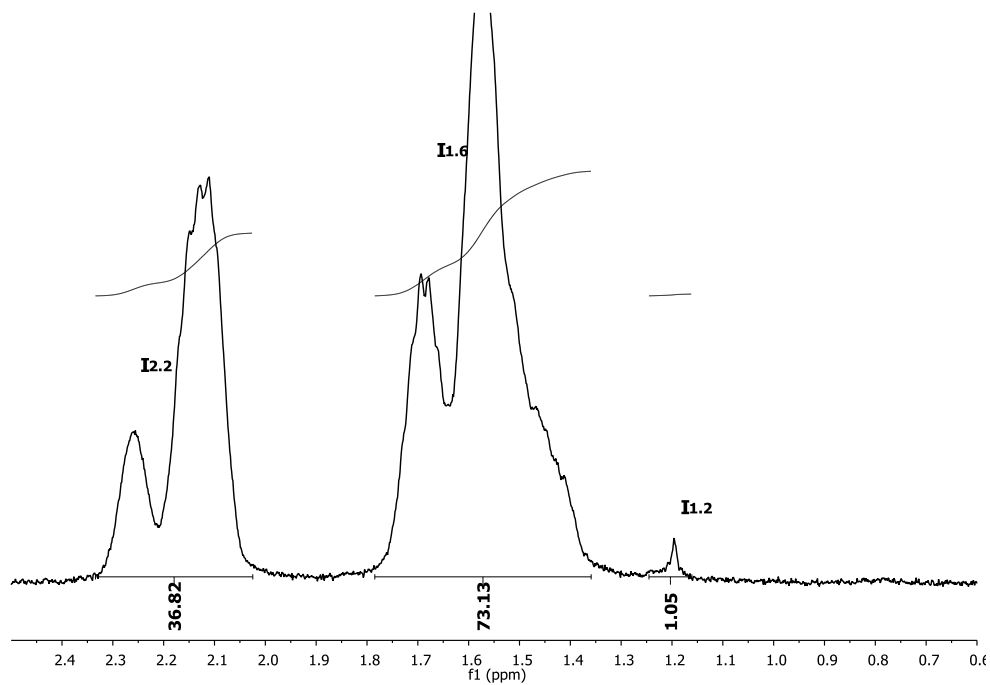


Figure 3.11. ¹H NMR spectrum of poly(acrylamide-co-n-octadecyl acrylamide) (AOD3).

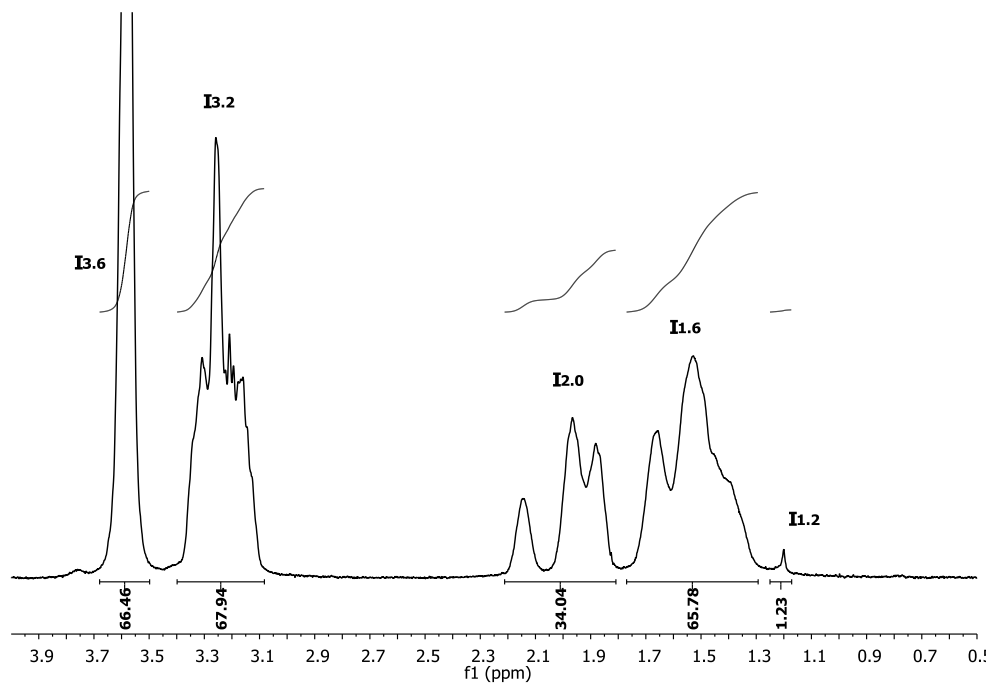


Figure 3.12. ¹H NMR spectrum of poly(N-hydroxyethyl acrylamide-co-n-octadecyl acrylamide) (HEOD1).

The content of hydrophobic monomer was also confirmed by elemental analysis. The analysis of the content of n-decyl acrylamide in poly(acrylamide-co-n-decyl acrylamide) and n-octadecyl acrylamide in poly(acrylamide-co-n-octadecyl acrylamide) is based on the formula 10 and 11, respectively:

$$DAAm(mol\%) = \frac{0.1\frac{C\%}{M_C} - 0.3\frac{N\%}{M_N}}{\frac{N\%}{M_N}} \cdot 100 \quad (10)$$

$$ODAAm(mol\%) = \frac{0.0555\frac{C\%}{M_C} - 0.167\frac{N\%}{M_N}}{\frac{N\%}{M_N}} \cdot 100 \quad (11)$$

The analysis of the content of n-decyl acrylamide in poly(N-hydroxyethyl acrylamide-co-n-decyl acrylamide) and n-octadecyl acrylamide in poly(N-hydroxyethyl acrylamide-co-n-octadecyl acrylamide) is based on the formula 12 and 13, respectively:

$$DAAm(mol\%) = \frac{0.125\frac{C\%}{M_C} - 0.626\frac{N\%}{M_N}}{\frac{N\%}{M_N}} \cdot 100 \quad (12)$$

$$ODAAm(mol\%) = \frac{0.0625\frac{C\%}{M_C} - 0.312\frac{N\%}{M_N}}{\frac{N\%}{M_N}} \cdot 100 \quad (13)$$

Where C% and N% are the weight percentages of carbon and nitrogen as determined by elemental analysis, M_C is the atomic mass of carbon $12.01 \text{ g}\cdot\text{mol}^{-1}$ and M_N is the atomic mass of nitrogen $14.01 \text{ g}\cdot\text{mol}^{-1}$.

The data is presented in Chapter 4 section 4.2.1 *Table 4.1* for copolymers of acrylamide and Chapter 6 section 6.2.1 *Table 6.1* for copolymers of N-hydroxyethyl acrylamide.

3.5.9. Determination of the degree of sulfonation

The degree of sulfonation in modified poly(styrene-*block*-butadiene) was determined using elemental analysis and calculated with the formula:

$$m_{CinPS}(g) = x_{PS} \cdot \left(\frac{1mol}{M_{PS}}\right) \cdot \left(\frac{8C}{1mol}\right) \cdot \left(\frac{M_C}{1C}\right) \quad (14)$$

$$m_{CinPB}(g) = y_{PB} \cdot \left(\frac{1mol}{M_{PB}}\right) \cdot \left(\frac{4C}{1mol}\right) \cdot \left(\frac{M_C}{1C}\right) \quad (15)$$

$$m_{Total C}(g) = m_{CinPS} + m_{CinPB} \quad (16)$$

$$n_{Total C}(moles) = \frac{(n_{PS}+n_{PB}) \cdot m_{C in EA}}{m_{Total C}} \quad (17)$$

$$S(mol\%) = \frac{m_{SEA}}{M_S} \cdot \frac{1}{n_{Total C}} \cdot 100 \quad (18)$$

Where m_{CinPS} is the mass of carbon in polystyrene, x_{PS} is the weight fraction of polystyrene in poly(styrene-*block*-butadiene) 83 wt%, M_{PS} is the molecular weight of styrene repeat unit 104.2 g·mol⁻¹, M_C is the atomic mass of carbon 12.01 g·mol⁻¹, m_{CinPB} is the mass of the carbon in polybutadiene, y_{PB} is the weight fraction of polybutadiene in poly(styrene-*block*-butadiene) 17 wt%, M_{PB} is the molecular weight of the butadiene repeat unit 54.048 g·mol⁻¹, $m_{Total C}$ is the total mass of carbon in polymer, $n_{Total C}$ is the total number of moles of carbon in polymer, n_{PS} is the number of moles of styrene in polymer, n_{PB} is the number of moles butadiene in polymer, $m_{C in EA}$ the mass of carbon in the copolymer obtained from elemental analysis, m_{SEA} is the mass of sulphur obtained from elemental analysis, M_S is the atomic mass of sulfur 32.065 g·mol⁻¹. The degree of sulfonation of sulfonated polymers is presented in Chapter 7 Section 7.2.1 *Table 7.1*.

3.5.10. Dynamic Light Scattering (DLS)

The hydrodynamic radius of polymer samples was determined using a Zetasizer Nano-S (Malvern, UK) equipped with a He-Ne laser source operating at $\lambda = 633\text{nm}$. Deionised water (“Option 4”, Water Purifier, ELGA) was used as a solvent and was filtered through 0.22 μm polyethersulfone membrane Milex syringe filter (Millipore Co.) before use. The polymer solutions were prepared by the dissolution of a known amount of polymer in the filtered solvent. After 48 hours of agitation on the shaker at 50 osc·min⁻¹ (KS 260 basic, IKA, Staufen, Germany), the solutions were filtered using a 0.22 μm polyethersulfone membrane Milex syringe filter

(Millipore Co.) directly into the measuring cuvette. The measurements were performed at 25°C with 120 s equilibration time and 120 s measurement time. Each sample was measured 10 times. Correlation curves were analysed with Zetasizer software v.6.01 through an inverse Laplace transformation using the constrained regularisation method (CONTIN).

3.5.11. Rheology

The rheology was carried out using an Anton Paar MCR 301 rheometer (Anton Paar GmbH, Ostfildern, Germany) equipped with double-gap Couette geometry. The measurements were performed at 25°C and the temperature was controlled with a Minichiller thermostatic bath (Huber, UK).

The apparent viscosity measurements at a constant shear of 10 s^{-1} were used to determine the apparent viscosity of the synthesized polymers at a range of concentrations and to determine the critical aggregation concentration (C_{agg}). Apparent viscosity measurements as a function of shear rate were also carried out to determine if polymers behave as Newtonian liquids. The curves were recorded in a stress-controlled mode. The tests were carried out three times to ensure reproducibility and the reported values are an average of these measurements. The error arising from equipment was 5%. Solutions for measurements were prepared by the dissolution of the polymer in deionised water to obtain a stock solution and agitated on the shaker set to $50 \text{ osc}\cdot\text{min}^{-1}$ for 48 hours. Sodium azide (0.02 % w/v) was added as a solid to every solution to prevent bacterial degradation. The stock solution was diluted to the required concentrations and shaken for a further 12 hours. The polymer samples containing α - and β -Cyclodextrin were prepared with the same method. α - and β -Cyclodextrin were added as solids or as a stock solution after the dissolution of polymer was complete. These solutions were shaken for a further 24 hours. The stock solution of each Cyclodextrin was prepared by dissolution of 0.015 g of solid in 30 g of deionised water. The Cyclodextrin solutions were then agitated at $250 \text{ osc}\cdot\text{min}^{-1}$ for 24 hours.

3.5.12. Instantaneous and time dependent drag reduction measurements

The drag reduction of polymer solutions was measured using the method developed by Nakken *et al.* [73, 199] with a Physica US200 rheometer (Physica Messtechnik GmbH, Stuttgart, Germany) equipped with a double-gap Couette geometry. The aspect ratio $\Gamma = \frac{H}{\delta^*}$ was 222, where δ^* is the gap between the rotor and stator $\delta^* = 0.5$ mm and H is the active rotor height (Figure 3.13). The measured sample was located in interconnected stationary cylindrically shaped stators between which a thin walled tube-shaped-rotor was placed. Above a minimum value of the angular velocity of the rotor, Taylor vortices appear in the outer half of the measuring geometry.

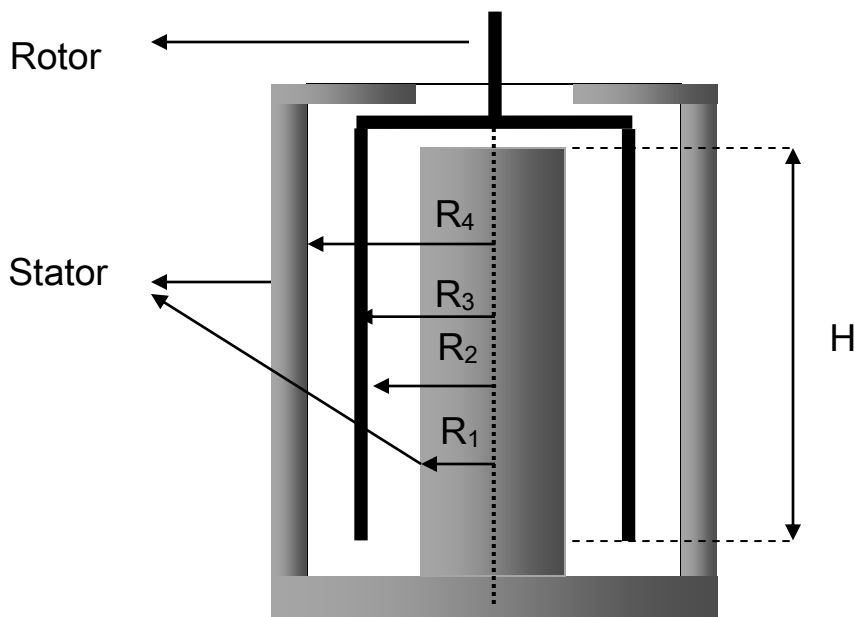


Figure 3.13. Schematic representation of the double gap cell with axial symmetry used for drag reduction study. The measuring cell active rotor height is $H = 111.00$ mm and the radii are $R1 = 22.25$ mm, $R2 = 22.75$ mm, $R3 = 23.50$ mm and $R4 = 24.00$ mm. The sample volume was 17 ml.

The drag reduction efficiency, the percentage of drag reduction (% DR), was calculated using the following equations [72, 73]:

$$DR(\%) = \left(100 - \frac{\eta_N^{Solution}}{\eta_N^{Solvent}} \cdot 100 \right)_{\eta_N=constant} \quad (19)$$

Where $\eta_N^{Solution/Solvent}$ is the normalized viscosity of the solvent and solution, respectively.

They are defined as:

$$\eta_N^{Solution} = \eta_{Taylor Area}^{Solution} - \eta_{Taylor Onset}^{Solution} \quad (20)$$

$$\eta_N^{Solvent} = \eta_{Taylor Area}^{Solvent} - \eta_{Taylor Onset}^{Solvent} \quad (21)$$

$$n_N = n_{Taylor Area} - n_{Taylor Onset} \quad (22)$$

Where $\eta_{Taylor Area}^{Solution/Solvent}$ and $\eta_{Taylor Onset}^{Solution/Solvent}$ is the apparent viscosity in the Taylor area and at the Taylor onset, respectively and n_N is a normalised rotor speed.

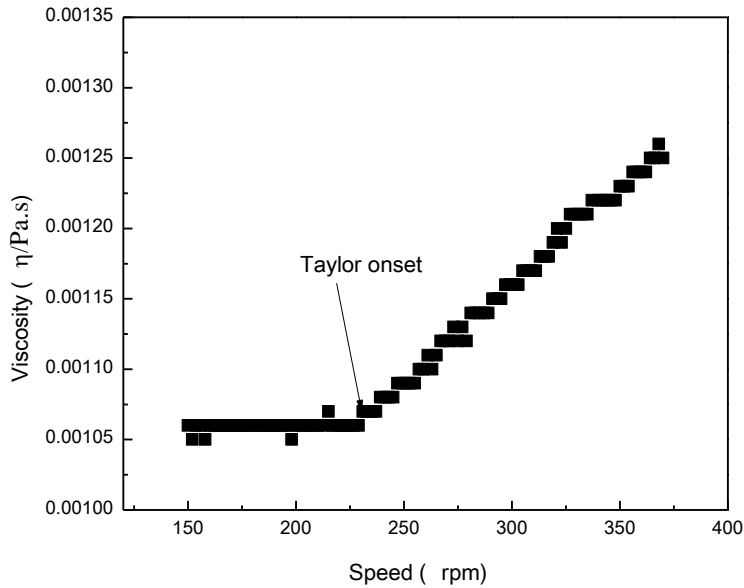


Figure 3.14. Taylor onset of polyacrylamide at $M_w = 1085$ kDa at $0.1 \text{ mg}\cdot\text{g}^{-1}$.

The viscosity at the Taylor onset was determined by measuring the apparent viscosity with increasing rotational speed of the rotor. Taylor onset can be observed as a rapid increase in

viscosity caused by the formation of Taylor vortices (*Figure 3.14*). The viscosity in the Taylor area (*Figure 3.15*) was measured at constant rotor speed of 2250 rpm which corresponds to a shear rate of 11200 s^{-1} and $Re \sim 2500$ in the Couette geometry and Re of 10^6 in a pipe flow. This shear rate was chosen since it is comparable to the shear rates experienced during hydraulic fracturing.

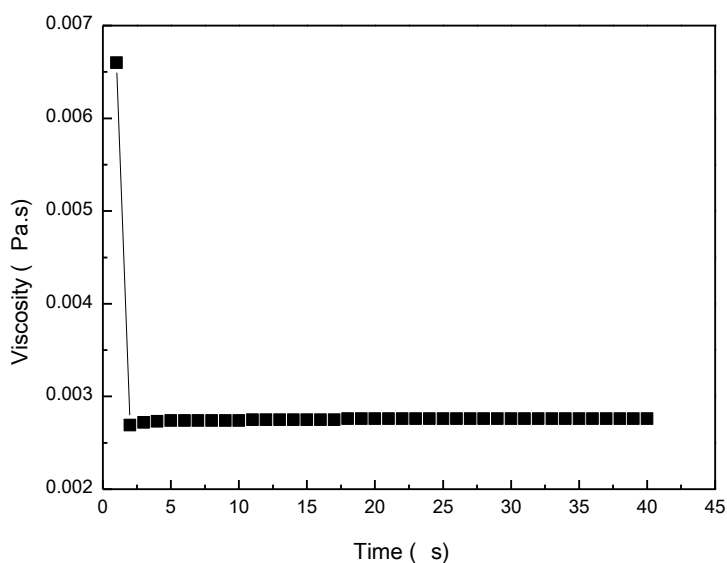


Figure 3.15. The apparent viscosity as a function of time at constant rotor speed of 2250 rpm (11200 s^{-1}) for polyacrylamide $M_w = 1085 \text{ kDa}$ at $0.1 \text{ mg} \cdot \text{g}^{-1}$.

Before each measurement, samples were equilibrated at zero shear for 5 minutes in order to reach the temperature equilibrium and polymer relaxation.

The measurements were carried out in triplicate using 17 ml of polymer sample. The temperature of the tests was set to $25 \pm 0.5^\circ\text{C}$ and controlled with a water circulatory thermostat (Julabo Series MV). During the time dependent drag reduction study; the sample was left for 1-3 hours in the cell in order to reach equilibrium after each pass at high shear rate, as well as to ensure full relaxation of the polymer. Polymer samples were prepared by dissolving a predetermined amount of polymer in deionised water to obtain a stock solution. The samples were shaken at $50 \text{ osc} \cdot \text{min}^{-1}$ for 24-48 hours. Sodium azide (0.02 % w/v) was added as a solid to each solution to prevent bacterial degradation. The stock solution was diluted to the required concentrations and

shaken for a further 12 hours. The polymer samples containing α - and β -Cyclodextrin were prepared using the same method as above. α - and β -Cyclodextrin were added as solids or as a stock solution after the dissolution of polymer was complete. These solutions were shaken for a further 24 hours. The stock solution of each Cyclodextrin was prepared by dissolution of 0.015 g of solid in 30 g of deionised water. The Cyclodextrin solutions were then shaken at $250 \text{ osc}\cdot\text{min}^{-1}$ for 24 hours.

API brine was prepared by the dissolution of 11.12 g of calcium chloride dihydrate and 90 g of sodium chloride in 900 ml of deionised water. The solvent was then filtered through a $0.45 \mu\text{m}$ syringe filter before use. The solution of 2 % (w/v) potassium chloride was obtained by dissolution of 20 g of KCl in 1 litre of tap water. The polymers containing API brine and KCl were first dissolved in deionised water to obtain stock solutions for 24-48 hours and the appropriate amount of salts was then added. This was done to avoid the prolonged dissolution time of hydrophobically modified PAAm copolymers in salt solutions. The solutions were diluted to the required concentrations with API brine or 2% (w/v) KCl solutions and shaken for a further 12 hours at $50 \text{ osc}\cdot\text{min}^{-1}$.

3.5.13. Adsorption and desorption study of polymers on silica

The adsorption of polymer from solution onto a silica surface and its subsequent desorption using Cyclodextrins was measured by Total Organic Carbon Analyser (TOC) (Shimadzu TOC-VCPN). Air was used as the carrier gas. In this method, the aqueous solution of a polymer at an unknown concentration is evaporised in the furnace of the TOC. The area of a peak determined and the concentration is calculated from the calibration curve. The calibration curve is obtained by running a series of polymer solutions at known concentrations. Polymer samples were prepared by dissolving a predetermined amount of polymer in deionised water to obtain a stock solution. The samples were agitated at $50 \text{ osc}\cdot\text{min}^{-1}$ for 24-48 hours. Sodium azide (0.02 % w/v) was added as a solid to each solution to prevent bacterial degradation. The stock solution was diluted to the required concentrations and shaken for a further 12 hours. The polymer samples used for calibration containing α - and β -Cyclodextrin (0.5, 1 and 100 mol eq. of Cyclodextrin with respect to 1 mol eq. of hydrophobic monomer) were prepared using the same method. α -

and β -Cyclodextrin were added as solids or as a stock solution after the dissolution of polymer was complete. These solutions were shaken for a further 24 hours. The stock solution of each Cyclodextrin was prepared by dissolution of 0.015 g of the solid in 30 g of deionised water. The Cyclodextrin solutions were then shaken at 200 osc·min⁻¹ for 24 hours.

The TOC equipment was calibrated using solutions of each polymer with and without Cyclodextrins at concentrations of 0.5 mg·g⁻¹, 0.25, 0.125, 0.08 and 0.05 mg·g⁻¹. The aqueous solutions of the polymers (15±0.05 g) at the predetermined concentration were added to microsilica (1±0.05 g) and shaken on a shaker at 200 osc·min⁻¹ at 25°C for 48 hours. These polymer solutions were used to determine the adsorption of polymers and were centrifuged (Sorvall Legend RT+, Thermoscientific) at 3000 rpm for 15 minutes. The polymer samples in deionised water at a concentration of 0.5 mg·g⁻¹ (used to determine the polymer desorption from a silica surface) were prepared as above. After 48 hours of polymer adsorption, α - or β -Cyclodextrin (0.5, 1 and 100 mol eq. of Cyclodextrin with respect to 1 mol of hydrophobic monomer) were added. The samples tubes were further shaken for 24 hours and then centrifuged as above. The supernatant was collected and the concentration of polymer in supernatant was tested by TOC. The measurements were performed in triplicate. The amount of adsorbed and desorbed polymer (Q_e) was calculated from the concentration of polymer in solution before and after adsorption (supernatant) from the mass balance equation as follows [200]:

$$Q_{e(mg \cdot g^{-1})} = (C_0 - C_e) \cdot \frac{W_p}{W_s} \quad (23)$$

Where C_0 and C_e are initial and equilibrium liquid-phase concentrations of polymers (concentration of polymer in supernatant) (mg·g⁻¹), respectively, W_p is the mass of polymer solution (g), and W_s is the mass of microsilica used (g).

3.5.14. Determination of solubility of sulfonated polymers

The solubility tests were performed using tetrahydrofuran, dimethyl sulfoxide, methanol, acetone and deionised water. Two concentrations were studied: 2.25 mg or 15 mg of each polymer was placed in a glass vial and 3 g of solvent was added. Samples were stirred using vortex mixer

(Votex Genie 2, G560, Scientific Industries Inc.) and shaken overnight on a shaker at 200 $\text{osc}\cdot\text{min}^{-1}$.

Solubility tests were also performed in THF/H₂O mixtures with compositions of 2, 5, 10, 15, 20, 25, 30, 35, 40, 45, 50 etc up to 95 vol % THF. The 2.25 mg of sample was placed in a glass vial and the solvent mixtures were added. Samples were stirred using vortex mixer (Votex Genie 2, G560, Scientific Industries Inc.) and shaken overnight on a shaker at 200 $\text{osc}\cdot\text{min}^{-1}$. The extent of polymer dissolution was determined visually.

3.5.15. Determination of solubility of hydrophobically modified polyacrylamide and poly(N-hydroxyethylacrylamide) copolymers

The solubility tests were performed using formamide and deionised water. 3 mg of each polymer was placed in a glass vial and 3 g of water or formamide was added. Samples were shaken for a minimum of 24 hours on a shaker at 200 $\text{osc}\cdot\text{min}^{-1}$. The extent of the polymer dissolution was verified visually i.e. when clear solutions were obtained dissolution was assumed.

Chapter 4

Hydrophobically modified polymers of acrylamide

4.1. Introduction

Drag reduction effect caused by polymers is affected by various parameters such as molecular weight of polymer, concentration of polymer, polymer-solvent interactions or the presence of associating groups in polymer [16, 17, 20, 21, 34, 35, 52, 55, 76]. Many theories to explain the mechanism of drag reductions have been proposed, however it is widely recognized that macromolecules interact with turbulent vortices and dissipate the energy thereby reducing the flow instabilities [56, 60, 77, 201, 202]. The subject of the utilisation of associating polymers as improved drag reducing agents has become topic of interest in the last decade [17, 18, 20]. This is due to the associating polymer's improved shear stability as compared to a non-associating homologue and the fact that intermolecular associations result in higher apparent molecular weight of the copolymer. It has been shown that although high molecular weight drag reducing polymers provide many advantages, they can undergo mechanical degradation in turbulent flow and lose their effectiveness after a short interval of time [75, 76]. The associated groups in associating polymers provide not only higher drag reduction due to the resulting higher apparent molecular weight of the associating copolymer but it is also recognised that the destruction of the secondary interactions rather than breakage of the polymer backbone is the foundation for improved shear stability [17, 20, 78, 79]. It is also predicted that the associating polymer would reassociate upon removal of the shear force and as a result could be reused again as a drag reducer. Hydrophobically modified associating polymers are water soluble polymers containing small quantities of hydrophobic groups. In aqueous solution, intermolecular associations with hydrophobic groups are formed resulting in enhanced viscosity as compared to unmodified homologue [25, 121, 124, 125, 128, 130, 203-207]. These copolymers have been recognised to reduce drag, however the information on some features of these polymers in regards to drag

reduction remain limited [19, 26, 27]. The role of the molecular variables, such as the alkyl chain length in the hydrophobic monomer or concentration of the hydrophobic moieties in the polymer backbone, in the shear stability of hydrophobically modified polyacrylamide were among the unresolved issues tackled in this Chapter.

In this Chapter, the synthesis of hydrophobically modified acrylamide polymers via micellar polymerisation is reported. The details of the synthesis and polymer characterisation procedures are reported in Chapter 3. This method of polymerisation was chosen because it offered the possibility to synthesise relatively high molecular weight water soluble polymers, in addition to creating polymers with hydrophobic groups randomly distributed as blocks along the polymer backbone. The incorporation of hydrophobic monomers as blocks is attributed to the high local concentration of hydrophobic monomer in the surfactant micelles and the high probability of the addition of all of the hydrophobic monomer residing in the interior of the surfactant micelles to the growing polyacrylamide radical as described by Hill *et al.* [122]. The influence of hydrophobic modification on rheology and drag reducing properties of hydrophobically modified PAAm in deionised water and in the presence of salts is demonstrated. The shear resistance of polymers as a function of the concentration of hydrophobic groups in copolymers was also studied.

4.2. Results and discussion

4.2.1. Synthesis and characterisation of polymers of acrylamide

Hydrophobically modified polymers of acrylamide were successfully synthesised via micellar copolymerisation in water. The concentration and type of the hydrophobic monomer was varied to obtain polymers with different associating behaviour and these parameters are shown in *Table 4.1*. Hydrophobic monomers containing short and long alkyl chains were chosen to study the influence of the monomer type on the strength of hydrophobic association. It is believed that the longer alkyl chain in n-octadecyl acrylamide should lead to stronger associations between hydrophobic groups. The initial concentration of monomers in water was set at 3 and 20 % (w/w) in order to obtain polymers with high molecular weight (according to Equation 24).

Sample	Yield (%)	M _w (kDa)	PDI	N _H	H (mol%) in feed	H (mol%) ^{EA}	H (mol%) ^{NMR}	Solubility H ₂ O/Formamide
AD1	2.042 75.0	Ns	ns	13.0	5.01	5.02	ns	-/+
AD2	2.256 87.8	Ns	ns	7.58	2.99	3.1	ns	-/+
AD3	2.353 95.7	Ns	ns	3.74	1.49	1.6	ns	-/+
AD4	2.034 90.9	Ns	ns	2.57	0.92	1.1	ns	-/+
AD5	2.348 97.3	210	1.4	2.11	0.85	0.89	0.85	+/+
AD6	2.107 87.8	486	1.8	1.61	0.61	0.62	0.61	+/+
AD7	2.134 88.4	974	2.8	2.06	0.79	0.64	0.65	+/+
AD8	2.108 87.8	864	1.2	1.58	0.62	0.55	0.54	+/+
AD9	1.887 79.1	1163	1.9	1.08	0.45	0.35	0.33	+/+
AD10	2.084 87.9	1074	1.5	0.60	0.29	0.23	0.21	+/+
AOD1	2.222 92.5	Ns	ns	1.08	0.43	0.44	ns	-/+
AOD2	2.001 84.1	Ns	ns	0.60	0.245	0.23	ns	-/+
AOD3	1.938 82.0	1345	1.7	0.24	0.099	0.10	0.09	+/+
PAAm0	1.954 83.0	1896	1.3	0	0	0	0	+/+

Table 4.1. Yield, molecular weight M_w, hydrophobic monomer content H and solubility of polymers in water and formamide obtained by micellar polymerisation. – or + denotes insoluble or soluble in deionised water or formamide, respectively. ns denotes insoluble in either GPC eluent, deionised water or D₂O, hence analysis not possible, **AD**= poly(acrylamide-co-n-decyl acrylamide). **AOD**= poly(acrylamide-co-n-octadecyl acrylamide).

The solubilisation of hydrophobic monomers was achieved by addition of sodium dodecyl sulfate kept at a constant level (concentrations above CMC, see Chapter 3, Section 3.2.1). In addition, solutions containing n-octadecyl acrylamide were heated to 80°C to aid monomer solubility. The number of hydrophobic monomers per surfactant micelle N_H (Equation 4 Chapter 3) was varied by modifying the initial proportion of hydrophobic monomer with respect to surfactant concentration. Homopolyacrylamide was also synthesised under identical conditions to the copolymers shown in *Table 4.1* at 20 % (w/w) initial monomer content and used as a reference in order to determine the effect of the modification on the polymer properties.

The presence of hydrophobic moieties in the copolymer and the composition of the copolymers were determined using 1H NMR. Elemental Analysis was additionally used to verify the results obtained by NMR and to determine the content of hydrophobic moieties in polymers that were insoluble in water. The 1H NMR spectra of n-decyl acrylamide and n-octadecyl acrylamide were recorded in $CDCl_3$ and their spectra are presented in *Figure 4.1* and *Figure 4.4*, respectively. The 1H NMR spectra of polyacrylamide and water soluble copolymers were recorded in D_2O . The spectrum of the homopolymer (**PAAm0**), a typical spectrum of poly(acrylamide-co-n-decyl acrylamide) (**AD7**) and poly(acrylamide-co-n-octadecyl acrylamide) (**AOD3**) are presented in *Figure 4.2*, *Figure 4.3* and *Figure 4.5*, respectively. Protons characteristic for polyacrylamide, n-decyl acrylamide and n-octadecyl acrylamide were identified and assigned (*Figure 4.1*, *Figure 4.2* and *Figure 4.4*). In the spectrum of n-decyl acrylamide and n-octadecyl acrylamide, the chemical shifts for protons from the methylene groups (CH_2) marked as B-I and J (or B-Q and R in n-octadecyl acrylamide) can be distinguished in the 1.2-1.6 ppm range and at 3.3 ppm, respectively. The strong triplet from the protons of the methyl groups (CH_3) signal A appears at 0.8 ppm. In the spectrum of polyacrylamide (**PAAm0**) (*Figure 4.2*), peaks in the range of 1.2 and 3.2 ppm correspond to the protons of the methylene (A) and methine (B) groups in the polymer backbone. All of the protons corresponding to **PAAm0** and the protons corresponding to the alkyl chains of n-decyl acrylamide, A and B-J could be identified and assigned in the 1H NMR spectrum of poly(acrylamide-co-n-decyl acrylamide) (*Figure 4.3*). This confirmed that n-decyl acrylamide was successfully incorporated into the copolymer structure.

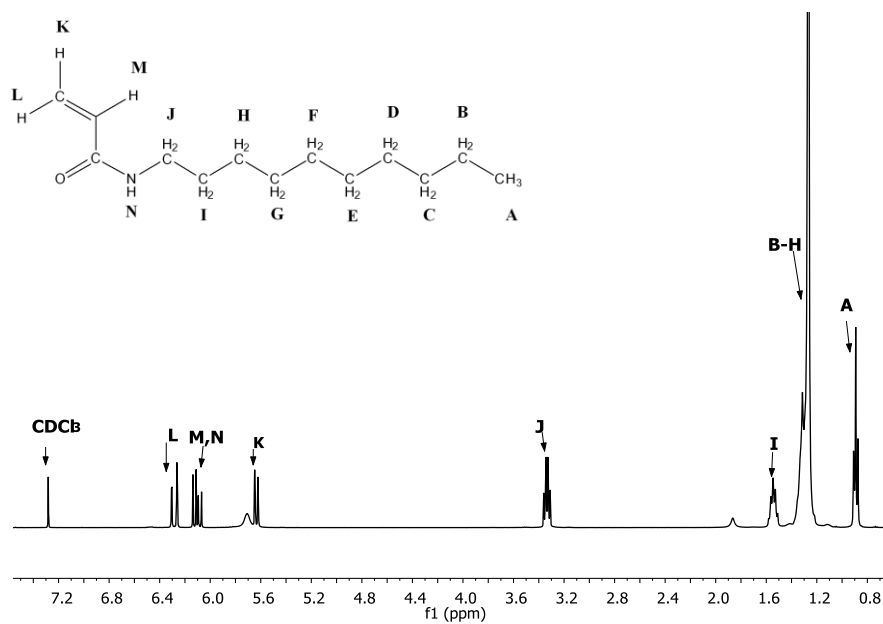


Figure 4.1. ¹H NMR spectrum of n-decyl acrylamide recorded in CDCl₃.

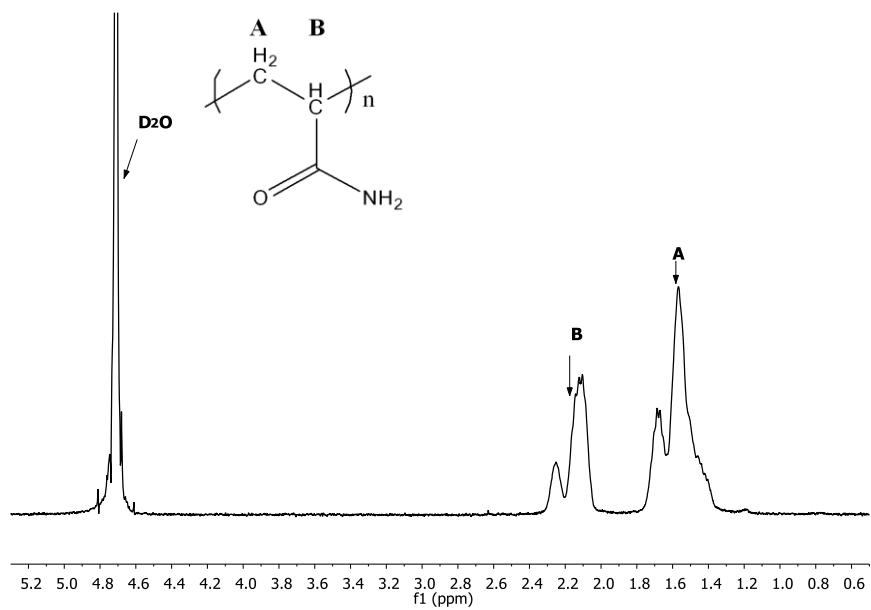


Figure 4.2. ¹H NMR spectrum of polyacrylamide acquired in D₂O (PAAm0).

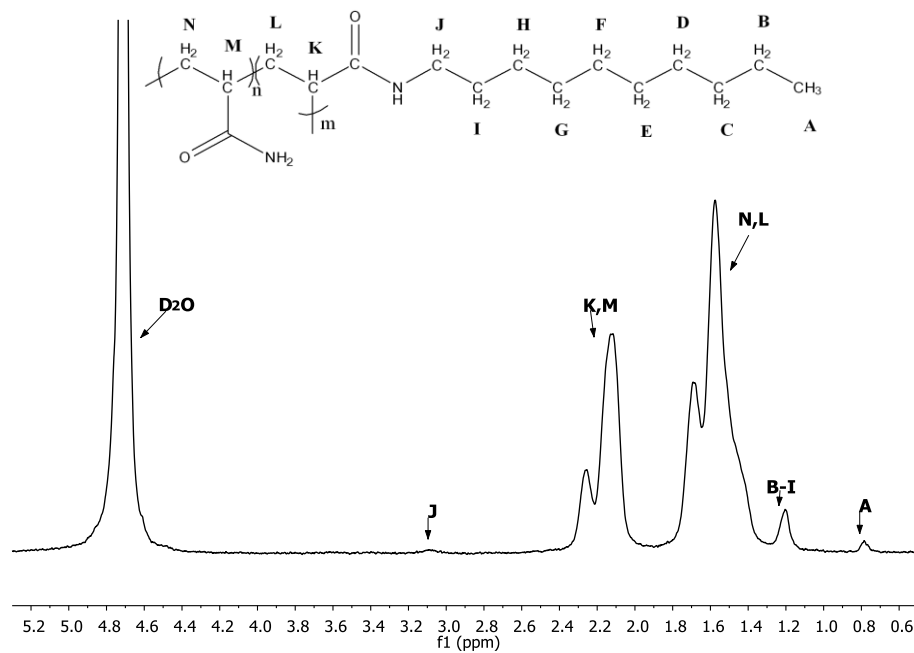


Figure 4.3. The example of ^1H NMR spectrum of poly(acrylamide-co-n-decyl acrylamide) in D_2O (**AD7**, 0.65 mol% DAAm).

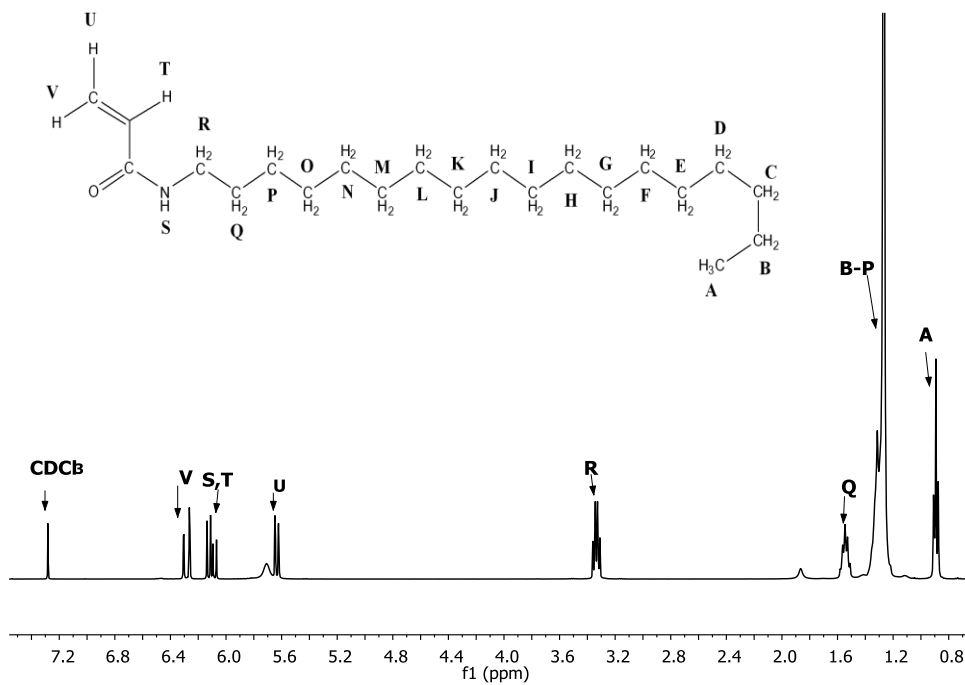


Figure 4.4. ^1H NMR spectrum of n-octadecyl acrylamide recorded in CDCl_3 .

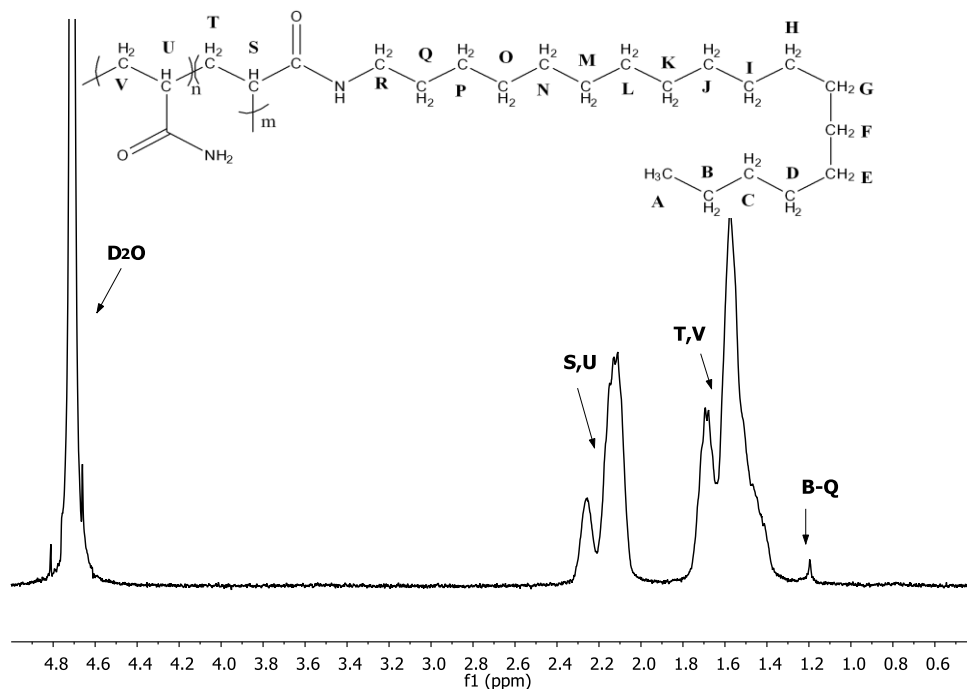


Figure 4.5. ¹H NMR spectrum of poly(acrylamide-co-n-octadecyl acrylamide) in D₂O (**AOD3**, 0.09 mol% ODAAm).

All of the protons for **PAAm0** and the protons from the alkyl chains of n-octadecyl acrylamide, B-Q could be identified and assigned in the ¹H NMR spectrum of poly(acrylamide-co-n-octadecyl acrylamide) (Figure 4.5). This confirmed that n-octadecyl acrylamide was successfully incorporated into the copolymer structure. Protons A and R could not be assigned due to low concentration of n-octadecyl acrylamide.

The extremely low concentration of hydrophobic moieties in copolymers led to difficulties in assessing the concentration of the hydrophobic monomer that was incorporated into the copolymer, since the sensitivity of the NMR technique (1-2 % [198]) was above the detection limit. Thus, the presented values from NMR analysis (Table 4.1) should be treated with a certain level of uncertainty. The polymer composition determined from both NMR and Elemental Analysis appeared to be in relatively good agreement. Some small composition drift from the initial monomer feed for some copolymers was however observed (see Table 4.1). This drift could be linked to compositional heterogeneity of copolymer with an increase in conversion due to rapid incorporation and early depletion of the hydrophobic monomer in the course of the

polymerisation. The initial rapid incorporation of hydrophobic monomer could be observed, especially at higher N_H ($N_H > 2.1$) and higher concentration of hydrophobic monomers ($[H] > 0.8-0.85$ mol%) which could be linked to the higher reactivity of hydrophobic monomer because of the solubilisation in the surfactant micelles [121, 124]. The drift in composition was also described by Hill *et al.* [122] to be due to the flux of the hydrophobic monomers from the swollen micelles to the micelles in which growing radical head presently resides. Hill *et al.* also suggested that the drift in composition could be due to the interaction of surfactant with the growing copolymer chain that affect the rate of this flux, and the partial intermixing of acrylamide and hydrophobic monomer in the interfacial micellar region.

During the micellar polymerisation procedure, the reaction mixtures remained homogeneous and viscous when the concentration of hydrophobic monomer in the feed and N_H was low ($[H] < 0.8-0.85$ mol% and $N_H < 2.1$). It appeared gel-like (hard gel) when the N_H number and the concentration of hydrophobic monomer in the feed was high ($[H] > 0.8-0.85$ mol% and $N_H > 2.1$). *Table 4.1* shows that there were a number of copolymers that was insoluble in water. The insolubility was particularly evident for copolymers synthesised at high values of N_H (> 2.1) (suggesting that the length of the hydrophobic monomer blocks increased with increasing N_H) and at high concentration of hydrophobic moieties ($[H] > 0.8-0.85$ mol%). These copolymers were not chemically crosslinked since they were readily soluble in formamide and in aqueous solution of the surfactant (sodium dodecyl sulfate). The dissolution of copolymers in aqueous solution of surfactant was due to the surfactant-copolymer interactions i.e. surfactant micelles solubilised hydrophobic moieties of the copolymer. This demonstrates that the water solubility was dominated by the strength of hydrophobic interaction. Thus, the extent of solubility of copolymers containing n-octadecyl acrylamide was reduced as compared to copolymers containing n-decyl acrylamide of identical initial hydrophobic monomer concentration. Copolymers containing > 0.1 mol% of n-octadecyl acrylamide ($N_H > 0.24$, **AOD1** and **AOD2**) were not soluble in water. Similarly the copolymers containing n-decyl acrylamide were not soluble in water at hydrophobic monomer concentrations above 0.8 and 0.85 mol% ($N_H > 2.1$). Similar dissolution problems were also reported in the literature for hydrophobically modified polyacrylamides [126, 130, 208].

The molecular weights of the water soluble polymers were determined by GPC in a mixture of 0.1 M sodium nitrate in deionised water and methanol (80 and 20 vol% respectively). Methanol was added to the eluent in order to disrupt the hydrophobic interactions. The molecular weights of the polymers were found to be largely dependent on the concentration of the hydrophobic moieties in copolymers and the initial concentration of hydrophobic and hydrophilic monomers in the polymerisation mixture. The molecular weights were found to increase with decreasing N_H and decreasing concentration of hydrophobic moieties in copolymers. Similar behaviour was observed for copolymers synthesised via micellar polymerisation by Biggs *et al.* [121] and Jianping *et al.* [209] and were attributed to an increase in the chain transfer on the surfactant, or on the impurities present in the surfactant, and the radical transfer reactions onto the hydrophobic groups. The increase in the molecular weight with an increase in the overall monomer concentration in the initial monomer mixture is consistent with Equation 24 [210, 211] indicating that with an increase in the initial concentration of monomer (for ideal polymerisation kinetics), the number average degree of polymerisation \overline{Xn} increases:

$$\overline{Xn} = \zeta \frac{k_p}{(2fk_d k_{t(pp)})^{1/2}} \cdot \frac{[M]}{[I]_0^{1/2}} \quad (24)$$

Where ζ is the degree of coupling of chains, k_p is the propagation rate constant, $k_{t(pp)}$ is the termination rate constant for 2 polymers (coupling or disproportionation), k_d is the initiator dissociation rate constant, f is the radical yield, $[M]$ is the monomer concentration in the feed and $[I]_0$ is the initial concentration of initiator,

The data in *Table 4.1* show that the yield of polymerisation was lower than 100 % (see *Table 4.1*). At high concentration of the monomers in the feed (20 wt%), the viscosity of the polymerisation mixture became high as the conversion of polymerisation increased; hence the polymerisation became controlled by diffusion of the propagating species [211]. The comparable effect was seen at high concentrations of hydrophobic monomer being incorporated ($N_H > 2.1$ and $[H] > 0.8-0.85$ mol%). The high concentration of hydrophobic monomer ($N_H > 2.1$ and $[H] > 0.8-0.85$ mol%) led to the enhanced viscosity of the monomer mixture during polymerisation due to

stronger intermolecular hydrophobic association (physical crosslinking of hydrophobic moieties due to overlap of macromolecules) [210].

4.2.2. Rheology of polymers of acrylamide

The effect of the content and the type of the hydrophobic moiety on the apparent viscosity of aqueous polymer solutions was studied as a function of copolymer concentration, using a rheometer equipped with double-gap geometry at constant shear rate of 10 s^{-1} . The results are illustrated in *Figure 4.6* and *Figure 4.7*.

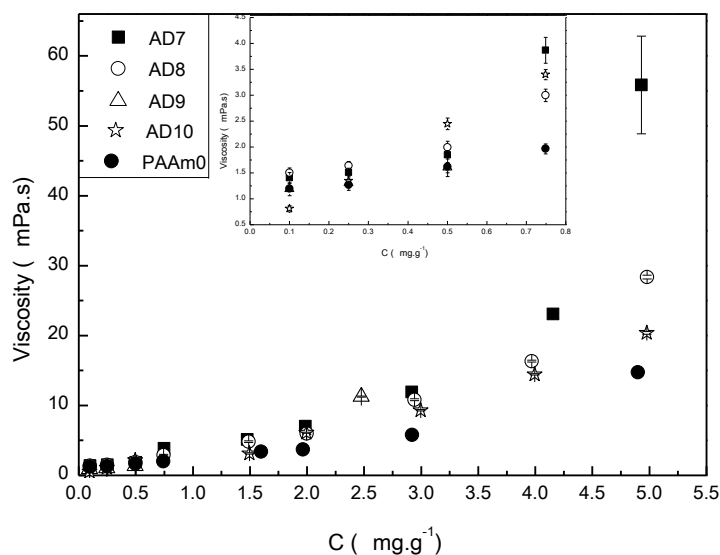


Figure 4.6. The apparent viscosity at $\dot{\gamma} = 10 \text{ s}^{-1}$ and at $T = 25^\circ\text{C}$ of the aqueous solutions of PAAm and its copolymers with n-decyl acrylamide as a function of polymer concentration (inset shows close-up of low concentrations).

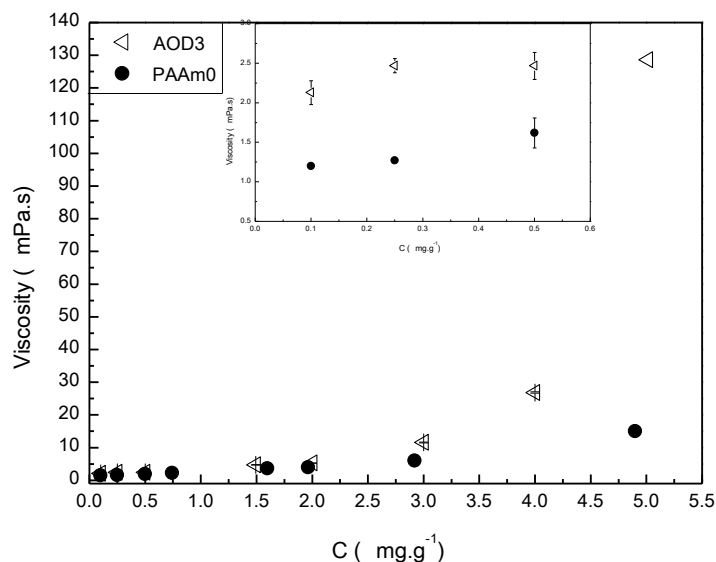


Figure 4.7. The apparent viscosity at 10 s^{-1} and at $T = 25^\circ\text{C}$ of the aqueous solutions of PAAm and its copolymer with n-octadecyl acrylamide (**AOD3**, 0.09 mol% ODAAm) as a function of concentration (inset shows close-up of low concentrations).

At low polymer concentration ($<1 \text{ mg}\cdot\text{g}^{-1}$) the apparent viscosity of aqueous polymer solutions of copolymers **AD9** (0.33 mol% DAAM, $N_{\text{H}} = 1.08$, $M_{\text{w}} = 1163 \text{ kDa}$) and **AD10** (0.21 mol% of DAAM, $N_{\text{H}} = 0.60$, $M_{\text{w}} = 1074 \text{ kDa}$), copolymers with short n-decyl acrylamide blocks, was comparable, whereas the viscosity of copolymers **AD7** (0.65 mol% DAAM, $N_{\text{H}} = 2.06$, $M_{\text{w}} = 974 \text{ kDa}$), **AD8** (0.54 mol% DAAM, $N_{\text{H}} = 1.58$, $M_{\text{w}} = 864 \text{ kDa}$) and **AOD3** (0.09 mol% ODAAM, $N_{\text{H}} = 0.24$, $M_{\text{w}} = 1345 \text{ kDa}$) was higher than the apparent viscosity of polyacrylamide (**PAAm0**, $M_{\text{w}} = 1896 \text{ kDa}$). Moreover, the copolymer containing n-octadecyl acrylamide **AOD3** had the highest apparent viscosity of all of the copolymers in the dilute region. The behaviour of poly(acrylamide-co-n-decyl acrylamide) copolymers (**AD** series) was as expected. The strength of the hydrophobic interaction increases with increasing the length of the hydrophobic block i.e. increasing N_{H} , therefore copolymers **AD7** and **AD8** had higher apparent viscosity than copolymers **AD9** and **AD10**. The general behaviour of the hydrophobically modified polyacrylamide is that at very dilute concentrations, the chains collapse due to the intramolecular hydrophobic associations, which results in viscosities lower than that of the homopolymer [122,

132]. The behaviour observed for some copolymers suggests that a certain degree of intermolecular hydrophobic aggregation between neighbouring alkyl chains in copolymers was present even in the dilute regime. Similar observation was made by Turner *et al.* [117], hang *et al.* [212], Grassl *et al.* [213] and Lin *et al.* [214] for water soluble hydrophobically modified polymers containing hydrophobic moieties with fluorine atoms, short alkyl chain hydrophobic moieties or hydrophobically modified polyacrylamide prepared by post-modification. The greater apparent viscosity of copolymer **AOD3** compared to all other copolymers could be associated with the greater hydrophobic character of the copolymers containing n-octadecyl acrylamide (due to longer alkyl chain), in comparison to the copolymers containing n-decyl acrylamide. The higher apparent viscosity of copolymer **AOD3** over the other copolymers in the **AD** series (poly(acrylamide-co-n-decyl acrylamide)) could be also attributed to its higher molecular weight (*Table 4.1*).

The apparent viscosity of polymers **AD8** (0.54 mol% DAAM, $N_H= 1.58$, $M_w= 864$ kDa), **AD9** (0.33 mol% DAAM, $N_H= 1.08$, $M_w= 864$ kDa), **AD10** (0.21 mol% DAAM, $N_H= 0.60$, $M_w= 1074$ kDa) and **PAAm0** ($M_w= 1896$ kDa) increased linearly with concentration. This behaviour was as expected. Above a polymer concentration of $2 \text{ mg}\cdot\text{g}^{-1}$, these copolymers showed an even greater increase in apparent viscosity (as compared to low concentration) in comparison to the apparent viscosity of **PAAm0**. The behaviour of copolymers could be attributed to the strengthening of intermolecular associations between the polymeric chains containing hydrophobic moieties due to overlap of macromolecules, and the resulting higher apparent molecular weights. The increase in apparent viscosity was in range of half to two times that of the apparent viscosity of polyacrylamide. The copolymers **AD7** (0.65 mol% DAAM, $N_H= 2.06$, $M_w= 974$ kDa) and **AOD3** (0.09 % ODAAM, $N_H= 0.24$, $M_w= 1345$ kDa) also demonstrated the linear development of apparent viscosity with concentration, however at a concentration above $2 \text{ mg}\cdot\text{g}^{-1}$ a more dramatic increase in apparent viscosity was observed as compared to other copolymers and **PAAm0**. Moreover at a concentration of $5 \text{ mg}\cdot\text{g}^{-1}$, the apparent viscosity of copolymer **AOD3** was twice as much as the value observed for copolymer **AD7** and ten times as much as compared to **PAAm0** (*Figure 4.6* and *Figure 4.7*). This behaviour was the result of the stronger interaction between the n-octadecyl acrylamide moieties in the copolymer **AOD3** leading to higher apparent

molecular weight. Copolymer **AD7** had the longest incorporated blocks of n-decyl acrylamide (highest N_H) therefore the strength of the intermolecular hydrophobic association in this copolymer was also the greatest above all copolymers is **AD** series. The dramatic increase in the apparent viscosity that was observed for all the copolymers, occurred at concentrations lower than the overlap concentration (C^*) of polyacrylamide at higher molecular weight (**PAAm0**, $M_w = 1896$ kDa, $C^* \sim 3$ mg·g⁻¹). This concentration corresponded to the critical aggregation concentration (C_{agg}) and the observations on the behaviour of hydrophobically modified polyacrylamide in this research work were in the agreement with previous reports [26, 215].

4.2.3. Instantaneous drag reduction study of polymers of acrylamide

The influence of the concentration of aqueous solutions of PAAm and its copolymers on their drag reduction effect was studied using a rheometer equipped with double-gap Couette geometry at 25°C. The drag reduction of polyacrylamide synthesized under micellar polymerisation conditions (**PAAm0**, $M_w = 1896$ kDa, PDI = 1.3) and commercial polyacrylamide (**PAAmC**, $M_w = 1085$ kDa, PDI = 2.05) was also studied as a comparison. The drag reduction values reported were the maximum drag reduction achieved in the first 5 minutes of measurements for all the polymer concentrations studied. The experimental results shown in *Figure 4.8* for the water soluble copolymer in the **AD** series (poly(acrylamide-co-n-decyl acrylamide)) and in *Figure 4.9* for copolymers in the **AOD** series (poly(acrylamide-co-n-octadecyl acrylamide)), indicated that the extent of the drag reduction effect caused by polymers increased with increasing polymer concentration. The drag reduction (DR) imparted by polymers as a function of concentration followed the classical trend, i.e. drag reduction increased with polymer concentration until a plateau was reached (*Figure 4.8* and *Figure 4.9*). This plateau is called the optimum polymer concentration C_{opt} . Beyond this concentration, any further increases in concentration did not lead to any significant increase in drag reduction effect [13, 73, 83].

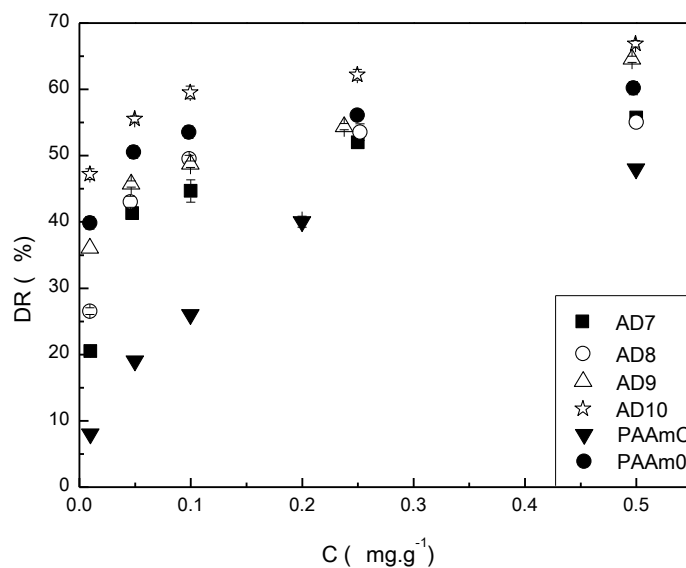


Figure 4.8. Percentage drag reduction as a function of polymer concentration for commercial PAAm (**PAAmC**, $M_w= 1085$ kDa), control **PAAm0** ($M_w= 1896$ kDa) and copolymers of PAAm with n-decyl acrylamide. Measured at shear rate $\gamma= 11200$ s⁻¹ and 25°C.

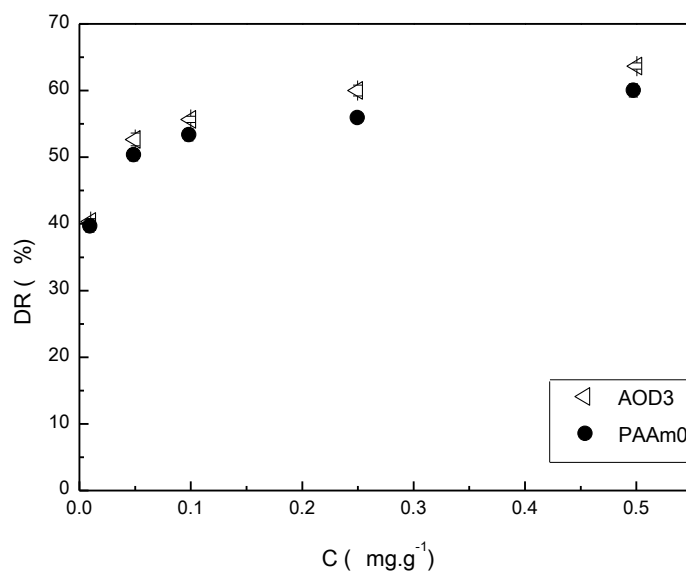


Figure 4.9. Percentage drag reduction as a function of polymer concentration for **PAAm0** ($M_w= 1896$ kDa) and its copolymer with n-octadecyl acrylamide (**AOD3**, $M_w= 1345$ kDa). Measured at shear rate $\gamma= 11200$ s⁻¹ and 25°C.

The comparative studies of drag reduction (DR) produced by copolymers and homopolymers indicated improved drag reduction performance for all copolymers at the concentrations studied. Although the percentage of the drag reduction for the copolymers of PAAm and n-decyl acrylamide was generally larger than the percentage drag reduction for **PAAmC** ($M_w=1085$ kDa), the values of the drag reduction for copolymers of PAAm (apart from copolymer **AD10**) were smaller than that of **PAAm0** ($M_w=1896$ kDa). The lower drag reduction performance of **AD7**, **AD8** and **AD9** in comparison to **PAAm0** was due to lower apparent molecular weight and rather strong hydrophobic interactions (than **AD10**). For example at polymer C= $0.5 \text{ mg}\cdot\text{g}^{-1}$, the drag reduction of the copolymers **AD10** ($M_w=1074$ kDa, 0.21 mol% DAAM) and **AOD3** ($M_w=1345$ kDa, 0.09 mol% ODAAM) was 66.67 ± 0.47 and 63.67 ± 0.47 % whereas for **PAAm0** ($M_w=1896$ kDa) and **PAAmC** ($M_w=1085$ kDa) it was $60\pm 1\%$ and 48%, respectively (*Table 4.2*). The improved performance of **AOD3** ($M_w=1345$ kDa, 0.09 mol% ODAAM) in comparison to **PAAm0** ($M_w=1896$ kDa) was not as evident. Taking into consideration the difference in the weight average molecular weight (M_w), this copolymer offered comparable drag reduction at lower molecular weight. The observed behaviour could be explained by the presence of intra- and intermolecular associations as evidenced by Dynamic Light Scattering (DLS) (*Table 4.2*) and rheology at constant shear rate (*Figure 4.6* and *Figure 4.7*). It is recognized that the coil volume has a profound effect on drag reduction. Polymers with greater hydrodynamic volume promote higher drag reduction [19, 201]. The hydrodynamic radius of all the copolymers was higher than the hydrodynamic radius of polyacrylamides, confirming the presence of intermolecular associations in aqueous solutions of copolymers. The presence of intramolecular associations can be also concluded from the size of the hydrodynamic radius. If only intermolecular hydrophobic associations were present in the copolymer, the radius of the copolymer would be expected to be twice the radius of the polyacrylamide. The hydrodynamic radius for the hydrophobically modified polyacrylamide was ~ 1.2 to 1.6 higher than the radius of commercial polyacrylamide (**PAAm0**). This suggests the presence of both intra- and intermolecular hydrophobic interactions in the aqueous solutions of hydrophobically modified polyacrylamide.

Sample	M_w (kDa)	PDI	N_H	H^{NMR} (mol%)	$DR_{0.5mg\cdot g^{-1}}$ (%)	R_H (nm)
AD7	974	2.8	2.06	0.65	55.7±0.43	95.8±3.70
AD8	864	1.2	1.58	0.54	55.0±0.00	78.5±1.50
AD9	1163	1.9	1.08	0.33	64.1±0.47	103±2.20
AD10	1074	1.5	0.60	0.21	66.7±0.47	98.0±6.00
AOD3	1345	1.7	0.24	0.09	63.7±0.47	92.9±1.80
PAAm0	1896	1.3	0	0	60.0±1.00	76.6±3.20
PAAmC	1085	2.1	0	0	48.0±0.00	63.6±2.70

Table 4.2. Weight average molecular weight M_w , polydispersity index PDI, hydrophobic monomer content H , drag reduction (DR) determined at $C=0.5mg\cdot g^{-1}$ and hydrodynamic radius R_H for copolymers and polymers of acrylamide; **AD**= poly(acrylamide-co-n-decyl acrylamide), **AOD**= poly(acrylamide-co-n-octadecyl acrylamide), **PAAm0** and **PAAmC** are homopolymers of acrylamide synthesised under micellar polymerisation conditions and obtained from a commercial source, respectively.

The drag reduction effect caused by copolymers of PAAm in the **AD** series (poly(acrylamide-co-n-decyl acrylamide)) was found to increase with decreasing concentration of the hydrophobic moieties and increasing the length of hydrophobic block (increasing N_H). This effect was found to be most evident at copolymers concentration of $\sim 0.01 mg\cdot g^{-1}$. One could argue that the observed trend in the drag reduction effect could be attributed to slightly higher molecular weight, however copolymer **AD10** had a lower molecular weight (1074 kDa, 0.21 mol% DAAM, $DR\%=66.7$ at $0.5 mg\cdot g^{-1}$ and $DR\%\sim 48$ at $0.01 mg\cdot g^{-1}$) than **AD9** (1163 kDa, 0.33 mol% DAAM, $DR\%=64.1$ at $0.5 mg\cdot g^{-1}$ and $DR\%\sim 35$ at $0.01 mg\cdot g^{-1}$) yet displayed higher drag reduction effect. The drag reduction effect imparted by polymers is related to ability of polymer to interact and disrupt turbulent vortices. The observed trend in drag reducing performance of the copolymers could be attributed to increasing concentrations and increasing block length of the hydrophobic moieties. Copolymer **AD7** contained the highest concentration of n-decyl acrylamide and longest hydrophobic block (0.65 mol% DAAM, $N_H= 2.08$) and was characterised by the strongest

hydrophobic interaction from all of the copolymers in the **AD** series (poly(acrylamide-co-n-decyl acrylamide)). This means that the copolymer **AD7** was unable to efficiently unravel during interactions with the Taylor vortices. A similar trend was observed by Bock *et al.* [27] and Mumick *et al.* [79].

4.2.4. Time dependent drag reduction of polymers of acrylamide

It is often observed that molecular chains in polymer solutions are subjected to mechanical scission under high shear in turbulent flow. This form of polymer degradation results in a decrease in the observed level of drag reduction [69, 83]. The degradation of the polymer can be linked to one of the proposed mechanism of drag reduction i.e. the macromolecules are elongated by shear stresses associated with turbulent flow [216]. It has been proposed that aggregates might offer some resistance to polymer shear degradation in turbulent flow since the breakage of secondary bonds should preferably occur instead of cleavage of the polymer backbone [20]. The secondary bonds could then reform in quiescent conditions and as a result, the polymer could be reused [18, 26]. The decrease in the drag reduction performance of polymers is generally attributed to the mechanical degradation of the polymer backbone and corresponding decrease in molecular weight. Changes in the drag reduction performance of aqueous solutions of acrylamide polymers in Taylor Flow over time were therefore investigated using a rheometer equipped with a Couette double-gap cell at 25°C. The shear stabilities of polymer solutions were elucidated at constant shear of 11200 s⁻¹ over 1800 s during 6 shearing cycles. The polymer was allowed to relax after each shearing cycle for 2-3 hours. The longer relaxation time was not attempted due to the possibility of the solvent evaporation during prolonged residence of the polymer in a Couette cell. The effect of repeated application of shearing force on the polymer solutions of acrylamide are shown in *Figure 4.10* and *Figure 4.11*.

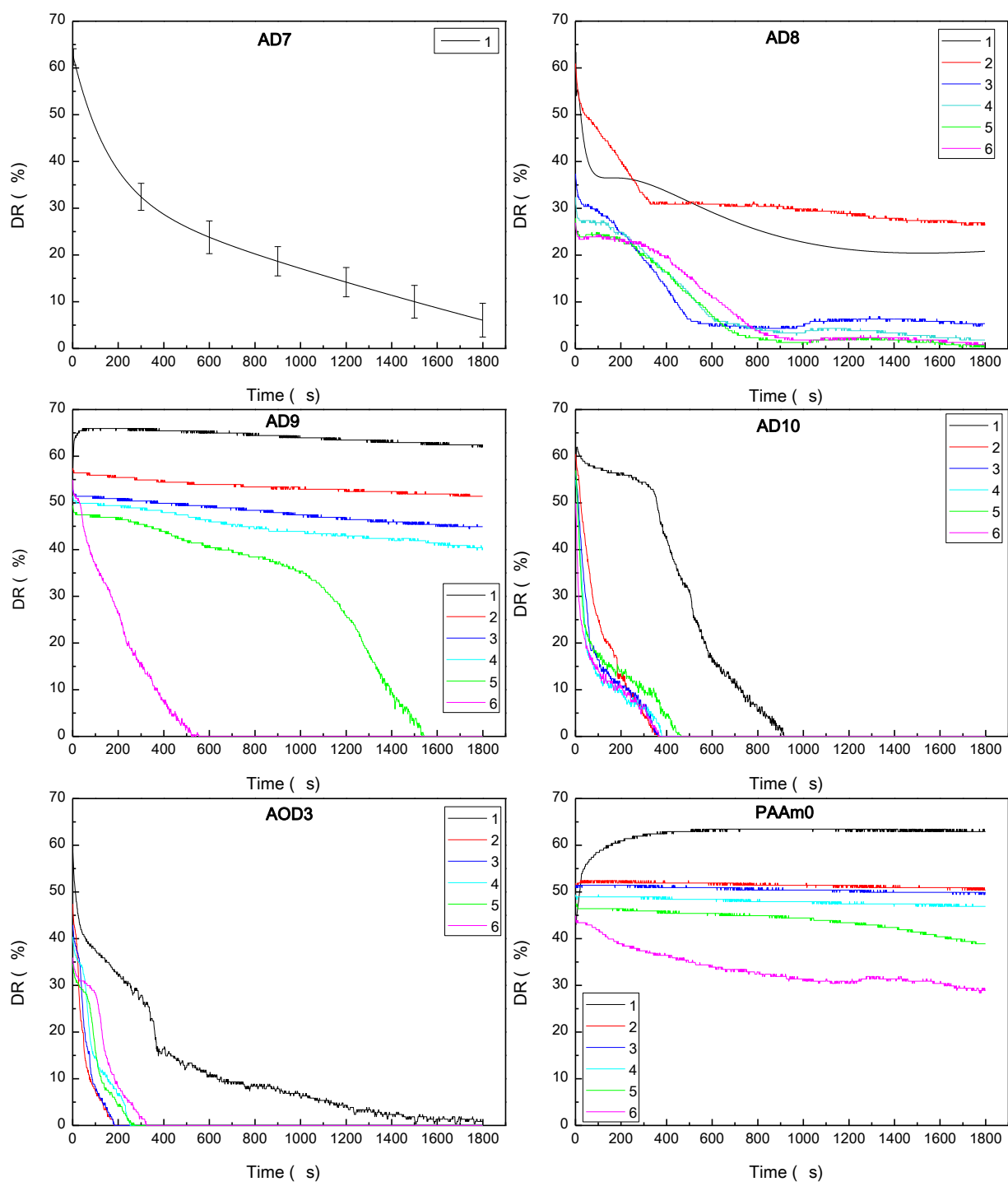


Figure 4.10. Evolution of drag reduction with shearing time for the polymers of acrylamide. Studied at a shear rate of 11200 s^{-1} , 25°C and at polymer $C = 0.5 \text{ mg}\cdot\text{g}^{-1}$. Error 0.5 to 1.5 %. 1 to 6 is the number of a shearing cycle.

The drag reduction of **PAAm0** (*Figure 4.10*, $M_w = 1896$ kDa) was found to increase as a function of time during the first shearing cycle and remained nearly constant during three subsequent shearing cycles. The similar behaviour for high molecular weight polyacrylamide was also demonstrated by Zadrazil, which was explained by the possible elongation of polymer molecules in turbulent flow [83]. The observed decrease in drag reduction effect for **PAAm0** from ~62 to ~54 % in the second cycle could be attributed to mechanical degradation of polyacrylamide [83]. The decrease in drag reduction effect caused by **PAAm0** in subsequent shearing cycles was found to be smaller. As a result, the final value of drag reduction displayed by **PAAm0** after the 6th cycle reached ~45 %. This behaviour is consistent with observation made by Zadrazil.

All of the copolymers, except copolymer **AD9** (0.33 mol% DAAM (n-decyl acrylamide)), demonstrated a decreased drag reduction effect as a function of time. The drag reduction imparted by copolymers **AD10** (0.21 mol% DAAM) and **AOD3** (0.09 mol% ODAAM (n-octadecyl acrylamide)) was found to decrease rapidly with time, with drag reduction disappearing completely after 900 s and 1200 s during the first shearing cycle, respectively and ~300 s during the subsequent cycles. The fast disappearance of drag reduction could be explained by the existence of weak intermolecular interactions that could become easily disrupted by the turbulent vortices. This behaviour was most likely due to the low content of hydrophobic moieties in these copolymers. The aforementioned copolymers resembled behaviour of weak surfactants that dissociated in turbulent flow and recovered its ability to reduce drag after removal of shearing force [35, 217]. The ability of the recovery of drag reduction was particularly evident for copolymer **AD10**, which showed its drag reduction almost unchanged during the second shearing cycle (*Figure 4.11*). This suggested that the intermolecular interactions became preferentially destroyed upon shearing instead of the scission of polymer backbone. The exposure of copolymer **AD10** to the turbulent flow in subsequent shearing cycles could have resulted in the mechanical scission of the polymer backbone, although it is also possible that the aggregates formed by an intermolecular hydrophobic association of polymer chains were not rebuilt. This was evident in the value of drag reduction in the final shearing cycle (6th), which was ~12 % lower than the initial value of drag reduction (DR_0 66.7 % to $DR_{\text{final pass}}$ ~53 %). Copolymer **AOD3** did not recover its ability to reduce drag

and the drag reduction effect was found to be lower by 10 % after the 1st shearing cycle, and this could have been due to either the mechanical degradation of this copolymer. The drag reduction effect was found to decrease further in the subsequent shearing cycles until a plateau of 35 % drag reduction was reached. The behaviour of the copolymer was most likely related to the small concentration of hydrophobic moieties (~ 0.09 mol%), which was not sufficient enough to prevent mechanical degradation of the backbone in this copolymer.

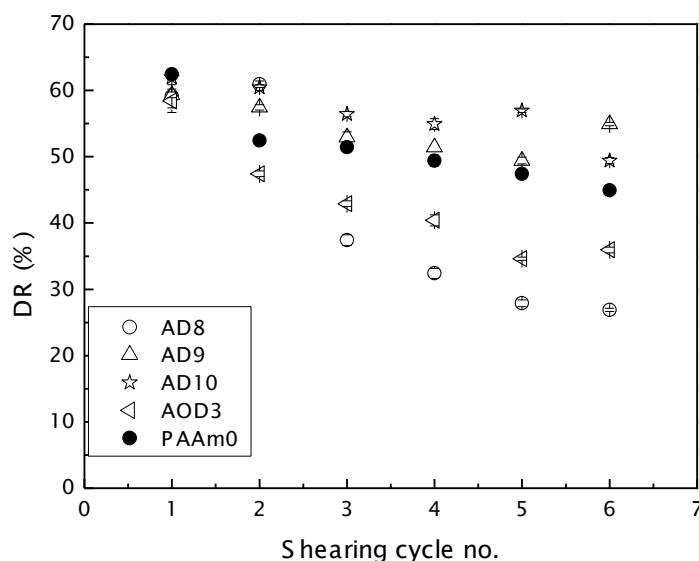


Figure 4.11. The variation of drag reduction as a function of shearing cycle number in Taylor flow for copolymers of PAAm. Measured with a double-gap cell at shear rate of 11200 s^{-1} , 25°C and at polymer $C=0.5 \text{ mg}\cdot\text{g}^{-1}$.

The drag reduction by copolymer **AD9** increased as a function of time during the first shearing cycle and remained constant in three subsequent shearing cycles. The observed initial increase in drag reduction effect by copolymer **AD9** could be caused by the formation of a transient gel-like network. This network is created by the physical interaction of the hydrophobic moieties introduced into the backbone of the copolymer and most likely formed during the elongation of the molecules in turbulent flow. The proposed mechanism is shown in *Figure 4.12*. The polymer in quiescent conditions exists in the intra- or/and intermolecularly associated form (as evidenced by the rheology and the size of hydrodynamic radius) (1). However in turbulent flow the polymer

elongates and absorbs and dissipates the energy from the vortices (2 and 3). Eventually, the elongated polymer coils meet in the near-wall region and form transient gel-like network connected via hydrophobic groups (4), which then interact with the remaining vortices. Due to absorption of turbulent energy, the polymer network becomes destroyed (5). Upon removal of the shearing force, the polymer recovers and intra- or/and intermolecular associations reform (6). As a result of gel-like network formation, the drag reduction of copolymer **AD9** was found to decrease only slightly during subsequent shearing cycles. This behaviour confirms that the formation of the flexible physical network is responsible for the shear resistance of this copolymer. The mechanism based on the formation of polymer layers in the near-wall region was recently proposed by Zadrazil [60, 83]. The author based his assumptions on the data obtained for poly(ethylene oxide) and polyacrylamide. This mechanism seems to be valid for the copolymers synthesised in this thesis.

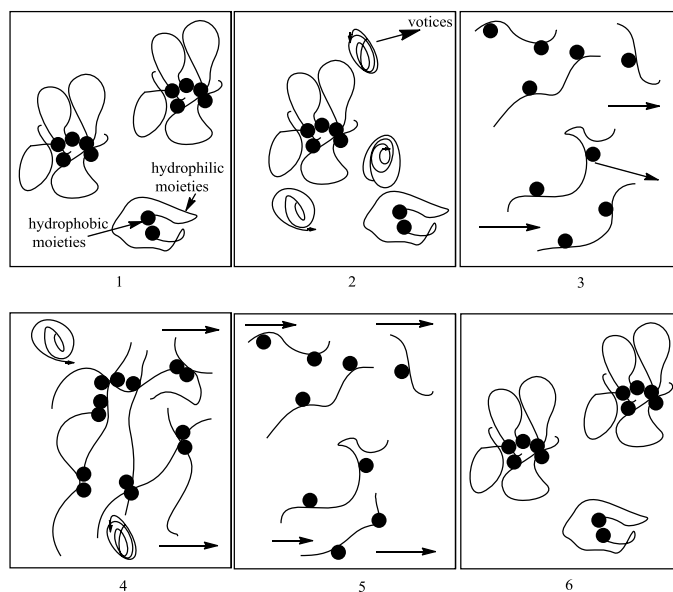


Figure 4.12. The schematic illustration of the proposed mechanism for the interaction of associating polymers of PAAm containing hydrophobic moieties with turbulent vortices. 1. Quiescent conditions, polymer in the intra- or/and intermolecularly associated form; 2. Collision of turbulent vortices and the resulting polymer elongation and vortices destruction; 3. Formation of a gel-like transient network with elongated chains containing associating groups; 4. Collision of turbulent vortices and gel-like network; 5. Dissociation of gel-like network under the shear; 6. Recovered associating polymer in quiescent conditions.

The drag reduction by copolymer **AD8** (0.54 mol% of DAAM) was maintained at its initial level during second shearing cycle which suggests that the formation of physically crosslinked network was responsible for the shear resistance of this copolymer. The subsequent shearing cycles however, were found to lower drag reduction (DR). Ultimately, the final drag reduction (6th shearing cycle) was found to plateau at ~33 % which was much lower than the initial drag reduction (55 %). This suggests that the mechanical degradation of the polymer backbone could be the cause of decreased drag reduction. Such behaviour cannot be attributed to the lack of the copolymer's ability to form a strong physically crosslinked network, since the concentration of the hydrophobic groups in this copolymer was greater than in copolymer **AD9**. To reveal the cause of the decrease in drag reduction, the viscosity of copolymer **AD8** was studied as a function of time at a constant shear rate of 1000 s⁻¹ after the 1st shearing cycle. *Figure 4.13* demonstrates the recovery of the copolymer to be very slow and complex.

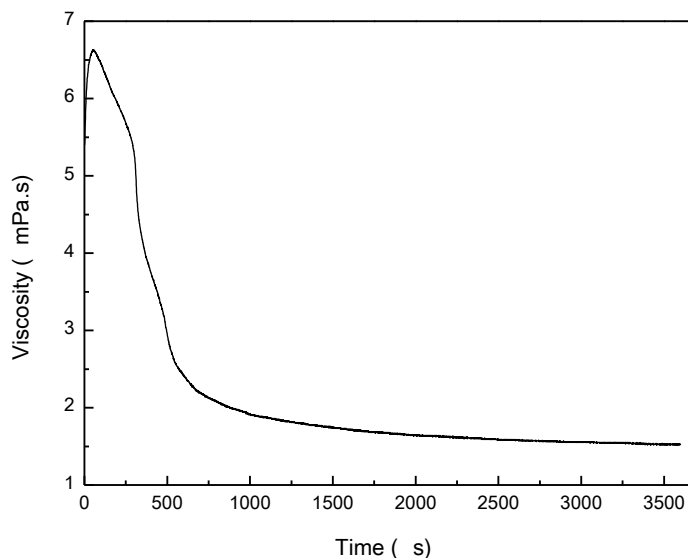


Figure 4.13. Apparent viscosity of poly(acrylamide-co-n-decyl acrylamide) (**AD8**, 0.54 mol% DAAM) as a function of time. Measured at 1000 s⁻¹ after 1st shearing cycle and after 60 min. relaxation at 0 shear rate.

Slow relaxation of the copolymer could imply only partial reformation of the intermolecular polymer network in the subsequent shearing cycles. The decrease in drag reduction in subsequent

shearing cycles for copolymer **AD8** could suggest that the physically crosslinked network did not reform and as a result lower drag reduction was observed for this copolymer. Lower drag reduction could have been also caused by the mechanical degradation of this copolymer.

It should be noted that the shear stability of copolymer **AD7** as a function of a number of shearing cycles was also quantified however the results are not shown. The reason for this is that the Taylor onset in the subsequent shearing cycles could not be determined. The relaxation of polymer upon removal of shearing force was not reached even after 3 hours. Long residence time in the rheological cell could result in the evaporation of water and therefore would result in changes in the polymer concentration. The longer relaxation time was therefore not attempted.

4.2.5. Influence of solvent quality on drag reduction of polymers of acrylamide

Although pure water is nowadays often used in hydraulic fracturing processes, surface, brackish or sea water are among the most common fluids used for the oilfield operations [218-220]. Solvent quality is an important factor affecting polymer's performance in the drag reduction. The presence of these ions is predicted to affect the efficiency of the associating polymers, since the hydrophobic interactions are enhanced in the presence of salts. It has also been suggested that the performance of polymers is influenced by the water structure [19, 79]. Thus, compounds promoting hydrophobic bonding such as small concentrations of salts were found to improve drag reduction performance, whereas additives such as urea promoting changes in structure of water were found to decrease the efficiency of drag reduction. The drag reduction by polymers was therefore studied in artificial sea water (API brine). Additionally, the effect of 2% (w/w) ($0.268 \text{ mol}\cdot\text{L}^{-1}$) of aqueous solution of potassium chloride, solvent that is also used in the hydraulic fracturing by oil-servicing companies, was also tested on selected polymers.

The results shown in *Figure 4.14* indicated that the drag reduction effect (DR) caused by the copolymers dissolved in brine containing high concentration of n-decyl acrylamide moieties (0.65 mol% and 0.54 mol% of DAAM) remained fairly unchanged. However, the drag reduction by copolymer **AD7** (0.65 mol% DAAM) decreased by 4% at a polymer concentration of $0.5 \text{ mg}\cdot\text{g}^{-1}$, whereas drag reduction by copolymer **AD8** (0.54 mol% DAAM) increased by 6% at the same polymer concentration.

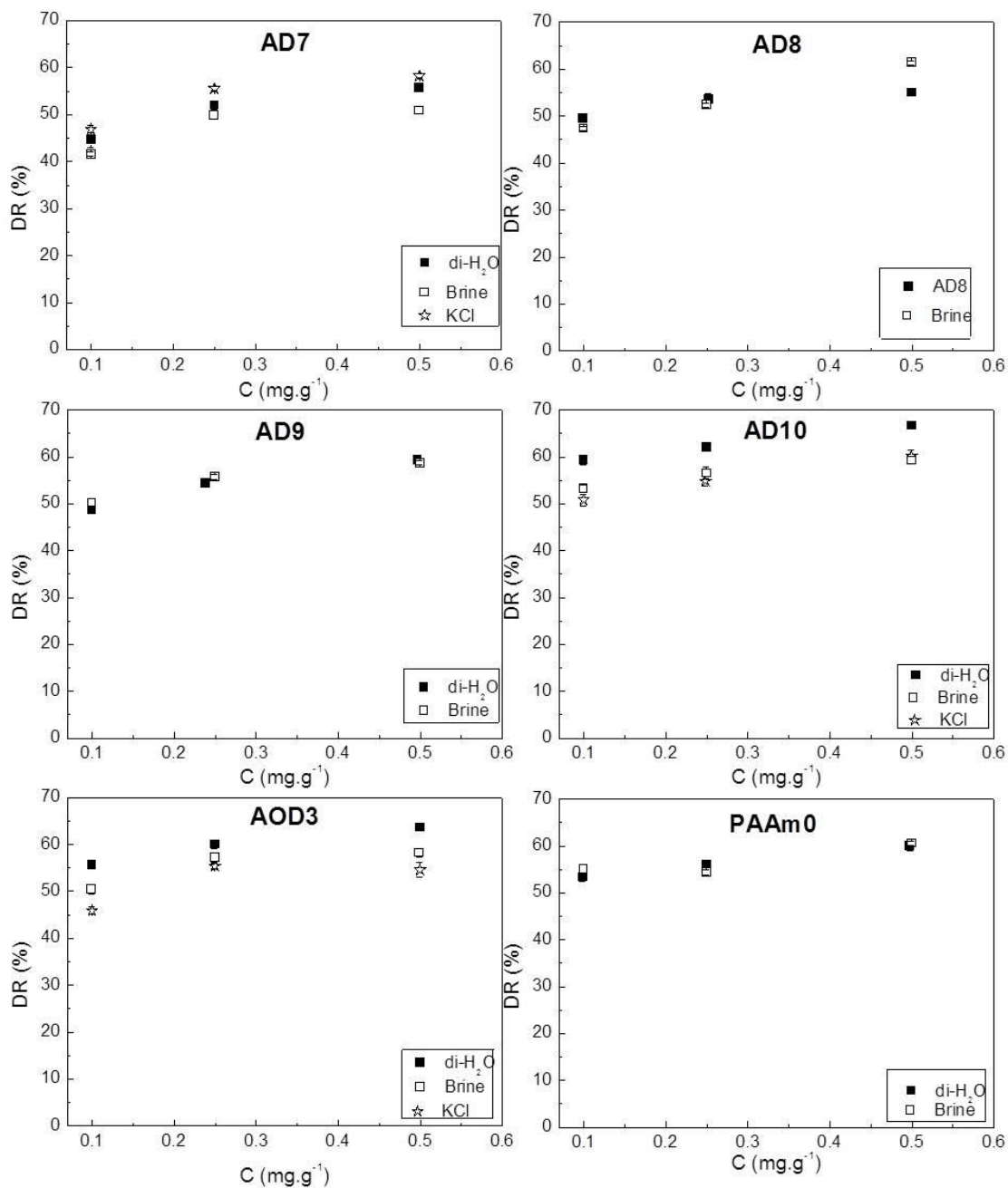


Figure 4.14 Percent drag reduction as a function of concentration for copolymers of acrylamide and polyacrylamide (PAAm0). Studied in deionised water, API brine (1.711 mol•L⁻¹ NaCl and 0.084 mol•L⁻¹ CaCl₂•2H₂O and 2% w/w (0.268 mol•L⁻¹) KCl (for selected polymers).

The increase in drag reduction was attributed to enhancement of interpolymer hydrophobic associations with addition of the high concentration of salt (brine) [221]. The decrease in the drag reduction performance caused by copolymer **AD7** at high concentrations ($0.5 \text{ mg}\cdot\text{g}^{-1}$) could be linked to the tight intra- or intermolecular associations that resulted in a loss of the polymer's ability to effectively unravel in the turbulent flow [79]. At low salt concentration (2% w/w ($0.268 \text{ mol}\cdot\text{L}^{-1}$) KCl) the drag reduction effect caused by copolymer **AD7** (0.65 mol% DAAM) slightly increased. The observed result imply that an intermediate concentration of salt (2 % w/w ($0.268 \text{ mol}\cdot\text{L}^{-1}$) KCl) resulted in the optimal strength of the intermolecular association between alkyl chains of hydrophobic moieties which did not affect drag reduction in a significant manner. This result is in agreement with observations reported by McCormick *et al.* [222] who studied changes in the properties of hydrophobically modified PAAM as a function of increasing salt concentration.

The drag reduction (DR) performance displayed by the copolymer containing an intermediate concentration of n-decyl acrylamide incorporated into a backbone (**AD9**, 0.33 mol% DAAM), remained unchanged upon addition of API brine. The drag reduction effect as a function of concentration by copolymers **AD10** (0.21 mol% DAAM) and **AOD3** (0.09 mol% ODAAM) was the highest in deionised water relative to brine and potassium chloride. Such behaviour was caused by enhanced intramolecular hydrophobic association within polymer chain in the presence of ions resulting in chain contraction. Drag reduction of **PAAM0** was unaffected by the addition of API brine. The invariance of PAAM's behaviour to salinity was as expected since polyacrylamide is a non-ionic and non-associating polymer [214, 221].

4.3. Summary

The aim of this chapter was to investigate the role of the molecular variables, such as the alkyl chain length in the hydrophobic monomer or concentration of the hydrophobic moieties in the copolymer, in the association of hydrophobically modified polyacrylamides. This was carried out to fill out the gaps in the literature and to identify the parameters influencing drag reduction and shear stability of these copolymers.

Water soluble polymers of acrylamide containing small amounts of hydrophobic moieties were successfully synthesised by micellar polymerisation. ^1H NMR confirmed the successful incorporation of the hydrophobic moieties into the copolymer structure. The water solubility of the obtained copolymers and the molecular weight was found to be dependent on the concentration of hydrophobic moieties; number of hydrophobic monomers per surfactant micelle (N_{H}) applied in polymerisation and type of incorporated hydrophobic moiety. Water solubility decreased with increasing concentration of hydrophobic moieties, increasing the length of alkyl chain and increasing the N_{H} (length of hydrophobic block). The molecular weight decreased with increasing concentration of the hydrophobic monomer used in the reaction and decreased with increasing N_{H} number. Rheological studies indicated that the associative properties were strongly governed by the nature and the concentration of hydrophobic moieties. The introduction of hydrophobic moieties induced an enhancement in the apparent viscosity of aqueous solutions of the copolymers due to the formation of intermolecular hydrophobic associations between alkyl chains in copolymers in addition to intramolecular hydrophobic associations within copolymer chains. Moreover intermolecular hydrophobic associations between hydrophobically modified PAAm were found to be present even in dilute concentrations for copolymers containing 0.09 mol% of ODAAm (**AOD3**) and copolymers containing 0.65 and 0.54 mol% of DAAM (**AD7** and **AD8**). The increase in apparent viscosity was even more pronounced at higher concentrations of copolymer solutions and was dependent on the length of the alkyl chain of the hydrophobic moiety and the concentration of the hydrophobic moieties in the copolymers.

The measurements of instantaneous drag reduction as a function of polymer concentration showed typical trend observed generally for drag reducing polymers, with drag reducing effect increasing with increasing polymer concentration until the optimum concentration was reached. The drag reduction effect achieved by all of the copolymers, studied in deionised water, was higher as compared to the commercial polyacrylamide. The drag reduction achieved by copolymers was higher despite the lower copolymers' molecular weights indicating the significance of intra- and intermolecular associations in the drag reduction mechanism. Moreover, drag reduction was dependent on the concentration of the incorporated hydrophobic moieties and the molecular weight of the copolymers. The strength of hydrophobic association

was found to affect the drag reduction performance of copolymers. The tight conformation (**AD7**, strong associations, the longest hydrophobic block, the highest concentration of n-decyl acrylamide 0.65 mol% of DAAM) was found to result in lowest drag reduction. This was attributed to lower efficiency of this copolymer towards interaction with the turbulent vortices. The time dependent measurements of drag reduction in the turbulent flow showed that the drag reduction caused by the majority of copolymers decreased with increasing shearing time and the number of shearing cycles. Moreover, the magnitude of the decrease in the drag reduction performance and shear resistance of copolymers was proportional to the concentration of hydrophobic groups. Copolymer containing intermediate concentration of n-decyl acrylamide (**AD9**, 0.33 mol% DAAM) was found to be the most effective drag reducer in terms of shear stability. This demonstrated that the copolymers containing small concentration of hydrophobic moieties are excellent drag reducers and offer higher shear stability in comparison to unmodified PAAm. Drag reduction of hydrophobically modified polymers of PAAm measured in the 2% (w/w) potassium chloride and brine was found to be dependent on the concentration of hydrophobic moieties. The copolymer **AD7** (highest concentration n-decyl acrylamide, 0.65 mol% DAAM) exhibited an increase in the drag reduction when dissolved in a solution with low ionic strength (2 % (w/w) ($0.268 \text{ mol}\cdot\text{L}^{-1}$) KCl). This was attributed to strengthening of hydrophobic intermolecular associations. The drag reduction effect caused by the majority of the copolymers in brine, exhibited a decrease in comparison to drag reduction achieved in deionised water. The drag reduction effect by copolymer containing intermediate concentration of n-decyl acrylamide (**AD9**, 0.33 mol% DAAM) was found to be unaffected by the presence of the monovalent and divalent ions. This demonstrates that this copolymer was the most efficient drag reducing agent in terms of performance, shear stability and resistance to salts.

Chapter 5

Influence of Cyclodextrins on the behaviour of the polymers of acrylamide

5.1. Introduction

Drag reducing agents such as polyacrylamide or polyacrylic acid are known to adsorb in oil and gas reservoirs [23, 223]. The adsorption of polymers especially in low permeability reservoirs requires expensive clean up operations and results in a decrease in the yield of the production of gas or oil [224-227]. A major disadvantage with the use of associating polymers as drag reducing agents is that adsorption on the well formation surface is more significant in comparison to homopolymers. This is due to the reformation of association when shear force is removed [22, 25, 228-231]. It is therefore desirable in certain applications to deactivate the hydrophobic associations. The effective method known in the literature is to deactivate hydrophobic interactions by utilisation of Cyclodextrins [110, 115]. Cyclodextrins are water-soluble cyclic oligosaccharides that have a hydrophobic inner cavity. The hydrophobic interactions between hydrophobic groups within polymer chain or between neighbouring polymer chains are switched off by the formation of inclusion complexes between the Cyclodextrin interior and the hydrophobic pendant groups on polymers [113, 114, 232]. The unique characteristic of inclusion complexes is the ability to recover the hydrophobic associations by the addition of surfactants or other chemicals. This provides the opportunity for the polymer (drag reducing agent) to be recovered [114, 141, 232].

This chapter tackles the influence of Cyclodextrins on the deactivation of hydrophobic interactions. The details on the synthesis and characterisation of the copolymers studied in this Chapter are presented in Chapter 3 and Chapter 4. The experimental procedures are also presented in Chapter 3. The effect of α - and β -Cyclodextrin on the rheology and drag reduction

of hydrophobically modified polyacrylamide is reported. Additionally the adsorption of polyacrylamides on the silica surface and their subsequent desorption from silica in the presence of Cyclodextrins is demonstrated.

5.2. Results and discussion

5.2.1. Influence of Cyclodextrins on the deactivation of hydrophobic interactions in polymers of acrylamide

Cyclodextrins (CD) are hydrophilic compounds that form inclusion complexes with hydrophobic molecules. This encapsulation allows modulation of the hydrophobic interactions. Complexation with polymers is known to affect rheological properties dramatically [112, 115]. The advantage of using Cyclodextrin to form complexes with hydrophobically modified polymers is the possibility of the recovery of the hydrophobic associations upon addition of surfactants or compounds that have a stronger binding affinity to Cyclodextrins e.g. ferrocenecarboxylic acid [114, 141, 233]. This presents benefit from an economical point of view since the polymer (drag reducing agent) could be recycled.

An insight into the complexation between Cyclodextrins and hydrophobic moieties in the hydrophobically modified polyacrylamide has been obtained using ^1H NMR. This technique has been used by many researchers to study the association characteristics of polymers and Cyclodextrins [110, 115, 234]. *Figure 5.1* and *Figure 5.2* demonstrates a typical ^1H NMR spectrum of poly(acrylamide-co-n-decyl acrylamide), **AD8** (0.54 mol% of n-decyl acrylamide), α - and β -Cyclodextrin and inclusion complexes of this copolymer with Cyclodextrins recorded in D_2O . Both the methyl and methylene protons in the decyl side chain of poly(acrylamide-co-n-decyl acrylamide) in the inclusion complexes with β -Cyclodextrin were shifted downfield from $\delta=0.86$ to 0.90 ppm and $\delta=1.28$ to 1.32 ppm, respectively as shown in *Figure 5.3*. Interaction of poly(acrylamide-co-n-decyl acrylamide) with α -Cyclodextrin (100 mol eq) caused a greater downfield shift by 0.08 ppm for both methyl and methylene protons. The higher shift in α -Cyclodextrin in comparison to β -Cyclodextrin was related to the ring size of α -Cyclodextrin. Previous studies indicated that α -Cyclodextrin has a higher binding affinity over β -Cyclodextrin although this depends on the bulkiness (steric effects and polymer conformation) of the

hydrophobic groups [113, 235]. The formation of the inclusion complexes was additionally confirmed by the downfield shift of the Cyclodextrin protons observed at $\delta=5.02$ ppm to $\delta=5.07$ ppm for β -Cyclodextrin and $\delta=5.02$ to $\delta=5.07$ ppm for α -Cyclodextrin, respectively. The protons in the region 3.5 to 4 ppm (peaks arising from Cyclodextrin H2 to H6) were shifted downfield by 0.04-0.05 for β -Cyclodextrin (*Figure 5.5*) and by 0.04-0.08 for α -Cyclodextrin, respectively (*Figure 5.4*). The observed shifts in the proton resonances indicate the interaction of the alkyl chains from hydrophobic moieties in copolymers with Cyclodextrins. As shown in *Figure 5.3*, the extent of the downfield shift was dependent on the concentration of Cyclodextrin used and increased with increasing Cyclodextrin concentration. At a 1:1 molar ratio of the hydrophobic moiety to β -Cyclodextrin, the shifts of the methyl and methylene protons in the alkyl chain of the hydrophobic moiety were shifted by +0.02ppm and +0.02ppm. The proton resonance at 5.02 ppm corresponding to Cyclodextrin (H1 peak) was shifted downfield to 5.07 ppm. This shows that the degree of shift of protons arising from Cyclodextrin did not depend on the concentration of Cyclodextrin used. The other peaks belonging to Cyclodextrin appeared to be not of high enough intensity for analysis at this concentration of Cyclodextrin. The shifts in the peak resonances were found to be independent on the concentration and type of the hydrophobic moiety and the slight increase in the shift by 0.05 (comparing to 0.04 for poly(acrylamide-co-n-decyl acrylamide)) was observed for the methyl and methylene peaks for the poly(acrylamide-co-n-octadecyl acrylamide), **AOD3**.

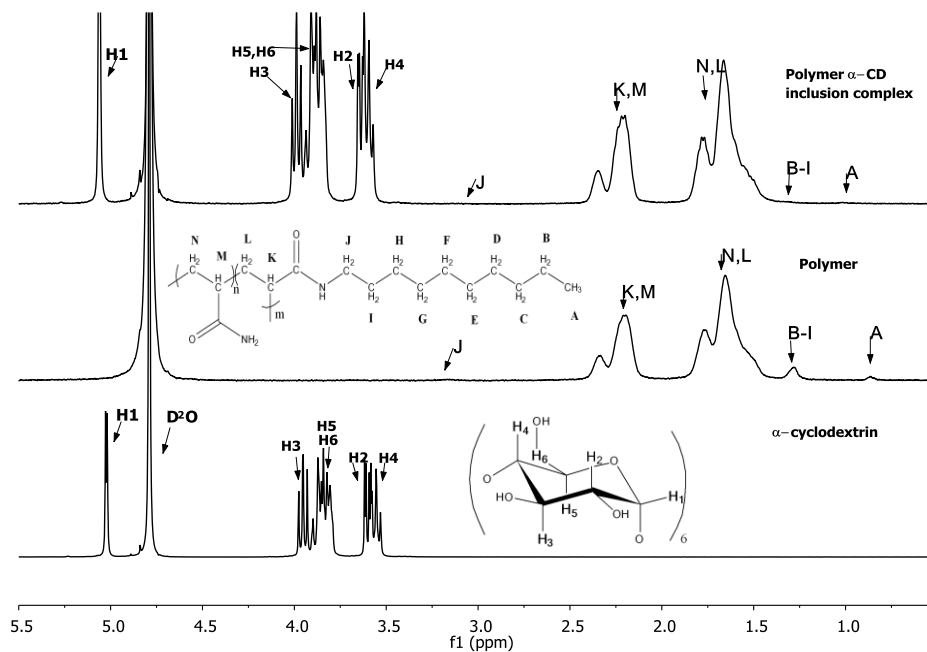


Figure 5.1. An example of ^1H NMR spectrum in D_2O of poly(acrylamide-co-n-decyl acrylamide) (**AD8**), α -CD and inclusion complex of poly(acrylamide-co-n-decyl acrylamide) (**AD8**) with 100 meq α -CD.

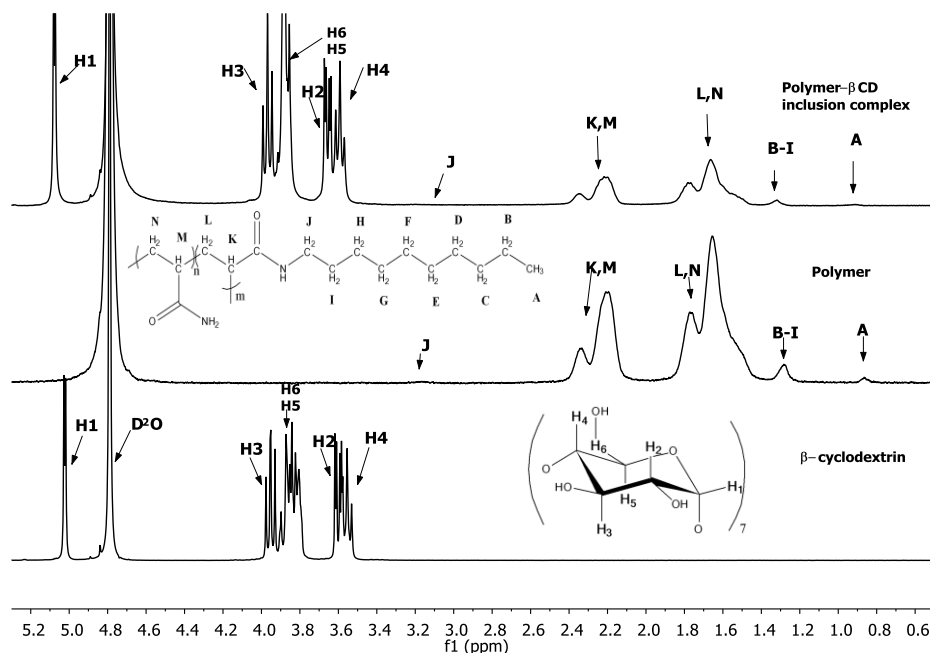


Figure 5.2. An example of ^1H NMR spectrum of poly(acrylamide-co-n-decyl acrylamide) (**AD8**), β -CD and inclusion complex of poly(acrylamide-co-n-decyl acrylamide) (**AD8**) and 100 meq β -CD studied in D_2O .

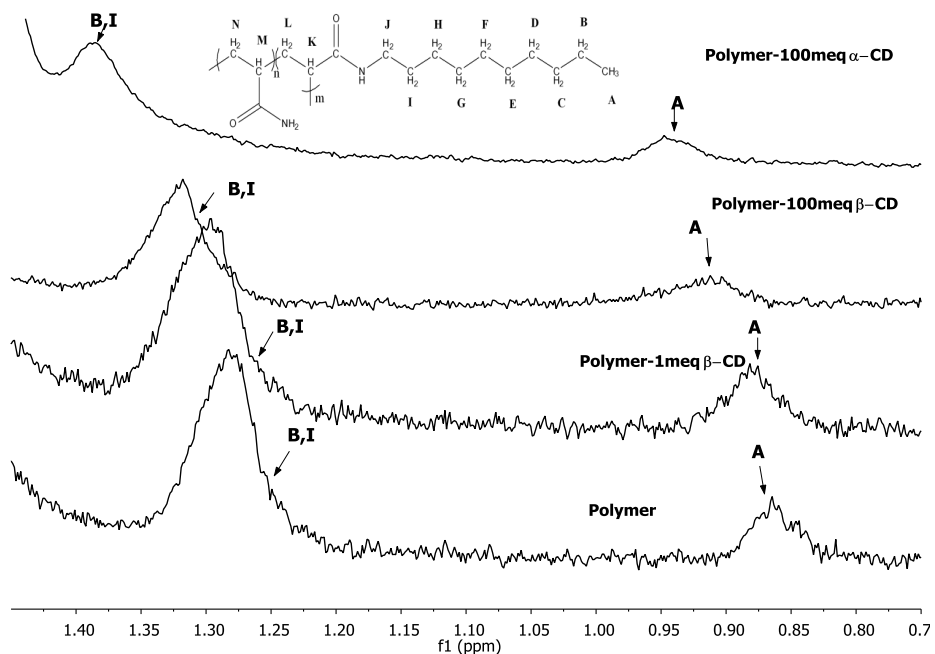


Figure 5.3. Part of the ^1H NMR spectrum in D_2O showing protons in poly(acrylamide-co-n-decyl acrylamide) (AD8) and inclusion complexes at 1 and 100 meq of β -CD and 100 meq α -CD.

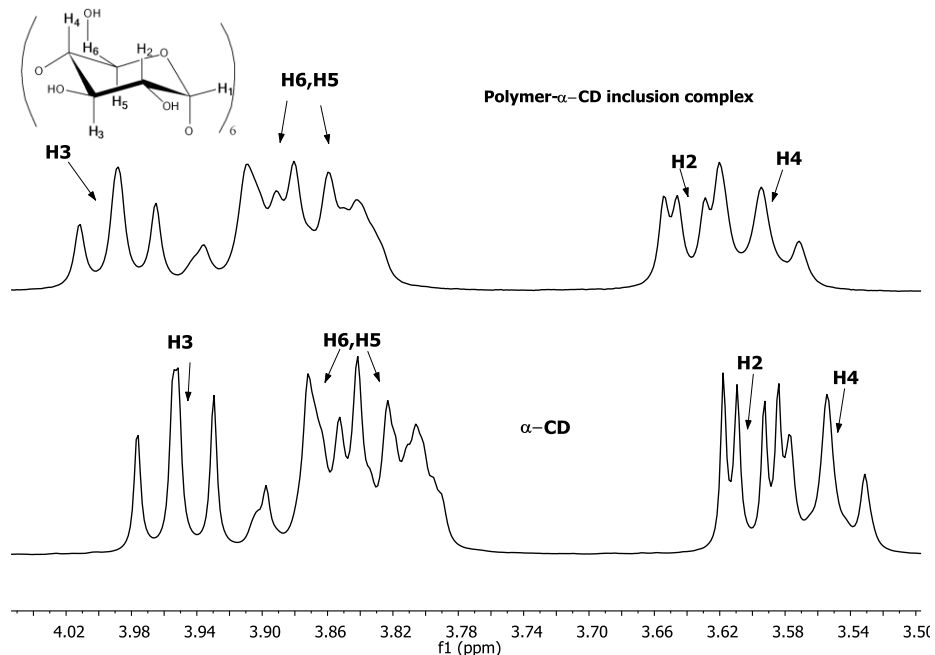


Figure 5.4. Part of the ^1H NMR spectrum in D_2O showing protons in α -Cyclodextrin (CD) and inclusion complex of poly(acrylamide-co-n-decyl acrylamide) (AD8, 0.54 mol% of DAAM) with 100 meq α -CD.

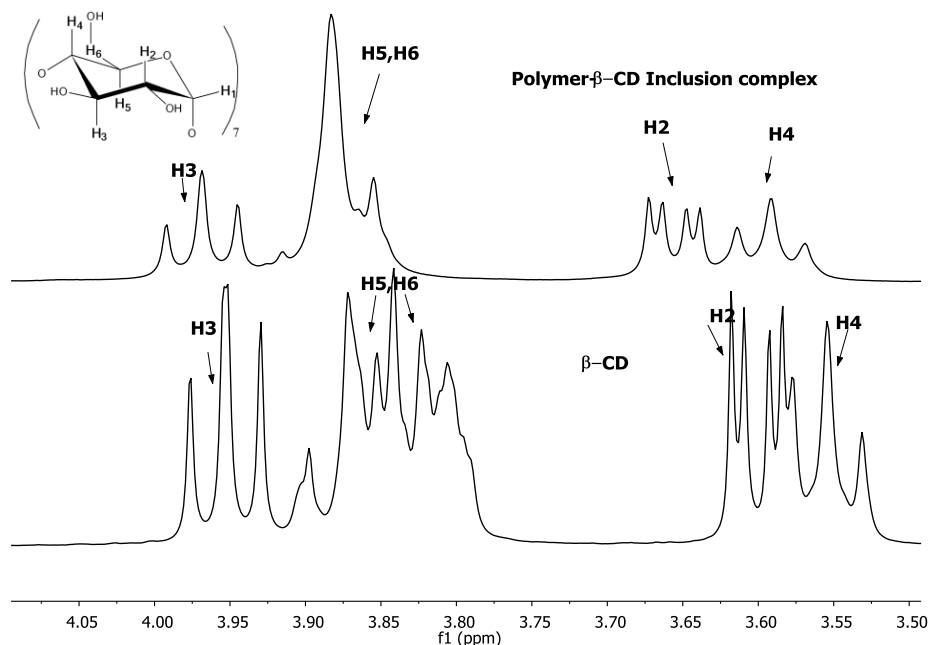


Figure 5.5. Part of the ¹H NMR spectrum in D₂O showing protons of β-Cyclodextrin (CD) and inclusion complex of poly(acrylamide-co-n-decyl acrylamide) (**AD8**, 0.54 mol% of DAAM) with 100 meq of β-CD.

The hydrophobically modified copolymers had a higher apparent viscosity than the PAAm homopolymer at the same concentration. Thus it is apparent that the addition of Cyclodextrin to the associated polymer should result in a noticeable decrease in the apparent viscosity. Indeed, the apparent viscosity of the polymer solution of poly(acrylamide-co-n-decyl acrylamide) **AD8** at $C=5 \text{ mg}\cdot\text{g}^{-1}$ (well above critical aggregation concentration), decreased significantly upon addition of 100 meq of β-Cyclodextrin (β-CD) (Figure 5.6); the polymer gel turned into liquid. This was due to the dissociation of the associated n-decyl groups in the copolymer and the formation of host-guest complexes between the n-decyl acrylamide groups and the Cyclodextrin interior [113, 115, 236].

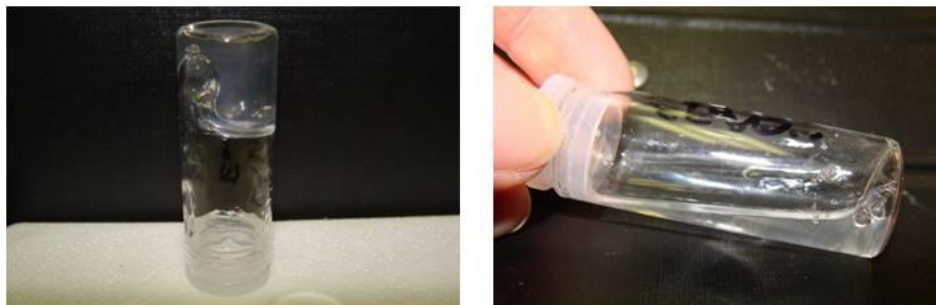


Figure 5.6. Photographs of the transition of the polymer gel formed by poly(acrylamide-co-n-decyl acrylamide) **AD8** (0.54 mol% of DAAM) at $C=5 \text{ mg}\cdot\text{g}^{-1}$ (left) into solution (right) upon addition of 100 meq of β -CD.

The influence of Cyclodextrins on the dissociation capability of the hydrophobic physical links in the hydrophobically modified PAAm was also studied as a function of shear rate at a semi-dilute polymer concentration of $0.5 \text{ mg}\cdot\text{g}^{-1}$. This maximum concentration is typically used in drag reduction studies.

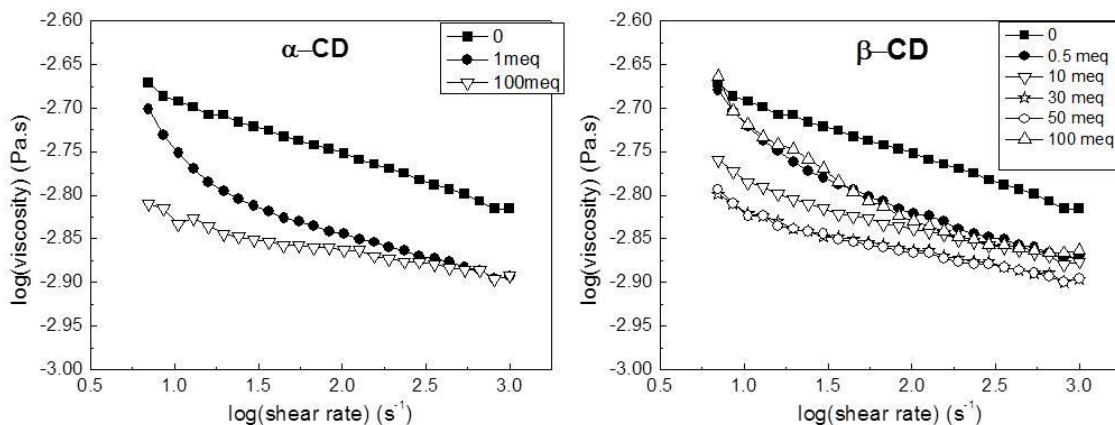


Figure 5.7. Influence of α - and β -Cyclodextrin addition on the apparent viscosity of solutions of poly(acrylamide-co-n-decyl acrylamide) (**AD7**, 0.65 mol% DAAM). Studied at polymer $C=0.5 \text{ mg}\cdot\text{g}^{-1}$ and $25 \text{ }^\circ\text{C}$.

The interaction of the polymers with Cyclodextrins resulted in visible changes to the viscoelastic properties due to masking of the hydrophobic associations. As shown in *Figure 5.7*, the addition of α -Cyclodextrin and β -Cyclodextrin to copolymer **AD7** resulted in a decrease in the apparent viscosity of polymer solution and the extent of the apparent viscosity decrease was dependent on

the concentration of Cyclodextrin. Upon addition of 1 mol eq. of α -Cyclodextrin, the apparent viscosity of copolymer **AD7** decreased by the 20 %. Any further increases in the concentration of Cyclodextrin did not affect the polymer's behaviour significantly. When β -Cyclodextrin was used, a decrease in apparent viscosity was also seen. At a 1:1 mol eq. Cyclodextrin to hydrophobic monomer ratio, a 30 % decrease in the apparent viscosity was observed. The observed apparent viscosity reduction with addition of either α -Cyclodextrin or β -Cyclodextrin was caused by the deactivation of hydrophobic associations, due to the formation of inclusion complexes with between hydrophobic moieties and Cyclodextrins [232, 237, 238]. Additionally, the extent of the reduction of the copolymer's apparent viscosity upon addition of β -Cyclodextrin was higher (by 10 %) in comparison to α -Cyclodextrin. This finding was opposite to literature reports on binding studies between polymers and Cyclodextrins [113, 235, 239] and ^1H NMR studies. On the other hand Karlson [111] and Harada *et al.* [240] indicated that the increased size of β -Cyclodextrin's cavity often results in a higher tendency for complex formation with sterically hindered or bulky hydrophobes and the binding is dependent on the polymer conformation. Copolymer **AD7** had the longest hydrophobic blocks (bulky groups) and strongest hydrophobic interaction out of all other copolymers therefore it had higher affinity towards β -Cyclodextrin.

It should be noted that the apparent viscosity of the copolymer **AD7** increased at high concentrations of β -Cyclodextrin. This behaviour was observed in previous studies on interactions of hydrophobically modified polymers of alginate and hydroxyethyl cellulose with Cyclodextrins. Kjøniksen *et al.* [241] and Bu *et al.* [242] suggested that the increase in apparent viscosity was due to cross-linking of hydrophobically modified polymers, via assembling of the Cyclodextrin molecules into complexes at junction zones and the formation of large aggregates or crystallites. Wang and Banerjee [243] studied complexes of Cyclodextrins and copolymers of polyacrylamide with cationic monomers and showed that the increase in apparent viscosity and hydrodynamic volume was due to polymer agglomeration above a certain threshold of Cyclodextrin concentration.

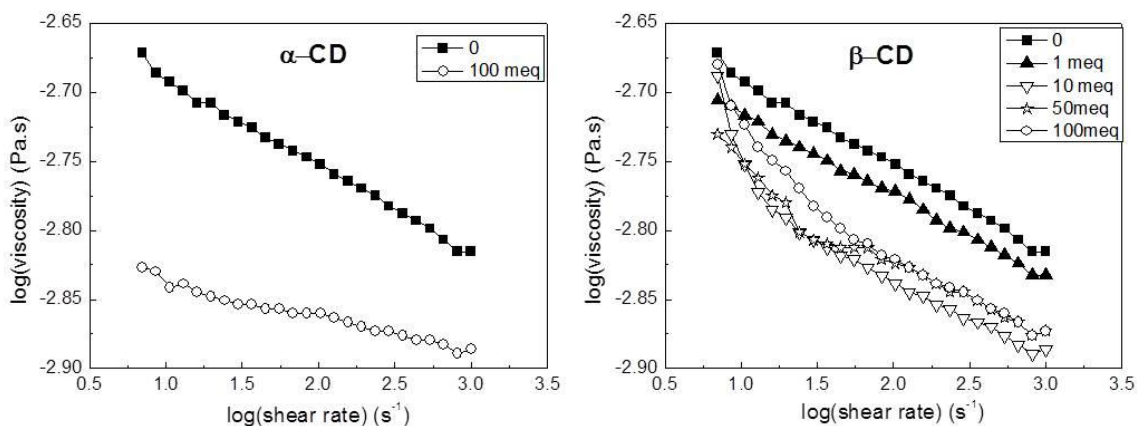


Figure 5.8. Influence of α - and β -Cyclodextrin addition on the apparent viscosity of solutions of poly(acrylamide-co-n-decyl acrylamide) (**AD8**, 0.54 mol% DAAM). Studied at polymer $C = 0.5 \text{ mg}\cdot\text{g}^{-1}$ and $25 \text{ }^\circ\text{C}$.

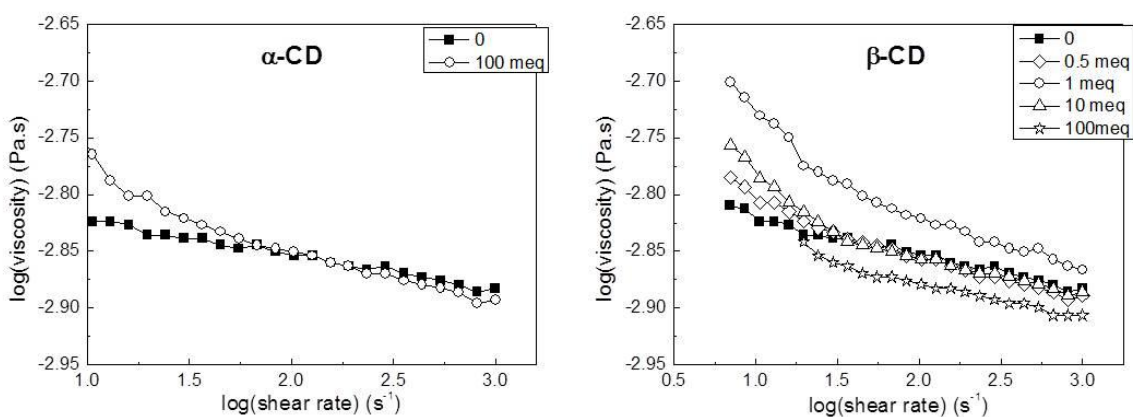


Figure 5.9. Influence of α - and β -Cyclodextrin addition on apparent viscosity of solutions of poly(acrylamide-co-n-decyl acrylamide) (**AD9**, 0.33 mol% DAAM). Studied at $C = 0.5 \text{ mg}\cdot\text{g}^{-1}$ and $25 \text{ }^\circ\text{C}$.

The addition of Cyclodextrins to copolymer **AD8** (Figure 5.8) resulted in a decrease in the apparent viscosity for both α - and β -Cyclodextrin-polymer complexes by up to 14 %. The reduction in apparent viscosity was caused by the annihilation of the hydrophobic interactions in this copolymer. The addition of both α - or β -Cyclodextrin to copolymer **AD9** (Figure 5.9) did not result in any significant changes to this polymer's rheology and upon addition of β -Cyclodextrin to this polymer apparent viscosity decreased by only 7 %. This could be due to the

low concentration of the hydrophobic moieties (0.33 mol%) incorporated into this copolymer. As a result, the deactivation of hydrophobic interactions by Cyclodextrins did not cause detectable changes in the observed apparent viscosity.

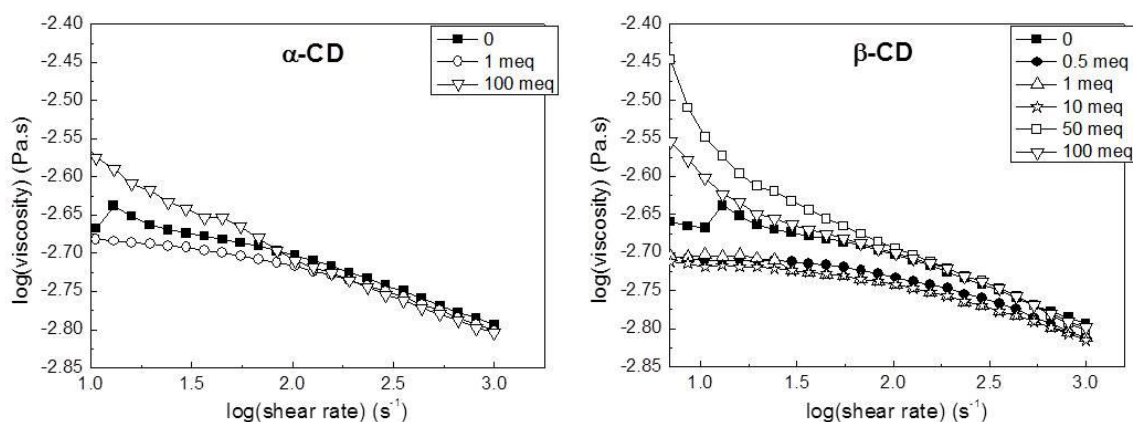


Figure 5.10. Influence of α - and β -Cyclodextrin addition on the apparent viscosity of solutions of poly(acrylamide-co-n-decyl acrylamide) (**AD10**, 0.21 mol% DAAM). Studied at $C = 0.5 \text{ mg}\cdot\text{g}^{-1}$ and 25°C .

The rheological behaviour of copolymer **AD10** was found to be not significantly affected by addition of α - or β -Cyclodextrin (*Figure 5.10*) and only small changes in the apparent viscosity were observed at low shear rates. This was most likely due to the small concentration of n-decyl acrylamide in the copolymer. Upon dissociation of the hydrophobic groups, the difference in the apparent viscosity was not large enough to be detected by the rheometer.

The rheological study in *Figure 5.11* indicated that complexation of copolymer **AOD3** with α -Cyclodextrin did not affect the apparent viscosity of aqueous polymer solution significantly. When β -Cyclodextrin was introduced instead, the apparent viscosity of aqueous polymer solution decreased more dramatically and at 10 mol eq of β -Cyclodextrin (with respect to 1 mol eq of hydrophobic chains) a polymer solution behaved almost like a Newtonian liquid (40 % decrease in apparent viscosity). This indicated the deactivation of the hydrophobic associations due to complexation with Cyclodextrin. The higher tendency of β -Cyclodextrin to form complexes with longer alkyl chains is related to steric effects, arising from inclusion of the C18 alkyl chain. The

larger cavity of β -Cyclodextrin as compared to α -Cyclodextrin results in the lower affinity of the latter towards bulky alkyl chains [115, 240, 244].

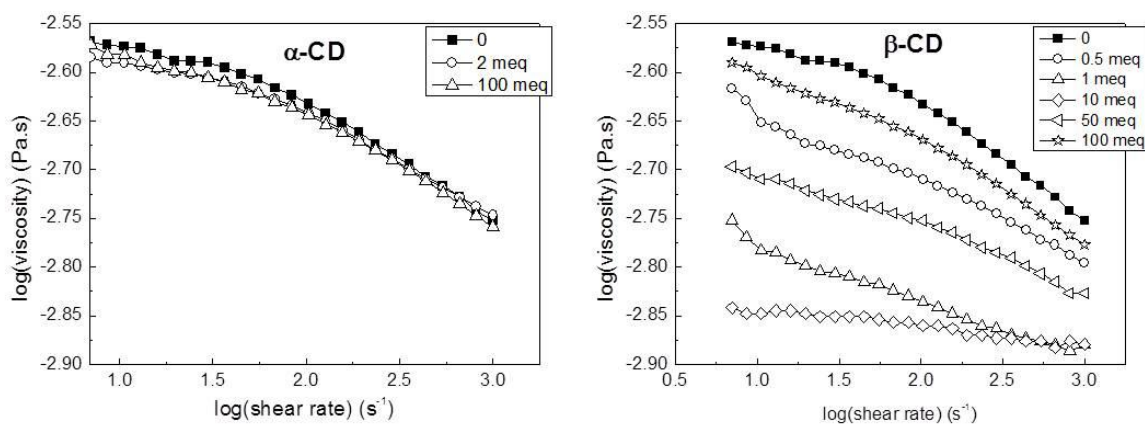


Figure 5.11. Influence of α - and β -Cyclodextrin addition on apparent viscosity of solutions of poly(acrylamide-co-n-octadecyl acrylamide) (AOD3, 0.09 mol% ODAAm). Studied at polymer $C= 0.5 \text{ mg}\cdot\text{g}^{-1}$.

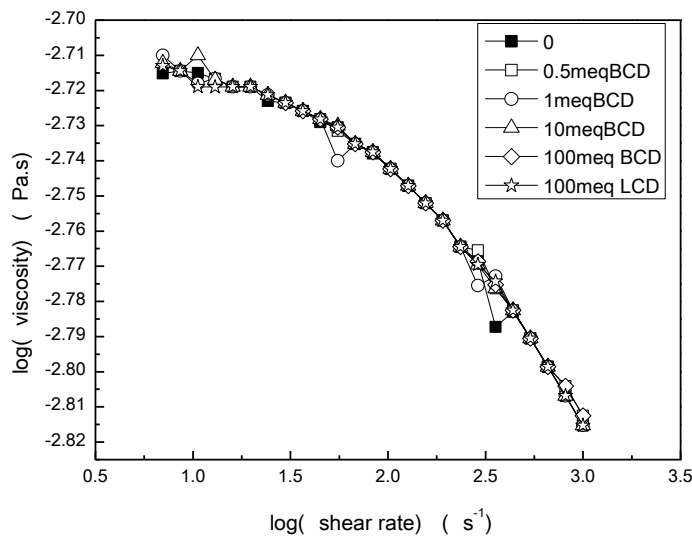


Figure 5.12 Influence of α - and β -Cyclodextrin addition on apparent viscosity of solutions of PAAm0. Studied at polymer $C= 0.5 \text{ mg}\cdot\text{g}^{-1}$

As before, the formation of aggregates of complexes at higher concentrations of Cyclodextrin resulted in an increase in the apparent viscosity. As expected no changes in rheological behaviour of **PAAm0** were observed upon addition of Cyclodextrins (results shown in *Figure 5.12*).

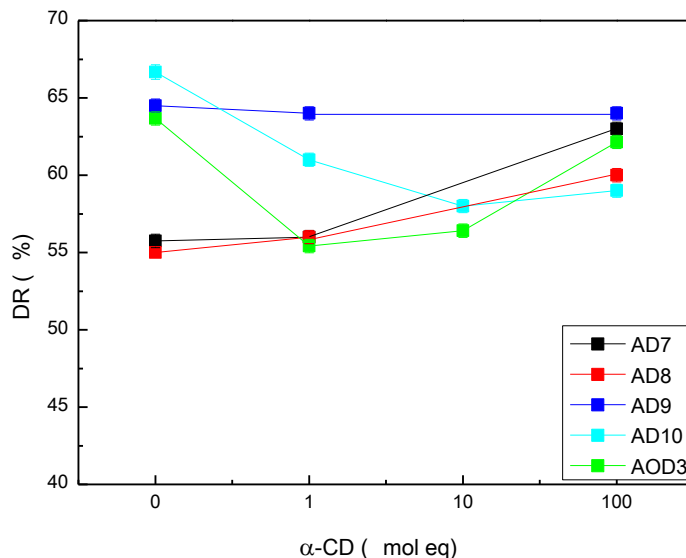


Figure 5.13. Influence of α -CD addition on the drag reduction of PAAm copolymers. Studied at 11200 s⁻¹, at 25°C and at polymer C= 0.5 mg·g⁻¹.

The effect of complexation of copolymers with Cyclodextrins on drag reduction has been studied, at a constant shear rate of 11200 s⁻¹ and a constant polymer concentration of 0.5 mg·g⁻¹. Drag reduction is expected to be affected by addition of Cyclodextrins, since formation of inclusion complexes between Cyclodextrin and polymer would result in the dissociation of hydrophobic links, therefore results in a decrease in an apparent molecular weight. Drag reduction profiles for the copolymer complexes with α - and β -Cyclodextrin are shown in *Figure 5.13* and *Figure 5.14*, respectively.

Increases in the concentration of α -Cyclodextrin resulted in an increase in observed drag reduction (DR) for copolymers **AD7** (0.65 mol% DAAM) and **AD8** (0.54 mol% DAAM) by 7 and 4.5 %, respectively (*Figure 5.13*). The observations were in contrast to what was expected, since the decrease in apparent viscosity (measured by rheometer, *Figure 5.7* and *Figure 5.8*)

suggested deactivation of the hydrophobic associations. It can be therefore hypothesised that the disruption of the hydrophobic associations and complexation by α -Cyclodextrin, resulted in a more open conformation of the copolymer. As a result, the polymer complex was more flexible and more efficient in suppressing the Taylor vortices.

The drag reduction of copolymer **AD9** (0.33 mol% DAAM) was found to be largely unaffected by complexation with α -Cyclodextrin. This is in agreement with apparent viscosity data obtained from the rheological measurements (*Figure 5.9*) and the values of the hydrodynamic radius (R_H) obtained by Dynamic Light Scattering (DLS) (*Table 5.1*). The unchanged performance of the copolymer could be due the small concentration of hydrophobic moieties present, which upon complexing with Cyclodextrin did not affect its energy absorbing abilities from turbulent microdisturbances.

The drag reduction (DR) efficiency upon complexing the copolymer **AD10** (0.21 mol% DAAM) with α -Cyclodextrin was lowered by 7 % and with an increase in the Cyclodextrin concentration, the drag reduction levelled off (*Figure 5.13*). The dissociation of intra- and intermolecular hydrophobic groups was facilitated for the copolymer, due to the loosely connected weak associations. This is consistent with results achieved by dynamic light scattering (DLS) although the rheology was found to be only slightly affected at low shear rates (*Table 5.1* and *Figure 5.10*).

The drag reduction of copolymer **AOD3** (0.09 mol% ODAAM) decreased by 8 % at low concentrations of α -Cyclodextrin ($[CD] < 10$ mol eq.) which could be explained in a similar manner as for copolymer **AD10**. Rheological studies (*Figure 5.11*) showed only a small decrease in apparent viscosity at low shear rates. The increase of drag reduction upon addition of α -Cyclodextrin concentrations greater than 10 mol eq could not be attributed to the association of the Cyclodextrin-polymer complexes, since the apparent viscosity of the polymer complex and hydrodynamic radius (R_H) remained nearly unchanged upon complexation of **AOD3** with α -Cyclodextrin. Therefore it can be assumed that the hydrophobic associations between hydrophobic moieties in aqueous solutions of this copolymer were rather strong and upon addition of Cyclodextrin, a more open conformation was formed. This conformation was

therefore capable of a more efficient coil unravelling in turbulent flow and hence was more effective in the suppression of turbulence.

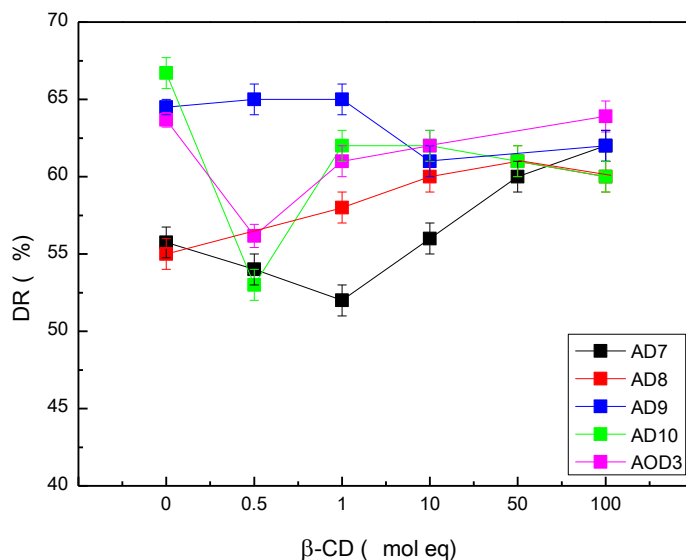


Figure 5.14. Influence of the addition of β -CD to aqueous solutions of PAAM copolymers on the drag reduction. Studied at 11200 s^{-1} , at 25°C and at polymer $C = 0.5 \text{ mg}\cdot\text{g}^{-1}$.

The effect of the complexation of copolymers **AD7** (0.65 mol% DAAM) and **AD8** (0.54 mol% DAAM) with β -Cyclodextrin on the drag reduction efficiency was found to follow similar trends (Figure 5.14). However, the drag reduction (DR) performance of copolymer **AD7** was found to initially decrease at Cyclodextrin concentrations below 10 mol eq. This behaviour could be the result of the destruction of hydrophobic interactions as suggested by the apparent viscosity trend from the rheology (Figure 5.7) and value of hydrodynamic radius from the DLS (Table 5.1). The increase in drag reduction for copolymer **AD7** at high concentrations of Cyclodextrin ($[\text{CD}] > 1 \text{ mol eq}$) was most likely due to formation of aggregates of inclusion complexes as evidenced by rheology. The data from the DLS was however inconclusive, since the changes in hydrodynamic radius were too small. Additionally, it is postulated that the interaction of complexes of copolymer **AD8** with vortices was higher due to the destruction of tightly associated molecules. This hypothesis was supported by the decrease in apparent viscosity of aqueous solutions as studied by rheology (Figure 5.8). The increase in the size of hydrodynamic radius for the

copolymer **AD8** (*Table 5.1*) makes this theory inconclusive and would suggest the formation of larger polymer-Cyclodextrin aggregates.

The drag reduction (DR) of copolymer **AD9** (0.33 mol% DAAM) was found to be unaffected by β -Cyclodextrin concentration below 1 mol eq and only slightly decreased upon addition of higher concentrations of Cyclodextrin. As a result, a decrease of $\sim 4\%$ in drag reduction was observed. This result was consistent with the rheological data shown in *Figure 5.9*, which illustrated only a small change in the apparent viscosity upon addition of β -Cyclodextrin. The DLS data shown in *Table 5.1* also demonstrated that the hydrodynamic radius was not largely affected by polymer complexation with β -Cyclodextrin.

The drag reduction (DR) efficiency of the complexes of copolymers **AD10** (0.21 mol% DAAM) and **AOD3** (0.09 mol% ODAAM) with β -Cyclodextrin followed similar trends. At 0.5 mol eq of β -Cyclodextrin, drag reduction for both copolymers was found to decrease by 14 and 8 %, respectively. The decrease in drag reduction performance for both copolymers was a result of the deactivation of weak hydrophobic interactions as indicated by the lower hydrodynamic radius (*Table 5.1*) and lower apparent viscosity (however copolymer **AD10** showed barely noticeable changes in viscosity, *Figure 5.10*). An increase in concentration of β -Cyclodextrin above 0.5 mol eq resulted in an increase in drag reduction (DR) performance. Further increases in the concentration of β -Cyclodextrin did not result in significant drag reduction performance changes in copolymer **AD10**, however an increase in drag reduction for copolymer **AOD3** was observed. The observed increase in the drag reduction of **AOD3** was a result of the aggregation of Cyclodextrin-copolymer complexes [243]. This was evidenced by an increase in hydrodynamic radius and apparent viscosity (*Table 5.1* and *Figure 5.11*).

Sample	M _w (kDa)	PDI	H ^{NMR} (mol%)	R _H (nm)	R _{H0.5β-CD} (nm)	R _{H1β-CD} (nm)	R _{H100β-CD} (nm)	R _{H100α-CD} (nm)
AD7	974	2.8	0.65	95.8±3.7	86.3±3.5	92.0±1.4	88.6±3.2	90.7±3.8
AD8	864	1.2	0.54	73.2±2.2	82.8±2.3	80.9±1.8	91.8± 4.0	90.6±7.3
AD9	1163	1.9	0.33	104.4±4.6	99.6±2.0	107.1±7.4	105.7±3.8	103.1±3.8
AD10	1074	1.5	0.21	98.0±6.0	88.4±3.3	NA	92.1±3.2	93.1±1.9
AOD3	1345	1.7	0.09	92.9±1.8	86.2±1.8	NA	92.4±1.0	84.9±3.0

Table 5.1. Weight average molecular weight M_w, polydispersity index PDI, hydrophobic moiety content H, and hydrodynamic radius R_H for PAAm and its copolymers with and without α- or β-Cyclodextrin addition; AD= poly(acrylamide-co-n-decyl acrylamide), AOD= poly(acrylamide-co-n-octadecyl acrylamide).

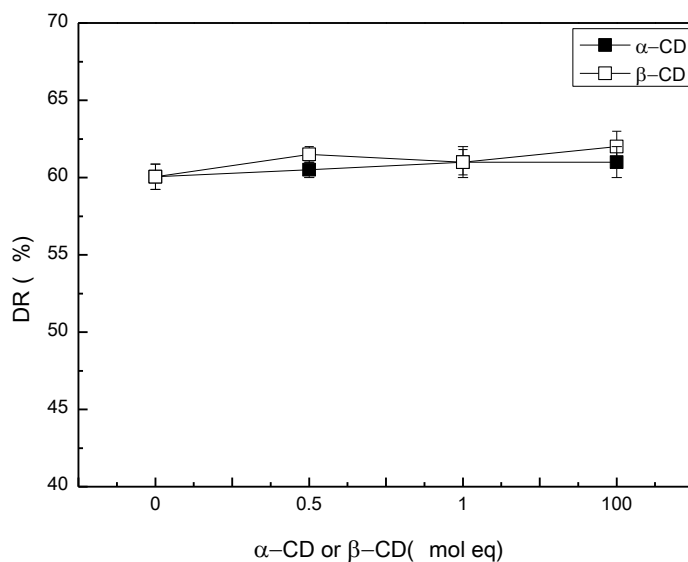


Figure 5.15. Percent DR of **PAAm0** (M_w=1896 kDa) as a function of α- and β-CD concentration studied in deionised water. Measured at 11200 s⁻¹, 25°C and polymer C= 0.5 mg·g⁻¹

Figure 5.15 illustrates the drag reduction performance of polyacrylamide (**PAAm0**) in deionised water upon addition of α- and β-Cyclodextrin. The drag reduction performance was constant for

the homopolymer of acrylamide in the presence of Cyclodextrins. Thus, the drag reduction performance of copolymers was clearly affected by the presence of hydrophobic moieties.

5.2.3. Adsorption of polymers of PAAm and desorption from silica using Cyclodextrins

Water soluble polymers are effective in reducing drag, however they are known to adsorb in gas and oil reservoirs [22, 24, 224]. The adsorption of polymers is particularly troublesome in low permeability reservoirs, which leads to undesirable polymer deposits and impacts on the recovery of hydrocarbons [23, 223]. Expensive clean up operations such as enzymatic degradation are usually required to remove polymers from the surface of the reservoir. The adsorption of associating polymers was found to be especially problematic since the existence of physical interactions between hydrophobic groups lead to increased adsorption of polymer [22, 25, 228, 231]. For these applications, the availability of additives capable to desorb the polymer from the solid surface would be very advantageous. Since hydrophobically modified polymers were found to be responsive to the addition of Cyclodextrins, the influence of these additives on the copolymers' desorption from a silica surface was investigated. The influence of the Cyclodextrins on desorption of **PAAm0** was also studied for comparison.

The adsorption of copolymers **AD10** (0.21 mol% DAAm, $M_w = 1074$ kDa) and **AOD3** (0.09 mol% ODAAm, $M_w = 1345$ kDa) and homopolymer **PAAm0** ($M_w = 1896$ kDa) as a function of concentration were determined quantitatively using Total Organic Carbon (TOC) Analyser and the results are shown in *Figure 5.16*. With increasing the polymer concentration, the adsorption of polymers on silica increased. The plateau of adsorption for both copolymers was observed in the concentration range between 0.25 to 0.5 $\text{mg}\cdot\text{g}^{-1}$. The levelling of adsorption was described by Argillier *et al.* [22] as being due to the aggregation of particles induced by the adsorption of high molecular weight polymers and the resulting decrease of the accessible surface for further adsorption.

Increasing the concentration of **PAAm0** resulted in the increase in the adsorbed amount of polyacrylamide and no plateau was achieved in the range of concentrations studied. Adsorption of polymers on solids is determined by the nature of the solid substrate such as the

hydrophilicity, the molecular weight of the polymer as well as the existence of physical interactions between polymer molecules and between polymer and the solid surface [22, 231]. It is established that the extent of adsorption of homopolymers and copolymers increases with molecular weight [228, 245]. The molecular weight of **PAAm0** studied in this investigation was higher than that of the copolymers; therefore the degree of adsorption of **PAAm0** was higher. The hydrophilicity of silica used was also a factor that could influence the adsorption of polymers.

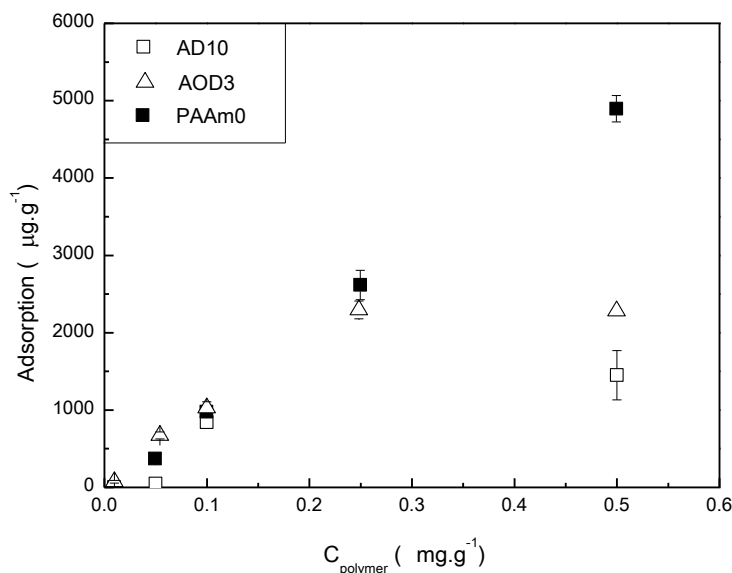


Figure 5.16. The adsorption of **PAAm0** and its copolymers with n-decyl acrylamide **AD10** and n-octadecyl acrylamide **AOD3** on silica (specific surface area of silica 45 m².g) as a function of polymer concentration. Measured in deionised water, at pH 7 and 25°C.

It is interesting to point out that the extent of adsorption of copolymers on the silica, as determined at polymer $C=0.5 \text{ mg}\cdot\text{g}^{-1}$, was found to be dependent on the content of the hydrophobic moieties (Table 5.2). The adsorption of copolymer **AD8** (0.54 mol% DAAM, $M_w=864 \text{ kDa}$) was found to be higher than the adsorption of other polymers and only slightly higher than the adsorption of **PAAm0**. The M_w of copolymer **AD8** was half that of **PAAm0**. Bottero *et al.* showed that the size of the loops formed by the adsorbed polymer increases with the length of polymer [245]. This demonstrates that the hydrophobically modified copolymer **AD8** had a

higher affinity to silica, since at this molecular weight adsorption of this copolymer on silica was expected to be lower. This also indicates that the physical interactions between polymer chains were responsible for the increased adsorption of hydrophobically modified polymers onto the silica. This observation is in agreement with previous studies on the adsorption of water soluble polymers containing hydrophobic groups [22, 25, 228].

The extent of desorption of polymers from the silica surface was determined under the same conditions as used in the adsorption study. The amount of polymer desorbed was determined quantitatively by TOC at a polymer concentration of $0.5 \text{ mg}\cdot\text{g}^{-1}$. The data presented in *Table 5.2* indicate that in presence of β -Cyclodextrin, copolymers **AD8** and **AOD3** became fully desorbed from the silica. It was also observed that the extent of desorption was connected to the efficiency with which the copolymers formed complexes with Cyclodextrins. α -Cyclodextrin was found to have little influence on rheological behaviour when complexed with copolymer **AD10** and **AOD3** (*Figure 5.10* and *Figure 5.11*). As such α -Cyclodextrin was the worst inhibitor of polymer adsorption with only a few percent of polymer recovery seen. β -Cyclodextrin was found to form stronger complexes with copolymers **AD8** and **AOD3** in comparison to copolymer **AD10** (rheological study, *Figure 5.8*, *Figure 5.11* and *Figure 5.10*). Thus, only ~53 % recovery of the copolymer **AD10** was seen.

It is interesting to point out that addition of α - and β -Cyclodextrin resulted in partial desorption of polyacrylamide. It is an unexpected phenomenon, since the rheological behaviour of polyacrylamide was found to be unaffected by the presence of Cyclodextrins. It is therefore hypothesised that the formation of hydrogen bonds between the hydroxyl groups of Cyclodextrin and the amide groups of polyacrylamide, could account for the partial desorption of homopolymer. It is also possible that the interaction of Cyclodextrin with silica surface was stronger than the interaction of polyacrylamide with silica. Therefore, it is feasible that Cyclodextrin displaced some of the polyacrylamide molecules on silica.

The obtained results indicate that β -Cyclodextrin is the most efficient additive for desorption of copolymers containing hydrophobic groups. The recovery of the polymer from the silica surface was nearly 100 % for the majority of copolymers. Moreover, the addition of β -Cyclodextrin to the silica slurry containing adsorbed polyacrylamide resulted in ~40 % of homopolymer

recovery. The results achieved demonstrate the superiority of the Cyclodextrin in desorption of both homopolyacrylamide and associating polyacrylamide.

Sample	M _w (kDa)	PDI	H (mol%) ^{NMR}	Ads _{0.5mg.g-1} (μg·g ⁻¹)	Des _{α-CD} (μg·g ⁻¹) (%)	Des _{β-CD} (μg·g ⁻¹) (%)
AD8	864	1.2	0.54	4981±108.7	-	4976.3±52.5 ³ 99.9
AD10	1074	1.5	0.21	1450.6±317.5	104.9 ¹ 7.2	768.8 ² 52.7
AOD3	1345	1.7	0.09	2262	200.04±49.9 ¹ 8.84	2246.7±0 ³ 99.4
PAAm0	1896	1.3	0	4892.2±120.7	1697.1±120 ¹ 34.7	1891.7±36.6 ² 38.1

Table 5.2. The amount of PAAm and its hydrophobically modified copolymers adsorbed and desorbed on and from silica as measured by TOC; ¹Amount desorbed with 100 α-CD, no desorption seen at 0.5 and 1 meq of α-CD, ²Amount desorbed with 100 β-CD, no desorption seen at 0.5 and 1 meq of β-CD, ³Amount desorbed with 0.5 and 100 meq β-CD.

5.3. Summary

The aim of the study carried out in this chapter was to identify suitable additives capable of dissociating hydrophobic interactions between or within polymer chains. Deactivation of hydrophobic interactions would result in reduced viscosity, quick partitioning of polymer into the water phase and reduced adsorption of polymer onto the surfaces of the well formation. Cyclodextrins were chosen as potential materials capable of dissociating hydrophobic interactions.

¹H NMR studies demonstrated that α- and β-Cyclodextrin formed inclusion complexes with the alkyl chains of n-decyl- and n-octadecyl acrylamide moieties. The formation of inclusion complexes of polyacrylamides with Cyclodextrins was further confirmed by rheology. This study showed the stronger tendency of β-Cyclodextrin to form complexes with the copolymers containing the highest concentration of n-decyl acrylamide (0.65 mol%) and n-octadecyl acrylamide (0.09 mol%). The measurements of instantaneous drag reduction as a function of Cyclodextrin concentration indicated, that the changes in drag reduction were caused by the modulation of the hydrophobic interactions. The drag reduction study carried out at higher

concentrations of Cyclodextrins ($[CD] > 1$ or 10 mol eq.) indicated the possible formation of copolymer-Cyclodextrin aggregates and formation of more flexible conformation in copolymers. This was evidenced by an increase in the observed value of drag reduction and the increase in the dimensions of the polymer's hydrodynamic radius.

The polymers exhibited an increase in polymer adsorption on silica as a function of polymer concentration. The extent of polymer adsorption was dependent on the molecular weight of the polymer studied and the strength of polymer-polymer interaction. The hydrophobic interactions were found to be responsible for the higher adsorption of the hydrophobically modified polyacrylamides on silica. The extent of polymer desorption from the surface of the silica was found to be dependent on the type of Cyclodextrin used. The nearly complete removal of the copolymers **AD8** (0.54 mol% of DAAM) and **AOD3** (0.09 mol% of ODAAM) and partial removal of copolymer **AD10** (0.21 mol% of DAAM, ~53 % of copolymer desorption) was achieved by β -Cyclodextrin. This was due to the formation of inclusion complexes between Cyclodextrin and the hydrophobic moieties. The lower value of desorption of the copolymer **AD10** from silica was due to weaker interaction of this copolymer with both α - and β -Cyclodextrin. The partial desorption of polyacrylamide by α - and β -Cyclodextrin (~34 and 38 %) was also demonstrated. This was considered to be due to either hydrogen bonding between the amide groups in the polymer and the hydroxyl groups in Cyclodextrins or partial displacement of polyacrylamide layers by Cyclodextrins due preferential adsorption of Cyclodextrins on silica over polyacrylamide. This study demonstrated that inexpensive Cyclodextrin can be utilised in removal of polymer from the surface of the well formation.

Chapter 6

Hydrophobically modified polymers of N-hydroxyethyl acrylamide

6.1. Introduction

Since the paper by Toms [9] on drag reduction effect caused by polymer solutions, many studies on various aspects of this phenomenon have followed. The molecular parameters that were found to affect the drag reduction performance of polymers were determined to be: the molecular structure, the chain flexibility, the length of polymeric molecules and the conformation of the random coil in various solvents [34, 77, 201].

The conformation of the polymer coils has an important influence on drag reduction. In turbulent flow, a random coil interacts with the flow and adsorbs kinetic energy from vortices [30]. It is also recognised that a good solvent promotes higher drag reduction, since the better interaction of the polymer results in an expanded polymer conformation i.e. higher hydrodynamic volume [83, 246]. It is therefore reasonable to assume that drag reduction performance is governed by the extent of the polymer/solvent interaction in a given solvent.

Poly(N-hydroxyethyl acrylamide) (PHEAAm) is a derivative of polyacrylamide with primary hydroxyl groups. It is more resistant to hydrolysis and more hydrophilic compared to polyacrylamide, and has been studied as a potential matrix for the capillary electrophoresis of DNA [161]. The synthesis of the poly(N-hydroxyethyl acrylamide) (PHEAAm) copolymers with a variety of monomers such as the *N*-acryloylmorpholine, *N,N*-dimethylacrylamide [163], 2,7-(9,9-dihexylfluorene) and *N*-isopropylacrylamide [247] or styrene has been reported. Saito *et al.* demonstrated that poly(N-hydroxyethyl acrylamide) was the most hydrophilic polymer of all known water soluble polymers [160]. Moreover, Skov *et al.* showed that this polymer has a higher radius of gyration in comparison to polyacrylamide of the same molecular weight [161]. Since drag reduction is largely dependent on the hydrodynamic volume, it can be considered that

the poly(N-hydroxyethyl acrylamide) could potentially provide better drag reduction in comparison to polyacrylamide. In addition, since poly(N-hydroxyethyl acrylamide) is more resistant to hydrolysis than polyacrylamide, it can be assumed that it could be used over a wider range of conditions (such as acidic or basic media) [162]. Furthermore, the incorporation of hydrophobic moieties into the polymer's backbone could potentially result in even higher drag reduction due to intermolecular hydrophobic associations between polymer chains and resulting higher apparent molecular weight.

The objective of the work described in this chapter was to investigate the possibility of the utilisation of poly(N-hydroxyethyl acrylamide) homopolymer and its copolymers as potential drag reducing agents. This chapter reports the micellar copolymerisation of N-hydroxyethyl acrylamide with varying amounts of n-decyl- and n-octadecyl acrylamide. The details of the synthesis and the characterisation procedures are described in Chapter 3. Micellar copolymerisation was chosen since it is known to result in high molecular weight water soluble copolymers. In addition, the hydrophobic groups are distributed as random blocks along the polymer backbone [116, 122, 124, 203]. The influence of the concentration of the hydrophobic monomers on the rheological and drag reducing properties of polymer solutions are reported. The effect of the size of the random coil of the copolymers on drag reduction is also demonstrated.

6.2. Results and Discussion

6.2.1. Synthesis and characterisation of polymers of N-hydroxyethyl acrylamide

A series of hydrophobically modified poly(N-hydroxyethyl acrylamide) copolymers were synthesized via the micellar copolymerisation procedure. The homopolymer was also synthesised via the same method and used as a control sample in all studies. It is well known that the properties of copolymers synthesised by micellar copolymerisation depend strongly on the hydrophobic monomer to surfactant ratio used in the polymerisation [126, 127, 132]. Thus, in this research, the size of the blocks and the concentration of hydrophobic moieties in the copolymers were controlled by altering the number of hydrophobes per surfactant micelle (N_H)

and concentration of the hydrophobic monomer in the feed. In Chapter 4, the water solubility of copolymers was found to be largely dependent on the N_H and on the initial concentration of hydrophobic monomer. The N_H number and the concentration of the hydrophobic monomer in this study was therefore kept below the specified value ($N_H < 2.1$ and $[H] < 0.85$ mol%) as indicated in the experimental conditions in Chapter 3 Sections 3.3.1 and 3.3.2. N-decyl acrylamide and n-octadecyl acrylamide were chosen as hydrophobic monomers in order to study the influence of length of the alkyl chain on the degree of association. It is alleged that longer alkyl chains lead to stronger hydrophobic association and the higher apparent molecular weight resulting in higher drag reduction effect and improved shear stability of copolymers.

The composition of the copolymers was determined using 1H NMR. Elemental analysis was additionally used to verify the results obtained by the NMR. The 1H NMR spectra of n-decyl acrylamide and n-octadecyl acrylamide were recorded in $CDCl_3$ and the spectra are presented in Chapter 4 *Figure 4.1* and *Figure 4.4*. The 1H NMR spectrum of poly(N-hydroxyethyl acrylamide) (**PHEAAm0**) and its copolymers with n-decyl acrylamide and n-octadecyl acrylamide were recorded in D_2O . The spectrum of **PHEAAm0**, a typical spectrum of poly(N-hydroxyethyl acrylamide-co-n-decyl acrylamide) (**HED1**, 0.73 mol% DAAM) and poly(N-hydroxyethyl acrylamide-co-n-octadecyl acrylamide) (**HEOD1**, 0.13 mol% ODAAM) is presented in *Figure 6.1*, *Figure 6.2* and *Figure 6.3*.

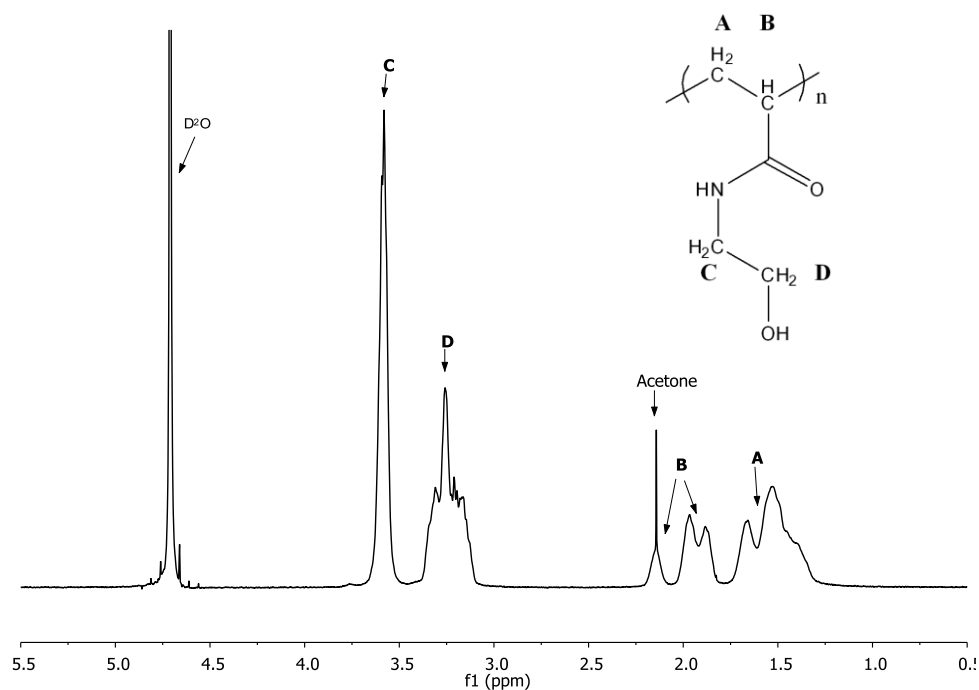


Figure 6.1. ¹H NMR spectrum of poly(N-hydroxyethyl acrylamide) acquired in D₂O (**PHEAAm0**).

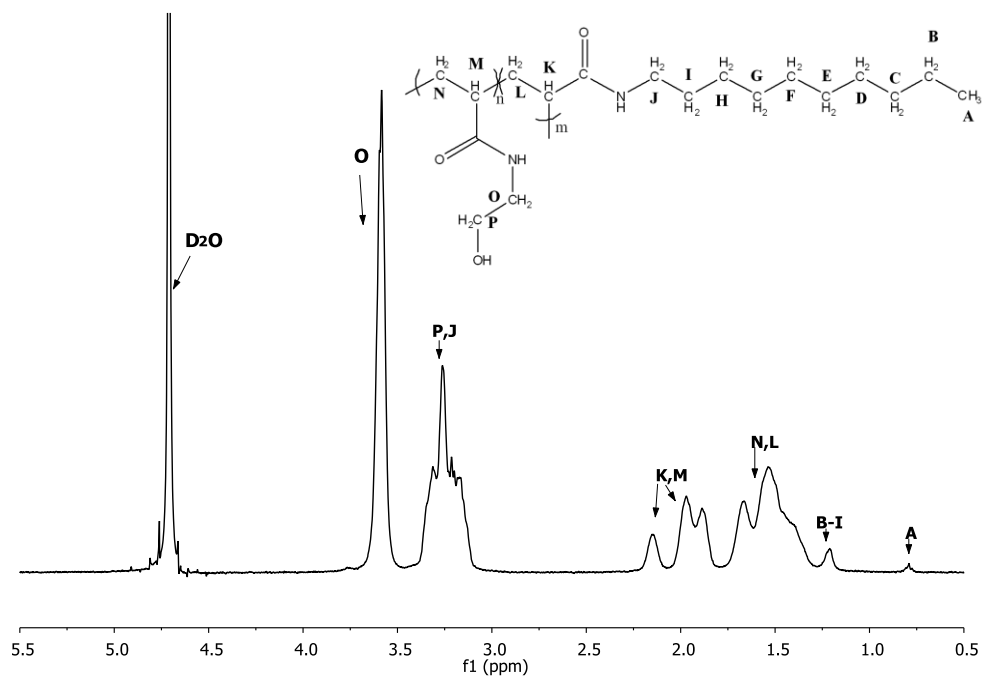


Figure 6.2. ¹H NMR spectrum of poly(N-hydroxyethyl acrylamide-co-n-decyl acrylamide) acquired in D₂O (**HED1**, 0.73 mol% DAAM).

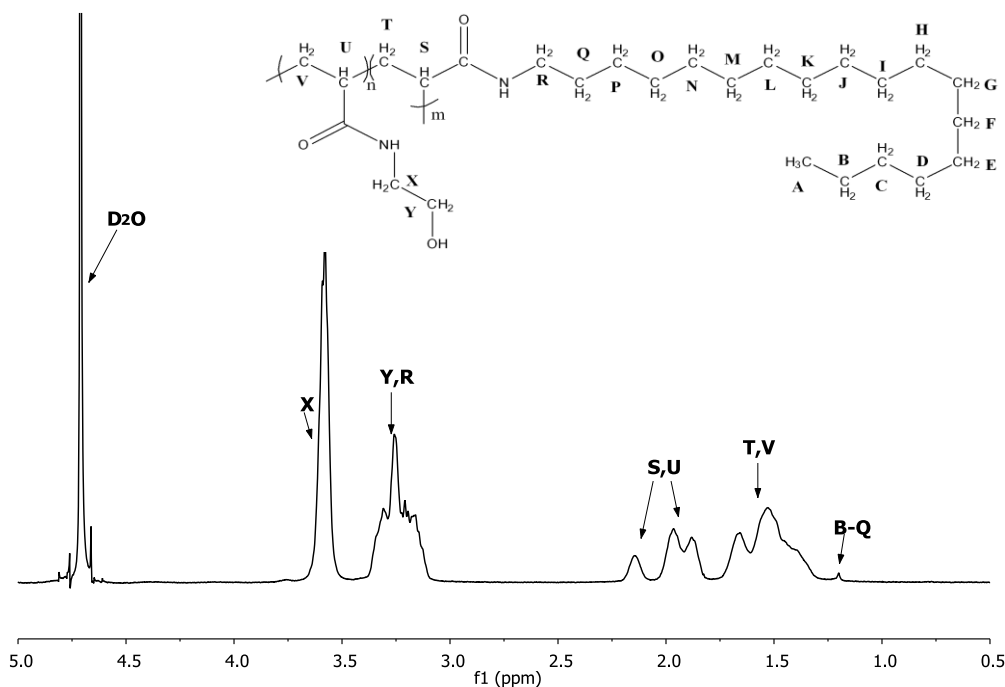


Figure 6.3. ^1H NMR spectrum of poly(N-hydroxyethyl acrylamide-co-n-octadecyl acrylamide) acquired in D_2O (**HEOD1**, 0.11 mol% ODAAm).

Protons characteristic for poly(N-hydroxyethyl acrylamide), n-decyl acrylamide and n-octadecyl acrylamide were identified and assigned (*Figure 6.2* and *Figure 6.3*). In the spectrum of n-decyl acrylamide and n-octadecyl acrylamide (*Figure 4.1* and *Figure 4.4*, Chapter 4), the chemical shifts for the protons from the methylene groups (CH_2) were marked as B-H, I and J (or B-P, Q and R in n-octadecyl acrylamide) and can be distinguished in the 1.2-1.6 ppm range and at 3.3 ppm, respectively. The strong triplet from the protons of the methyl groups (CH_3), signal A, appears at 0.8 ppm. In the spectrum of the poly(N-hydroxyethyl acrylamide) (**PHEAAm0**) (*Figure 6.1*), the peaks in the range of 1.2 and 3.2 ppm correspond to the protons of the methylene (A) and methine (B) groups in the polymer backbone. The methylene protons C and D in the side chain can be identified in the 3.1-3.6 ppm range. All of the protons for **PHEAAm0** polymer and protons from the alkyl chain of n-decyl acrylamide, A and B-J, could be identified and assigned in the ^1H NMR spectrum of poly(N-hydroxyethyl acrylamide-co-n-decyl acrylamide) synthesised via micellar polymerisation (*Figure 6.2*). This confirms the successful incorporation of the n-decyl acrylamide into the copolymer backbone.

All of the protons for **PHEAAm0** polymer and the protons from the alkyl chain of n-octadecyl acrylamide, B-Q could be identified and assigned in the ^1H NMR spectrum of poly(acrylamide-co-n-octadecyl acrylamide) (*Figure 6.3*). This confirmed that n-octadecyl acrylamide was successfully incorporated into the copolymer structure. Protons A and R could not be assigned due to low concentration of n-octadecyl acrylamide moieties in the copolymer.

In the ^1H NMR spectrum, the peaks of the terminal methyl and methylene groups in the alkyl chains of n-decyl- and methylene peak in n-octadecyl acrylamide and the peaks from methylene/methine groups in the polymer backbone were found to be sufficiently separated to allow the determination of the hydrophobic monomer concentration in the copolymers from their integrals. The data in *Table 6.1* indicates that the amount of n-decyl acrylamide (DAAm) and n-octadecyl acrylamide (ODAAm) in the copolymer is almost the same as the amount of the hydrophobic monomer in the feed. It should be noted however that the determination of the composition of copolymers determined by ^1H NMR, was a subject to a degree of uncertainty due to the low sensitivity of NMR (1-2%). However, based on the obtained results it can be stated that the composition of the copolymers is similar to the monomer feed composition used in the copolymerisation. This is in agreement with the research carried out by Candau *et al.* [122, 123, 132]. Candau and co-workers found that the micellar copolymerisation of acrylamide with hydrophobic monomers carried out to conversion below 50 %, leads to a copolymer composition equivalent to the monomer composition used in the feed. However, the final composition largely depends on the number of the hydrophobes per surfactant micelle N_{H} . This is due to the enhancement of the reactivity of hydrophobic monomers with increasing N_{H} number. This results in the fast and complete consumption of the hydrophobic monomer in the early stages of polymerisation. When N_{H} is 1 or smaller, the compositional heterogeneity is however minimized. On the basis of Candau's research, the fact that relatively low N_{H} numbers were used in the polymerisation and the similarity of N-hydroxyethyl acrylamide to acrylamide, it can be assumed that the composition of the copolymers is equal to the monomer composition used in the feed.

Sample	Yield (g) (%)	M _w (kDa)	PDI	H (mol%) Feed	N _H	H (mol%) ^{EA}	H (mol%) ^{NMR}
HED1	1.801 85.2	656	1.7	0.72	1.55	0.73	0.73
HED2	1.392 65.8	792	2.2	0.50	1.08	0.53	0.51
HED3	1.439 68.0	706	2.2	0.28	0.61	0.35	0.33
HEOD1	1.600 67.8	204	1.5	0.1	0.24	0.13	0.11
PHEAAm0	1.742 74.0	633	1.8	0	0	0	0

Table 6.1. Yield, molecular weight M_w and the content of hydrophobic moieties H in the copolymers obtained by micellar polymerisation; PDI is the polydispersity index, **HED**= poly(N-hydroxyethyl acrylamide-co-n-decyl acrylamide), **HEOD**= poly(N-hydroxyethyl acrylamide-co-n-octadecyl acrylamide), **PHEAAm0**= poly(N-hydroxyethyl acrylamide).

All polymerisations were carried out with high initial concentration of the monomers according to Equation 24 (~18 wt%) in order to obtain polymers with high molecular weight. The molecular weights achieved, as shown in *Table 6.1* were found to be reasonably high. The yield of the polymerisation was found to be relatively low. This can be explained by the viscosity effect. At high concentrations of monomer in the feed, the polymerisation mixture becomes so viscous with increasing conversion that the polymerisation becomes controlled by diffusion and the decrease in the mobility of the propagating species is observed [210].

6.2.2. Rheology of polymers of N-hydroxyethyl acrylamide

The apparent viscosity of the aqueous solutions of poly(N-hydroxyethyl acrylamide) copolymers was studied as a function of concentration at a constant shear rate of 10 s⁻¹. The influence of shear rate between 7 s⁻¹ and 1000 s⁻¹ was studied in order to determine the viscoelastic properties of the polymers. It can be seen from *Figure 6.4* that a linear evolution of apparent viscosity with concentration was observed for poly(N-hydroxyethyl acrylamide) (**PHEAAm0**).

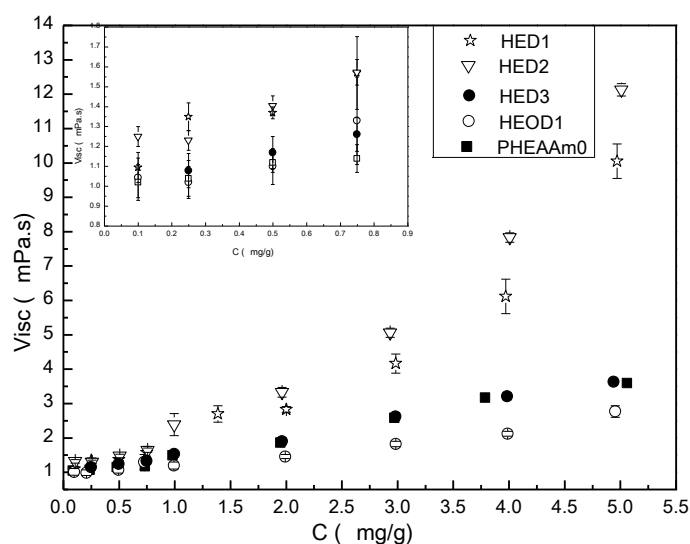


Figure 6.4. Apparent viscosity of the aqueous solutions of polymers of N-hydroxyethyl acrylamide as a function of polymer concentration. Measured at 10 s^{-1} and 25°C (inset shows close-up of low concentrations).

Copolymers containing 0.33 mol% of n-decyl acrylamide and synthesised at low N_H ($N_H = 0.61$, short length of the hydrophobic block) (**HED3**) and a low concentration of n-octadecyl acrylamide (**HEOD1**, 0.11 mol% ODAAm, $N_H = 0.24$, $M_w = 706 \text{ kDa}$) displayed the same behaviour as poly(N-hydroxyethyl acrylamide) (**PHEAAm0**, $M_w = 633 \text{ kDa}$). These concentrations of the hydrophobic moieties and the length of the hydrophobic block appear to be too low or too short to induce significant changes in the apparent viscosity. Changes in the apparent viscosity of copolymer **HEOD1** were also not observed despite incorporation of the very hydrophobic n-octadecyl acrylamide moieties into the polymer backbone. On the other hand the weight average molecular weight (M_w) of poly(N-hydroxyethyl acrylamide-co-n-octadecyl acrylamide) was relatively low compared to the homopolymer (**PHEAAm0**), and therefore, a lower apparent viscosity was expected.

The copolymers **HED1** ($N_H = 1.55$, $M_w = 656 \text{ kDa}$) and **HED2** ($N_H = 1.08$, $M_w = 792 \text{ kDa}$) containing 0.73 and 0.51 mol% of n-decyl acrylamide, respectively, and having longer hydrophobic block length than **HED3** displayed a noticeably different behaviour; the measured

apparent viscosity at polymer $C = 1 \text{ mg}\cdot\text{g}^{-1}$ increased significantly as a result of the strengthening of the hydrophobic intermolecular associations. The observed increase in the apparent viscosity occurred at a concentration lower than the overlap concentration (C^*) of the poly(N-hydroxyethyl acrylamide) (**PHEAAm0**). This concentration at which the apparent viscosity of the polymer solution abruptly increased corresponds to the critical aggregation concentration (C_{agg}). This observation is in agreement with previous research on hydrophobically modified polyacrylamide [26, 215, 248]. It can be also seen in *Figure 6.4* that the apparent viscosity of copolymers **HED1** and **HED2** was higher than the apparent viscosity of the homopolymer **PHEAAm0** at low concentrations. This indicates the existence of intermolecular interactions between hydrophobic moieties in hydrophobically modified poly(N-hydroxyethyl acrylamide) even in the dilute concentration regime in addition to intramolecular hydrophobic interactions. However, the apparent viscosity of the copolymer containing n-octadecyl acrylamide (**HEOD1**) was lower than the apparent viscosity of pure homopolymer (**PHEAAm0**), which had a higher molecular weight. This can be associated with the incorporation of longer alkyl chains which result in stronger intramolecular interactions, causing coil contraction, and therefore a lower apparent molecular weight [249]. This behaviour could be also associated with lower molecular weight of **HEOD1** ($M_w = 204 \text{ kDa}$).

The changes in the apparent viscosity of aqueous solutions of polymers measured as a function of shear rate were measured at polymer concentrations of 0.5 ($C < C_{\text{agg}}$) and 1 $\text{mg}\cdot\text{g}^{-1}$ (C_{agg}) for the copolymers and the homopolymer of poly(N-hydroxyethyl acrylamide). It is clearly demonstrated in *Figure 6.5* and *Figure 6.6* that the concentration of hydrophobic moieties in the polymer had a significant influence on the polymers behaviour.

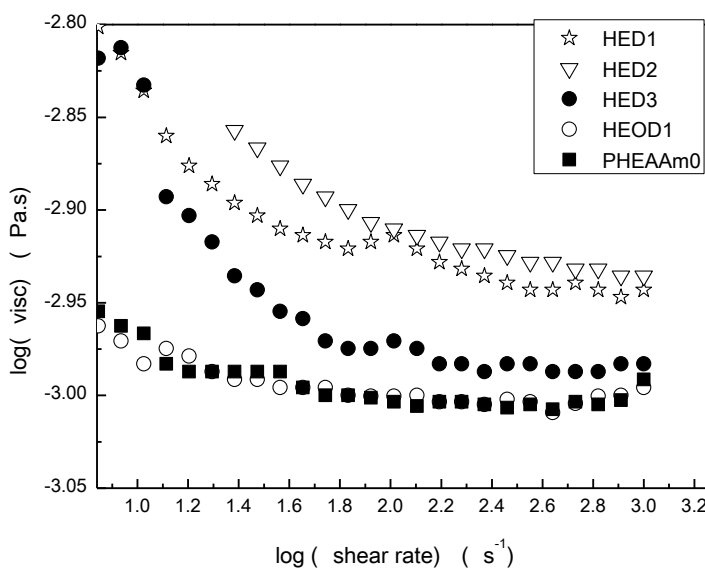


Figure 6.5. Apparent viscosity as a function of shear rate for aqueous solutions of poly(*N*-hydroxyethyl acrylamide) polymers at polymer concentration of $0.5 \text{ mg}\cdot\text{g}^{-1}$ and at 25°C (logarithmic scale).

The copolymer containing 0.11 mol% of *n*-octadecyl acrylamide (**HEOD1**) and homopolymer (**PHEAAm0**) displayed Newtonian behaviour and had comparable viscosities. However, the copolymers containing *n*-decyl acrylamide, **HED1** (0.73 mol% DAAM), **HED2** (0.51 mol% DAAM) and **HED3** (0.33 mol% DAAM) displayed pronounced shear thinning. This behaviour was a result of the increased apparent viscosity of the copolymers at lower shear rates. Moreover, the apparent viscosity increased with increasing concentration of *n*-decyl acrylamide moieties. This indicates an increase in the strength of hydrophobic interaction with increasing concentration of *n*-decyl acrylamide units and with increasing the length of the hydrophobic block in the polymer backbone. The apparent viscosity of copolymer **HED1** was lower than the apparent viscosity of copolymer **HED2** and this could be due to lower weight average molecular weight of **HED1** or stronger intramolecular hydrophobic interactions that cause contraction of the random coil. The sharper decrease in the apparent viscosity as a function of shear rate was the result of the orientation and the disentanglement of the polymer chains under shear, which is associated with the breaking of the hydrophobic intermolecular associations. The apparent

viscosity of copolymers containing n-decyl acrylamide **HED1**, **HED2** and **HED3** displayed at high shear rates, was however larger than the apparent viscosity of homopolymer **PHEAAm0**, suggesting the incomplete breakage of intermolecular hydrophobic associations. This behaviour is in agreement with previous findings for hydrophobically modified PAAm copolymers [109, 250].

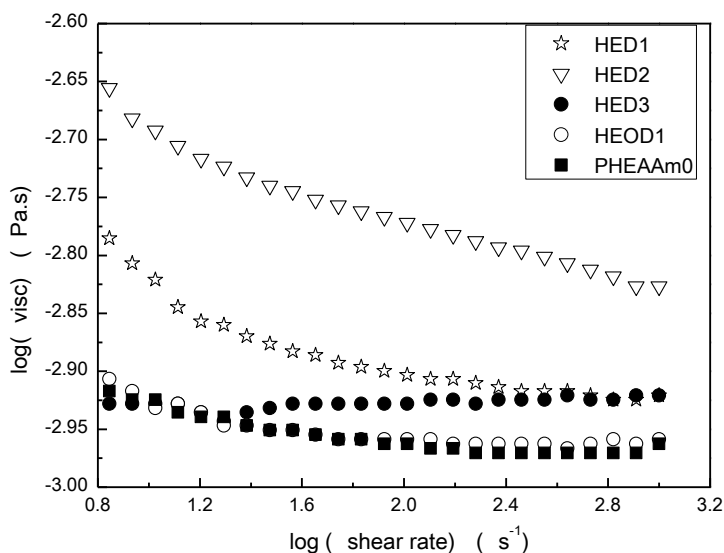


Figure 6.6. Apparent viscosity as a function of shear rate for aqueous solutions of poly(N-hydroxyethyl) polymers at polymer concentration of $1 \text{ mg}\cdot\text{g}^{-1}$ and at 25°C (logarithmic scale).

6.2.3. Instantaneous drag reduction study of polymers of N-hydroxyethyl acrylamide

The drag reduction effect caused by aqueous solutions of poly(N-hydroxyethyl acrylamide) polymers was studied as a function of concentration using a rheometer equipped with double-gap Couette geometry at 25°C . The drag reduction of commercial polyacrylamide ($M_w = 1085 \text{ kDa}$, $\text{PDI} = 2.05$) was also studied for comparison. The hydrodynamic radius was also studied by Dynamic Light Scattering (DLS) at concentrations below C_{agg} to study an influence of hydrodynamic volume on the drag reduction effect caused by poly(N-hydroxyethyl acrylamide) polymers. The percentage drag reduction reported was the maximum drag reduction achieved in

the first 5 minutes of measurements. Poly(N-hydroxyethyl acrylamide) (**PHEAAm0**, $M_w = 633$ kDa) and poly(N-hydroxyethyl acrylamide-co-n-octadecyl acrylamide) (**HEOD1**, $M_w = 204$ kDa, 0.11 mol% ODAAm) did not display a drag reduction effect at any concentration studied (Figure 6.8). The behaviour of latter could be attributed to the low molecular weight, since it is known that the lower polymer's molecular weight limit displaying drag reduction effect is around 500 kDa [10, 251]. The drag reduction of poly(N-hydroxyethyl acrylamide-co-n-decylacrylamide) copolymers was found to increase with concentration and was dependent on the concentration of n-decyl acrylamide moieties and the length of the hydrophobic block in the polymer backbone (Figure 6.7).

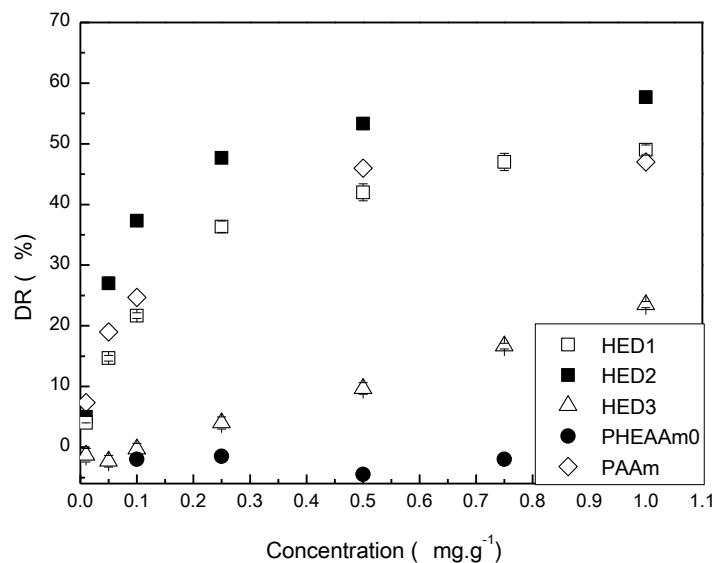


Figure 6.7. Percentage drag reduction as a function of polymer concentration for polyacrylamide (PAAm, $M_w = 1085$ kDa), **PHEAAm0** and poly(N-hydroxyethyl acrylamide-co-N-decylacrylamide) copolymers.

The drag reduction by poly(N-hydroxyethyl acrylamide-co-n-decyl acrylamide) polymers increased with the concentration of n-decyl acrylamide moieties and the length of the hydrophobic blocks (increase in N_H). The lower drag reduction of **HED1** in comparison to **HED2** could be attributed to lower molecular weight of **HED1**. The maximum drag reduction effect displayed by **HED2** containing 0.52 mol% of n-decyl acrylamide and with a molecular

weight of 792 kDa was found to be 53 % at $C= 0.5 \text{ mg}\cdot\text{g}^{-1}$ and 57 % at $C=1 \text{ mg}\cdot\text{g}^{-1}$. This level of drag reduction was found to be higher than the drag reduction of polyacrylamide of higher molecular weight (1085 kDa, DR= 45 %). Moreover, the drag reduction of sample **HED2** was found to slightly increase further with increasing concentration.

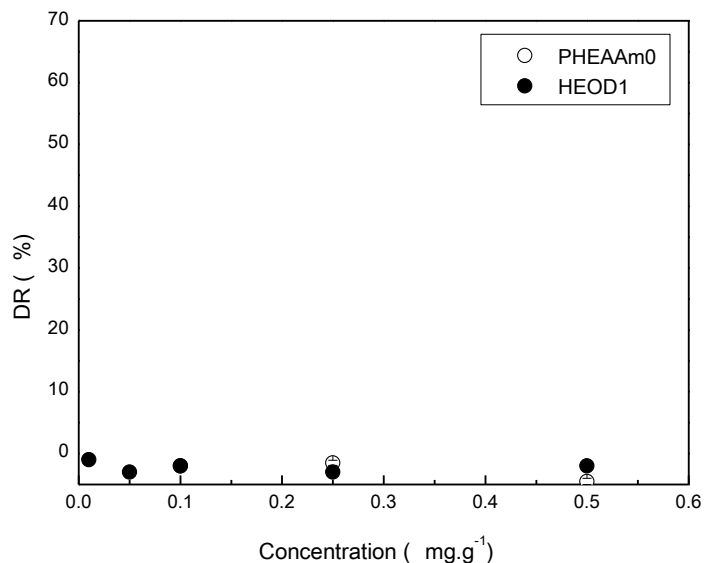


Figure 6.8. Percentage drag reduction as a function of polymer concentration for HEAAm homopolymer (**PHEAAm0**) and its copolymer with n-octadecyl acrylamide (**HEOD1**).

Drag reduction effect imparted by polymers depend on chemical structure, polymer flexibility, polymer-solvent interactions, presence of intermolecular associations and polymer molecular weight. The mechanism of drag reduction by polymers is strongly connected to the behaviour of polymer macromolecules when interacting with turbulent vortices and this behaviour in turn is linked to the above parameters. The lack of the ability of the homopolymer **PHEAAm** to reduce drag cannot be connected to the low molecular weight, since copolymers of comparable molecular weight reduce drag effectively. The higher hydrodynamic radius of poly(N-hydroxyethyl acrylamide) as compared to polyacrylamide should also result in higher drag reduction [246]. Lumley stated that polymer molecules become elongated due to interaction with turbulent vortices [34]. This elongation leads to an increase in the effective viscosity, which enhances the dissipation of turbulent forces. McCormick *et al.* also stated that more expanded

molecules are more effective at low Reynolds numbers since low shear rates are required to unravel these molecules. Based on this theory, it is possible that the expanded hydrodynamic radius of poly(N-hydroxyethyl acrylamide) **PHEAAm0** could be the cause of the worse suppression of turbulence at the Reynolds numbers studied in this research. As can be seen from the results summarised in *Table 6.2* the hydrodynamic radius of polyacrylamide (PAAm) of higher M_w was lower than the hydrodynamic radius of poly(N-hydroxyethyl acrylamide) (**PHEAAm0**). The incorporation of hydrophobic moieties into poly(N-hydroxyethyl acrylamide) resulted in an increase in the size of the hydrodynamic radius. The predicted hydrodynamic radius of copolymer **HED1** in the absence of any interactions should be 75.2 nm. If only intermolecular hydrophobic associations were present in the copolymers, the size of the hydrodynamic radius should be twice the size of poly(N-hydroxyethyl acrylamide) (**PHEAAm0**, $R_H = 74.3$ nm). The size of 87.2 nm suggests that intermolecular as well as intramolecular hydrophobic associations were present in the aqueous polymer solutions. The higher apparent viscosity of the copolymers at low concentrations and at constant shear rate (Section 6.2.2 *Figure 6.4*) supports the presence of intermolecular hydrophobic associations. Poly(N-hydroxyethyl acrylamide) itself did not have any drag reducing properties, however the results clearly showed that the simple modification of this polymer with pendant hydrophobic groups imparted drag reducing properties. McCormick *et al.* [19] showed in their studies, that the extent of polymer-polymer and polymer-solvent interactions have a great effect on drag reduction performance. Enhanced drag reduction (DR) was observed for hydrophobically modified polymers when intermolecular molecular associations were present, and the solvent promoting the intermolecular hydrophobic associations promoted higher drag reduction. From the obtained results two conclusions could be drawn: the introduction of hydrophobic moieties reduced solvent quality and resulted in more closed conformation (stronger polymer-polymer interactions) but in the same time hydrophobic moieties associated intermolecularly resulting in higher apparent molecular weight; therefore the efficient drag reduction effect was observed

Sample	M_w (kDa)	PDI	H (mol%) ^{NMR}	N_H	$DR_{0.5mg\cdot g^{-1}}$ (%)	R_H (nm)
HED1	656	1.7	0.73	1.55	43	87.2±1.65
HED2	792	2.2	0.51	1.08	53	90.7±1.2
HED3	706	2.2	0.33	0.61	8	85.9±2.9
HEOD1	204	1.5	0.11	0.24	0	62.4±1.8
PHEAAm0	633	1.8	0	0	0	74.3±3.3
PAAm	1085	2.1	0	0	45	63.6±2.7

Table 6.2. Molecular parameters of the modified poly(N-hydroxyethyl acrylamide) copolymers obtained from the GPC analysis and Dynamic Light Scattering (DLS). Where N_H is the number of hydrophobes per surfactant micelle, M_w is the weight average molecular weight, PDI is the polydispersity index, H (mol%) is the molar percentage of hydrophobic moieties in polymer and R_H is the hydrodynamic radius. **HED**= poly(N-hydroxyethyl acrylamide-co-n-decyl acrylamide) **HEOD**= poly(N-hydroxyethyl acrylamide-co-n-octadecyl acrylamide), **PHEAAm0**= poly(N-hydroxyethyl acrylamide).

6.3. Summary

The objective of the work described in this chapter was to investigate the possibility of the utilisation of poly(N-hydroxyethyl acrylamide) and its copolymers as a potential drag reducing agents. The water-soluble hydrophobically modified poly(N-hydroxyethyl acrylamide) copolymers with varying degree of hydrophobicity were successfully synthesised using micellar polymerisation. ¹H NMR spectra of the water soluble polymers demonstrated the successful incorporation of hydrophobic groups into the copolymers. The effect of the concentration of the incorporated hydrophobic moieties and the length of the hydrophobic block on the properties of polymers was demonstrated by rheology. It was shown that hydrophobic intermolecular associations as well as intramolecular hydrophobic interactions exist even in dilute concentration regime. The polymers containing high concentrations of n-decyl acrylamide (**HED1** and **HED2**) showed a sharp increase in apparent viscosity with increasing concentration of polymers (above 1 mg·g⁻¹) due to strong intermolecular hydrophobic association. The pronounced shear thinning

for copolymers **HED1** (0.73 mol% DAAM) and **HED2** (0.51 mol% DAAM) was associated with the orientation and the disentanglement of polymer chains under the shear, which was a result of the breaking up of the hydrophobic intermolecular associations.

Drag reduction studies carried out for the water soluble samples showed that the homopolymer **PHEAAm0** did not reduce drag. This was due most likely due to highly expanded open random coil conformation, incapable of suppression of turbulence at the Reynolds numbers studied. The incorporation of hydrophobic moieties was found to impart drag reduction behaviour into poly(N-hydroxyethyl acrylamide), due to two effects: weakened polymer-solvent interactions resulting in less expanded conformation and intermolecular hydrophobic associations resulting in higher apparent molecular weight. The drag reduction of hydrophobically modified poly(N-hydroxyethyl acrylamide) was found to be higher than that of polyacrylamide. This was linked to the presence of intermolecular hydrophobic associations resulting in higher hydrodynamic radii and higher apparent molecular weight.

This study demonstrated that the incorporation of a small concentration of hydrophobic moieties into poly(N-hydroxyethyl acrylamide) imparted its drag reducing properties. The drag reduction effect created by the incorporation of the associating hydrophobic moieties exceeded the drag reduction of polyacrylamide.

Chapter 7

Sulfonated copolymers of styrene and butadiene

7.1. Introduction

In the previous chapters, the influence of the molecular characteristics of polymers on drag reduction performance was demonstrated. It was established that the incorporation of small amounts of hydrophobic moieties into the polymeric structures was sufficient to induce or improve the drag reduction efficiency and shear stability of polymers. For example, the introduction of hydrophobic groups into water soluble poly(N-hydroxyethyl acrylamide) was found to induce drag reducing properties in water.

Hydrophobic polymers are also known to reduce drag as effectively as water soluble polymers. Polystyrene and polybutadiene are examples of hydrophobic homopolymers displaying such properties in organic solvent [76, 87, 199, 252, 253]. It would therefore be of interest to investigate the modification of these polymers to render them water soluble, in order to determine if they are able to reduce drag in water.

The functionalisation of polymers of styrene has been demonstrated in Chapter 2 to occur via the aromatic electrophilic substitution, and the sulfonation of block polymers containing moieties with π -bonds is well known [180, 254, 255]. It has been shown that the partial sulfonation of the diblock or triblock copolymers of styrene and isoprene can create polymers that form micellar-like structures in water due to hydrophobic interactions [192, 193]. The presence of sulfonate functionalities and hydrophobic moieties in the polymers of acrylamide has been also demonstrated to increase the shear stability and salt resistance of these polymers, as well as an increased stability to high temperatures [256]. Perricone *et al.* also showed that vinyl sulfonate copolymers are more effective drag reducing agents in high temperature oil field operations because they are more hydrolytically and enzymatically stable [257]. The partial sulfonation of polystyrene and polybutadiene was therefore performed to impart water solubility. It is

postulated that these polymers would be able to reduce drag (via hydrophobic associations) in aqueous solutions with the added benefit of being able to withstand the high temperature that can be encountered in oil and gas reservoirs.

In this chapter, the synthesis, the rheology and the drag reducing properties of sulfonated poly(styrene-*block*-butadiene) copolymers is described. The details of the synthesis and characterisation procedures are presented in Chapter 3. The influence of the acetyl sulfate concentration, the sulfonation time and the reaction temperature on the degree of sulfonation is demonstrated. The influence of the degree of sulfonation in water-soluble polymers on chain mobility, thermal stability, rheology and drag reducing properties is also reported. The shear resistance of polymers as a function of the degree of sulfonation of the block copolymers is also reported.

7.2. Results and discussion

7.2.1. Sulfonation of poly(styrene-*block*-butadiene)

A series of sulfonated poly(styrene-*block*-butadiene) polymers were synthesized using variable concentrations of acetyl sulfate with respect to the polymer. Polymers generally become more water soluble with the increasing amount of sulfonate groups that are incorporated. However, there is a higher probability of crosslinking occurring (sulfone formation) with increasing amounts of sulfonate groups [176]. The amount of the sulfonating agent, sulfonation time and temperature was therefore varied in order to achieve optimal water solubility without occurrence of crosslinking. The extent of sulfonation was evaluated by elemental analysis and the data is presented in *Table 7.1*, together with the obtained degrees of sulfonation.

Sample	Yield (g) (%)	SD designed (mol%)	SD (mol%)	Solubility THF/H ₂ O %/%
SSB1	0.4102 84.5	72	6.68	90/10
SSB2	0.441 71.96	72	21.74	56/44
SSB3	0.520 83.2	140	43.5	25/75
SSB4	0.520 79.83	290	46.33	15/85
SSB5	0.512 77.21	574	46.98	10/90
SSB6	0.556 66.78	574	66.28	0/100
SSB7	0.414 70.57	1149	24.89	60/40
SSB8	0.664 98.54	1149	53.55	2/98
SSB9	0.407 61.99	1149	42.27	27/73
SSB10	0.656 92.06	1149	57.06	0/100
SSB11	0.571 93.94	1720	33.72	40/60
SSB12	0.5688 93.75	2295	33.07	40/60

Table 7.1. Properties of sulfonated poly(styrene-*block*-butadiene). SD is the degree of sulfonation (extent of sulfonation) determined by elemental analysis and calculated from equations (14)-(18) in Chapter 3 section 3.5.9.

The extent of sulfonation was found to be lower than desired degree of sulfonation (See *Table 7.1* and *Table 3.4* Chapter 3). Additionally the degree of sulfonation at a constant temperature was found to increase before reaching a maximum point, after which the extent of sulfonation

decreased (*Figure 7.1*). This suggests that sulfonation became more difficult as the degree of sulfonation increased. The reason behind this could be due to the decrease in the solubility of the more polar sulfonated polymers in a less polar solvent that was used in the sulfonation reaction, which caused contraction of the polymeric chains [180, 182, 188].

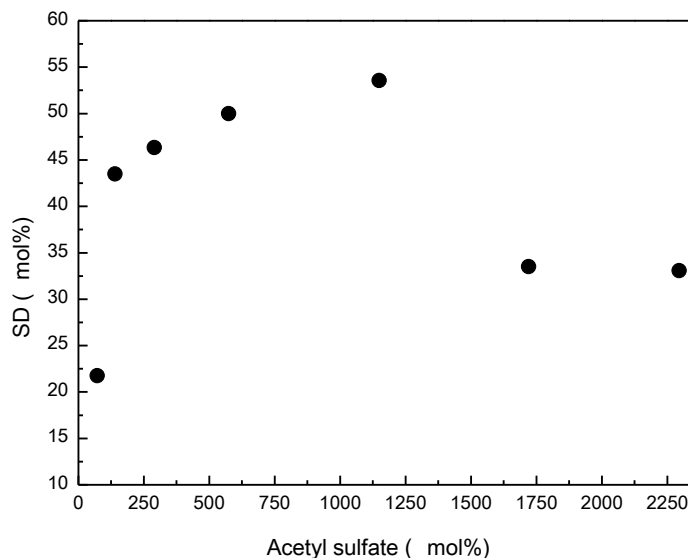


Figure 7.1. Yield of sulfonation of poly(styrene-*block*-butadiene) at 25°C and at a sulfonation time of 24 hours.

The decrease in the degree of sulfonation at high concentrations of acetyl sulfate (above 1250 mol%) could be also explained by the reversibility of the reaction. Since each reaction step was in equilibrium, the conditions of the reaction could heavily affect the yield through disruption of this equilibrium [178, 258]. High concentrations of acetyl sulfate used also mean that high concentrations of acetic acid were produced. This shifted the equilibrium to the left and desulfonation occurred (*Figure 7.2*).

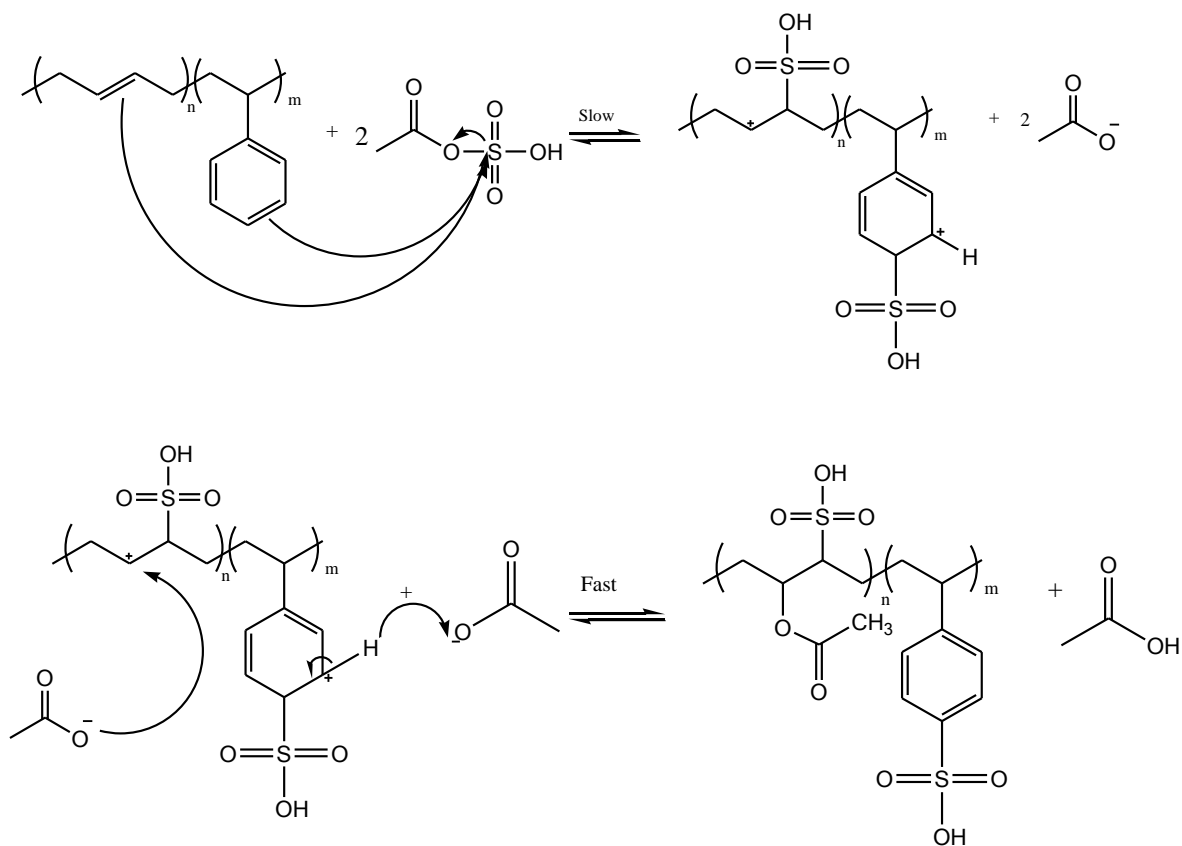


Figure 7.2. The mechanism of sulfonation of poly(styrene-*block*-butadiene) by acetyl sulfate. For clarity 1,2 butadiene sulfonation is omitted.

The dependence of the extent of sulfonation on reaction time is presented in *Figure 7.3*. The degree of sulfonation was found to initially increase with time before reaching a maximum, whereupon it started to decrease. Idibie *et al.* observed polymer degradation at high concentrations of chlorosulfonic acid (another type of sulfonating agent) [254]. This implies that there is an optimal degree of sulfonation and any further attempts to increase the degree of sulfonation will result in polymer degradation. The extent of sulfonation was also found to increase with temperature. When the reaction temperature was raised from 25 °C to 40°C, almost 20 % increase in the degree of sulfonation was observed when the concentration of acetyl sulfate was at moderate level (574 mol%, see *Table 3.4*, samples **SSB5** and **SSB6**). At higher concentrations of the sulfonating agent, the extent of this increase was not that large (1149 mol

%, **SSB8** and **SSB10**). This is in agreement with previous reports on the sulfonation of polyvinyl aromatics [178].

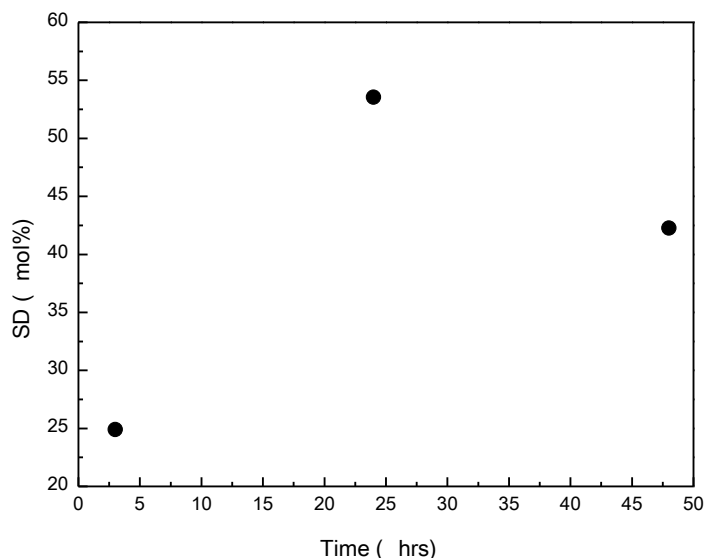


Figure 7.3. Time dependence of the degree of sulfonation of poly(styrene-*block*-butadiene). Studied at 25°C and with 5.74 mol eq. of acetyl sulfate to 1 mol eq. of polymer.

The synthesized polymers were all soluble in mixtures of tetrahydrofuran and deionised water. As expected, the water solubility was found to increase with increasing degree of sulfonation. Moreover, samples **SSB6** (SD= 66.28 mol%) and **SSB10** (SD= 57.06 mol%) were found to be soluble in deionised water and in mixtures of water with dimethyl sulfoxide (DMSO) or methanol (MeOH). Sample **SSB8** (SD= 53.55 mol%) was found to be soluble in a mixture of water and acetone; however some small gel particles were observed in deionised water.

The weight average molecular weight of the sulfonated copolymers could not be determined by Gel Permeation Chromatography, due to strong interactions between the sulfonate groups and the column, as well as interactions within the hydrophobic chains.

7.2.3. Characterisation of sulfonated poly(styrene-*block*-butadiene)

FT-IR and $^1\text{H-NMR}$ analyses were used to confirm sulfonation and to determine the extent of sulfonation. *Figure 7.4* and *Figure 7.5* compares the FT-IR spectra of poly(styrene-*block*-butadiene) before and after sulfonation.

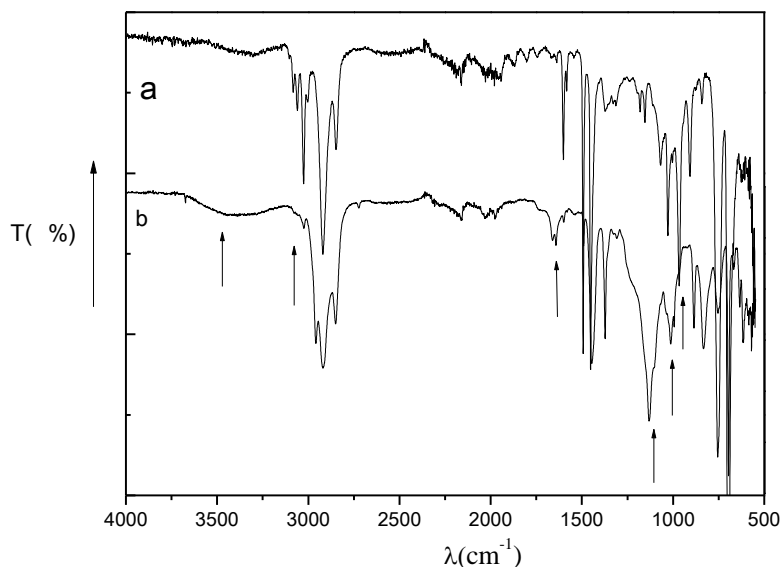


Figure 7.4. Infrared spectrum of poly(styrene-*block*-butadiene) before (a) and (b) after sulfonation (**SSB1**, SD= 6.68 mol%).

The characteristic absorption bands for polybutadiene units were observed at 966, 1640 and 3100 cm^{-1} and those at 750, 905, 1650 cm^{-1} were due to the phenyl rings of the polystyrene units. The existence of the absorption band at 3490 cm^{-1} was attributed to the OH stretch from the sulfonic acid group and was observed even at very low degree of sulfonation (*Figure 7.4*). The adsorption bands at 1034 and 1162 cm^{-1} were due to the vibration of the sulfonic acid group (O=S=O) in the sulfonated polymer. The band at 1650 cm^{-1} became more intense with increasing degree of sulfonation. This wave number is characterised by the vibration modes of the phenyl group. Additionally, the sulfonated polymers showed a clear decrease in the relative intensity of the C-H (3100 cm^{-1}) and C=C (966 cm^{-1}) adsorption bands which corresponds to the adsorption of butadiene, although band at 3100 cm^{-1} also corresponds to adsorption of C-H in benzene ring.

This demonstrates that sulfonation occurred not only at polystyrene segments but also at the polybutadiene segments.

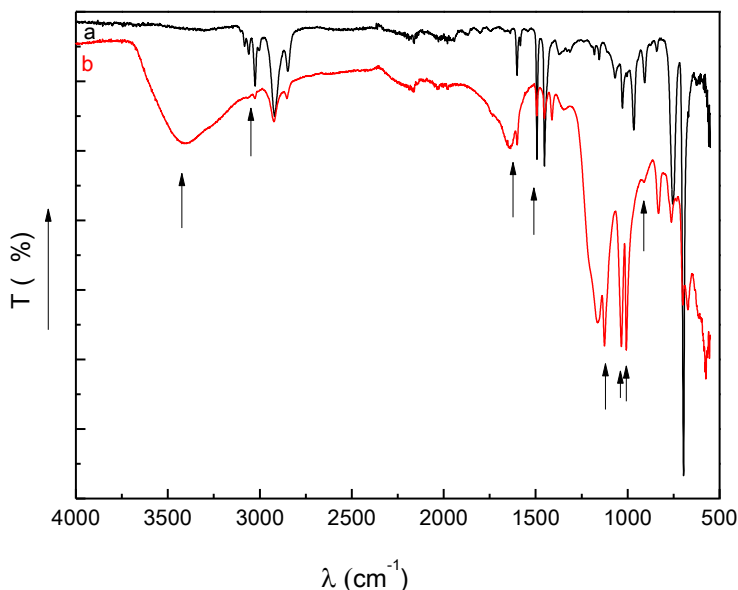


Figure 7.5. Infrared spectrum of poly(styrene-*block*-butadiene) before (a) and (b) after sulfonation (**SSB6**, SD= 66.28 mol%).

Figure 7.6 and *Figure 7.7* show the ^1H NMR spectra of poly(styrene-*block*-butadiene) before and after sulfonation (**SSB6**, SD= 66.28 mol%), respectively. The proposed structure is presented in *Figure 7.8*. The spectrum of the sulfonated sample was taken in a mixture of 25% deuterated THF and 75% D_2O . Samples in pure D_2O were very viscous and therefore the ^1H NMR spectra could not be obtained. The disappearance of the signals at 2.0, 2.5 and 5.0-5.7 ppm (attributed to polybutadiene) was observed in the sulfonated polymer, confirming that the sulfonation of polybutadiene did occur. Additionally, the appearance of a new signal at 7.5 ppm, attributed to the substituted polystyrene (the aromatic hydrogen signals absorption range), could be assigned to the successful sulfonation of polystyrene.

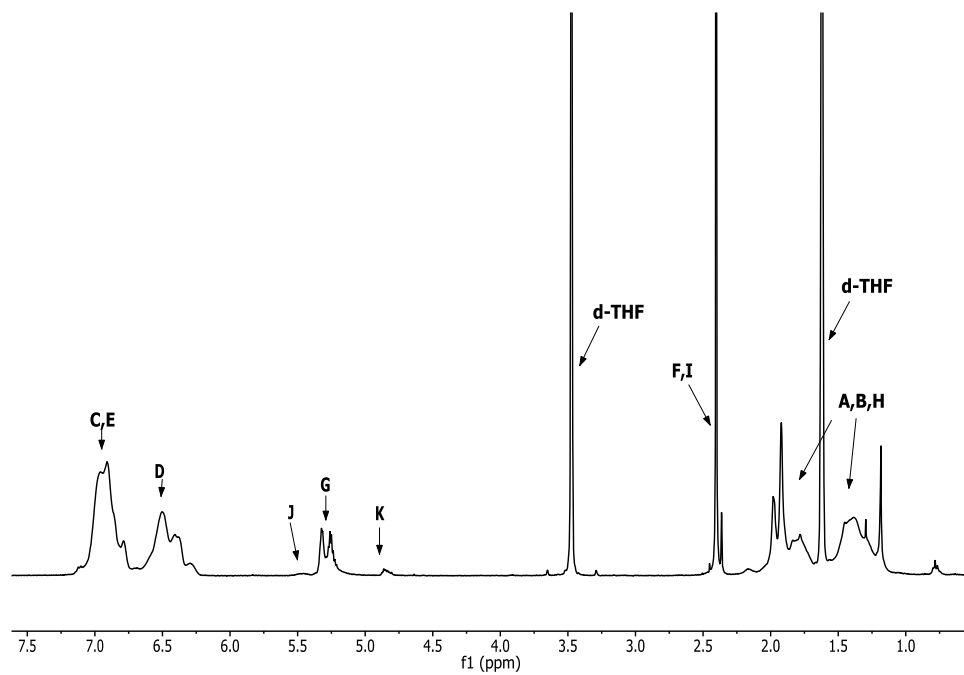


Figure 7.6. ^1H NMR spectrum of poly(styrene-*block*-butadiene) before sulfonation in d_8 -THF.

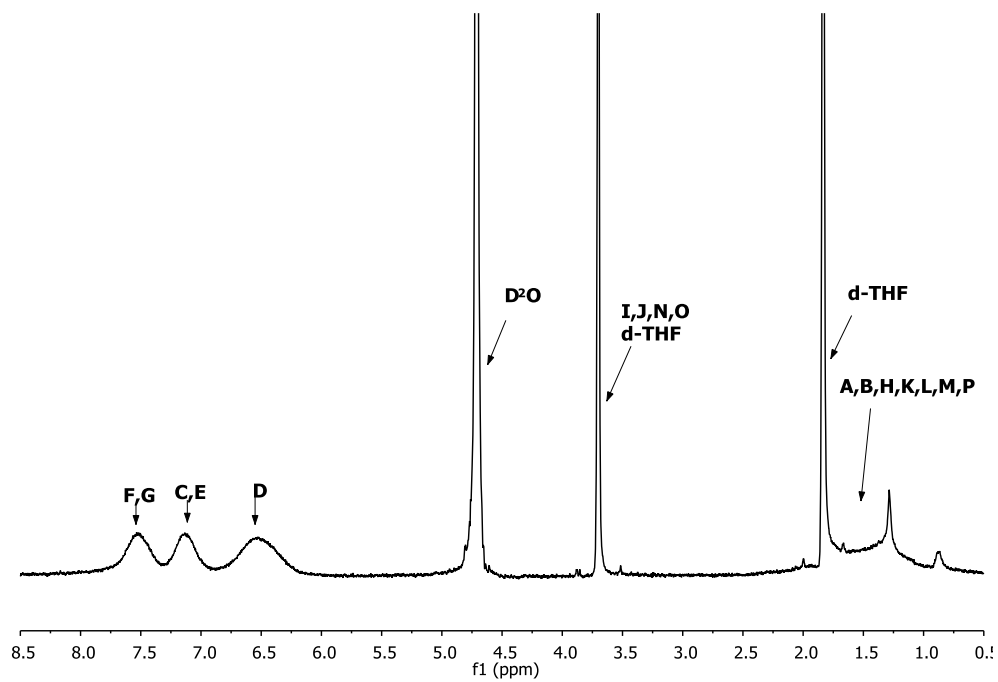


Figure 7.7. ^1H NMR spectrum of poly(styrene-*block*-butadiene) after sulfonation in a mixture of 25% d_8 -THF and 75% D_2O (SSB6, SD= 66.28 mol%).

The peaks arising from the protons adjacent to the sulfonic acid and carbonyl groups in sulfonated polybutadiene were expected to appear at ~3.7 ppm, however the peaks could not be distinguished due to signal overlap with d_8 -THF. The small peak at 0.8 and the sharp peak at 1.4 ppm can be assigned to the end groups from the tert-butyl lithium initiator. This is in agreement with literature reports [259, 260].

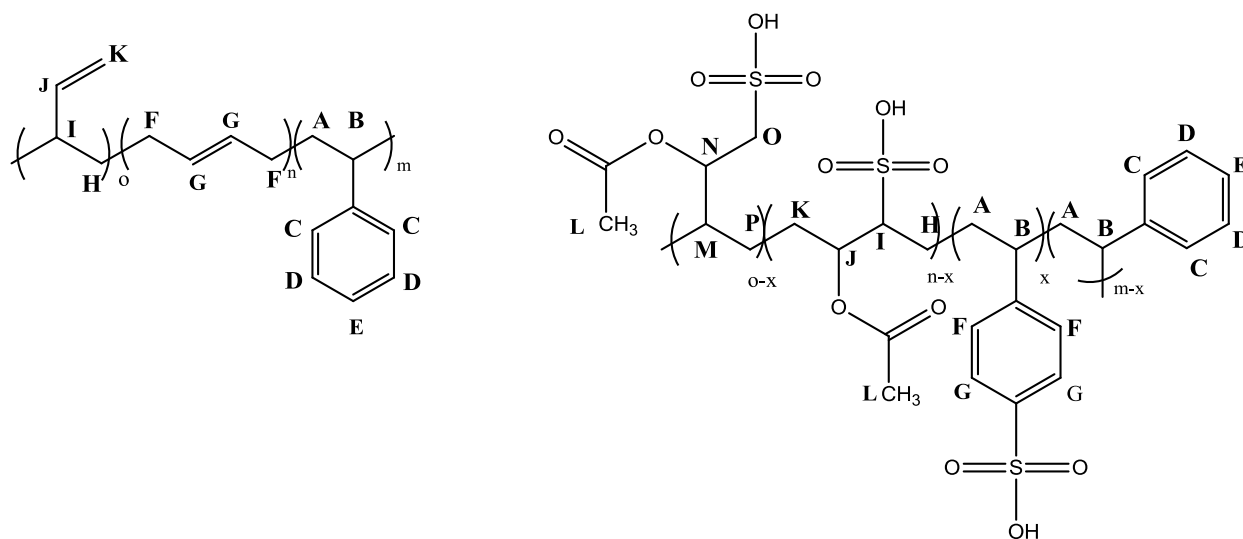


Figure 7.8. Chemical structure of poly(styrene-*block*-butadiene) before and after sulfonation with acetyl sulfate.

7.2.4. Thermal analysis of sulfonated poly(styrene-*block*-butadiene)

The thermal properties of sulfonated poly(styrene-*block*-butadiene) were studied using Thermogravimetric Analysis (TGA) and Differential Scanning Calorimetry (DSC) but if the glass transition temperature (T_g) could not be determined by DSC, Dynamic Mechanical Analysis (DMA) was used. These studies were performed in order to determine an influence of the degree of sulfonation on the thermal stability and the chain flexibility of polymers.

The thermal stability of poly(styrene-*block*-butadiene) and sulfonated derivatives was studied under nitrogen at a heating rate of $10^\circ\text{C}\cdot\text{min}^{-1}$ in the range of temperature of 30°C to 600°C . The analysis revealed that a thermal stability for **SSB6** (SD= 66.28 mol%) and **SSB10** (SD= 57.06

mol%) decreased in comparison to the unmodified poly(styrene-*block*-butadiene) (Figure 7.9 and Figure 7.10).

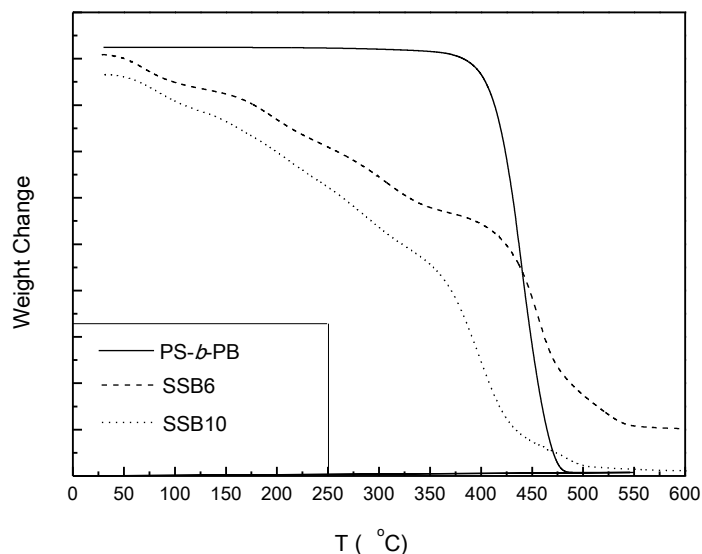


Figure 7.9. Thermogravimetric curves of poly(styrene-*block*-butadiene) (PS-*b*-PB) and sulfonated water soluble poly(styrene-*block*-butadiene) **SSB6** (SD= 66.28 mol%) and **SSB10** (SD= 57.06 mol%).

The sulfonated polymers exhibited three different distinct degradation steps. The first weight loss corresponded to the loss of water molecules that were strongly bound via hydrogen bonding to the sulfonic acid groups. The second weight loss at around 230°C was due to the loss of the sulfonic acid group -SO₃H (desulfonation). The third weight loss around 339-369°C was due to the degradation of the polymer chains. Poly(styrene-*block*-butadiene) showed a weight loss process, with its onset at approximately 339°C and a single step decomposition was observed (Figure 7.10). The degradation temperature was within close proximity to the values reported in literature [182]. Even though the thermal stability of polymers **SSB6** (SD= 66.28 mol%) and **SSB10** (SD= 57.06 mol%) decreased with increasing degree of sulfonation, the degradation temperature of the polymer's backbone was found to increase. This could be due to an increase in the rigidity in copolymers with increases in the degree of sulfonation. Nevertheless, the temperature stability of sulfonated copolymers remained relatively high and was comparable to

polyacrylamide [261]. The degradation temperatures of the copolymers are summarised in *Table 7.2*.

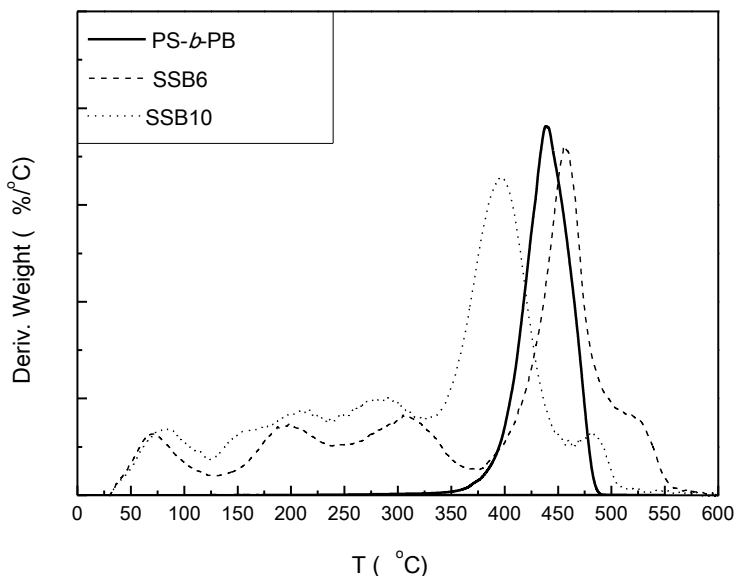


Figure 7.10. Thermogravimetric derivative weight curves for poly(styrene-*block*-butadiene) (PS-*b*-PB) and sulfonated water soluble poly(styrene-*block*-butadiene) **SSB6** (SD= 66.28 mol%) and **SSB10** (SD= 57.06 mol%).

It is well known that drag reduction is strongly affected by the flexibility of the polymers used [10, 34, 77]. It is therefore vital to test the level of flexibility of these polymers to predict their behaviour as drag reducing agents. Differential Scanning Calorimetry (DSC) and Dynamic Mechanical Analysis (DMA) have been used to study the thermal behaviour of the synthesised sulfonated block copolymers and starting polymer. All samples were investigated in the temperature range of -150°C to 250°C at a heating rate of $10^{\circ}\text{C}\cdot\text{min}^{-1}$. The thermograms of the sulfonated water soluble polymers **SSB6** (SD= 66.28 mol%), **SSB10** (SD= 57.06 mol%) and poly(styrene-*block*-butadiene) are presented in *Figure 7.11* (first heating curve) and *Figure 7.12* (second heating curve). The dynamic mechanical curves were obtained at a heating rate of $5^{\circ}\text{C}\cdot\text{min}^{-1}$ at frequency of 1 Hz and are additionally presented in *Figure 7.13*. Only $\tan \delta$ values were used since the loss and storage modulus obtained from this analysis were not attributed to the properties of the sample but to the metal powder cell. The glass transition temperatures of the

copolymers were determined from the second heating cycles and DMA curves. The glass transition temperatures of poly(styrene-*block*-butadiene) and sulfonated poly(styrene-*block*-butadiene) are summarised in *Table 7.2*.

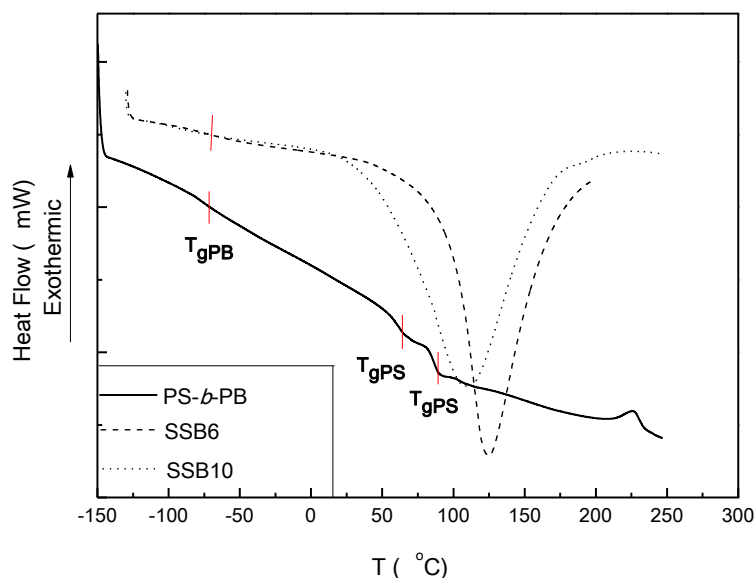


Figure 7.11. DSC curves of poly(styrene-*block*-butadiene) (PS-*b*-PB) and water soluble sulfonated poly(styrene-*block*-butadiene) **SSB6** (SD= 66.28 mol%) and **SSB10** (SD= 57.06 mol%) for the 1st heating cycle.

Both samples of sulfonated poly(styrene-*block*-butadiene) exhibited an endothermic peak at 110°C (**SSB10**, SD= 57.06 mol%) and 125°C (**SSB6**, SD= 66.28 mol%) as shown in the first heating curves in *Figure 7.11*. This is attributed to the presence of the sulfonic acid groups on the polymer chains [179, 262]. These transitions were irreversible as indicated in the second heating curves (*Figure 7.12*). Two glass transition temperatures of 64.6°C and 86.0°C were also observed for the unmodified poly(styrene-*block*-butadiene) (*Figure 7.11*). This could be attributed to phase separation arising from the chemical composition of poly(styrene-*block*-butadiene), which was supplied as a blend of poly(styrene-*block*-butadiene) and pure polystyrene (5 % polystyrene) [263]. The broad exothermic peak observed in the DSC thermogram of poly(styrene-*block*-butadiene) (as shown in the first heating curve at 208°C in *Figure 7.11*) can be the result of the vulcanisation of the polybutadiene [264].

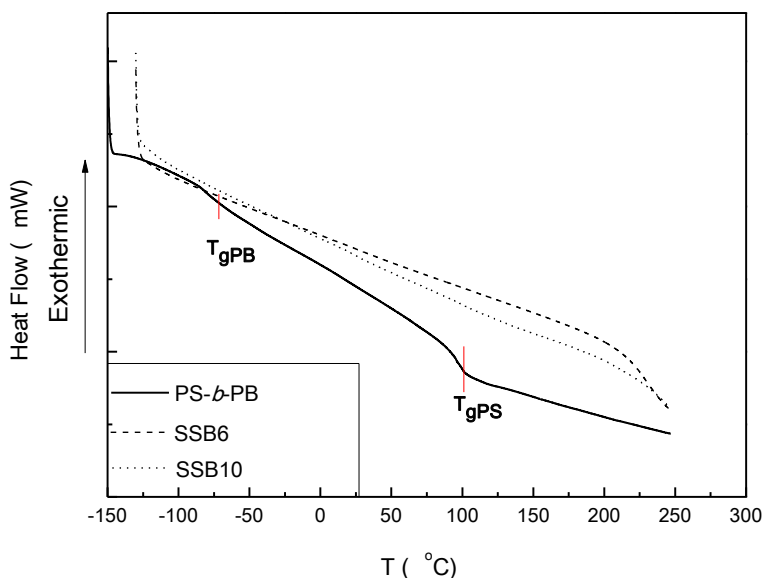


Figure 7.12. DSC curves of poly(styrene-*block*-butadiene) (PS-*b*-PB) and water soluble sulfonated poly(styrene-*block*-butadiene) **SSB6** (SD= 66.28 mol%) and **SSB10** (SD= 57.06 mol%) for the 2nd heating cycle.

The glass transition temperatures of polystyrene (T_{gPS}) and polybutadiene (T_{gPB}) segments were shifted to higher temperatures (T_{gPS} from 85.7°C (DMA value, 100°C DSC value) to 140°C for **SSB10** (SD= 57.06 mol%) and 168.3°C for **SSB6** (SD= 66.28 mol%), T_{gPB} from -80.5 °C to -81°C for **SSB10** and -70.9°C for **SSB6**) as compared to poly(styrene-*block*-butadiene) (from DMA analysis *Figure 7.13*, maximum peak value of $\tan \delta$ and DSC *Figure 7.11*, *Figure 7.12* and *Table 7.2*). The introduction of sulfonate groups resulted in an increase in molecular interaction by the pendant sulfonate groups and introduced bulkiness into the copolymers (change in microstructure). These effects hindered the chain movements of the polymer molecule and resulted in an increase in the glass transition temperatures for the sulfonated polymers [265]. The results indicated that the copolymers became more rigid upon sulfonation and the rigidity increased with degree of sulfonation. These results are in agreement with literature reports [179]. The changes in the glass transition temperatures of the polybutadiene and polystyrene segments confirmed that the sulfonation of polymer occurred in both polystyrene and polybutadiene. This indicates that acetyl sulfate was not selective towards styrene segments.

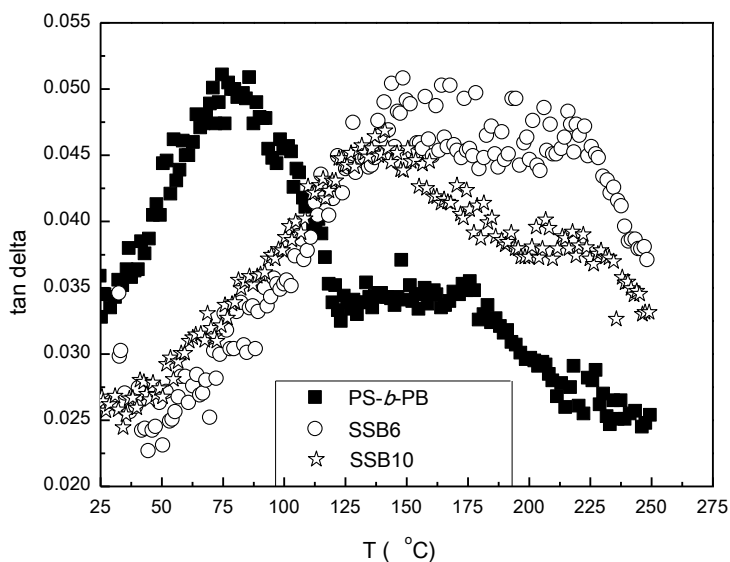


Figure 7.13. DMA $\tan \delta$ curves of poly(styrene-*block*-butadiene) (PS-*b*-PB) and water soluble sulfonated poly(styrene-*block*-butadiene) **SSB6** and **SSB10** obtained at 1 Hz.

Sample	SD (mol%)	T_{g1PB} (°C) DSC	T_{g2PS} (°C) DSC	T_{gPS} (°C) DMA	T_{d1} (°C) (%)	T_{d2} (°C) (%)	T_{d3} (°C) (%)
poly(styrene- <i>block</i> -butadiene)	0	-80.5	64.6 and 86.0 (1 st heat), 100.7 (2 nd heat)	85.7	339.0 98.4	-	-
SSB6	66.28	-70.9	-	168.3	130.7 8.0	241.4 10.7	368.7 32.6
SSB10	57.06	-81.0	-	140	123.7 11.5	235.9 11.2	339.7 35.9

Table 7.2. T_g of polybutadiene and polystyrene segments and T_d with corresponding weight loss for poly(styrene-*block*-butadiene) and water-soluble sulfonated polymers **SSB6** and **SSB10** as measured by DSC, DMA and TGA.

7.2.5. Rheology of water soluble sulfonated poly(styrene-*block*-butadiene)

The influence of the concentration of aqueous solutions of sulfonated poly(styrene-*block*-butadiene) on flow properties of sulfonated copolymers was studied (at constant shear rate of 10 s^{-1} and at shear rate ramp from 7 s^{-1} to 1000 s^{-1}). It can be seen from *Figure 7.14* that the apparent viscosity of sample **SSB10**, containing 57.07 mol% of sulfonic acid groups, was higher than the apparent viscosity of sample **SSB6**, containing 66.28 mol% sulfonic acid groups, throughout the concentration range studied.

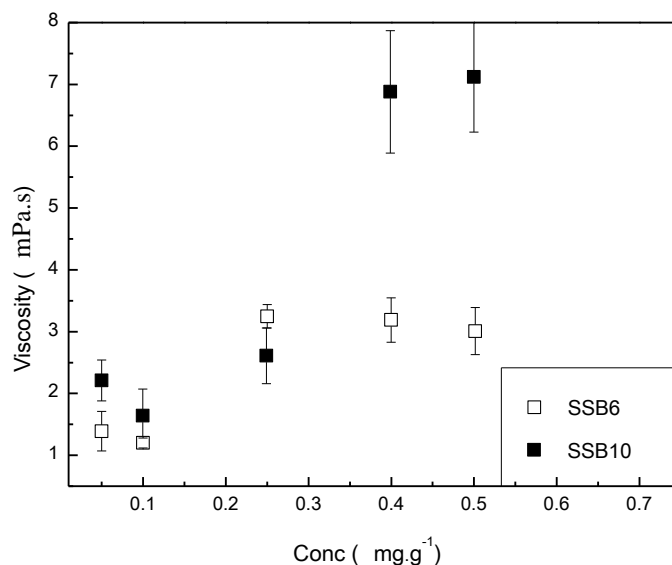


Figure 7.14. Apparent viscosity as a function of concentration of the aqueous solutions of sulfonated polymers poly(styrene-*block*-butadiene) **SSB6** (SD= 66.28 mol%) and **SSB10** (SD= 57.06 mol%) at 10 s^{-1} and 25°C .

The higher apparent viscosity of polymer **SSB10** (SD= 57.06 mol%) in comparison to polymer **SSB6** (SD= 66.28 mol%) can be explained by the higher amount of hydrophobic moieties present. The higher amount of hydrophobic moieties resulted in stronger intermolecular hydrophobic association, which in turn led to a higher apparent viscosity and higher apparent molecular weight [26, 208]. Additionally, the apparent viscosity of both samples increased at a concentration between 0.25 to 0.4 mg.g^{-1} . This behaviour is well-known for hydrophobically

modified polymers and the inflection point above which the apparent viscosity increased is called critical aggregation concentration [130, 203].

The influence of the strength of the hydrophobic association on apparent viscosity was also evident in *Figure 7.15* and *Figure 7.16*.

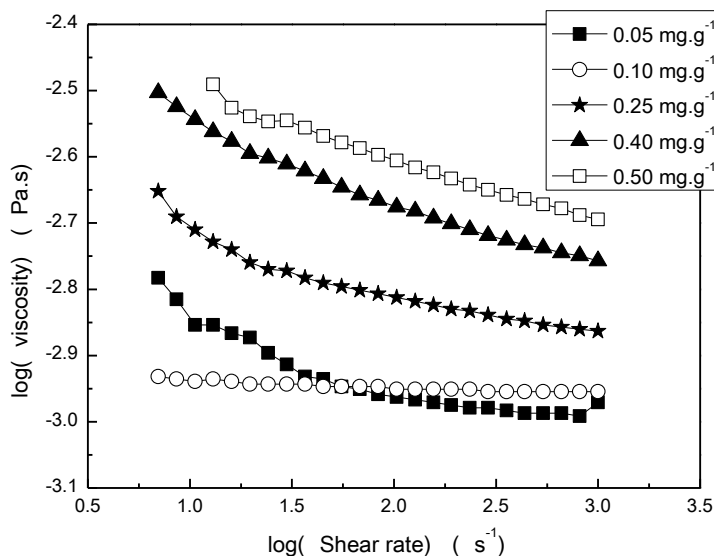


Figure 7.15. Shear rate dependence on the apparent viscosity of the aqueous solutions of sulfonated poly(styrene-block-butadiene) SSB6 (SD= 66.28 mol%) studied at various polymer concentrations at 25°C (logarithmic scale).

At low concentrations, both polymers showed slight shear-thinning behaviour. However, at higher concentrations a more pronounced shear thinning behaviour was observed for sample **SSB6** (SD= 66.28 mol%) and conversely for sample **SSB10** (SD= 57.06 mol%), shear-thickening behaviour at concentrations of 0.4 and 0.5 mg.g⁻¹. The shear-thinning behaviour of copolymer **SSB6** was due to the orientation and disentanglement of the polymer chains under shear, which was associated with the breaking of the hydrophobic intermolecular associations. The shear-thickening behaviour of hydrophobically modified polymers has been the object of several theoretical approaches [266, 267]. The most common explanation of this phenomenon is that the shear stress shifts the balance between intra- and intermolecular hydrophobic associations. Witten and Cohen [268] suggested that intermolecular associations are favoured

over intramolecular associations due to chain stiffening under shear. The shear thickening behaviour of sulfonated polymers containing a certain concentration of hydrophobic moieties can be attributed to the effect of chains stretching and rotation under applied shear, which induces the formation of a gel-like network, formed of polymer chains connected via hydrophobic junctions (Figure 7.17).

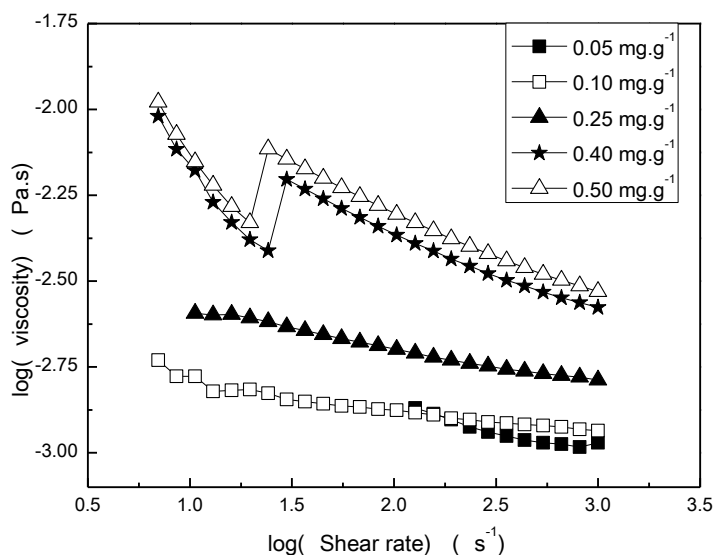


Figure 7.16. Shear rate dependence on the apparent viscosity of the aqueous solutions of sulfonated poly(styrene-block-butadiene) SSB10 (SD= 57.06 mol%) studied at various polymer concentrations at 25°C (logarithmic scale).

When the shear rate was increased even further, shear-thinning was observed for copolymer **SSB10**. This behaviour can be attributed to the breakage of hydrophobic junctions in the gel-like network, due to the limiting shear rate being reached [221]. From the obtained data, it is apparent that shear-thickening behaviour is only observed if the sulfonated poly(styrene-*block*-butadiene) contains a certain concentration of hydrophobic moieties. The concentration required has to be high enough to form a strong transient gel-like network and, therefore no shear-thickening behaviour was observed for sample **SSB6** (SD= 66.28 mol%), which contained 10 % less hydrophobic groups in comparison to sample **SSB10** (SD= 57.06 mol%).

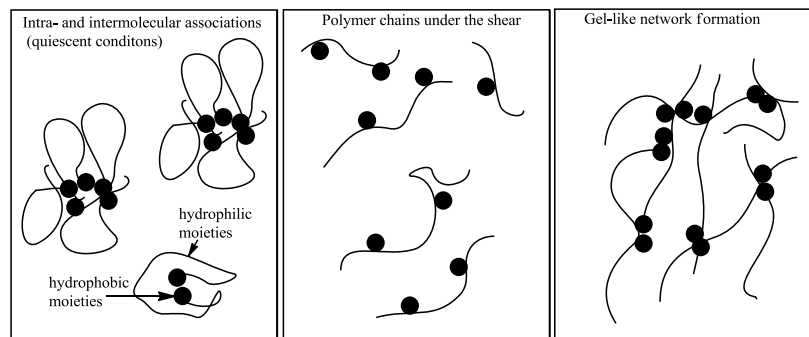


Figure 7.17. Illustration of shear-thickening behaviour in associating polymers [266].

7.2.6. Instantaneous drag reduction of sulfonated poly(styrene-*block*-butadiene)

The influence of the concentration of solutions of sulfonated poly(styrene-*block*-butadiene) on drag reduction was studied using a rheometer with double-gap geometry at 25°C. The drag reduction value reported was the maximum drag reduction achieved in the first 5 minutes of a measurement. For both polymers, the percentage of drag reduction increased with increasing polymer concentration (*Figure 7.18*). However, drag reduction did not plateau in the range of concentrations studied suggesting that further increases in drag reduction could be obtained. The levelling of drag reduction with increasing polymer concentration is a characteristic behaviour for many commercially available polymers for example PAAm (*Figure 7.18*). The value of drag reduction achieved by polymer **SSB10** (SD= 57.06 mol%) was found to be similar to that of polyacrylamide at the polymer $C = 0.5 \text{ mg}\cdot\text{g}^{-1}$, however the molecular weight of the sulfonated polymer was considerably lower than that of the polyacrylamide ($M_w = 1085 \text{ kDa}$). The weight average molecular weight of the unmodified poly(styrene-*block*-butadiene) was equal to 143 kDa. The theoretical molecular weight of the fully sulfonated copolymer, calculated from equation 25, was equal to $M_w \sim 316.5 \text{ kDa}$ and the approximate weight average molecular weight of sulfonated polymers (assuming that all of the butadiene repeat units were sulfonated) **SSB6** and **SSB10** was around 210-220 kDa:

$$M_{wSulf} = DP_{PB} \cdot M_{wSB} + DP_{PS} \cdot M_{wSS} \quad (25)$$

Where DP_{PB} is the weight average degree of polymerisation of the polybutadiene segments ($DP_{PB} = 450$), DP_{PS} is the weight average degree of polymerisation of the polystyrene segments ($DP_{PS} = 1141$), M_{wSB} is the molecular weight of the sulfonated butadiene unit, $236.074 \text{ g}\cdot\text{mol}^{-1}$ and M_{wSS} is the molecular weight of the sulfonated styrene unit, $184.255 \text{ g}\cdot\text{mol}^{-1}$.

The behaviour of sulfonated poly(styrene-*block*-butadiene) could be explained by the formation of large macromolecules of higher apparent molecular weight as a result of intermolecular hydrophobic associations. The achievement of such high drag reduction using water soluble polymers with molecular weights well under 500 kDa was not yet reported in the literature. Moreover, it was stated that polymers with molecular weights below 500 kDa did not reduce drag effectively [10].

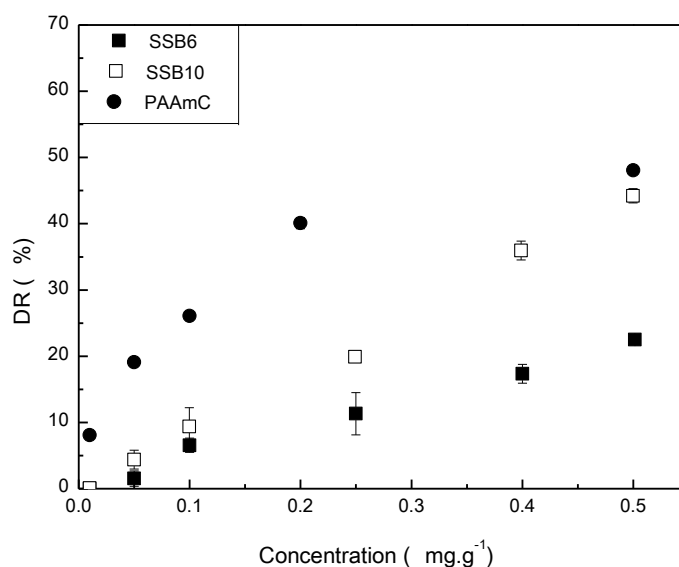


Figure 7.18. Percentage drag reduction as a function of polymer concentration for sulfonated poly(styrene-*block*-butadiene) **SSB6** ($SD = 66.28 \text{ mol}\%$) and **SSB10** ($SD = 57.06 \text{ mol}\%$) and commercial PAAm (**PAAmC** $M_w = 1085 \text{ kDa}$) obtained at 25°C in turbulent Taylor Flow.

The higher drag reduction of polymer **SSB10** ($SD = 57.06 \text{ mol}\%$) over polymer **SSB6** ($SD = 66.28 \text{ mol}\%$) can not be explained in terms of molecular weight, since the molecular weight of

polymers with higher degrees of sulfonation should be even higher. The higher drag reduction could be explained by the existence of stronger intermolecular associations in **SSB10**, due to higher concentration of hydrophobic moieties. The stronger associations in this polymer resulted in a higher apparent molecular weight, that of the sulfonated poly(styrene-*block*-butadiene) aggregate, hence a higher drag reduction was seen. The lower drag reduction observed for **SSB6** could be also explained in terms of chain flexibility and the number of side branches (sulfonic acid groups). It is well known that rigidity of polymers and the degree of branching affects drag reduction [30]. Flexible polymers interact with the turbulent vortices more effectively than rigid polymers and the more branched the polymer is, the less effective the drag reduction. Polymer **SSB6** (SD= 66.28 mol%) had higher degree of bulky sulfonic acid groups than copolymer **SSB10** (SD= 57.06 mol%). These bulky sulfonic acid groups prevented free chain movement and constrained polymer rotation and stretching while interacting with turbulent Taylor vortices therefore affected polymer's flexibility. Highly sulfonated polymer **SSB6** therefore exhibited lower drag reduction. The data obtained by the DLS showed that the hydrodynamic radius of copolymer **SSB6** (SD=66.3 mol%) in deionised water was equal to 302.6 ± 6.2 nm and the hydrodynamic radius of copolymer **SSB10** (SD=57 mol%) was equal to 157.8 ± 10.2 nm. Based on these results more open conformation of copolymer **SSB6** should result in higher drag reduction. However, it is known that the polymers assuming highly expanded conformation are more effective in reducing drag at lower Reynolds numbers since low shear rates are only required to unravel these polymers. Consequently, at the Reynolds numbers and concentrations of polymers studied in this research, less open conformation of **SSB10** was more effective than highly expanded conformation of **SSB6**.

7.2.7. Time dependent drag reduction of sulfonated poly(styrene-*block*-butadiene)

The introduction of sulfonic acid groups into polymers was found by Sabhapondit *et al.* to improve the shear stability of polymers of acrylamide [256]. It is also known that the introduction of hydrophobic groups into polyacrylamide results in the formation of hydrophobic aggregates that improves shear stability of polymers, allowing polymers to be reused [109].

Therefore the drag reduction of sulfonated polymers was studied at constant shear rate of 11200 s^{-1} and at the polymer concentration of $0.5 \text{ mg}\cdot\text{g}^{-1}$. The polymers were sheared in six consecutive cycles lasting 30 minutes each. After each shearing cycle the shearing force was removed and polymer was allowed to rest for an hour in a double-gap cell to allow full relaxation of the polymer chains to its original structure.

The drag reduction (DR) by **SSB6** (SD= 66.28 mol%) (Figure 7.19) slightly increased initially and thereafter remained constant. The drag reduction of **SSB10** (SD= 57.06 mol%) (Figure 7.20) also increased initially however it decreased after 5 minutes of shearing to level off at a lower level.

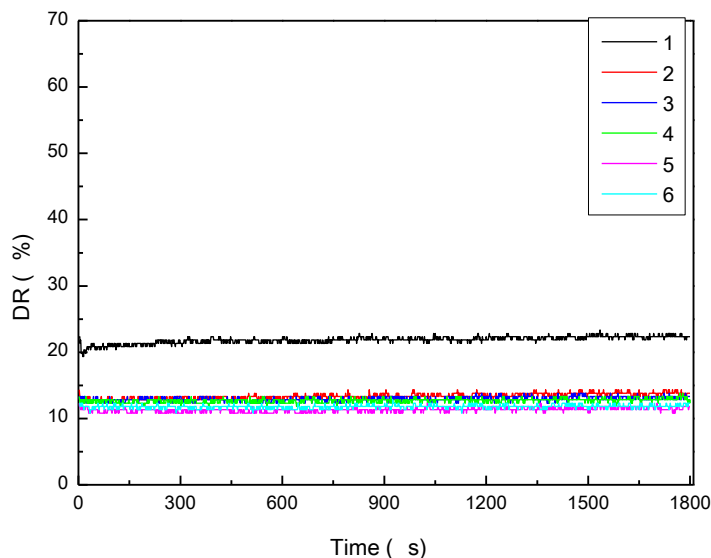


Figure 7.19. Drag reduction as a function of time for sulfonated poly(styrene-*block*-butadiene) **SSB6** (SD= 66.28 mol%) measured at $\gamma= 11200 \text{ s}^{-1}$ and polymer concentration $C= 0.5 \text{ mg}\cdot\text{g}^{-1}$. Error 0.5-1.5 %. 1 to 6 is the number of shearing cycle.

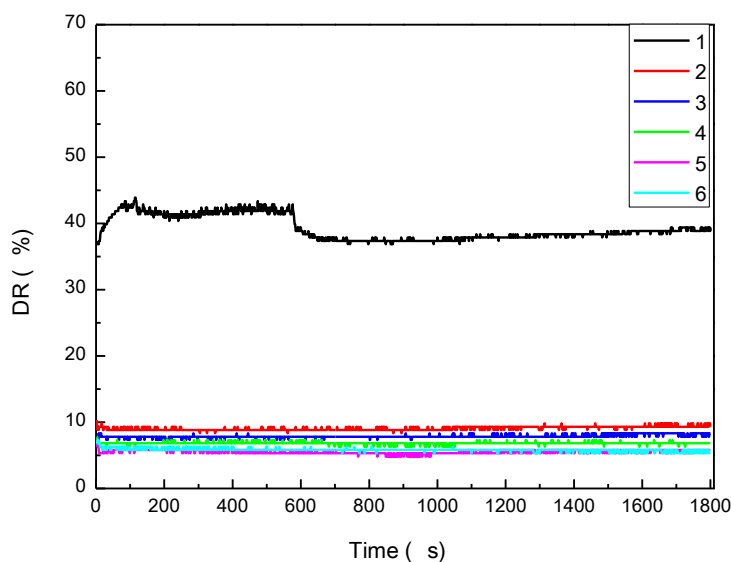


Figure 7.20. Drag reduction as a function of time for sulfonated poly(styrene-*block*-butadiene) **SSB10** (SD= 57.06 mol%) measured at $\gamma= 11200 \text{ s}^{-1}$ and polymer concentration $C= 0.5 \text{ mg}\cdot\text{g}^{-1}$. Error 0.5-1.5 %. 1 to 6 is the number of shearing cycle.

The increase in the drag reduction by polymers could be attributed to the creation of a gel-like network connected by the formation hydrophobic junctions. In turbulent Taylor flow, the polymer chains are elongated and unravelled as they absorb kinetic energy [34]. This elongation allows the further intermolecular hydrophobic associations to form, however the polymer molecules can only be stretched up to a certain extent until the gel-like network is destroyed and the non-associated polymer molecules become responsible for the observed drag reduction. The drag reduction of both polymers decreased after the 1st shearing cycle (*Figure 7.19* to *Figure 7.21*), which suggests that the polymers underwent mechanical degradation. The decrease in drag reduction however, was less drastic for polymer **SSB6**. This was contrary to what was expected, since the polymer **SSB10** associated to a greater extent due to its higher hydrophobicity. Since the extent of the drag reduction of copolymer **SSB10** was dependent on the strength of hydrophobic associations thus, destruction of the physically crosslinked network would result in lower drag reduction of the copolymer. It is therefore possible that the reformation of the physically crosslinked network upon start of the second shearing cycle was not complete.

The higher shear resistance of **SSB6** could be also attributed to higher rigidity imposed by higher concentration of sulfonic acid groups that acted as branches [30]. As a result the stress that **SSB6** experienced was most likely distributed among the individual polymer chains. Moreover, the sulfonic acid groups prevented free chain movements and as a result unravelling of the polymer chains in this polymer was sterically hindered. Therefore even though the initial drag reduction for **SSB6** was lower, the steric hinderance imparted by sulfonic acid groups resulted in greater shear resistance.

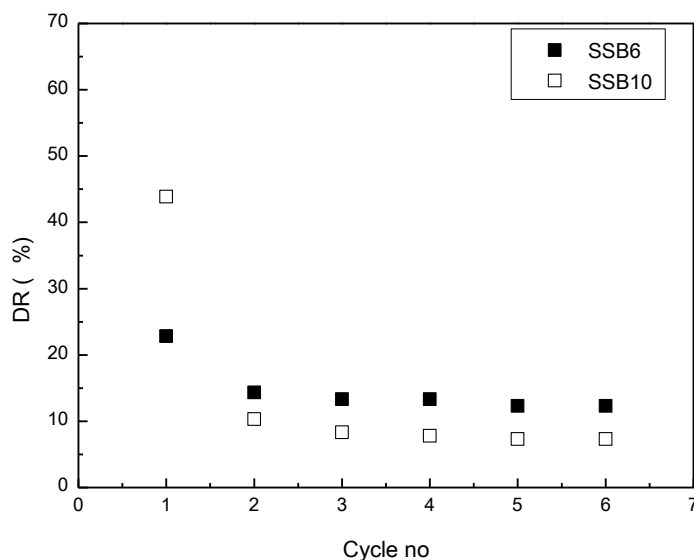


Figure 7.21. Drag reduction as a function of number of shearing cycles for sulfonated poly(styrene-*block*-butadiene) **SSB6** and **SSB10** as measured at polymer $C=0.5 \text{ mg}\cdot\text{g}^{-1}$ and $\dot{\gamma}=11200 \text{ s}^{-1}$. Error 0.5-1.5 %.

7.3. Summary

The aim of the research described in this chapter was to investigate the drag reducing properties of partially sulfonated poly(styrene-*block*-butadiene) in water. Water-soluble poly(styrene-*block*-butadiene) with varying degrees of sulfonation were successfully synthesised by aromatic electrophilic substitution with acetyl sulfate. FT-IR and Elemental Analysis confirmed the presence of sulfonic acid groups in polymers. The ^1H NMR spectrum of the water soluble sulfonated poly(styrene-*block*-butadiene) demonstrated that sulfonation occurred on both the

polystyrene and polybutadiene segments illustrating the low selectivity of the sulfonating agent towards one monomer. The thermal properties by DSC, DMA and TGA showed that the sulfonated polymers were less thermally stable than the starting unsulfonated poly(styrene-*block*-butadiene) and that the overall rigidity of the polymer increased with increasing extent of sulfonation.

The effect of the partial sulfonation of poly(styrene-*block*-butadiene) on the viscoelastic properties was determined by rheology. The apparent viscosity as a function of polymer concentration was found to be lower for **SSB6** (SD= 66.28 mol%) in comparison to **SSB10** (SD= 57.06 mol%). This was explained by the greater hydrophobicity of **SSB10** and stronger intermolecular hydrophobic association.

The polymer with the lower degree of sulfonation (**SSB10**, SD= 57.06 mol%) exhibited shear-thickening behaviour, which was attributed to the strong association between hydrophobic segments in this copolymer. **SSB6** exhibited shear-thinning behaviour, which was attributed to the breakdown of the hydrophobic associations in polymer and the deformation of polymeric coils under the applied shear. Drag reduction studies carried out for the water-soluble sulfonated poly(styrene-*block*-butadiene) showed that copolymers were efficient drag reducers. The **SSB10** exhibited excellent drag reducing performance at a much lower (nominal) molecular weight than polyacrylamide and the molecular weight that is necessary to impart good drag reducing properties. This finding was contrary to literature reports and showed that polymers of certain molecular characteristics can exhibit drag reducing performance exceeding commercially available polymers. The drag reduction by **SSB10** was higher than the drag reduction by **SSB6** and this was attributed to stronger intermolecular hydrophobic association between unmodified segments in **SSB10**, higher flexibility due to lower concentration of bulky sulfonic acid groups and less expanded conformation. The shear stability of sulfonated poly(styrene-*block*-butadiene) was found to be dependent on the degree of sulfonation. **SSB6** exhibited higher shear resistance, which was explained by the higher rigidity that was imparted by bulky sulfonic acid groups.

This study demonstrated that the partial sulfonation of poly(styrene-*block*-butadiene) resulted in creation of excellent drag reducing agents. The high drag reduction of the sulfonated block

copolymer was achieved at molecular weights below the lower molecular weight limit that was reported to be necessary to achieve any drag reduction performance.

Chapter 8

Summary and future work

The main objective of the research described in this thesis was to synthesise water-soluble polymers that would display improved drag reducing properties and resistance to shear degradation. It was demonstrated that associating polymers exhibit these properties hence this class of polymers was primarily chosen for investigation. The second objective of this research was to identify suitable additives capable of breaking the hydrophobic associations between and within polymer chains in aqueous solutions. This would prevent or reduce the adsorption of polymers onto reservoir surfaces.

8.1. Summary of the results

To achieve the objectives of this research work firstly water-soluble hydrophobically modified polyacrylamide were synthesised by micellar polymerisation. The polymers were synthesised in order to investigate the role of molecular variables such as the influence of the strength of the hydrophobic association on the drag reducing performance. This research was carried out to fill the gaps in the literature such as understanding a role of the molecular variables, the alkyl chain length in the hydrophobic monomer, the length of the hydrophobic block or concentration of the hydrophobic moieties in the copolymer, in the shear stability of hydrophobically modified polyacrylamide.

^1H NMR confirmed the successful incorporation of the hydrophobic moieties into the copolymers backbone. The water-solubility and the rheology of the obtained copolymers and the molecular weight were found to be dependent on the concentration and the type of the incorporated hydrophobic moieties as well as on the length of the hydrophobic blocks. The introduction of hydrophobic moieties into the polyacrylamide backbone was found to enhance the apparent viscosity of copolymers (as determined at low shear rate), due to the

intermolecularly associating hydrophobic groups. The increase in apparent viscosity was even more pronounced at higher polymer concentrations. The increase in the observed apparent viscosity was dependent on the length of the alkyl chain, the length of the block and the amount of incorporated hydrophobic moieties.

The measurement of the instantaneous drag reduction for hydrophobically modified polyacrylamide showed that the drag reduction in deionised water was higher (55 to 67 %) for all of the copolymers studied in comparison to commercial polyacrylamide (48 %), despite the copolymers having lower molecular weights, and was dependent on the concentration of hydrophobic moieties and the molecular weight of copolymers. This indicated higher apparent molecular weights for hydrophobically modified polyacrylamide and the importance of intra- and intermolecular hydrophobic associations or of secondary bonds in the drag reduction.

The time dependent measurements of drag reduction in the turbulent Taylor flow, showed that the drag reduction of the majority of copolymers decreased with increasing shearing time and the number of shearing cycles. Moreover, the magnitude of the decrease in the drag reduction and the shear resistance of copolymers was proportional to the concentration of the hydrophobic groups. Copolymer containing 0.33 mol% of n-decyl acrylamide (**AD9**) was found to be the most effective drag reducer in terms of shear stability.

Drag reduction of copolymers measured in the 2% (w/w) potassium chloride and brine was found again to be dependent on the concentration of hydrophobic moieties. The copolymer containing the highest amount of n-decyl acrylamide moieties (0.65 mol%) exhibited an increase in drag reduction when dissolved in aqueous potassium chloride. This was attributed to the strengthening of the hydrophobic intermolecular associations. The percentage drag reduction of the majority of the copolymers in brine was lower than that of the same copolymers in deionised water. The drag reduction of copolymer containing 0.33 mol% of n-decyl acrylamide (**AD9**) was found to be unaffected by the presence of the monovalent and divalent ions. This demonstrated that this copolymer was the most efficient drag reducing agent in terms of performance, shear stability and resistance to salts.

Moreover, a further aim of this work was to identify suitable additives capable of dissociating (or breaking) the hydrophobic associations between polymers or within a polymer chain. The ^1H

NMR demonstrated that α - and β -Cyclodextrin formed inclusion complexes with the alkyl chains of n-decyl- and n-octadecyl moieties, which were incorporated into polyacrylamide. The formation of inclusion complexes of hydrophobically modified polyacrylamide with Cyclodextrins was further confirmed by rheology. This study showed a stronger tendency of β -Cyclodextrin to form complexes with the copolymers containing the highest concentration of n-decyl acrylamide (0.65 mol%) or n-octadecyl acrylamide. The instantaneous drag reduction as a function of Cyclodextrin concentration indicated that the changes in the drag reduction were caused by the modulation of the hydrophobic interactions. However, increasing the concentration of β -Cyclodextrin beyond the optimum ($[\text{CD}] > 1 \text{ mol eq.}$) mediated formation of polymer-Cyclodextrin aggregates. This was evidenced by an increase in the observed percentage of drag reduction and increasing apparent viscosity.

Drag reducing agents such as polyacrylamide or polyacrylic acid have been known to adsorb in oil and gas reservoirs. The adsorption of polymers especially in low permeability reservoirs requires expensive clean up operations and can result in a decrease in the yield of the production of gas or oil. A major disadvantage with the use of associating polymers as drag reducing agents is that adsorption on the reservoir surface has been shown to be more significant in comparison to non-associating polymer. This is due to the reformation of association when shear force is removed. It was therefore desirable to deactivate the hydrophobic associations to prevent adsorption of polymers in the low permeability reservoir. The amount of polymer adsorption on silica was found to increase as a function of the polymer concentration and was dependent on the molecular weight of the polymer studied and the strength of the polymer-polymer interaction. The hydrophobic interactions were found to be responsible for a higher adsorption of the hydrophobically modified polyacrylamides onto the silica. The extent of polymer desorption from silica was found to be dependent on the type of Cyclodextrin used. It was possible to almost completely remove the majority of the copolymers studied by adding β -Cyclodextrin. This was due to the formation of strong inclusion complexes between Cyclodextrin and the hydrophobic moieties. It was even possible to partially desorb polyacrylamide by the addition of both α - and β -Cyclodextrin. This was considered to be either due to hydrogen bonding between the amide groups in PAAm and the hydroxyl groups present in Cyclodextrin or partial displacement of

polyacrylamide by the Cyclodextrins. This study demonstrated that inexpensive Cyclodextrin could potentially be utilised in the removal of polymer layers, which formed by the adsorption of drag reducing polymers, from the surface of the oil and gas reservoirs.

Another objective of this research was to investigate drag reducing properties of poly(N-hydroxyethyl acrylamide) and hydrophobically modified poly(N-hydroxyethyl acrylamide). Water-soluble poly(N-hydroxyethyl acrylamide) polymers with varying concentrations of hydrophobic moieties were synthesised by micellar polymerisation. ^1H NMR spectra of the water soluble polymers demonstrated the successful incorporation of hydrophobic groups into the polymer backbone. The effect of the concentration of the incorporated hydrophobic moieties and the length of the hydrophobic blocks on the apparent viscosity of copolymer solutions was demonstrated by rheology. It was shown that hydrophobic intermolecular associations exist even in the dilute concentration regime. The polymers containing high concentrations of n-decyl acrylamide showed a sharp increase in apparent viscosity with increasing concentration (above $1 \text{ mg}\cdot\text{g}^{-1}$). This was due to the strong intermolecular hydrophobic association. The pronounced shear thinning for the copolymers of poly(N-hydroxyethyl acrylamide) and n-decyl acrylamide **HED1** (0.73 mol% of n-decyl acrylamide) and **HED2** (0.51 mol% of n-decyl acrylamide) was associated with the orientation and disentanglement of the polymer chains under the shear. This behaviour was the result of the breaking up of the hydrophobic intermolecular associations.

Drag reduction studies carried out for the water soluble samples showed that poly(N-hydroxyethyl acrylamide) did not reduce drag. This was thought to be due to open conformation of this polymer which was incapable of suppressing turbulence at the Reynolds numbers studied in this research work. The incorporation of the hydrophobic moieties into the polymer structure was found to impart excellent drag reduction performance into poly(N-hydroxyethyl acrylamide). The drag reduction performance of copolymer of N-hydroxyethyl acrylamide and n-decyl acrylamide (**HED2**, 0.51 mol% of n-decyl acrylamide) was found to reach 53 %. Moreover the drag reduction achieved with this copolymer was found to be higher than that of the commercially available polyacrylamide (48 %). This behaviour was linked to the intermolecular hydrophobic associations in the poly(N-hydroxyethyl acrylamide-co-n-decyl acrylamide) which resulted in higher apparent molecular weight.

The final objective of this research was to functionalise poly(styrene-*block*-butadiene) to impart water solubility and to investigate the drag reducing properties of water-soluble sulfonated poly(styrene-*block*-butadiene). Water-soluble poly(styrene-*block*-butadiene) with varying degrees of sulfonation were synthesised by aromatic electrophilic substitution with acetyl sulfate. Elemental Analysis confirmed the presence of the sulfonic acid groups in the polymers and FT-IR and ¹H NMR spectra of the water-soluble poly(styrene-*block*-butadiene) demonstrated that sulfonation occurred at both polystyrene and polybutadiene segments. This demonstrated the low selectivity of the sulfonating agent towards one monomer. The study of the thermal properties by DSC, DMA and TGA showed that the sulfonated polymers were less thermally stable than poly(styrene-*block*-butadiene) and that the rigidity of the polymers increased with increasing extent of sulfonation.

The effect of the partial sulfonation of these polymers on the viscoelastic properties was demonstrated by rheology. The **SSB10** (SD=57.06 mol%) had higher apparent viscosity than **SSB6** (SD=66.28 mol%) and showed shear-thickening behaviour and this was due to the stronger intermolecular hydrophobic association in copolymer **SSB6**.

Drag reduction studies carried out for the water-soluble sulfonated poly(styrene-*block*-butadiene) showed that the sulfonated polymers were efficient drag reducers and the percentage of drag reduction was dependent on the degree of sulfonation. **SSB6** (SD=66.28 mol%) was less efficient due to more open structure and higher rigidity imparted by bulky sulfonic acid groups; hence it could not interact with Taylor vortices as effectively as **SSB10** (SD=57.06 mol%). Moreover, **SSB10** exhibited excellent drag reduction performance at molecular weights lower than the commonly accepted limit of the molecular weight necessary to observe good drag reduction effect. This finding was contrary to the literature reports and showed that polymers of certain molecular characteristics could exhibit drag reducing performance exceeding commercially available polymers.

The study carried out in this thesis demonstrated excellent drag reducing properties of three different classes of hydrophobically modified polymers, hydrophobically modified polyacrylamide, hydrophobically modified poly(N-hydroxyethyl acrylamide) and sulfonated poly(styrene-*block*-butadiene). Moreover, the hydrophobically modified polymers of acrylamide

indicated higher shear resistance to mechanical degradation than polyacrylamide. This showed that these polymers could be successfully recycled in the repetitive hydraulic fracturing operations. The research also established that inexpensive Cyclodextrin could be used to desorb hydrophobically modified polymers completely from the surface of the reservoir. Moreover, it was even possible to partially desorb polyacrylamide.

8.2. Future work

The work presented in this thesis was focused on the synthesis of polymers with improved drag reducing properties and on addressing the problems associated with commercially available drag reducing agents. These problems were mechanical degradation of polymers and adsorption of commercially available drag reducing polymers such as polyacrylamide and its hydrophobically modified polymers onto the oil and gas reservoir surfaces. The obtained systems were found to be potentially useful drag reducing agents and the issue of polymer adsorption in the reservoir has been addressed and resolved. However, there are a number of actions which should be taken in order to fully characterize and further improve the developed systems. The following actions are recommended as a future work:

- *Synthesis of polyacrylamide and poly(N-hydroxyethyl acrylamide) polymers with higher molecular weight*

Knowing that the drag reducing effect caused by the polymers increase with increasing molecular weight, the synthesis of copolymers with as high molecular weight as possible should be attempted. Water in oil emulsion or microemulsion polymerisation is recommended as the preferable approach to obtain high molecular weight polymers at rapid reaction rates. The time dependent drag reduction of the poly(N-hydroxyethyl acrylamide) copolymers should be then determined. The drag reduction effect of homopolymer of N-hydroxyethyl acrylamide should be also studied at various Reynolds numbers to find the reason behind the lack of the drag reducing properties.

- *Synthesis of block polymers and triblock polymers of styrene and butadiene with high molecular weight and subsequent sulfonation*

Drag reduction of sulfonated polymers was found to be sufficiently high in the turbulent Taylor flow; however polymers of higher molecular weight offer the benefits of the utilisation of lower polymer concentrations. Free radical emulsion polymerisation of styrene and butadiene results in very high molecular weight latex and could be used if the control over the structure is not important and random polymers are required. However, the conversion has to be kept relatively low to avoid crosslinking [269]. On the other hand, if a well-defined polymer structure, high and controlled molecular weight is required then living sequential polymerisation is the suggested method for obtaining these block copolymers. For example, living anionic polymerisation or combination of living anionic polymerisation and ATRP polymerisation could be used to obtain block copolymers of butadiene and styrene. ATRP has been shown to result in high molecular weights of over 10^6 Da [270].

- *Scaling up the polymerisation process*

In order to investigate the behaviour of the polymers in pipe flow and whether the polymers could actually be used on industrial scale, a scale up synthesis protocol should be devised. The first step should be to quantify the drag reduction in actual turbulent pipe flow in the rig described by Zadrazil *et al.* [60].

References

1. Skov, A.M., *World Energy Beyond 2050*. Annual Technical Conference and Exhibition, 29 September-2 October 2002, San Antonio, Texas, 2002. **SPE 77506**.
2. Conti, J. and P. Holtberg, *U.S. Energy Information Administration*. International Energy Outlook 2011, September 2011.
3. King, R.F., *Chapter 2: Natural Gas and the Environment*, in *Natural Gas 1998: Issues and Trends*. 1999. p. 49-71.
4. Boyer, C., J. Kieschnick, R. Suarez-Rivera, R.E. Lewis, and G. Waters, *Producing Gas from Its Source* Oilfield Review, 2006. **18**(3): p. 36-49.
5. Soeder, D.J., *Porosity and Permeability of Eastern Devonian Gas Shale*. SPE Formation Evaluation, 1988. **3**(1): p. 116-124.
6. Arthur, J.D., B. Bohm, and M. Layne, *Hydraulic Fracturing Considerations for Natural Gas Wells of the Marcellus Shale*, in *The Ground Water Protection Council 2008 Annual Forum*. 2008: Cincinnati, Ohio. p. 1-16.
7. Haimson, B. and C. Fairhurst, *Initiation and Extension of Hydraulic Fractures in Rocks*. 1967.
8. Bahamdan, A., *Hydrophobic Guar Gum Derivatives Prepared by Controlled Grafting Processes for Hydraulic Fracturing Applications*. 2005, PhD Thesis, Louisiana State University.
9. Toms, B.A., *Some Observations on the Flow of Linear Polymer Solutions Through Straight Tubes at Large Reynolds Numbers*. Proceedings of the 1st International Congress on Rheology, 1948: p. 135-141.
10. Morgan, S.E. and C.L. McCormick, *Water-Soluble Polymers in Enhanced Oil Recovery*. Progress in Polymer Science, 1990. **15**(1): p. 103-145.
11. Kim, C.A., S.T. Lim, H.J. Choi, J.I. Sohn, and M.S. Jhon, *Characterization of Drag Reducing Guar Gum in a Rotating Disk Flow*. Journal of Applied Polymer Science, 2002. **83**(13): p. 2938-2944.
12. Al-Wahaibi, T., M. Smith, and P. Angeli, *Effect of Drag-Reducing Polymers on Horizontal Oil-Water Flows*. Journal of Petroleum Science and Engineering, 2007. **57**(3-4): p. 334-346.

13. Bizotto, V.C. and E. Sabadini, *Poly(ethylene oxide) × Polyacrylamide. Which One is More Efficient to Promote Drag Reduction in Aqueous Solution and Less Degradable?* Journal of Applied Polymer Science, 2008. **110**(3): p. 1844-1850.
14. Escudier, M.P., F. Presti, and S. Smith, *Drag Reduction in the Turbulent Pipe Flow of Polymers*. Journal of Non-Newtonian Fluid Mechanics, 1998. **81**(3): p. 197-213.
15. Liberatore, M.W., E.J. Pollauf, and A.J. McHugh, *Shear-Induced Structure Formation in Solutions of Drag Reducing Polymers*. Journal of Non-Newtonian Fluid Mechanics, 2003. **113**(2-3): p. 193-208.
16. Bismarck, A., L. Chen, J.M. Griffen, J.F. Hewitt, and J.C. Vassilicos, *Polymer Drag Reduction*. Heat Exchanger Design Updates, 2006. **11**(1): p. 2.14.2-1- 2.14.2-25.
17. Malik, S. and R.A. Mashelkar, *Hydrogen Bonding Mediated Shear Stable Clusters as Drag Reducers*. Chemical Engineering Science, 1995. **50**(1): p. 105-116.
18. Malik, S., S.N. Shintre, and R.A. Mashelkar, *Enhancing the Shear Stability in Drag-reducing Polymers Through Molecular Associations*. Macromolecules, 1993. **26**(1): p. 55-59.
19. McCormick, C.L., R.D. Hester, S.E. Morgan, and A.M. Safieddine, *Water-Soluble Copolymers. 31. Effects of Molecular Parameters, Solvation, and Polymer Associations on Drag Reduction Performance*. Macromolecules, 1990. **23**(8): p. 2132-2139.
20. Kowalik, R.M., I. Duvdevani, D.G. Peiffer, R.D. Lundberg, K. Kitano, and D.N. Schulz, *Enhanced Drag Reduction via Interpolymer Associations*. Journal of Non-Newtonian Fluid Mechanics, 1987. **24**(1): p. 1-10.
21. Shetty, A.M. and M.J. Solomon, *Aggregation in Dilute Solutions of High Molar Mass Poly(ethylene) oxide and Its Effect on Polymer Turbulent Drag Reduction*. Polymer, 2009. **50**(1): p. 261-270.
22. Argillier, J.F., A. Audibert, J. Lecourtier, M. Moan, and L. Rousseau, *Solution and Adsorption Properties of Hydrophobically Associating Water-Soluble Polyacrylamides*. Colloids and Surfaces A: Physicochemical and Engineering Aspects, 1996. **113**(3): p. 247-257.
23. Amro, M.M., A.A.H. El-Sayed, E.S. Al-Homahdi, M.A. Al-Saddique, and M.N. Al-Awad, *Investigation of Polymer Adsorption on Rock Surface of Highly Saline Reservoirs*. Chemical Engineering & Technology, 2002. **25**(10): p. 1005-1013.
24. Graveling, G.J., K. Vala Ragnarsdottir, G.C. Allen, J. Eastman, P.V. Brady, S.D. Balsley, and D.R. Skuse, *Controls on Polyacrylamide Adsorption to Quartz, Kaolinite, and Feldspar*. Geochimica et Cosmochimica Acta, 1997. **61**(17): p. 3515-3523.

25. Lu, H. and Z. Huang, *Solution and Adsorption Properties of Hydrophobically Associating Polyacrylamide Prepared in Inverse Microemulsion Polymerization*. Journal of Macromolecular Science, Part A, 2009. **46**(4): p. 412 - 418.
26. Camail, M., A. Margaillan, and I. Martin, *Copolymers of N-alkyl- and N-arylalkylacrylamides with Acrylamide: Influence of Hydrophobic Structure on Associative Properties. Part I: Viscometric Behaviour in Dilute Solution and Drag Reduction Performance*. Polymer International, 2009. **58**(2): p. 149-154.
27. Bock, J., R.M. Kowalik, D.B. Siano, and S.R. Turner, *Aqueous Drag Reduction with Novel Acrylamide-N-alkyl Acrylamide Copolymers*. Patent H577, 1989.
28. Cengel, Y.A., *Fundamentals of Convection*, in *Heat Transfer: a Practical Approach*. 2002. p. 343-366.
29. Bismarck, A., L. Chen, J.M. Griffin, G.F. Hewitt, and J.C. Vassilicos, *Drag Reduction: Introduction*. Heat Exchanger Design Updates, 2006. **11**(3): p. 2.14.1-1.
30. Berman, N.S., *Drag Reduction by Polymers*. Annual Review of Fluid Mechanics, 1978. **10**(1): p. 47-64.
31. Bonn, D., Y. Amarouchène, C. Wagner, S. Douady, and O. Cadot, *Turbulent Drag Reduction by Polymers*. Journal of Physics: Condensed Matter, 2005. **17**: p. S1195-S1202.
32. Brostow, W., H. Ertepinar, and R.P. Singh, *Flow of Dilute Polymer Solutions: Chain Conformations and Degradation of Drag Reducers*. Macromolecules, 1990. **23**(24): p. 5109-5118.
33. Choi, H.J. and M.S. Jhon, *Polymer-Induced Turbulent Drag Reduction*. Industrial & Engineering Chemistry Research, 1996. **35**(9): p. 2993-2998.
34. Lumley, J.L., *Drag Reduction by Additives*. Annual Review of Fluid Mechanics, 1969. **1**(1): p. 367-384.
35. Zhang, Y., J. Schmidt, Y. Talmon, and J.L. Zakin, *Co-solvent Effects on Drag reduction, Rheological Properties and Micelle Microstructures of Cationic Surfactants*. Journal of Colloid and Interface Science, 2005. **286**(2): p. 696-709.
36. Qi, Y., K. Littrell, P. Thiyagarajan, Y. Talmon, J. Schmidt, Z. Lin, and J.L. Zakin, *Small-Angle Neutron Scattering Study of Shearing Effects on Drag-Reducing Surfactant Solutions*. Journal of Colloid and Interface Science, 2009. **337**(1): p. 218-226.
37. Bismarck, A., L. Chen, J.M. Griffen, G.F. Hewitt, and J.C. Vassilicos, *Surfactant Drag Reduction*. Heat Exchanger Design Updates, 2006. **11**(3): p. 2.14.3-1-2.14.3-5.

38. Shenoy, A.V., *A Review on Drag Reduction with Special Reference to Micellar Systems*. Colloid & Polymer Science, 1984. **262**(4): p. 319-337.
39. Doulah, M.S., *Mechanism of Drag Reduction in Turbulent Pipe Flow by the Addition of Fibers*. Industrial & Engineering Chemistry Fundamentals, 1981. **20**(1): p. 101-102.
40. Gillissen, J.J.J., B.J. Boersma, P.H. Mortensen, and H.I. Andersson, *Fibre-Induced Drag Reduction*. Journal of Fluid Mechanics, 2008. **602**(-1): p. 209-218.
41. Gutierrez Torres, C.D.C., Y.A. Hassan, J.A. Jiminez, and J.G. Barbosa Saldana Bernal, *Drag Reduction by Microbubble Injection in a Channel Flow*. Revista mexicana de física, 2008. **54**(8-14).
42. Chen, Y., Y.C. Chen, W. Huang, R.Y. Hu, K.M. Yao, and F.X. Wang, *Experiment Investigation of Drag Reduction Using Riblets for a Slender Body*. Shiyuan Liuti Lixue/Journal of Experiments in Fluid Mechanics, 2012. **26**(2): p. 42-45.
43. Zhao, D.-Y., Z.-P. Huang, M.-J. Wang, T. Wang, and Y. Jin, *Vacuum Casting Replication of Micro-Riblets on Shark Skin for Drag-Reducing Applications*. Journal of Materials Processing Technology, 2012. **212**(1): p. 198-202.
44. Burger, E.D., L.G. Chorn, and T.K. Perkins, *Studies of Drag Reduction Conducted over a Broad Range of Pipeline Conditions when Flowing Prudhoe Bay Crude Oil*. Journal of Rheology, 1980. **24**(5): p. 603-626.
45. Fink, J.K., *Hydraulic Fracturing Fluids*, in *Oil Field Chemicals*. 2003, Gulf Professional Publishing. p. 233-275.
46. Sellin, R.H.J. and M. Ollis, *Polymer Drag Reduction in Large Pipes and Sewers: Results of Recent Field Trials*. Journal of Rheology, 1980. **24**(5): p. 667-684.
47. Figueredo, R.C.R. and E. Sabadini, *Firefighting Foam Stability: the Effect of the Drag Reducer Poly(ethylene) oxide*. Colloids and Surfaces A: Physicochemical and Engineering Aspects, 2003. **215**(1-3): p. 77-86.
48. Khalil, M.F., S.Z. Kassab, A.A. Elmiligui, and F.A. Naoum, *Applications of Drag-Reducing Polymers in Sprinkler Irrigation Systems: Sprinkler Head Performance*. Journal of Irrigation and Drainage Engineering, 2002. **128**(3): p. 147-152.
49. Moore, K.J., T.D. Ryan, C.M. Moore, and T.A. Boyce, *Method to Increase the Efficiency of Polymer Drag Reduction for Marine and Industrial Applications*. Patent US 8039055, 2009.
50. Greene, H.L., R.F. Mostardi, and R.F. Nokes, *Effects of Drag Reducing Polymers on Initiation of Atherosclerosis*. Polymer Engineering & Science, 1980. **20**(7): p. 499-504.

51. Rosen, M.W. and N.E. Cornford, *Fluid Friction of Fish Slimes*. Nature, 1971. **234**(5323): p. 49-51.
52. Virk, P.S., *Drag Reduction Fundamentals*. AIChE Journal, 1975. **21**(4): p. 625-656.
53. Nadolink, R.H. and W.W. Haigh, *Bibliography on Skin Friction Reduction With Polymers and Other Boundary-Layer Additives*. Applied Mechanics Reviews, 1995. **48**(7): p. 351-460.
54. Bismarck, A., L. Chen, J.C. Vassilicos, G.F. Hewitt, and J.M. Griffin, *Drag Reduction in Multiphase Flow*. Heat Exchanger Design Updates, 2006. **11**(3): p. 2.14.4-1- 2.14.4.-6.
55. Benzi, R., *A Short Review on Drag Reduction by Polymers in Wall Bounded Turbulence*. Physica D: Nonlinear Phenomena, 2010. **239**(14): p. 1338–1345.
56. Brostow, W., *Drag Reduction in Flow: Review of Applications, Mechanism and Prediction*. Journal of Industrial and Engineering Chemistry, 2008. **14**: p. 409–416.
57. Hoyt, J.W., *Drag-Reduction Effectiveness of Polymer Solutions in the Turbulent-Flow Rheometer: A Catalog*. Journal of Polymer Science Part B: Polymer Letters, 1971. **9**(11): p. 851-862.
58. Virk, P.S. and H. Baher, *The Effect of Polymer Concentration on Drag reduction*. Chemical Engineering Science, 1970. **25**: p. 1183-1189.
59. Kim, N.-J., S. Kim, S.H. Lim, K. Chen, and W. Chun, *Measurement of Drag Reduction in Polymer Added Turbulent Flow*. International Communications in Heat and Mass Transfer, 2009. **36**(10): p. 1014-1019.
60. Zadrazil, I., A. Bismarck, G.F. Hewitt, and C.N. Markides, *Shear Layers in the Turbulent Pipe Flow of Drag Reducing Polymer Solutions*. Chemical Engineering Science, 2012. **72**: p. 142-154.
61. Pereira, A.S. and E.J. Soares, *Polymer Degradation of Dilute Solutions in Turbulent Drag Reducing Flows in a Cylindrical Double Gap Rheometer Device*. Journal of Non-Newtonian Fluid Mechanics, 2012. **179-180**: p. 9-22.
62. Phukan, S., P. Kumar, J. Panda, B.R. Nayak, K.N. Tiwari, and R.P. Singh, *Application of Drag Reducing Commercial and Purified Guar gum for Reduction of Energy Requirement of Sprinkler Irrigation and Percolation Rate of the Soil*. Agricultural Water Management, 2001. **47**(2): p. 101-118.
63. Marhefka, J.N., P.J. Marascalco, T.M. Chapman, A.J. Russell, and M.V. Kameneva, *Poly(N-vinylformamide) A Drag-Reducing Polymer for Biomedical Applications*. Biomacromolecules, 2006. **7**(5): p. 1597-1603.

64. Singh, R.P., G.P. Karmakar, S.K. Rath, N.C. Karmakar, S.R. Pandey, T. Tripathy, J. Panda, K. Kanan, S.K. Jain, and N.T. Lan, *Biodegradable Drag Reducing Agents and Flocculants Based on Polysaccharides: Materials and Applications*. Polymer Engineering & Science, 2000. **40**(1): p. 46-60.
65. Bewersdorff, H.-W. and R.P. Singh, *Rheological and Drag Reduction Characteristics of Xanthan Gum Solutions*. Rheologica Acta, 1988. **27**: p. 617-627.
66. Wyatt, N.B., C.M. Gunther, and M.W. Liberatore, *Drag Reduction Effectiveness of Dilute and Entangled Xanthan in Turbulent Pipe Flow*. Journal of Non-Newtonian Fluid Mechanics, 2011. **166**(1-2): p. 25-31.
67. Ueberschär, O., C. Wagner, T. Stangner, K. Kühne, C. Gutsche, and F. Kremer, *Drag Reduction by DNA-Grafting for Single Microspheres in a Dilute λ -DNA Solution*. Polymer, 2011. **52**(18): p. 4021-4032.
68. Japper-Jaafar, A., M.P. Escudier, and R.J. Poole, *Turbulent Pipe Flow of a Drag-Reducing Rigid "Rod-Like" Polymer Solution*. Journal of Non-Newtonian Fluid Mechanics, 2009. **161**: p. 86-93.
69. Kalashnikov, V.N., *Degradation Accompanying Turbulent Drag Reduction by Polymer Additives*. Journal of Non-Newtonian Fluid Mechanics, 2002. **103**: p. 105-121.
70. Fernandes, R.L.J., B.M. Jutte, and M.G. Rodriguez, *Drag Reduction in Horizontal Annular Two-Phase Flow*. International Journal of Multiphase Flow, 2004. **30**: p. 1051-1069.
71. Lee, K.H., K. Zhang, and H.J. Choi, *Time Dependence of Turbulent Drag Reduction Efficiency of Polyisobutylene in Kerosene*. Journal of Industrial and Engineering Chemistry, 2010. **16**(4): p. 499-502.
72. Nakken, T., M. Tande, and A. Elgsaeter, *Measurements of Polymer Induced Drag Reduction and Polymer Scission in Taylor Flow Using Standard Double-Gap Sample Holders With Axial Symmetry*. Journal of Non-Newtonian Fluid Mechanics, 2001. **97**(1): p. 1-12.
73. Nakken, T., M. Tande, and B. Nystrom, *Effect of Molar Mass, Concentration and Thermodynamic Conditions on Polymer-Induced Flow Drag Reduction*. European Polymer Journal, 2004. **40**: p. 181-186.
74. Peyser, P. and R.C. Little, *The Drag Reduction of Dilute Polymer Solutions as a Function of Solvent Power, Viscosity, and Temperature*. Journal of Applied Polymer Science, 1971. **15**: p. 2623-2637.

75. Zakin, J.L. and D.L. Hunston, *Effects of Solvent Nature on the Mechanical Degradation of High Polymer Solutions*. Journal of Applied Polymer Science, 1978. **22**(6): p. 1763-1766.
76. Liaw, G.-C., J.L. Zakin, and G.K. Patterson, *Effects of Molecular Characteristics of Polymers on Drag Reduction*. AIChE Journal, 1971. **17**(2): p. 391-397.
77. Kulicke, W.M., M. Kötter, and H. Gräger, *Drag Reduction Phenomenon with Special Emphasis on Homogeneous Polymer Solutions*. Polymer Characterization/Polymer Solutions, in *Advances in Polymer Science*. 1989, Springer Berlin / Heidelberg. p. 1-68.
78. McCormick, C.L., R.D. Hester, S.E. Morgan, and A.M. Safieddine, *Water-Soluble Copolymers. 30. Effects of Molecular Structure on Drag Reduction Efficiency*. Macromolecules, 1990. **23**(8): p. 2124-2131.
79. Mumick, P.S., R.D. Hester, and C.L. McCormick, *Water Soluble Copolymers. 55: N-Isopropylacrylamide-co-Acrylamide. Copolymers in Drag Reduction: Effect of Molecular Structure, Hydration, and Flow Geometry on Drag Reduction Performance*. Polymer Engineering and Science, 1994. **34**(18): p. 1429-1439.
80. Mumick, P.S., P.M. Welch, L.C. Salazar, and C.L. McCormick, *Water-Soluble Copolymers. 56. Structure and Solvation Effects of Polyampholytes in Drag Reduction*. Macromolecules, 1994. **27**(2): p. 323-331.
81. Kim, O.K., R.C. Little, R.L. Patterson, and R.Y. Ting, *Polymer Structures and Turbulent Shear Stability of Drag Reducing Solutions*. Nature, 1974. **250**(5465): p. 408-410.
82. Lim, T.S., H.G. Choi, D. Biswal, and R.P. Singh, *Turbulent Drag Reduction Characteristics of Amylopectin and Its Derivative*. e-Polymers, 2004. **066**: p. 1-10.
83. Zadrazil, I., *Various Aspects of Polymer Induced Drag Reduction in Turbulent Flow*. PhD Thesis. 2011: Imperial College London.
84. Banijamali, S.H., E.W. Merrill, K.A. Smith, and J. L. H. Peebles, *Turbulent Drag Reduction by Polyacrylic Acid*. AIChE Journal, 1974. **20**(4): p. 824-826.
85. Donald, M.M., *Tube Flow of Non-Newtonian Polymer Solutions: Part II. Turbulent Flow*. AIChE Journal, 1964. **10**(6): p. 881-884.
86. Little, R.C., *Flow Properties of Polyox Solutions*. Industrial & Engineering Chemistry Fundamentals, 1969. **8**(3): p. 557-559.
87. Peyser, P. and R.C. Little, *The Drag Reduction of Dilute Polymer Solutions as a Function of Solvent Power, Viscosity, and Temperature*. Journal of Applied Polymer Science, 1971. **15**(11): p. 2623-2637.

88. Parker, C.A. and A.H. Hedley, *A structural Basis for Drag-Reducing Agents*. Journal of Applied Polymer Science, 1974. **18**(11): p. 3403-3421.
89. Pereira, A.S. and E.J. Soares, *Polymer degradation of dilute solutions in turbulent drag reducing flows in a cylindrical double gap rheometer device*. Journal of Non-Newtonian Fluid Mechanics, 2012. **179-180**: p. 9-22.
90. Oliver, D.R. and S.I. Bakhtiyarov, *Drag Reduction in Exceptionally Dilute Polymer Solutions*. Journal of Non-Newtonian Fluid Mechanics, 1983. **12**(1): p. 113-118.
91. Zhang, K., H. Choi, and C. Jang, *Turbulent drag reduction characteristics of poly(acrylamide-co-acrylic acid) in a rotating disk apparatus*. Colloid & Polymer Science, 2011. **289**(17): p. 1821-1827.
92. Kim, J.T., C.A. Kim, K. Zhang, C.H. Jang, and H.J. Choi, *Effect of Polymer-Surfactant Interaction on Its Turbulent Drag Reduction*. Colloids and Surfaces A: Physicochemical and Engineering Aspects, 2011. **391**: p. 125-129.
93. Bueche, F., *Mechanical Degradation of High Polymers*. Journal of Applied Polymer Science, 1960. **4**(10): p. 101-106.
94. Moussa, T., C. Tiu, and T. Sridhar, *Effect of Solvent on Polymer Degradation in Turbulent Flow*. Journal of Non-Newtonian Fluid Mechanics, 1993. **48**(3): p. 261-284.
95. Moussa, T. and C. Tiu, *Factors Affecting Polymer Degradation in Turbulent Pipe Flow*. Chemical Engineering Science, 1994. **49**(10): p. 1681-1692.
96. Toonder, J.M.J., A.A. Draad, G.D.C. Kuiken, and F.T.M. Nieuwstadt, *Degradation Effects of Dilute Polymer Solutions on Turbulent Drag Reduction in Pipe Flows*. Applied Scientific Research, 1995. **55**(1): p. 63-82.
97. Brostow, W., H. Ertepinar, and R.P. Singh, *Flow of Dilute Polymer Solutions: Chain Conformations and Degradation of Drag Reducers*. Macromolecules, 1990. **23**(24): p. 5109-5118.
98. Brostow, W., S. Majumdar, and R.P. Singh, *Drag Reduction and Solvation in Polymer Solutions*. Macromolecular Rapid Communications, 1999. **20**(3): p. 144-147.
99. Choi, S.U.S., Y.I. Cho, and K.E. Kasza, *Degradation Effects of Dilute Polymer Solutions on Turbulent Friction and Heat Transfer Behavior*. Journal of Non-Newtonian Fluid Mechanics, 1992. **41**(3): p. 289-307.
100. Choi, H.J., C.A. Kim, J.-I. Sohn, and M.S. Jhon, *An Exponential Decay Function for Polymer Degradation in Turbulent Drag Reduction*. Polymer Degradation and Stability, 2000. **69**(3): p. 341-346.

101. Rho, T., J. Park, C. Kim, H.-K. Yoon, and H.-S. Suh, *Degradation of Polyacrylamide in Dilute Solution*. *Polymer Degradation and Stability*, 1996. **51**(3): p. 287-293.
102. Singh, R.P., *Turbulent Drag Reduction by Polymer-Based Mixtures and Graft Copolymers*. *Current Science*, 1995. **68**(7): p. 736-739.
103. Stelter, M., T. Wunderlich, S.K. Rath, G. Brenn, A.L. Yarin, R.P. Singh, and F. Durst, *Shear and Extensional Investigations in Solutions of Grafted/Ungrafted Amylopectin and Polyacrylamide*. *Journal of Applied Polymer Science*, 1999. **74**(11): p. 2773-2782.
104. Bello, J.B., A.J. Müller, and A.E. Sáez, *Effect of Intermolecular Cross Links on Drag Reduction by Polymer Solutions*. *Polymer Bulletin*, 1996. **36**(1): p. 111-118.
105. Dunlop, E.H. and L.R. Cox, *Influence of Molecular Aggregates on Drag Reduction*. *Physics of Fluids*, 1977. **20**(10): p. S203-S213.
106. Lundberg, R.D., D.G. Peiffer, I. Duvdevani, and R.M. Kowalik, *Drag reduction Utilising Water Soluble Interpolymer Complexes*. Patent US4489180, 1984.
107. Sabadini, E., K.R. Francisco, and L. Bouteiller, *Bis-Urea-Based Supramolecular Polymer: The First Self-Assembled Drag Reducer for Hydrocarbon Solvents*. *Langmuir*, 2010. **26**(3): p. 1482-1486.
108. Mancera, R.L., *Influence of Salt on Hydrophobic Effects: A Molecular Dynamics Study Using the Modified Hydration-Shell Hydrogen-Bond Model*. *The Journal of Physical Chemistry B*, 1999. **103**(18): p. 3774-3777.
109. Camail, M., A. Margailan, and I. Martin, *Copolymers of N-alkyl- and N-arylalkylacrylamides with Acrylamide: Influence of Hydrophobic Structure on Associative Properties. Part II: Rheological Behaviour in Semi-Dilute Solution*. *Polymer International*, 2009. **58**(2): p. 155-162.
110. Del Valle, E.M.M., *Cyclodextrins and Their Uses: a Review*. *Process Biochemistry*, 2004. **39**(9): p. 1033-1046.
111. Karlson, L., *Hydrophobically Modified Polymers Rheology and Molecular Associations*. PhD Thesis. 2002: Lund University.
112. Ogoshi, T., Y. Takashima, H. Yamaguchi, and A. Harada, *Chemically-Responsive Sol-Gel Transition of Supramolecular Single-Walled Carbon Nanotubes (SWNTs) Hydrogel Made by Hybrids of SWNTs and Cyclodextrins*. *Journal Of American Chemical Society*, 2007. **129**: p. 4878-4879.
113. Mahammad, S., G.W. Roberts, and S.A. Khan, *Cyclodextrin-Hydrophobe Complexation in Associative Polymers*. *Soft Matter*, 2007. **3**: p. 1185-1193.

114. Talwar, S., J. Harding, K.R. Oleson, and S.A. Khan, *Surfactant-Mediated Modulation of Hydrophobic Interactions in Associative Polymer Solutions Containing Cyclodextrins*. *Langmuir*, 2009. **25**: p. 794-802.
115. Hashidzume, A. and A. Harada, *Recognition of polymer side chains by cyclodextrins*. *Polymer Chemistry*, 2011. **2**: p. 2146-2154.
116. Turner, S.R., D.B. Siano, and J. Bock, *Micellar Process for the Production of Acrylamide-Alkyl Acrylamide Copolymers*. Patent US5428348, 1985.
117. Turner, S.R., D.B. Siano, and J. Bock, *Acrylamide-Alkylacrylamide Copolymers*. US Patent 4520182, 1985.
118. Ezzell, S.A. and C.L. McCormick, *Water-Soluble Copolymers. 39. Synthesis and Solution Properties of Associative Acrylamido Copolymers with Pyrenesulfonamide Fluorescence Labels*. *Macromolecules*, 1992. **25**(7): p. 1881-1886.
119. Zhong, C., P. Luo, Z. Ye, and H. Chen, *Characterization and Solution Properties of a Novel Water-soluble Terpolymer For Enhanced Oil Recovery*. *Polymer Bulletin*, 2009. **62**(1): p. 79-89.
120. Gouveia, L.M., B. Grassl, and A.J. Müller, *Synthesis and Rheological Properties of Hydrophobically Modified Polyacrylamides with Lateral Chains of Poly(propylene oxide) Oligomers*. *Journal of Colloid and Interface Science*, 2009. **333**(1): p. 152-163.
121. Biggs, S., A. Hill, J. Selb, and F. Candau, *Copolymerization of Acrylamide and a Hydrophobic Monomer in an Aqueous Micellar Medium: Effect of the Surfactant on the Copolymer Microstructure*. *The Journal of Physical Chemistry*, 1992. **96**(3): p. 1505-1511.
122. Hill, A., F. Candau, and J. Selb, *Properties of Hydrophobically Associating Polyacrylamides: Influence of the Method of Synthesis*. *Macromolecules*, 1993. **26**(17): p. 4521-4532.
123. Volpert, E., J. Selb, and F. Candau, *Influence of the Hydrophobe Structure on Composition, Microstructure, and Rheology in Associating Polyacrylamides Prepared by Micellar Copolymerization*. *Macromolecules*, 1996. **29**(5): p. 1452-1463.
124. Camail, M., A. Margailan, I. Martin, A.L. Papailhou, and J.L. Vernet, *Synthesis of N-alkyl- and N-aryllalkylacrylamides and Micellar Copolymerization with Acrylamide*. *European polymer journal*, 2000. **36**(9): p. 1853-1863.
125. Penott-Chang, E.K., L. Gouveia, I.J. Fernández, A.J. Müller, A. Díaz-Barrios, and A.E. Sáez, *Rheology of Aqueous Solutions of Hydrophobically Modified Polyacrylamides and*

- Surfactants*. Colloids and Surfaces A: Physicochemical and Engineering Aspects, 2007. **295**(1-3): p. 99-106.
126. Zhu, Z., O. Jian, S. Paillet, J. Desbrières, and B. Grassl, *Hydrophobically Modified Associating Polyacrylamide (HAPAM) Synthesized by Micellar Copolymerization at High Monomer Concentration*. European Polymer Journal, 2007. **43**(3): p. 824-834.
 127. Gao, B., H. Guo, J. Wang, and Y. Zhang, *Preparation of Hydrophobic Association Polyacrylamide in a New Micellar Copolymerization System and Its Hydrophobically Associative Property*. Macromolecules, 2008. **41**(8): p. 2890-2897.
 128. Volpert, E., J. Selb, and F. Candau, *Associating Behaviour of Polyacrylamides Hydrophobically Modified with Dihexylacrylamide*. Polymer, 1998. **39**(5): p. 1025-1033.
 129. Candau, F., S. Biggs, A. Hill, and J. Selb, *Synthesis, Structure and Properties of Hydrophobically Associating Polymers*. Progress in Organic Coatings, 1994. **24**(1-4): p. 11-19.
 130. Xue, W., I.W. Hamley, V. Castelletto, and P.D. Olmsted, *Synthesis and Characterization of Hydrophobically Modified Polyacrylamides and Some Observations on Rheological Properties*. European Polymer Journal, 2004. **40**(1): p. 47-56.
 131. Gao, B., *Microstructure and Association Property of Hydrophobically Modified Polyacrylamide of a New Family*. European Polymer Journal, 2007. **43**(10): p. 4530.
 132. Candau, F. and J. Selb, *Hydrophobically-Modified Polyacrylamides Prepared by Micellar Polymerization*. Advances in Colloid and Interface Science, 1999. **79**(2-3): p. 149-172.
 133. Ivanova, E.M., I.V. Blagodatskikh, O.V. Vasil'eva, A.I. Barabanova, and A.R. Khokhlov, *Synthesis of Hydrophobically Modified Poly(acrylamides) in Water-in-Oil Emulsions*. Polymer Science, 2008. **50**(1): p. 9-17.
 134. Kobitskaya, E., *Synthesis of Hydrophobically Modified Polyacrylamide in Inverse Miniemulsion*. PhD Thesis, der Universität Ulm, 2008.
 135. Wu, S. and R. Shanks, *Synthesis and Characterisation of Hydrophobic Modified Polyacrylamide*. Polymer International, 2004. **53**: p. 1821- 1830.
 136. Li, Y. and J.C.T. Kwak, *Rheology and Binding Studies in Aqueous Systems of Hydrophobically Modified Acrylamide and Acrylic Acid Copolymers and Surfactants*. Colloids and Surfaces A: Physicochemical and Engineering Aspects, 2003. **225**: p. 169-180.

137. Philippova, O.E., D. Hourdet, R. Audebert, and A.R. Khokhlov, *pH-Responsive Gels of Hydrophobically Modified Poly(acrylic acid)*. *Macromolecules*, 1997. **30**(26): p. 8278-8285.
138. Zhou, H., G.-Q. Song, Y.-X. Zhang, J. Chen, M. Jiang, T.E. Hogen-Esch, R. Dieing, L. Ma, and L. Haeussling, *Hydrophobically Modified Polyelectrolytes, 4. Synthesis and Solution Properties of Fluorocarbon-Containing Poly(acrylic acid)*. *Macromolecular Chemistry and Physics*, 2001. **202**(15): p. 3057-3064.
139. Zhuang, D.-q., J.C. Ai-hua Da, Y.-x. Zhang, R. Dieing, L. Ma, and L. Haeussling, *Hydrophobically Modified Polyelectrolytes II: Synthesis and Characterization of Poly(acrylic acid-co-alkyl acrylate)*. *Polymers for Advanced Technologies*, 2001. **12**(11-12): p. 616-625.
140. Baßmann-Schnitzler, F. and J.-M. Séquaris, *Sorption Properties of Hydrophobically Modified Poly(acrylic acids) as Natural Organic Matter Model Substances to Pyrene*. *Colloids and Surfaces A: Physicochemical and Engineering Aspects*, 2005. **260**: p. 119-128.
141. Guo, X., A.A. Abdala, B.L. May, S.F. Lincoln, S.A. Khan, and R.K. Prud'homme, *Rheology Control by Modulating Hydrophobic and Inclusion Associations in Modified Poly(acrylic acid) Solutions*. *Polymer*, 2006. **47**(9): p. 2976-2983.
142. Wang, J., L. Li, X. Guo, L. Zheng, D.-T. Pham, S.F. Lincoln, H.T. Ngo, P. Clements, B.L. May, R.K. Prud'homme, and C.J. Easton, *Aggregation of Hydrophobic Substituents of Poly(acrylate)s and Their Competitive Complexation by β - and γ -Cyclodextrins and Their Linked Dimers in Aqueous Solution*. *Industrial & Engineering Chemistry Research*, 2011. **50**(12): p. 7566-7571.
143. Saitoh, T., N. Ono, and M. Hiraide, *Effective Collection of Hydrophobic Organic Pollutants in Water with Aluminum Hydroxide and Hydrophobically Modified Polyacrylic Acid*. *Chemosphere*, 2012. **89**(6): p. 759-763.
144. Padmanabha Iyer, N., D. Hourdet, M.V. Badiger, C. Chassenieux, P. Perrin, and P.P. Wadgaonkar, *Synthesis and Swelling Behaviour of Hydrophobically Modified Responsive Polymers in Dilute Aqueous Solutions*. *Polymer*, 2005. **46**(26): p. 12190-12199.
145. Shedge, A.S., A.K. Lele, P.P. Wadgaonkar, D. Hourdet, P. Perrin, C. Chassenieux, and M.V. Badiger, *Hydrophobically Modified Poly(acrylic acid) Using 3-Pentadecylcyclohexylamine: Synthesis and Rheology*. *Macromolecular Chemistry and Physics*, 2005. **206**(4): p. 464-472.
146. Perrin, P. and F. Lafuma, *Low Hydrophobically Modified Poly(Acrylic Acid) Stabilizing Macroemulsions: Relationship between Copolymer Structure and Emulsions Properties*. *Journal of Colloid and Interface Science*, 1998. **197**(2): p. 317-326.

147. Wang, K.T., I. Iliopoulos, and R. Audebert, *Viscometric Behaviour of Hydrophobically Modified Poly(sodium acrylate)*. Polymer Bulletin, 1988. **20**(6): p. 577-582.
148. Dimitrov, P., E. Hasan, S. Rangelov, B. Trzebicka, A. Dworak, and C.B. Tsvetanov, *High Molecular Weight Functionalized Poly(ethylene oxide)*. Polymer, 2002. **43**: p. 7171–7178.
149. Petrov, P., S. Rangelov, C. Novakov, W. Brown, I. Berlinova, and C.B. Tsvetanov, *Core-Corona Nanoparticles Formed by High Molecular Weight Poly(ethylene oxide)-b-Poly(alkylglycidyl ether) Diblock Copolymers*. Polymer, 2002. **43**: p. 6641–6651.
150. Petrov, P., I. Berlinova, C.B. Tsvetanov, S. Rosselli, A. Schmid, A.B. Zilaei, T. Miteva, M. Dur, A. Yasuda, and G. Nelles, *High- Molecular- Weight Polyoxirane Copolymers and Their Use in High- Performance Dye- Sensitised Solar Cells*. Macromolecular Materials and Engineering, 2008. **293**: p. 598- 604.
151. Rufier, C., A. Collet, M. Viguier, J. Oberdisse, and S. Mora, *Asymmetric End-Capped Poly(ethylene oxide). Synthesis and Rheological Behavior in Aqueous Solution*. Macromolecules, 2008. **41**(15): p. 5854-5862.
152. Rufier, C., A. Collet, M. Viguier, J. Oberdisse, and S. Mora, *Influence of Surfactants on Hydrophobically End-Capped Poly(ethylene oxide) Self-Assembled Aggregates Studied by SANS*. Macromolecules, 2011. **44**(18): p. 7451-7459.
153. Kolnibolotchuk, N.K., V.J. Klenin, and S.Y. Frenkel, *Formation of Supermolecular Order in Aqueous Solutions of Poly(vinyl alcohol) in a Turbulent Flow*. Journal of Polymer Science: Polymer Symposia, 1974. **44**(1): p. 119-129.
154. Shakhovskaya, L.I., T.A. Lemesheva, and Y.G. Kryazhev, *Influence of Structure of Aqueous Polymer Solutions on the Toms Effect*. Journal of Engineering Physics, 1978. **34**(1): p. 52-55.
155. Minsk, L.M., W.J. Priest, and W.O. Kenyon, *The Alcoholysis of Polyvinyl Acetate**. Journal of the American Chemical Society, 1941. **63**(10): p. 2715-2721.
156. Bravar, M., J. Rolich, N. Ban, and V. Gnjatovic, *Studies of Alcoholysis of Poly (vinyl acetate) to Poly (vinyl alcohol)*. Journal of Polymer Science: Polymer Symposia, 1974. **47**(1): p. 329-334.
157. Park, S. and H. Yoon, *Acid-Catalysed Hydrolysis Reaction of Poly(vinyl acetate)*. Polymer(Korea), 2005. **29**(3): p. 304-307.
158. Yahya, G.O., S.A. Ali, M.A. Al-Naafa, and E.Z. Hamad, *Preparation and Viscosity Behavior of Hydrophobically Modified Poly(vinyl alcohol) (PVA)*. Journal of Applied Polymer Science, 1995. **57**(3): p. 343-352.

159. Marstokk, O. and J. Roots, *Synthesis and Characterization of Hydrophobically Modified Poly(vinyl alcohol)*. Polymer Bulletin, 1999. **42**(5): p. 527-533.
160. Saito, N., T. Sugawara, and T. Matsuda, *Synthesis and Hydrophilicity of Multifunctionally Hydroxylated Poly(acrylamides)*. Macromolecules, 1996. **29**(1): p. 313-319.
161. Albarghouthi, M.N., B.A. Buchholz, P.J. Huiberts, T.M. Stein, and A.E. Barron, *Poly-N-Hydroxyethylacrylamide (polyDuramide): A Novel, Hydrophilic, Self-Coating Polymer Matrix for DNA Sequencing by Capillary Electrophoresis*. Electrophoresis, 2002. **23**(10): p. 1429-1440.
162. Albarghouthi, M.N., T.M. Stein, and A.E. Barron, *Poly-N-Hydroxyethylacrylamide as a Novel, Adsorbed Coating for Protein Separation by Capillary Electrophoresis*. Electrophoresis, 2003. **24**(7-8): p. 1166-1175.
163. Narumi, A., Y. Chen, M. Sone, K. Fuchise, R. Sakai, T. Satoh, Q. Duan, S. Kawaguchi, and T. Kakuchi, *Poly(N-hydroxyethylacrylamide) Prepared by Atom Transfer Radical Polymerization as a Nonionic, Water-Soluble, and Hydrolysis-Resistant Polymer and/or Segment of Block Copolymer with a Well-Defined Molecular Weight*. Macromolecular Chemistry and Physics, 2009. **210**(5): p. 349-358.
164. Gunes, D., O. Batu Kurtarel, and N. Bicak, *Poly(N-hydroxyethyl acrylamide)-b-Polystyrene by Combination of ATRP and Aminolysis Processes*. Journal of Applied Polymer Science, 2013. **127**(4): p. 2684-2689.
165. Bahamdan, A. and W.H. Daly, *Hydrophobic Guar Gum Derivatives Prepared by Controlled Grafting Processes*. Polymers for Advanced Technologies, 2007. **18**(8): p. 652-659.
166. Lapasin, R., L. De Lorenzi, S. Pricl, and G. Torriano, *Flow Properties of Hydroxypropyl Guar Gum and Its Long-Chain Hydrophobic Derivatives*. Carbohydrate Polymers, 1995. **28**(3): p. 195-202.
167. Zhang, L.M., *Cellulosic Associative Thickeners*. Carbohydrate Polymers, 2001. **45**(1): p. 1-10.
168. Landoll, L.M., *Nonionic Polymer Surfactants*. Journal of Polymer Science: Polymer Chemistry Edition, 1982. **20**(2): p. 443-455.
169. Cohen-Stuart, M.A., R.G. Fokkink, P.M. van der Horst, and J.W.T. Lichtenbelt, *The Adsorption of Hydrophobically Modified Carboxymethylcellulose on a Hydrophobic Solid: Effects of pH and Ionic Strength*. Colloid & Polymer Science, 1998. **276**(4): p. 335-341.

170. Nishimura, H., N. Donkai, and T. Miyamoto, *Preparation and Properties of a New Type of Comb-Shaped, Amphiphilic Cellulose Derivative*. Cellulose, 1997. **4**(2): p. 89-98.
171. Shih, J.S., *Heterocyclic Quaternized Nitrogen-Containing Cellulosic Graft Polymers* Patent US5037930, 1991.
172. Tomanova, V., I. Srokova, A. Malovikova, and A. Ebringerova. *Surface-Active and Viscous Behavior of HM-CMC in Aqueous Solutions*. in *9th International Conference on Frontiers of Polymers and Advanced Materials*. 2007. Cracow, POLAND: Taylor & Francis Ltd.
173. Odian, G., *Reactions of Polymers*, in *Principles of Polymerisation*. 2004. p. 729-788.
174. Luca, C., S. Drăgan, V. Bărboiu, and M. Dima, *Chloromethylated Polystyrene Reaction with Tris(2-hydroxyethyl)amine. I. Crosslinked Polymers Prepared by Chloromethylated Polystyrene with Tris(2-hydroxyethyl)amine*. Journal of Polymer Science: Polymer Chemistry Edition, 1980. **18**(2): p. 449-454.
175. Zeng, Q.H., Q.L. Liu, I. Broadwell, A.M. Zhu, Y. Xiong, and X.P. Tu, *Anion Exchange Membranes Based on Quaternized Polystyrene-block-Poly(ethylene-ran-butylene)-block-Polystyrene for Direct Methanol Alkaline Fuel Cells*. Journal of Membrane Science, 2010. **349**: p. 237-243.
176. Roth, H.H., *Sulfonation of Poly (vinyl Aromatics)*. Industrial & Engineering Chemistry, 1957. **49**(11): p. 1820-1822.
177. Thaler, W.A., *Hydrocarbon-Soluble Sulfonating Reagents. Sulfonation of Aromatic Polymers in Hydrocarbon Solution Using Soluble Acyl Sulfates*. Macromolecules, 1983. **16**(4): p. 623-628.
178. Kučera, F. and J. Jančář, *Homogeneous and Heterogeneous Sulfonation of Polymers: A Review*. Polymer Engineering & Science, 1998. **38**(5): p. 783-792.
179. Martins, C.R., G. Ruggeri, and M.-A. de Paoli, *Synthesis of Pilot Plant Scale and Physical Properties of Sulfonated Polystyrene* Journal of the Brazilian Chemical Society, 2003. **14**(5): p. 797-802.
180. Carvalho, A.J.F. and A.A.S. Curvelo, *Effect of Sulfonation Level on Solubility and Viscosity Behavior of Low to Medium Charged Sulfonated Polystyrenes*. Macromolecules, 2003. **36**: p. 5304-5310.
181. Sułkowski, W.W., K. Nowak, A. Słkowska, A. Wolińska, W.M. Bajdur, D. Pentak, and M. B., *Study of the Sulfonation of Expanded Polystyrene Waste and of Properties of the Products Obtained*. Pure and Applied Chemistry, 2009. **81**(12): p. 2417-2424.

182. Picchioni, F., I. Giorgi, E. Passaglia, G. Ruggeri, and M. Aglietto, *Blending of Styrene-block-butadiene-block-styrene Copolymer with Sulfonated Vinyl Aromatic Polymers*. Polymer International, 2001. **50**: p. 714-721.
183. Kim, J., B. Kim, and B. Jung, *Proton Conductivities and Methanol Permeabilities of Membranes Made from Partially Sulfonated Polystyrene-block-Poly(ethylene-ran-butylene)-block-Polystyrene Copolymers*. Journal of Membrane Science, 2002. **207**(1): p. 129-137.
184. Hwang, H.Y., S.Y. Ha, and S.Y. Nam, *Sulfonated SEBS Membranes for HVAC Systems*. Macromolecular Symposia, 2006. **245-246**: p. 450-456.
185. Hwang, H.Y., H.C. Koh, J.W. Rhim, and S.Y. Nam, *Preparation of Sulfonated SEBS Block Copolymer Membranes and Their Permeation Properties*. Desalination, 2008. **233**: p. 173-182.
186. Barra, G.M.O., L.B. Jacques, R.L. Oréface, and J.R.G. Carneiro, *Processing, Characterization and Properties of Conducting Polyaniline-Sulfonated SEBS Block Copolymers*. European Polymer Journal, 2004. **40**(9): p. 2017-2023.
187. Johnson, D., D. Williamson, A.J. Pasquale, J. Lizotte, and T. Long, *In-Paraller Synthetic Methodologies for Stable Free Radical Polymerisation and Selective Sulfonation of Block Copolymers*. 2001, Shaw University, Raileigh, NC.
188. Elabd, Y.A. and E. Napadensky, *Sulfonation and Characterisation of poly(styrene-isobutylene-styrene) Triblock Copolymers at High Ion-Exchange Capacities*. Polymer, 2004. **45**: p. 3037-3043.
189. Xie, H.-Q., D.-G. Liu, and D. Xie, *Preparation, Characterization, and Some Properties of Ionomers from a Sulfonated Styrene-Butadiene-Styrene Triblock Copolymer Without Gelation*. Journal of Applied Polymer Science, 2005. **96**(4): p. 1398-1404.
190. Idibie, C.A., S.A. Abdulkareem, C.H.v. Pienaar, S.E. Iyuke, and L. vanDyk, *Mechanism and Kinetics of Sulfonation of Polystyrene- Butadiene Rubber with Chlorosulfonic Acid*. Industrial & Engineering Chemistry Research, 2010. **49**(4): p. 1600-1604.
191. Weiss, R.A., R.D. Lundberg, and A. Werner, *The Synthesis of Sulfonated Polymers by Free Radical Copolymerization. Poly(butadiene-co-sodium styrene sulfonate)*. Journal of Polymer Science: Polymer Chemistry Edition, 1980. **18**(12): p. 3427-3439.
192. Szczubiałka, K., K. Ishikawa, and Y. Morishima, *Micelle Formation of Diblock Copolymers of Styrene and Sulfonated Isoprene in Aqueous Solution*. Langmuir, 1998. **15**(2): p. 454-462.

193. Szczubiałka, K., K. Ishikawa, and Y. Morishima, *Associating Behavior of Sulfonated Polyisoprene Block Copolymers with Short Polystyrene Blocks at Both Chain Ends*. Langmuir, 1999. **16**(5): p. 2083-2092.
194. Gatsouli, K.D., S. Pispas, and E.I. Kamitsos, *Development and Optical Properties of Cadmium Sulfide and Cadmium Selenide Nanoparticles in Amphiphilic Block Copolymer Micellar-like Aggregates*. The Journal of Physical Chemistry C, 2007. **111**(42): p. 15201-15209.
195. Wang, X., M. Goswami, R. Kumar, B. G. Sumpter, and J. Mays, *Morphologies of Block Copolymers Composed of Charged and Neutral Blocks*. Soft Matter, 2012. **8**(11): p. 3036-3052.
196. Uchman, M., M. Štěpánek, K. Procházka, G. Mountrichas, S. Pispas, I.K. Voets, and A. Walther, *Multicompartment Nanoparticles Formed by a Heparin-Mimicking Block Terpolymer in Aqueous Solutions*. Macromolecules, 2009. **42**(15): p. 5605-5613.
197. Pispas, S., *Double Hydrophilic Block Copolymers of Sodium(2-sulfamate-3-carboxylate)isoprene and Ethylene Oxide*. Journal of Polymer Science Part A: Polymer Chemistry, 2006. **44**(1): p. 606-613.
198. Robins, M.J., S. Sarker, and S.F. Wnuk, *What Are the Practical Limits for Detection of Minor Nucleoside Reaction Products with HPLC (UV Detection), H NMR, and TLC (UV Detection)?* Nucleosides and Nucleotides, 1998. **17**(4): p. 785-790.
199. Nakken, T., M. Tande, and A. Elgsaeter, *Measurements of Polymer Induced Drag Reduction and Polymer Scission in Taylor Flow Using Standard Double-Gap Sample Holders With Axial Symmetry*. Journal of Non-Newtonian Fluid Mechanics, 2001. **97**(1): p. 1-12.
200. Tekin, N., A. Dinçer, Ö. Demirbaş, and M. Alkan, *Adsorption of Cationic Polyacrylamide Onto Sepiolite*. Journal Of Hazardous Materials 2006. **B134**: p. 211-219.
201. Morgan, S.E. and C.L. McCormick, *Water-Soluble Copolymers XXXII: Macromolecular Drag Reduction. A review of Predictive Theories and the Effects of Polymer Structure*. Progress in Polymer Science, 1990. **15**(3): p. 507-549.
202. Little, R.C., R.J. Hansen, D.L. Hunston, O.-K. Kim, R.L. Patterson, and R.Y. Ting, *The Drag Reduction Phenomenon. Observed Characteristics, Improved Agents, and Proposed Mechanisms*. Industrial & Engineering Chemistry Fundamentals, 1975. **14**(4): p. 283-296.
203. Gao, B., H. Haopeng, G. Jian Wang, and Y. Zhang, *Preparation of Hydrophobic Association Polyacrylamide in a New Micellar Copolymerization System and Its Hydrophobically Associative Property*. Macromolecules, 2008. **41**: p. 2890-2897.

204. Yahaya, G.O., A.A. Ahdab, S.A. Ali, B.F. Abu-Sharkh, and E.Z. Hamad, *Solution Behavior of Hydrophobically Associating Water-Soluble Block Copolymers of Acrylamide and N-benzylacrylamide*. *Polymer*, 2001. **42**(8): p. 3363-3372.
205. Zhang, P., Y. Wang, Y. Yang, J. Zhang, X. Cao, and X. Song, *The Effect of Microstructure on Performance of Associative Polymer: In Solution and Porous Media*. *Journal of Petroleum Science and Engineering*, 2012. **90-91**: p. 12-17.
206. Dai, Y.-H., F.-P. Wu, M.-Z. Li, and E.J. Wang, *Properties and Influence of Hydrophobically Associating Polyacrylamide Modified with 2-Phenoxyethylacrylate*. *Frontiers of Materials Science in China*, 2008. **2**(1): p. 113-118.
207. Nakashima, K. and P. Bahadur, *Aggregation of Water-Soluble Block Copolymers in Aqueous Solutions: Recent Trends*. *Advances in Colloid and Interface Science*, 2006. **123-126**: p. 75-96.
208. Camail, M., A. Margailan, I. Martin, A.L. Papailhou, and J.L. Vernet, *Synthesis of N-alkyl- and N-arylalkylacrylamides and Micellar Copolymerization with Acrylamide*. *European polymer journal*, 2000. **36**(9): p. 1853-1863.
209. Jianping, Z., S. Yonggang, W. Qiang, and Z. Qiang, *Hydrophobically Modified Poly(sodium 2-acrylamido-2-methylpropanesulfonate): Synthesis and Viscosity of Aqueous Solution*. *Polymer International*, 2009. **58**(11): p. 1275-1282.
210. Cowie, J.M.G., *Free Radical Addition Polymerisation*, in *Polymers: Chemistry and Physics of Modern Materials*. 1991. p. 52-82.
211. Odian, G., *Principles of Polymerisation*. 2004. **Fourth Edition**: p. 236.
212. Zhang, Y.X., A.H. Da, G.B. Butler, and T.E. Hogen-Esch, *A Fluorine-Containing Hydrophobically Associating Polymer. I. Synthesis and Solution Properties of Copolymers of Acrylamide and Fluorine-Containing Acrylates or Methacrylates*. *Journal of Polymer Science Part A: Polymer Chemistry*, 1992. **30**(7): p. 1383-1391.
213. Grassl, B., L. Billon, O. Borisov, and J. François, *Poly(ethylene oxide)- and Poly(acrylamide)-Based Water-Soluble Associative Polymers: Synthesis, Characterisation, Properties in Solution*. *Polymer International*, 2006. **55**(10): p. 1169-1176.
214. Lin, Y., L. Kaifu, and H. Ronghua, *A study on P(AM-DMDA) Hydrophobically Associating Water-Soluble Copolymer*. *European Polymer Journal*, 2000. **36**(8): p. 1711-1715.
215. Shashkina, Y.A., Y.D. Zaroslov, V.A. Smirnov, O.E. Philippova, A.R. Khokhlov, T.A. Pryakhina, and N.A. Churochkina, *Hydrophobic Aggregation in Aqueous Solutions of*

- Hydrophobically Modified Polyacrylamide in the Vicinity of Overlap Concentration*. Polymer, 2003. **44**(8): p. 2289-2293.
216. Barnardi, B.J.S. and R.H.J. Sellin, *Degradation of Dilute Solutions of Drag-reducing Polymer*. Nature Physical Science, 1972. **236**: p. 12-14.
217. Gasljevic, K., K. Hoyer, and E.F. Matthys, *Temporary Degradation and Recovery of Drag-reducing Surfactant Solutions*. Journal of Rheology, 2007. **51**(4): p. 645-667.
218. *Hydraulic Fracturing Fluids, in Underground Injection Control Program*. June 2004, US Environmental Protection Agency.
219. Bukovac, T., R. Belhaouas, D. Perez, A. Dragomir, V. Ghita, and C. Carlos Webel. *Successful Multistage Hydraulic Fracturing Treatments Using a Seawater-Based Polymer-Free Fluid System Executed From a Supply Vessel; Lebada Vest Field, Black Sea Offshore Romania*. in *EUROPEC/EAGE Conference and Exhibition, 8-11 June 2009, Amsterdam, The Netherlands*. 2009.
220. *Water Management Associated with Hydraulic Fracturing*. 2010, Americal Petroleum Institute.
221. Feng, Y., B. Grassl, L. Billon, A. Khoukh, and J. Francois, *Effects of NaCl on Steady Rheological Behaviour in Aqueous Solutions of Hydrophobically Modified Polyacrylamide and Its Partially Hydrolyzed Analogues Prepared by Post-Modification*. Polymer International, 2002. **51**: p. 939-947.
222. McCormick, C.L., T. Nonaka, and C.B. Johnson, *Water-Soluble Copolymers: 27. Synthesis and Aqueous Solution Behaviour of Associative Acrylamide N-Alkylacrylamide Copolymers*. Polymer, 1988. **29**(4): p. 731-739.
223. Zaitoun, A. and N. Kohler, *The Role of Adsorption in Polymer Propagation Through Reservoir Rocks*, in *SPE International Symposium on Oilfield Chemistry*. 1987, 1987 Copyright 1987 Society of Petroleum Engineers, Inc.: San Antonio, Texas.
224. Hollander, A.F., P. Somasundaran, and C.C. Gryte, *Adsorption Characteristics of Polyacrylamide and Sulfonate-Containing Polyacrylamide Copolymers on Sodium Kaolinite*. Journal of Applied Polymer Science, 1981. **26**(7): p. 2123-2138.
225. Zitha, P.L.J. and C.W. Botermans, *Bridging Adsorption of Flexible Polymers in Low-Permeability Porous Media*. SPE Production & Operations, 1998. **13**(1): p. 15-20.
226. Zitha, P.L.J., K.G.S. van Os, and K.F.J. Denys, *Adsorption of Linear Flexible Polymers During Laminar Flow Through Porous Media: Effect of the Concentration*, in *SPE/DOE Improved Oil Recovery Symposium*. 1998, Society of Petroleum Engineers: Tulsa, Oklahoma.

227. Shah, S., S.A. Heinle, and J.E. Glass, *Water-Soluble Polymer Adsorption From Saline Solutions*, in *SPE Oilfield and Geothermal Chemistry Symposium*. 1985, 1985 Copyright 1985, Society of Petroleum Engineers: Phoenix, Arizona.
228. Volpert, E., J. Selb, F. Candau, N. Green, J.F. Argillier, and A. Audibert, *Adsorption of Hydrophobically Associating Polyacrylamides on Clay*. *Langmuir*, 1998. **14**(7): p. 1870-1879.
229. Ren, H., Y. Li, S. Zhang, J. Wang, and Z. Luan, *Flocculation of Kaolin Suspension with the Adsorption of N,N-disubstituted Hydrophobically Modified Polyacrylamide*. *Colloids and Surfaces A: Physicochemical and Engineering Aspects*, 2008. **317**: p. 388-393.
230. Xiao, L., G.-Y. Xu, A.-M. Chen, and S.-L. Yuan, *The Adsorption of Hydrophobically Modified Polyacrylates at Interfaces of Quartz/Liquid and Gas/Liquid*. *Colloids and Surfaces A: Physicochemical and Engineering Aspects*, 2003. **219**: p. 233-242.
231. Samoshina, Y., A. Diaz, Y. Becker, T. Nylander, and B. Lindman, *Adsorption of Cationic, Anionic and Hydrophobically Modified Polyacrylamides on Silica Surfaces*. *Colloids and Surfaces A: Physicochemical and Engineering Aspects*, 2003. **231**: p. 195-205.
232. Tomatsu, I., A. Hashidzume, and A. Harada, *Gel-to-Sol and Sol-to-Gel Transitions Utilizing the Interaction of α -Cyclodextrin with Dodecyl Side Chains Attached to a Poly(acrylic acid) Backbone*. *Macromolecular Rapid Communications*, 2005. **26**(10): p. 825-829.
233. Tomatsu, I., A. Hashidzume, and A. Harada, *Redox-Responsive Hydrogel System Using the Molecular Recognition of β -Cyclodextrin*. *Macromolecular Rapid Communications*, 2006. **27**(4): p. 238-241.
234. Schneider, H.J., F. Hacket, V. Ruediger, and H. Ikeda, *NMR Studies of Cyclodextrins and Cyclodextrin Complexes*. *Chemical Reviews*, 1998. **98**: p. 1755-1785.
235. Taura, D., A. Hashidzume, and A. Harada, *Macromolecular Recognition: Interaction of Cyclodextrins with an Alternating Copolymer of Sodium Maleate and Dodecyl Vinyl Ether*. *Macromolecular Rapid Communications*, 2007. **28**(24): p. 2306-2310.
236. Tomatsu, I., K. Peng, and A. Kros, *Photoresponsive Hydrogels for Biomedical Applications*. *Advanced Drug Delivery Reviews*, 2011. **63**: p. 1257-1266.
237. Guo, X., A.A. Abdala, B.L. May, S.F. Lincoln, S.A. Khan, and R.K. Prud'homme, *Novel Associative Polymer Networks Based on Cyclodextrin Inclusion Compounds*. *Macromolecules*, 2005. **38**(7): p. 3037-3040.

238. Tomatsu, I., A. Hashidzume, and A. Harada, *Photoresponsive Hydrogel System Using Molecular Recognition of α -Cyclodextrin*. *Macromolecules*, 2005. **38**(12): p. 5223-5227.
239. Wenz, G., B.H. Han, and A. Muller, *Cyclodextrin Rotaxanes and Polyrotaxanes*. *Chemical Reviews*, 2006. **106**: p. 782-817.
240. Harada, A., H. Adachi, Y. Kawaguchi, and M. Kamachi, *Recognition of Alkyl Groups on a Polymer Chain by Cyclodextrins*. *Macromolecules*, 1997. **30**(17): p. 5181-5182.
241. Kjøniksen, A.-L., C. Galant, K.D. Knudsen, G.T.M. Nguyen, and B. Nyström, *Effects of β -Cyclodextrin Addition and Temperature on the Modulation of Hydrophobic Interactions in Aqueous Solutions of an Associative Alginate*. *Biomacromolecules*, 2005. **6**(6): p. 3129-3136.
242. Bu, H., S.N. Naess, N. Beheshti, K. Zhu, K.D. Knudsen, A.-L. Kjoniksen, A. Elgsaeter, and B. Nystrom, *Characterization of Thermally Sensitive Interactions in Aqueous Mixtures of Hydrophobically Modified Hydroxyethylcellulose and Cyclodextrins*. *Langmuir*, 2006. **22**(21): p. 9023-9029.
243. Wang, Y. and S. Banerjee, *Cyclodextrins Modify the Properties of Cationic Polyacrylamides*. *Journal of Colloid and Interface Science*, 2009. **339**(2): p. 325-329.
244. Li, L., X. Guo, L. Fu, R.K. Prudhomme, and S.F. Lincoln, *Complexation Behavior of α , β , and γ -Cyclodextrin in Modulating and Constructing Polymer Networks*. *Langmuir*, 2008. **24**(15): p. 8290-8296.
245. Bottero, J.Y., M. Bruant, J.M. Cases, D. Canet, and F. Fiessinger, *Adsorption of Nonionic Polyacrylamide on Sodium Montmorillonite: Relation Between Adsorption, ζ Potential, Turbidity, Enthalpy of Adsorption Data and ^{13}C -NMR in Aqueous Solution*. *Journal of Colloid and Interface Science*, 1988. **124**(2): p. 515-527.
246. Martin, J.R. and B.D. Shapella, *The Effect of Solvent Solubility Parameter on Turbulent Flow Drag Reduction in Polyisobutylene Solutions*. *Experiments in Fluids*, 2003. **34**(5): p. 535-539.
247. Lin, S.-T., K. Fuchise, Y. Chen, R. Sakai, T. Satoh, T. Kakuchi, and W.-C. Chen, *Synthesis, Thermomorphic Characteristics, and Fluorescent Properties of Poly[2,7-(9,9-dihexylfluorene)]-block-Poly(N-isopropylacrylamide)-block-Poly(N-hydroxyethylacrylamide) Rod-Coil-Coil Triblock Copolymers*. *Soft Matter*, 2009. **5**(19): p. 3761-3770.
248. Blagodatskikh, I.V., O.V. Vasil'eva, E.M. Ivanova, S.V. Bykov, N.A. Churochkina, T.A. Pryakhina, V.A. Smirnov, O.E. Philippova, and A.R. Khokhlov, *New Approach to the Molecular Characterization of Hydrophobically Modified Polyacrylamide*. *Polymer*, 2004. **45**(17): p. 5897-5904.

249. Wu, S., R.A. Shanks, and G. Bryant, *Properties of Hydrophobically Modified Polyacrylamide with Low Molecular Weight and Interaction with Surfactant in Aqueous Solution*. Journal of Applied Polymer Science, 2006. **100**(6): p. 4348-4360.
250. Aubry, T. and T. Moan, *Polymères hydrophobiquement associatifs comme modificateurs de rhéologie*. Oil & Gas Science and Technology, 1997. **52**(2): p. 129-132.
251. Kulik, V.M., *Drag Reduction Change of Polyethyleneoxide Solutions in Pipe Flow*. Experiments in Fluids, 2001. **31**(5): p. 558-566.
252. Nesyn, G., V. Manzhai, Y. Suleimanova, V. Stankevich, and K. Konovalov, *Polymer Drag-Reducing Agents for Transportation of Hydrocarbon Liquids: Mechanism of Action, Estimation of Efficiency, and Features of Production*. Polymer Science Series A, 2012. **54**(1): p. 61-67.
253. David, R.L.A., M.-H. Wei, D. Liu, B.F. Bathel, J.P. Plog, A. Ratner, and J.A. Kornfield, *Effects of Pairwise, Self-Associating Functional Side Groups on Polymer Solubility, Solution Viscosity, and Mist Control*. Macromolecules, 2009. **42**(4): p. 1380-1391.
254. Idibie, C.A., S.A. Abdulkareem, C.H. vZ Pienaar, S.E. Iyuke, and L. vanDyk, *Mechanism and Kinetics of Sulfonation of Polystyrene-Butadiene Rubber with Chlorosulfonic Acid*. Industrial & Engineering Chemistry Research, 2010. **49**: p. 1600-1604.
255. Huang, R.Y.M., P. Shao, C.M. Burns, and X. Feng, *Sulfonation of poly(ether ether ketone)(PEEK): Kinetic study and characterization*. Journal of Applied Polymer Science, 2001. **82**(11): p. 2651-2660.
256. Sabhapondit, A., A. Borthakur, and I. Haque, *Characterization of Acrylamide Polymers for Enhanced Oil Recovery*. Journal of Applied Polymer Science, 2003. **87**(12): p. 1869-1878.
257. Perricone, A.C., D.P. Enright, and J.M. Lucas, *Vinyl Sulfonate Copolymers for High-Temperature Filtration Control of Water-Based Muds*. SPE Drilling Engineering, 1986. **1**(5): p. 358-364.
258. Solomons, T.W.G., *Organic Chemistry*. 1996, John Wiley & Sons, Inc. p. 661-662.
259. Kim, T.Y., J.E. Kim, Y.S. Kim, T.H. Lee, W.J. Kim, and K.S. Suh, *Preparation and Characterisation of Poly(3,4-ethylenedioxythiophene) (PEDOT) Using Partially Sulfonated poly(styrene-butadiene-styrene) Triblock Copolymer as a Polyelectrolyte*. Current Applied Physics, 2009. **9**: p. 120-125.
260. Liang, G.-D., J.-T. Xu, and Z.-Q. Fan, *Synthesis of Polystyrene-b-Poly(ethylene-co-butene) Block Copolymers by Anionic Living Polymerization and Subsequent*

- Noncatalytic Hydrogenation*. Journal of Applied Polymer Science, 2006. **102**: p. 2632-2638.
261. Silva, M.E.S.R., E.R. Dutra, V. Mano, and J.C. Machado, *Preparation and thermal study of polymers derived from acrylamide*. Polymer Degradation and Stability, 2000. **67**(3): p. 491-495.
262. Monroy-Barreto, M., J.L. Acosta, C. del Río, M.C. Ojeda, M. Muñoz, J.C. Aguilar, E. Rodríguez de San Miguel, and J. de Gyves, *Preparation, Characterization and Evaluation of Proton-Conducting Hybrid Membranes Based on Sulfonated Hydrogenated Styrene-Butadiene and Polysiloxanes for Fuel Cell Applications*. Journal of Power Sources, 2010. **195**(24): p. 8052-8060.
263. Zhao, J., M.D. Ediger, Y. Sun, and L. Yu, *Two DSC Glass Transitions in Miscible Blends of Polyisoprene/Poly(4-tert-butylstyrene)*. Macromolecules, 2009. **42**(17): p. 6777-6783.
264. Guo, B., F. Chen, Y. Lei, X. Liu, J. Wan, and D. Jia, *Styrene-Butadiene Rubber/Halloysite Nanotubes Nanocomposites Modified by Sorbic Acid*. Applied Surface Science, 2009. **255**(16): p. 7329-7336.
265. Wang, F., M. Hickner, Y.S. Kim, T.A. Zawodzinski, and J.E. McGrath, *Direct Polymerization of Sulfonated poly(arylene ether sulfone) Random (Statistical) Copolymers: Candidates for New Proton Exchange Membranes*. Journal of Membrane Science, 2002. **197**(1-2): p. 231-242.
266. Ballard, M.J., R. Buscall, and F.A. Waite, *The Theory of Shear-Thickening Polymer Solutions*. Polymer, 1988. **29**(7): p. 1287-1293.
267. Indei, T., *Necessary Conditions for Shear Thickening in Associating Polymer Networks*. Journal of Non-Newtonian Fluid Mechanics, 2007. **141**(1): p. 18-42.
268. Witten, T.A. and M.H. Cohen, *Crosslinking in Shear-Thickening Ionomers*. Macromolecules, 1985. **18**(10): p. 1915-1918.
269. Ushakov, V.D., L.P. Mezhirova, L.A. Galata, A.G. Kostyuk, Z.S. Khusnutdinova, S.S. Medvedev, A.D. Abkin, and P.M. Khomikovskii, *The Emulsion Polymerization of Styrene and of Butadiene-Styrene Mixtures with Redox Initiator Systems- I. The Effect of the Nature of the Peroxidic Compound on the Polymerization Rate*. Polymer Science U.S.S.R., 1962. **3**(6): p. 1081-1089.
270. Nicolaÿ, R., Y. Kwak, and K. Matyjaszewski, *A Green Route to Well-Defined High-Molecular-Weight (Co)polymers Using ARGET ATRP with Alkyl Pseudohalides and Copper Catalysis*. Angewandte Chemie International Edition, 2010. **49**(3): p. 541-544.